INFORMATION TO USERS

This manuscript has been reproduced from the microfilm master. UMI films the text directly from the original or copy submitted. Thus, some thesis and dissertation copies are in typewriter face, while others may be from any type of computer printer.

The quality of this reproduction is dependent upon the quality of the copy submitted. Broken or indistinct print, colored or poor quality illustrations and photographs, print bleedthrough, substandard margins, and improper alignment can adversely affect reproduction.

In the unlikely event that the author did not send UMI a complete manuscript and there are missing pages, these will be noted. Also, if unauthorized copyright material had to be removed, a note will indicate the deletion.

Oversize materials (e.g., maps, drawings, charts) are reproduced by sectioning the original, beginning at the upper left-hand corner and continuing from left to right in equal sections with small overlaps.

Photographs included in the original manuscript have been reproduced xerographically in this copy. Higher quality 6" x 9" black and white photographic prints are available for any photographs or illustrations appearing in this copy for an additional charge. Contact UMI directly to order.

Bell & Howell Information and Learning
300 North Zeeb Road, Ann Arbor, MI 48106-1346 USA
800-521-0600

DEVELOPMENT AND APPLICATION OF NOVEL NMR TECHNIQUES FOR THE STUDY OF LIGNIN

by

Behzad C. Ahvazi

A thesis submitted to the Faculty of Graduate Studies and Research in partial fulfilment of the requirements for the degree of Doctor of Philosophy

Department of Chemistry
McGill University
Montréal, Québec, Canada

April 1998

The essential is to meet the challenge

Primo Levi

Dedicated to my wonderful family

ABSTRACT

Solid-state and solution NMR techniques were used in order to study the transformation of various functional groups present in lignin and cellulose when wood is exposed to a wide range of pH's and pulping reagents.

Solid-state proton spin-lattice relaxation times (T_{1H}) allowed the determination of the molecular mobilities of carbohydrates and lignin as a function of pH for black spruce softwood. Similar measurements on isolated cellulose and cuoxam lignin were also conducted. These studies showed that the mobilities of the polymeric constituents of wood are affected by ionization processes occurring on the various functional groups present in lignin and cellulose.

Quantitative ^{31}P NMR spectroscopy was also used to derive the fundamental thermodynamic parameters that are involved in the stereoselective degradation of the two diastereomeric forms of the most abundant structural (arylglycerol-β-aryl ether) units of lignin under kraft pulping conditions. It was shown that the *erythro* isomers of the arylglycerol-β-aryl ether units in softwood milled wood lignin cleave faster than their *threo* counterparts. The general stability of the *threo* diastereomers toward kraft pulping seems to be the manifestation of a considerably slower reaction of the pulping reagents with the *threo* diastereomers of arylglycerol-β-aryl ethers. Quantitative ^{31}P NMR was also used for the identification and quantification of accumulated condensed diphenylmethane (DPM) moieties during conventional kraft, extended modified continuous cooking (EMCC®) and soda pulping processes.

A novel method that permits the quantitative detection and classification of various carbonyls in lignin was also developed. The proposed selective fluoride-induced trifluoromethylation method was optimized for a series of carbonyl-containing lignin-like model compounds. This was followed by ^{19}F NMR spectral analyses of the resulting fluorine derivatives allowing for thorough understanding of their structure/^{19}F NMR chemical shift relationships. Our studies demonstrated that the proposed method is a new analytical tool for the classification and quantification of various carbonyl groups that may be present in soluble lignins.

RÉSUMÉ

Des techniques RMN d'analyse à l'état solide et liquide ont été utilisées pour étudier la transformation de divers groupements fonctionnels présents dans la lignine et la cellulose lorsque le bois est exposé à divers degrés de pH et à divers réactifs pour la cuisson.

Des temps de relaxation spin-milieu de protons à l'état solide (T_{1H}) ont permis de déterminer les mobilités moléculaires des hydrates de carbone et de la lignine en tant que fonction du pH pour l'épinette noire. Des mesures similaires ont aussi été effectuées sur de la lignine de cuoxam et de cellulose isolées. Ces études ont démontré que les processus d'ionisation survenant avec les divers groupements fonctionnels présents dans la lignine et la cellulose avaient un effet sur les mobilités des composants polymériques du bois.

La spectroscopie quantitative RMN ^{31}P a aussi été utilisée pour déterminer les paramètres thermodynamiques fondamentaux impliqués dans la dégradation stéréosélective des deux formes diastéréomériques des unités structurales (éther arylglycérol-β-aryle) de lignine les plus abondantes dans des conditions de mise en pâte kraft. Il a été démontré que les isomères *érythro* des unités d'éther arylglycérol-β-aryle dans la lignine de bois de résineux broyé se clivent plus rapidement que les *thréo*. La stabilité générale des diastéréomères *thréo* lors de la mise en pâte kraft semble être la manifestation d'une réaction considérablement plus lente des réactifs dans la pâte avec les diastéréomères *thréo* des éthers arylglycérol-β-aryle. La RMN ^{31}P quantitative a aussi été utilisée pour identifier et quantifier les groupes de diphénylméthane (DPM) condensés accumulés lors de la mise en pâte kraft, la cuisson en continu modifiée prolongée (EMCC®), et la mise en pâte à la soude.

Une nouvelle méthode permettant la détection quantitative et la classification de divers carbonyles dans la lignine a aussi été mise au point. La méthode de la trifluorométhylation sélective provoquée par du fluor a été optimisée pour une série de composés modèles de type lignine contenant des carbonyles. Cette analyse a été suivie d'analyses spectrales RMN ^{19}F des dérivés de fluor apparus, ce qui a permis de bien comprendre les relations entre leur structure et le déplacement chimique en RMN ^{19}F.

Nos études ont démontré que la méthode proposée est un nouvel outil d'analyse pour la classification et la quantification de divers groupes carbonyles qui pourraient être présents dans les lignines solubles.

FOREWARD

This thesis was prepared in a manuscript-based structure, as described in section 3 of the McGill University, Faculty of Graduate Studies and Research Guidelines for Thesis Preparation, September 1994 revision. This section states:

> Candidates have the option of including, as part of the thesis, the text of a paper(s) submitted or to be submitted for publication, or the clearly-duplicated text of a published paper(s). These text must be bound as an integral part of the thesis.
>
> If this option is chosen, **connecting texts that provide logical bridges between the different papers are mandatory**. The thesis must be written in such a way that is more than a mere collection of manuscripts; in other words, results of a series of papers must be integrated.
>
> The thesis must still conform to all other requirements of the "Guidelines for Thesis Preparation" . **The thesis must include:** A Table of Contents, an abstract in English and French, an introduction which clearly states the rationale and objectives of the study, a comprehensive review of the literature, a final conclusion and summary, and a thorough bibliography or reference list.
>
> Additional material must be provided where appropriate (e.g. in appendices) and in sufficient detail to allow a clear and precise judgement to be made of the importance and originality of the research reported in the thesis.
>
> In the case of manuscripts co-authored by the candidate and others, **the candidate is required to make an explicit statement in the thesis as to who contributed to such work and to what extent**. Supervisors must attest to the accuracy of such statements at the doctoral oral defence. Since the task of the examiners is made more difficult in these cases, it is in the candidate's interest to make perfectly clear the responsibilities of all the authors of the co-authored papers. **Under no circumstances can a co-author of any component of such a thesis serve as an examiner for that thesis.**

This dissertation is presented in six chapters. Chapter 1 is a general introduction to the chemistry of lignin and its structural elucidation by application of NMR spectroscopy other than the investigation reported herein. The intervening chapters present the principle results of the research conducted. Each has been written in a paper

format, with an abstract, an introduction to the specific field discussed in the chapter, an experimental section, results and discussion, conclusions, acknowledgements when appropriate, and references. Tables and figures have been interleaved as near as possible to their mention in the text, mostly on separate pages.

The following publications contain material appearing in this thesis:

1. Ahvazi, B. C., and Argyropoulos, D. S., Quantitative trifluoromethylation of carbonyl-containing lignin model compounds., J. Fluorine Chem., 78, 195-198, 1996.

2. Ahvazi, B. C., and Argyropoulos, D. S., ^{19}F nuclear magnetic resonance spectroscopy for the elucidation of carbonyl groups in lignins: 1. Model compounds., J. Agric. Food Chem., 44(8), 2167-2175, 1996.

3. Ahvazi, B. C., and Argyropoulos, D. S., Thermodynamic parameters governing the stereoselective degradation of arylglycerol-β-aryl ether bonds in milled wood lignin under kraft pulping conditions., Nord. Pulp Pap. Res. J., 12(4), 282-288, 1997.

4. Ahvazi, B. C., and Argyropoulos, D. S., Quantitative detection of carbonyl groups in technical and native lignins using ^{19}F NMR spectroscopy., The 9th Int. Symp. Wood and Pulp. Chem., Montréal, Québec, Canada, 7-1 to 7-5, 1997.

5. Ahvazi, B. C., Pageau, G., and Argyropoulos, D. S., On the formation of diphenylmethane structures in lignin under kraft, EMCC$^{\bullet}$ and soda pulping conditions., Accepted in Can. J. Chem., Feb. 1998.

6. Ahvazi, B. C., and Argyropoulos, D. S., Proton spin-lattice relaxation time measurements of solid wood and its constituents as a function of pH., to be submitted to Wood Sci. Technol., 1998.

7. Ahvazi, B. C., Crestini, C., and Argyropoulos, D. S., ^{19}F nuclear magnetic resonance spectroscopy for the quantitative detection and classification of carbonyl groups in lignins., to be submitted to J. Agric. Food Chem., 1998.

CONTRIBUTIONS OF AUTHORS

Each of the above publications was written by the author of this dissertation under the supervision of Dr. D. S. Argyropoulos; the only exception being publication #7. The latter publication was written jointly with Dr. C. Crestini (visiting Postdoctoral Fellow) and adapted for inclusion in this thesis. The contribution of Dr. D. S. Argyropoulos to this thesis beyond the conception of the original objectives and the major experimental routes to be applied, included continuous guidance and in depth discussions on problems encountered. The contribution of Dr. Crestini to this effort was carrying out the 2D-NMR spectra of Figure 6.7 and the selective Dakin and hydrosulphite reactions. The contribution of Mr. G. Pageau in publication #5 was in developing a sampling protocol under real industrial conditions.

The material in Chapter 2 is to be submitted as publication #6; Dr. F. Morin contributed some of the T_{1H} measurements reported in this chapter. Chapters 3 and 4 have been published as publications #3 and #5, respectively. Chapter 5 is an expanded version of publications #1 and #2. Key results from Chapter 6 were reported in publication #4, with complete results to be submitted as publication #7.

ACKNOWLEDGEMENTS

I would like to express my deepest gratitude towards my thesis supervisor, Dr. D. S. Argyropoulos, for the immeasurable interest and numerous invaluable comments he contributed to this work. His enthusiasm, devotion to scientific inquiry and professional and personal generosity have all been inspiring. It has been a great pleasure to learn from a true *επιστήμων*. I would also like to thank him for accommodating my often unusual working schedule.

I would like to extend my appreciation to all those professors in the department of Chemistry, Pulp and Paper Research Centre and PAPRICAN from whom I gained the knowledge and background to carry out this research. In particular, Dr. C. Langford, my first academic supervisor for showing me the "way", Dr. D. F. R. Gilson, Dr. L. Reven, and specially Dr. F. Morin and Dr. F. Sourial for their patience and great kindness in teaching me the concept and the operation of both solid and solution NMR spectrometers. Thanks are also due to Dr. R. Brown, Dr. D. Patterson, Dr. A. Eisenberg, Dr. T. G. M. van de Ven, Dr. R. H. Marchessault and Dr. D. G. Gray. I also wish to thank Dr. R. St. John Manley and Dr. C. Heitner. It has been a privilege to work, and learn among people who are, not only knowledgable in their respective field, but also enjoy their work and the company of their colleagues. Thank you for making these years happy and memorable ones.

Thanks are also due to all my colleagues, co-workers and group members for their helpful and valuable discussions. Special thanks are expressed to both technical specialists Mr. G. Suranyi and Mr. Y. J. Sun for providing most of the lignins and also for their continuous encouragement during the course of this research. I am very greatful to Mr. P. Halevy and I. De Souza for thier great friendship, and timeless assistance in preparing this thesis.

I would also like to acknowledge my very special friends: Dr. G. Michalakis (*ψάλτης*), H. A. Kyriazopoulos, Dr. A. Spyros, Dr. C. M. P. Crestini, A. Taghizadeh, S. Fardad, for their endless support, love and encouragement.

Finally, I would like to thank all my wonderful family members: Dad and Mom for their unconditional love. My brothers: Dr. Bijan Ahvazi, Dr. Behrouz Ahvazi, and

Dr. Bahman Ahvazi for their guidance, and for their ability to inspire me through all the tough times. Thanks to all my lovely sisters, Mitra, Mina, Mehrnoosh and Lori Sobel Ahvazi for their patience, and their everlasting love and support; even though I was a pain..!!!

This research was supported by the Canadian Pulp and Paper Industry and a National Network Centres of Excellence Grant that was provided by the Natural Science and Engineering Research Council (NSERC).

TABLE OF CONTENTS

Chapter 6: ^{19}F Nuclear Magnetic Resonance (NMR) Spectroscopy for the Quantitative Detection and Classification of Carbonyl Groups in Lignins

LIST OF TABLES

LIST OF FIGURES

LIST OF ABBREVIATIONS AND SYMBOLS

S1, S2, S3	outer, middle and innermost layer of the secondary wall
NMR	nuclear magnetic resonance
δ	chemical shifts
J	coupling constants
DD	dipolar decoupling
CP	cross polarization
MAS	magic angle spinning
NOE	nuclear Overhauser effect
INEPT	insensitive nuclei enhanced by polarization transfer
T_1	spin-lattice relaxation time
$T_{1\rho}$	spin-lattice relaxation time in the rotating frame
T_2	spin-spin relaxation time
τ_2, τ_c	molecular rotational, angular momentum correlation time
ω_0	precessional frequency
CMP, CTMP	chemimechanical, chemithermomechanical pulp
RMP, TMP	refiner mechanical, thermomechanical pulp
DTPA	diethylenetriaminepentaacetic acid
Ka, pKa	dissociation constant, -log [Ka]
β-O-4	arylglycerol-β-aryl ether structural unit
INADEQUATE	incredible natural abundance double quantum transfer experiment
k	rate constant of a chemical reaction
A	pre-exponential factor
E_a	activation energy
R	gas constant
ΔG	Gibbs free energy
ΔH	enthalpy
ΔS	entropy

κ	Boltzmann's constant
h	Planck's constant
DPM	diphenylmethane
MCC	modified continuous cooking
EMCC	extended modified continuous cooking
RDH	rapid displacement heating
ECF	elemental chlorine free
γ	gyromagnetic ratio
H	Hamiltonian
I	spin angular momentum
r	vector distance
τ	rotational correlation time
$J(\omega)$	spectral density function
η	asymmetry chemical shift tensor
TBAF	tetra-n-butylammonium fluoride
TMAF	tetramethylammonium fluoride
THF	tetrahydrofuran
HMQC	heteronuclear multiple quantum correlation

Chapter 1

General Introduction

1.0. INTRODUCTION

Wood is a naturally occurring material familiar in at least some way to everyone. Wood has always held a significant place within the human economy. It represents one of the most important renewable natural resources, and its annual growth is sufficient to satisfy many essential needs indefinitely into the future. Wood has served man as a structural material for his buildings, furnishings, tools, weapons, and until recently as his only readily available fuel[1]. Wood is obtained from three main parts of a tree, namely the stem, the roots and the branches of the crown. Generally, trees belong to seed-bearing plants (spermatophytes) subdivided into two broad categories of plants known commercially as softwoods and hardwoods. Softwoods are tree species of a class of plants called gymnosperms (seeds are borne naked), and hardwoods are woody, dicotyledonous (two seed leaves) angiosperms (seeds are borne in a fruit structure). Both softwoods and hardwoods contain various fibrous and nonfibrous cells[2]. They grow and develop in various geometrical shapes and in different manners[3].

1.1. The MACROSCOPIC STRUCTURE of WOOD

In order to obtain the proper spatial concept for the structure of wood the stem from the trees must be considered. A log may be pictured with good approximation, as a truncated cone through which three sections may be cut perpendicular to each other. These are the transverse (T), or cross section, at right angles to the stem axis; the radial section (R), parallel to the axis on a radius of the stem; and the tangential section, parallel to the axis and perpendicular to the radius. Examination of three cutting planes of a stem (Figure 1.1) suggests[2] the processes of formation of wood cells and their final transformation into wood tissues. In Figure 1.1 the centrally located pith represent the growth of the plant. Ten growth rings represent the growth of the plant in each year. Each ring is composed of earlywood and latewood.

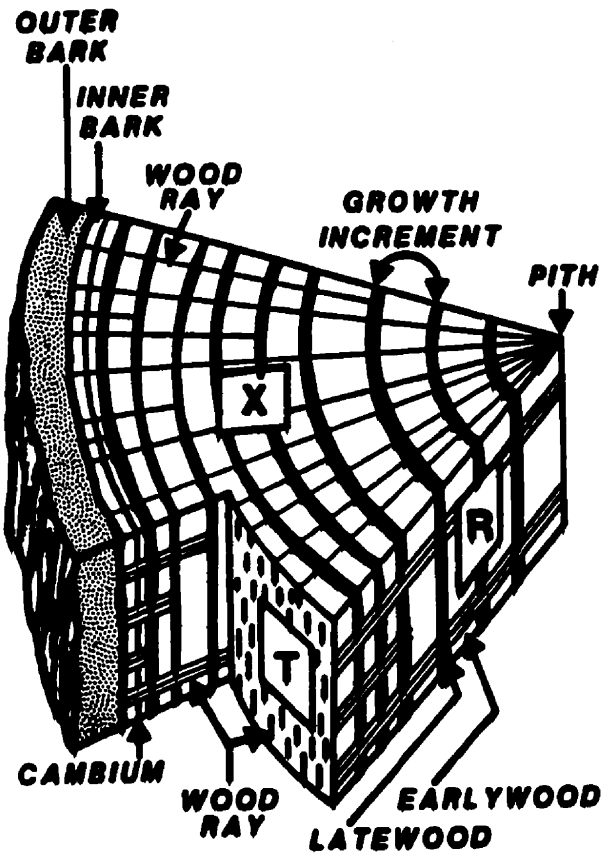

Figure 1.1. Representation of a tree cross section cut to reveal the three major structural planes of wood. This particular stem was cut in the spring of its 10th growing season[2].

The rings accumulated during the course of years collectively constitute the wood or xylem. To the outside of the wood lies the cambium, inner bark (phloem), and outer bark. Cambium is a very thin layer of living cells lying between wood (xylem) and inner bark (phloem). It is in this layer that the vital actions of cell division and radial growth of the tree proceed. Each cell formed through the division of a mother cell (in cambium), after growth and development, becomes part of the wood xylem. The division of phloem cells is less frequent than that of xylem cells and therefore they do not significantly contribute to the total volume of wood. But they do become incorporated into the outer bark, which acts as a protective shield and is important to the survival and growth of the plant.

1.1.1. The cell wall

Plant cell walls are built up of cellulose microfibrils orientated at various directions (Figure 1.2), and incrusted with a number of other compounds. They are subdivided into primary walls and secondary walls according to the time of their formation. The primary wall develops first and is often stretched during the differentiation of the cell. It is the only wall found in some cells. The secondary wall is laid down on the inside of the primary wall, usually after elongation of the cell has ceased, and is a characteristic feature of almost all wood cells[4].

The primary or outer wall of a wood cell consists of a thin network of cellulose microfibrils, irregularly and loosely arranged and incrusted with hemi-cellulose, lignin, and other compounds. The secondary wall is laid down inside the primary wall and in most xylem[5] cells is considerably the thicker of the two. It can be subdivided into three layers according to the orientation of the microfibrils within it. The layer nearest the primary wall is termed the S1 layer and the microfibrils in it are orientated nearly perpendicular to the long axis of the cell. The middle, or S2 layer is by far the thickest and is built up of microfibrils running at a small angle to the long axis of the cell. The S3 layer, lying nearest to the cell lumen, is a thin layer with the microfibrils again orientated in a nearly transverse direction. There may by a gradual transition in microfibril orientation from one layer to the next. The secondary wall is also incrusted with hemicellulose, and deposits of lignin and other substances. The S3 layer may be overlaid inside the cell lumen by a covering termed the warty layer[6]. This layer when present, so named on account of its small protrusions, is laid down just prior to death of the cell protoplast and covers the entire S3 layer, pit cavities and any other wall scupturings.

Individual cells are joined together by intercellular material between their primary walls. This middle lamella is an amorphous mass, rich in lignin and composed largely of pectin substances. It is readily dissolved away by macerating solutions.

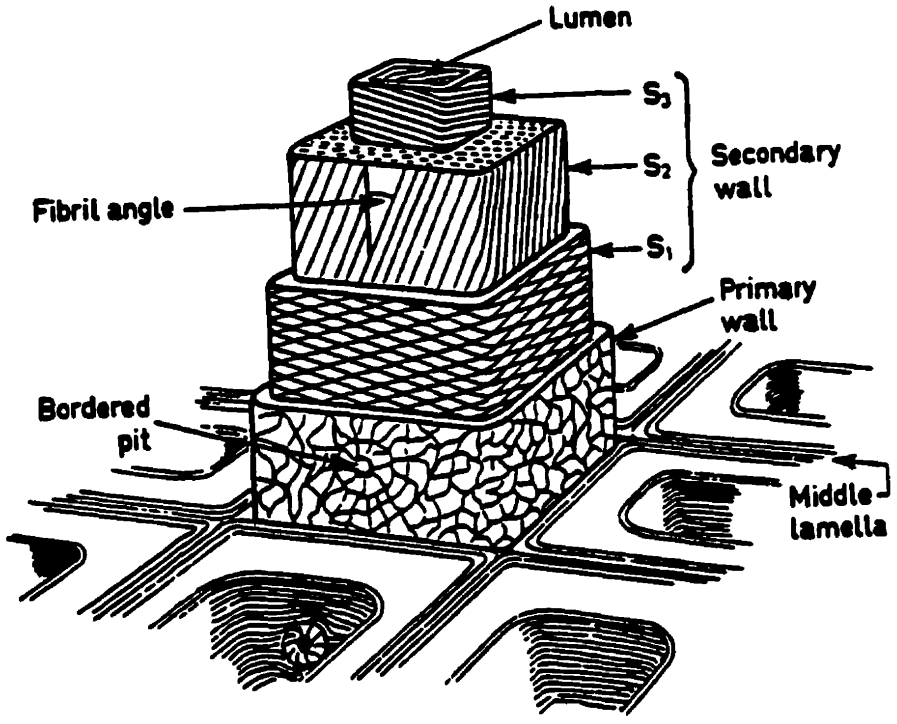

Figure 1.2. Schematic structural diagram[7] of a typical softwood tracheid[8]. **S1**, outer layer of the secondary wall; **S2**, middle layer of the secondary wall; **S3**, innermost layer of the secondary wall.

1.1.2. Gymnosperm wood

The secondary xylem of the gymnosperms, commonly called softwood, is simpler and more homogeneous than that of the angiosperms. The main differences between the two types of wood are the presence of vessels in the angiosperms and their absence in the gymnosperms (with the exception of one small order of plants) and the relatively small amount of axial parenchyma found in the gymnosperms. The axial system of the gymnospermous wood is compose almost entirely of tracheids though small amounts of axial parenchyma are found in some species[9]. The tracheids are long cells with several ray contacts and their ends overlapping each other. The cells are pitted in an opposite or alternate pattern, principally on their radial walls, and these pits in members of the

Coniferales and some other genera are of the conifer bordered pit type where the pit membranes possess tori. The pits are normally concentrated at the ends of the tracheids and on those portions of the walls adjacent to rays. Resin canals occur in a number of gymnosperms[10]. Growth rings are usually prominent, the latewood tracheids developing thicker walls with reduced bordered pits. The ray system conducts material horizontally across the stem. It contains ray parenchyma and ray tracheids, the latter being distinguished by their thicker walls, bordered pits and lack of a living protoplast at maturity. In the majority of gymnosperms the rays are also uniseriated. Horizontal resin canals may occur[11].

Although the tracheids fulfil the double function of support and conducting, and the wood lacks the apparent sophistication of vessels with open perforations and other modifications found in the angiosperms, the xylem of gymnosperms appears to be a highly efficient system. The giant redwoods of North America (*Sequioa sempervirens* D. Don.), for example, grow to more than 300 feet in height. The trunks of these giant trees, therefore, act as water-conducting pathway for a remarkable distance when it is remembered how comparatively small the cells of the xylem are. These trunks also hold huge weights of branches and foliage against severe wind loads.

1.1.3. Angiosperm wood

Although some monocotyledonous plants (e.g. the palms) do show some secondary growth, they do not possess a complete cylinder of vascular cambium and hence their stems do not contain wood in the usual sense of the word. Many dicotyledonous angiosperms, however, produce considerable amounts of secondary xylem This wood, generally referred to as hardwood, is considerably more complex than that found in the conifers since it contains a greater variety of cell types. Whereas in the softwood the axial system is built up almost entirely of tracheids, hardwoods have evolved two different cell types for conduction and support. Vessels, built up of individual vessel members joined end to end, provide a very efficient pathway for the ascent of sap up the tree. These vessels are variously distributed within the growth rings[12].

The function of mechanical support in angiosperm wood is carried out by the wood fibres. These extremely long cells with thick walls, arranged in various groupings within the growth rings, act as reinforcing members within the axial system. Libriform fibres are longer then fibre tracheids and have only simple pits. Fibre tracheids are shorter and have reduced bordered pits. In some plants the fibres can occupy more than half the volume of the wood and form the bulk of the fibrous mass obtained when the wood is pulped. Axial parenchyma cells are more abundant in hardwoods than in softwoods where they occur only rarely[13].

It is generally accepted that vessel members and fibres in hardwoods have evolved from tracheids, so that two separate cell types have become specialized to fulfil the two functions undertaken by the tracheid in other plant. Primitive dicotyledonous woods possess long vessel members with very oblique scalariform perforation plates while more specialized woods contain short wide vessel members with transverse simple perforation plates.

Rays occupy a higher proportion of the wood volume in angiosperms than in gymnosperms. They are usually multiseriate and may contain both procumbent and upright cells[14].

1.2. CHEMICAL COMPOSITIONS of WOOD

The chemical composition of wood is complex. The woody tissue is made up of many components which are distributed non-uniformly as a result of its anatomical structure, and not present in simple physical admixture. Consequently, the chemical behaviour of wood cannot be deduced in detail from the properties of the component substances.

The greater part of the wood substance is composed of materials of high molecular weight, and wood has been aptly described as an interpenetrating system of high molecular weight polymers. Although the separation and isolation of these polymers without significant modification is a difficult task, the components that are generally present in wood can be classified chemically in the following way.

1.2.1. Extractives

All wood species and other plant tissue contain small amounts, and in some cases quite appreciable quantities, of substances in addition to cellulose, hemicelluloses, and lignin. To distinguish them from the major cell wall components, these constituents are known as the extraneous components. Many of these substances are extractable with neutral organic solvents, and are referred to as extractives. The extractives can be regarded as nonstructural wood components, constituting 4-10% of the dry weight of normal wood species that grow in temperate climates. They could constitute as much as 20% of the wood of tropical species. The term extraneous components embraces a wide range of chemicals and includes a very large number of individual extracellular and low-molecular-weight compounds[15]. However, no single species contains all the possible compounds or even all the different classes of compounds.

The extractives occupy certain morphological sites in the wood structure. For example, the resin acids are located in the resin canals, whereas the fats and waxes are present in the ray parenchyma cells. Phenolic extractives are present mainly in the heartwood and in bark. The extractives often play an important role in the utilization of wood, and influence the physical properties of wood[16]. Different types of extractives are necessary to maintain the diversified biological functions of the tree. For example, fats constitute the energy source of the wood cells, whereas lower terpenoids, resin acids, and phenolic substances protect the wood against microbiological damage or insect attack. Traces of certain metal ions are present usually as functional parts of the enzymes which are needed as catalysts for biosynthesis.

1.2.2. Hemicelluloses

The cellulose and lignin of plant cell walls are closely interpenetrated by a mixture of polysaccharides called hemicelluloses. Hemicelluloses belong to a group of heterogeneous polysacchrides which are formed through biosynthetic routes different from that of cellulose. In contrast to cellulose which is a homopolysaccharide, hemicelluloses are heteropolysaccharides. The hemicelluloses are water-insoluble, alkali-

soluble substances which are more readily hydrolysed by acids to their monomeric components consisting of D-glucose, D-mannose, D-galactose, D-xylose, L-arabinose, and small amounts of L-rhamnose in addition to D-glucuronic acid, 4-O-methyl-D-glucuronic acid, and D-galacturonic acid[17].

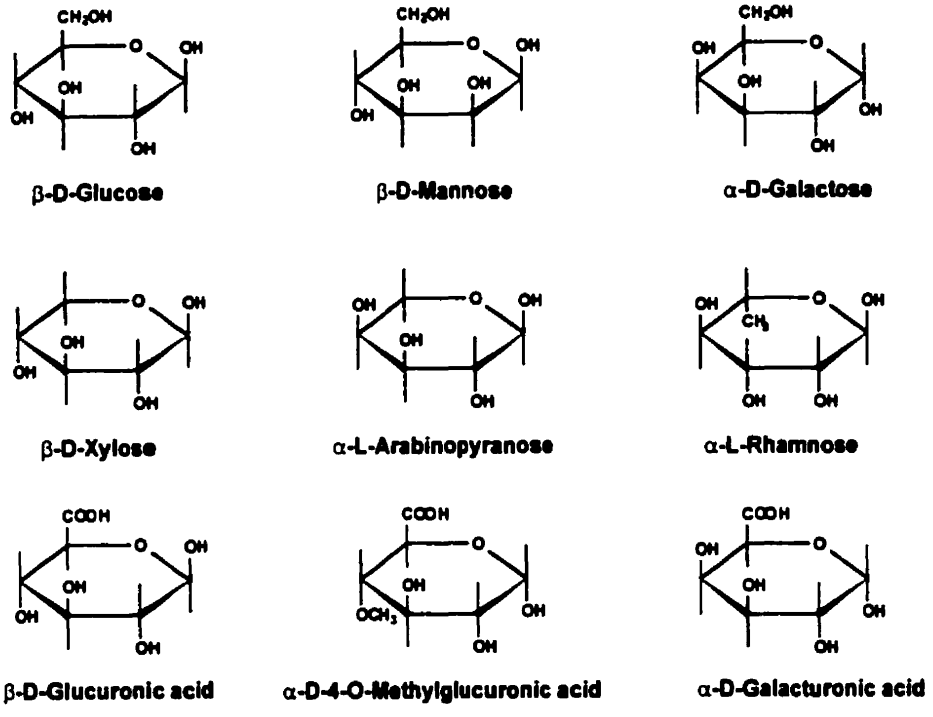

Figure 1.3. Monomeric components of hemicelluloses[17].

Generally, hemicelluloses are of much lower molecular weight than cellulose. Some wood polysaccharides are extensively branched (Figure 1.4) and are readily soluble in water. Most hemicelluloses have a degree of polymerization of only 200. Like cellulose most hemicelluloses function as supporting material for the cell wall. They are intimately associated with cellulose and appear to be a structural component of the plant. Some hemicelluloses are present in abnormally large amounts when the plant is under stress. For example, compression wood has a higher than normal galactose content and a higher lignin content[18].

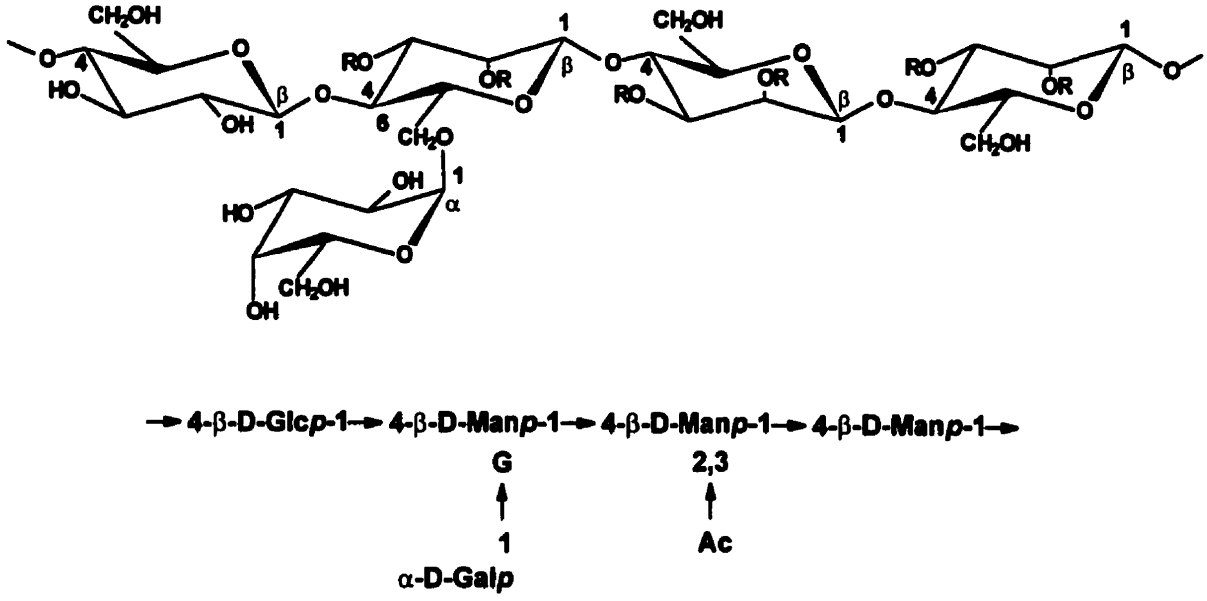

Figure 1.4. Principal structure of galactoglucomannans. Sugar units: β-D-glucopyranose (Glc*p*); β-D-mannopyranose (Man*p*); β-D-galactopyranose (Gla*p*). R=CH_3CO or H. Below is the abbreviated formula showing the proportions of the units (galactose-rich fraction)[19].

1.2.3. Cellulose

Cellulose is the structural basis of the plant cells and hence it follows that it is the most important natural substance produced by living organisms. It is distributed in all plants from highly developed trees to primitive organisms such as sea-weeds, flagellates and bacteria.

Cellulose is the main constituent of wood. Approximately 40-45% of the dry substance in most wood species is cellulose, located predominantly in the secondary cell wall. Cellulose is a homopolysaccharide composed of β-D-glucopyranose units which are linked together by (1→4)-glycosidic linkages (Figure 1.5)[20]. Two adjacent glucose units are linked by elimination of one molecule of water between their hydroxyl groups at C1 and 4. The repeating unit of the cellulose chain is the cellobiose unit (Figure 1.5). Though there are OH-groups at both ends of the cellulose chain, these OH-groups show

different behaviour. The C1-OH is an aldehyde group resulting from the ring formation by an intramolecular hemiacetal linkage. That is why the OH-group at the C1-end has reducing properties, while the OH-group at the C4-end of the cellulose chain is an alcoholic hydroxyl with no-reducing properties (Figure 1.5).

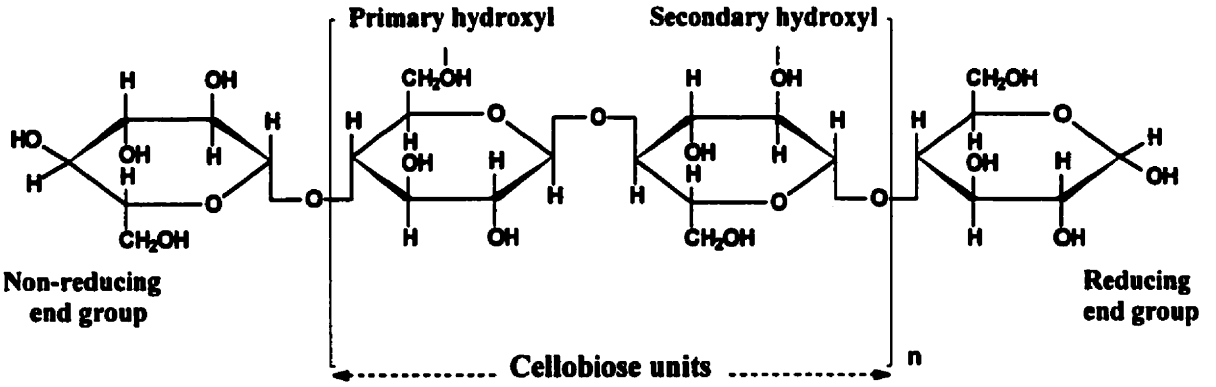

Figure 1.5. Partial molecular structure of cellulose in the 1,4-β-D-glucopyranose form[20].

The number of glucose units in cellulose varies from 7,000 to 10,000. The cellulose molecules are linked laterally by hydrogen bonds into linear bundles. The extremely large number of hydrogen bonds results in a strong lateral association of the linear cellulose molecules. This strong association and almost perfect alignment of the cellulose molecules gives rise to crystallinity. X-ray measurements show that the crystalline regions are interrupted every 600 Å with non-crystalline (amorphous) regions. Whether this is due to minor imperfections in the crystalline lattice or a real structural entity is not completely clear. The most widely held concepts is the latter in which the cellulose molecules are highly oriented (crystalline) for a distance of about 600 Å, then pass through an area of poor orientation (amorphous) and re-enter a crystalline region. The pattern repeats throughout the length of the cellulose molecule.

The chemical formula for cellulose is $(C_6H_{10}O_5)_n$, where n is the number of repeating sugar units or the degree of polymerization. The value of n varies with the different sources of cellulose and the treatment received. Most papermaking fibers have a weight-averaged DP in the 600-1500 range.

Cellulose is insoluble in most solvents including strong alkali. It is difficult to isolate it from wood in pure form because it is intimately associated with the lignin and hemicelluloses.

1.2.4. Lignin

Next to cellulose lignin is the most abundant and important polymeric organic substance in the plant kingdom. Lignin is a three-dimensional, highly branched, and polyphenolic molecule of complex structure and of high molecular weight. Lignin is frequently compared to an incrustant substance because it enjoys an essentially ubiquitous distribution in fully mature wood tissue. It permeates both cell walls and intercellular regions, or middle lamella, and renders wood a hard, rigid material able to withstand considerable mechanical stress. The middle lamella region (Figure 1.2) is composed of 70-80% lignin by weight and is the cementing material that binds all wood cells together. Although the middle lamella region has a very high lignin content, about 70% or more of the total wood lignin is located in the cell walls themselves. The amount of lignin present in different plants is quite variable[21-27].

Lignin is a mixture of macromolecules formed by an essentially random free-radical polymerization of idealized phenylpropane monomer units and its average structure is usually discussed in terms of its most pronounced repeat unit although its structure in totality is of course extremely heterogeneous in nature[28].

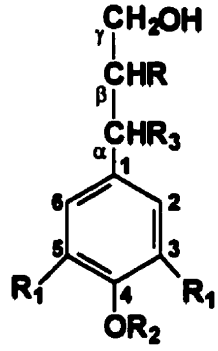

Where:

R = Another phenylpropane unit
R_1 = H, or OCH_3, or OR
R_2 = H, or R
R_3 = OH, or R

Generally, there are three types of lignins. These are the *Guaiacyl* or (G) lignins, the *Syringyl* or (S) lignins and the *para*-hydroxyphenyl or (H) lignins depending on the substitution patterns on the phenylpropanoids.

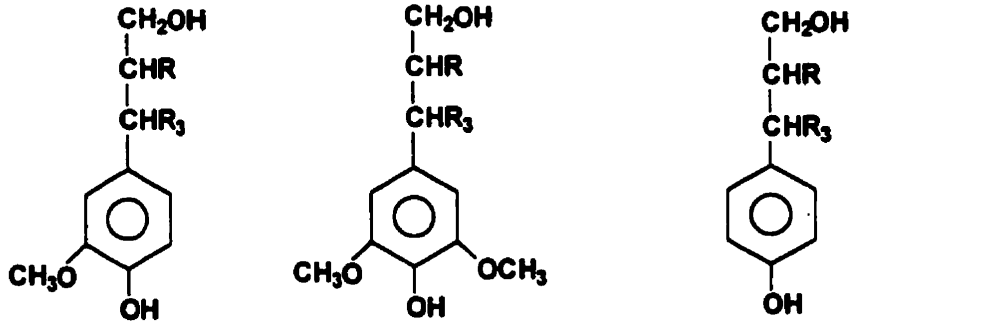

Guaiacyl(G) Syringyl(S) *Para*-Hydroxyphenyl (H)

Figure 1.6. The elementary phenylpropane building blocks of various lignins.

Softwoods contain almost exclusively (G) whereas hardwoods contain both (S) and (G). *Para*-hydroxyphenyl or (H) are present in hardwoods and in vascular plants. For the more complex hardwood lignins there are variations in the proportion of (S) to (G) to (H) lignins even amongst the different cell wall layers. Because the guaiacyl unit has a greater number of potential reactive sites, a higher degree of crosslinking exists. Furthermore lignin formed primarily from guaiacyl has, on the average, a higher molecular weight. A typical hardwood lignin is made up of an equal number of guaiacyl and syringyl units, whereas in softwoods only guaiacyl units exist. Therefore, hardwood lignins are more easily degraded than softwood lignins.

The building-up of the lignin macromolecules by the plant comprises complicated biological, biochemical and chemical systems which have been extensively studied and repeatedly reviewed[29-34]. Methods based on classical organic chemistry led to the conclusion that lignin is built up of phenylpropane units. These units are joined together with a variety of both C-O-C (ether) and C-C linkages. The ether linkages dominate; approximately two thirds or more are of this type, and the rest are of the carbon-carbon type. Detailed knowledge about the characteristics of these linkages is of great theoretical

and practical interest and necessary for a thorough insight into the degradation reactions of lignin in technical processes, such as pulping and bleaching. The dominating bond types[35-37] and their approximate proportions in lignin are shown in Table 1.1.

Table 1.1. Types and frequencies of interunit linkages in lignin models (Number of linkages per 100 C9-units)[17].

Linkages	Glasser, Glasser[35]	Erickson et al.[36]	Nimz[37]
β-O-4	} 55	49-51	} 65
α-O-4		6-8	
β-5	16	9-15	6
β-1	9	2	15
5-5	9	9.5	2.3
4-O-5	3	3.5	1.5
β-β	2	2	5.5
β-β*	-	-	2
α/γ-O-γ	10	-	-
α-β	11	-	2.5
β-6, ó-5	2	} 4.5-5	-
1-O-4, 1-5	(only 1-5)		
Total	117	85.5-96	99.8

* THF: Tetrahydrofuran structure

Based on the information obtained from studies of biosynthesis as well as analysis of the various linkages and functional groups, structural formulas for lignin have been constructed. The first lignin model was constructed by Freudenberg[38,39] for spruce lignin represented 18 phenylpropane (C_9) units. The formula has attained general acceptance with an empirical formula of $C_9H_{7.95}O_{2.40}(OMe)_{0.92}$ as a section of the total molecule which was assumed to be of more than 100 units in its native state. Adler's formula[40] for spruce lignin consisted of 16 prominent phenylpropane (C_9) units and it represents only a segment of the lignin macromolecule. The empirical formula of softwood lignin was proposed as $C_9H_{7.95}O_{2.41}(OMe)_{0.93}$ by Sakakibara[41] in 1980. The description of softwood lignin was demonstrated as a section of 28 C_9-units with several alternative structural elements. The most recent concept[35] comprises 94 units, corresponding to a total molecular weight of more than 17000 in milled wood lignin from loblolly pine (*Pinus*

taeda) as shown in Figure 1.7.

Depite intensive studies and a large number of analytical data available today on the composition of functional groups, this information can not be summarized in a simple way because of large individual variations among the wood species.

The intriguing macromolecular behaviour of lignin and its derivatives has yielded to ever greater measures of explicability; the properties of lignin-based polymeric materials have become amenable to modification over a considerable range, even in a predictable fashion. Significant developments in both macromolecular behaviour and property modification owe a great deal to the application of physico-chemical techniques that have been made accessible through profound improvements in commercially available instrumentation and related supplies. However, no method of isolating lignin is known which does not, in some way, alter its chemical and physical structure, for lignin in its natural state is believed to be a high polymer or even an infinitly cross-linked gel[42]. In connection with pulping and bleaching and new technologies of lignin utilization the analytical characterization of lignins has become increasingly important. Sophisticated analytical techniques have been developed for the determination of functional groups in lignin. Although the chemical methods are still important, much new information has emerged from the application of physical spectroscopic methods, especially NMR spectroscopy.

Advancement depends in part on understanding the molecular origin of macroscopic behaviour; it is here that numerous nuclear magnetic resonance (NMR) techniques make notable contributions toward comprehending the various morphological domains and the way in which it influences the overall macroscopic properties of the polymer. Indeed, recently developed techniques give promise of an increasing role for NMR. Since the various functional groups present in lignin greatly affect its reactivity, reliable and quantitative functional group information is important.

The flexibility achieved in both solution and solid state nuclear magnetic resonance spectroscopy by various spectroscopic techniques during the last 20 years has been invaluable in documenting the macromolecular properties of lignin.

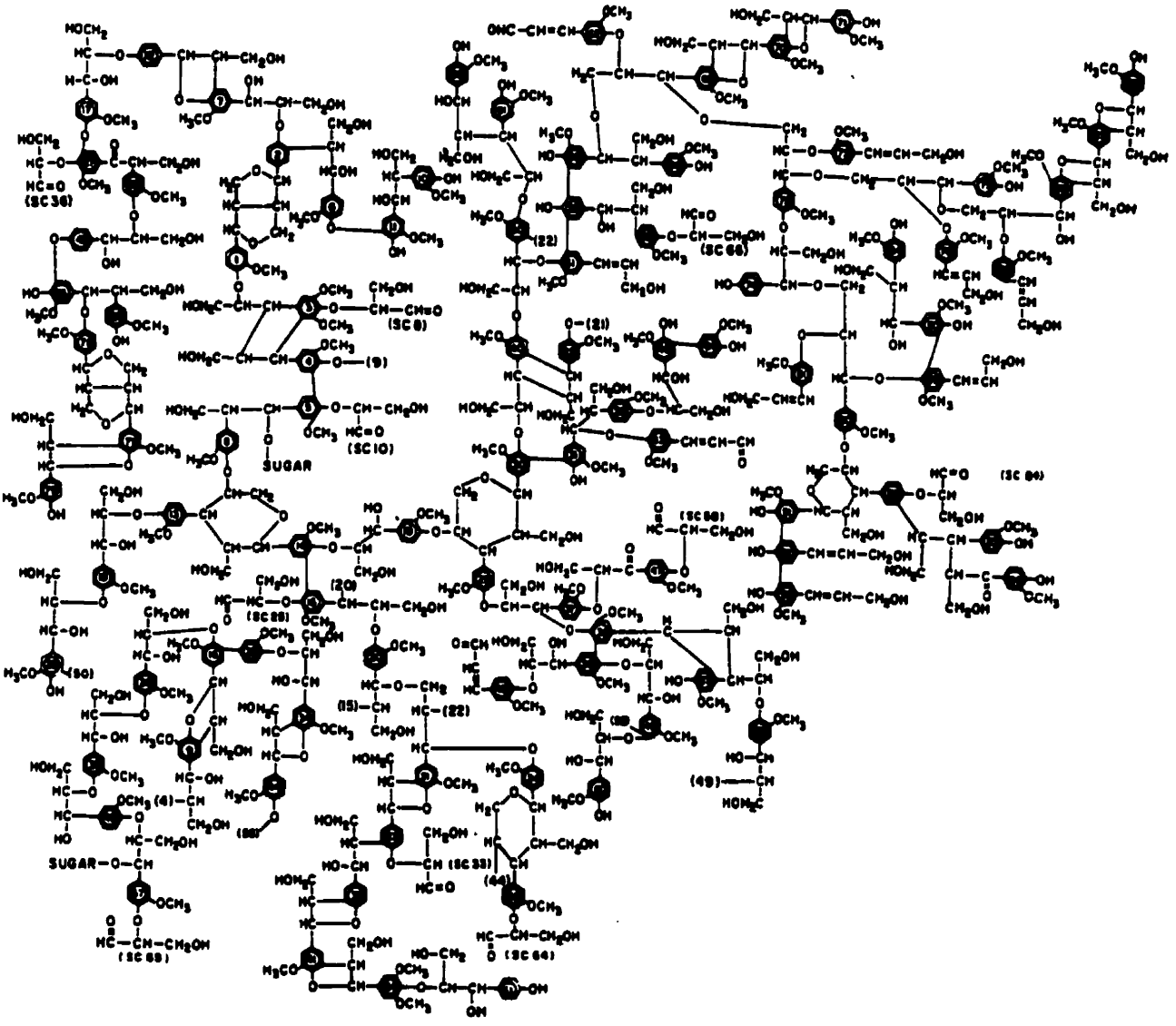

Figure 1.7. Softwood lignin model designed by computerized evaluation according to Glasser and Glasser[35].

1.3. NUCLEAR MAGNETIC RESONANCE SPECTROSCOPY

Nuclear magnetic resonance spectroscopy (NMR) has progressed at a vigorous pace since the introduction of the first commercial spectrometers in the early 1960s, in part due to the introduction of superconducting magnets which can maintain stable fields higher than electromagnets. In parallel, microprocessor development for signal acquisition and data manipulation, coupled with a deeper and evolving understanding of magnetic resonance phenomena, have led to invaluable methods which spurred structural determinations on numerous natural products and polymers[43]. The Fourier transform method applied to ^{13}C NMR, in combination with other spectrometric measurements, has increased our knowledge of the structure of organic molecules in general, and lignins in particular.

NMR parameters such as chemical shifts (δ), coupling constants (J), relaxation times, and signal intensities are closely related to electronic structure and chemical environments of nuclei involved in the resonance phenomenon. NMR is an appropriate tool for structural investigation: it reflects with precision chemical structures, functionalities, and the nature of chemical bonding within the lignin macromolecule. Lignin analyses using chemical methods often involve degradation of the polymer. These methods suffer from the drawback that both the lignin and resulting degradation products may undergo structural changes other than those generally associated with the procedure. Furthermore, the isolation of degradation products is time-consuming and product yield may be low. Thus, physical methods having as high a sensitivity as possible are preferred.

1.3.1. Solid State NMR Spectroscopy

One of the most important chemical aspects of a solid is the structural determination of its molecules. There are dynamic as well as static aspects of solid-state structures and NMR may be used to study the motions of molecules in solids which may be related to their mechanical and other physical properties. Solid state NMR can provide chemical information on species which impossible to examine in solution. In addition,

the compounds may dissociate in solution in a low energy process, yielding only exchange average solution NMR spectra but their structure may be well defined in the solid state. The development of methodology to obtain high resolution spectra of solids has greatly enhanced the range of potential NMR applications. Recently, techniques have been developed which enable NMR spectra of moderate resolution to be obtained from completely solid systems and these will undoubtedly prompt a resurgence of chemical interest in the solid state, particularly, for studies of low natural abundance nuclei such as ^{13}C.

Under normal conditions used to obtain ^{13}C NMR spectra of liquids, a solid sample would yield only an extremely broad featureless spectrum. A large contribution to the broadening arises from static dipolar interactions. ^{13}C spectra of solids obtained using high power proton irradiation (Dipolar Decoupling, DD) can have much of the initial broadening removed, but still may have linewidths of 5-10 kHz or more. This broadening is due to chemical shift anisotropy. The observed broad envelope is a result of contributions from the many individual chemical shifts of nuclei in molecules oriented differently within the sample. The anisotropy can be effectively removed if the sample is spun rapidly at an angle of 54.7° (Magic Angle Spinning, MAS) with respect to the external magnetic field.

Using the techniques of dipolar decoupling and magic angle spinning, it is possible to produce spectra in solids having nearly the same resolution as in liquids. However, the low natural abundance of ^{13}C nuclei, and their longer spin-lattice relaxation times (T_1) in solids compared with liquids severely limits the signal-to-noise ratio that can be obtained in a given time for a solid sample. This sensitivity problem can be overcome using the technique of cross polarization (CP), which not only brings about an increase in sensitivity, by allowing the magnetization from the abundant ^{1}H nuclear spins to be transferred to the dilute ^{13}C nuclei, but also allows signal accumulation to be repeated at intervals related to the shorter ^{1}H relaxation times rather than the longer ^{13}C relaxation times. It is also usual to perform the unrelated MAS experiment in conjunction with cross polarization[44]. In fact, the first CP/MAS spectra published[45] included a spectrum of wood in which both the cellulose and the lignin components could be clearly identified. Solid-

state ^{13}C CP/MAS NMR has the potential advantage of detecting all of the components in a system in a non-invasive and completely non-destructive manner.

^{13}C CP/MAS has been used to elucidate the chemical[46], conformational[47], and even the effect of moisture content[48] of some insoluble polysaccharides and Chitins[49, 50]. Similar techniques have been also implemented toward the study of lignins.

Maciel and coworkers[51] have used solid-state ^{13}C CP/MAS NMR to characterize lignins extracted by various procedures while Schaefer, Stejskal and co-workers[52] monitored the chemical transformation of lignin by fungal catabolism (degradation). However, these measurements are made on only one part of the total lignin and they are subject to the additional complications of material loss and possible structural alterations caused during the extraction process. The potential of the technique for the characterization of intact lignins has not been fully exploited to date.

1.3.2. Solution NMR Spectroscopy

1.3.2.1. ^{1}H NMR Spectroscopy

^{1}H NMR spectroscopy has been used for the characterization and classification of lignins and its structural determination. Most of the early work in this field was focused on proton NMR spectroscopy[53, 54]. The 100% natural abundance of the ^{1}H nucleus, resulting in high sensitivity during an NMR experiment, is among the advantages of proton NMR spectroscopy. Ludwig[55] reviewed the literature dealing with the ^{1}H NMR spectroscopy of lignins and a comprehensive ^{1}H NMR study of lignins and lignin model compounds. In this study, the lignins were analyzed as acetate derivatives using deuteriochloroform as the solvent. The methodology developed by Ludwig et al.[53, 54] has been applied to numerous studies[56-59]. Several ^{1}H NMR studies of lignins have been published in which conditions other than those used by Ludwig et al.[54] (acetate derivatives, chloroform solutions) have been employed. Acetylation or other derivatization procedures may cause unwanted chemical modification of the lignin samples. This complication is avoided when underivatized lignins are examined[60-67].

During the preferred method for ^1H NMR analysis of lignins, the samples are examined as acetate derivatives using chloroform as the solvent. In these respect, the conditions used by Ludwig et al.[53, 54] have thus been retained. One advantage in doing this is that a vast amount of the reported ^1H NMR spectral data for lignins and lignin model compounds remains relevant for reference purposes[68-78]. Nevertheless, there are some essential limitations to ^1H NMR spectroscopy of lignins. These include the rather limited range of chemical shifts (12 ppm), extensive signal overlapping and proton coupling effects. The technique is only suitable for the qualitative study of the proton distribution on lignins, while carbon containing groups and labile proton functionalities (OH< COOH< SH) remain beyond the capabilities of the technique.

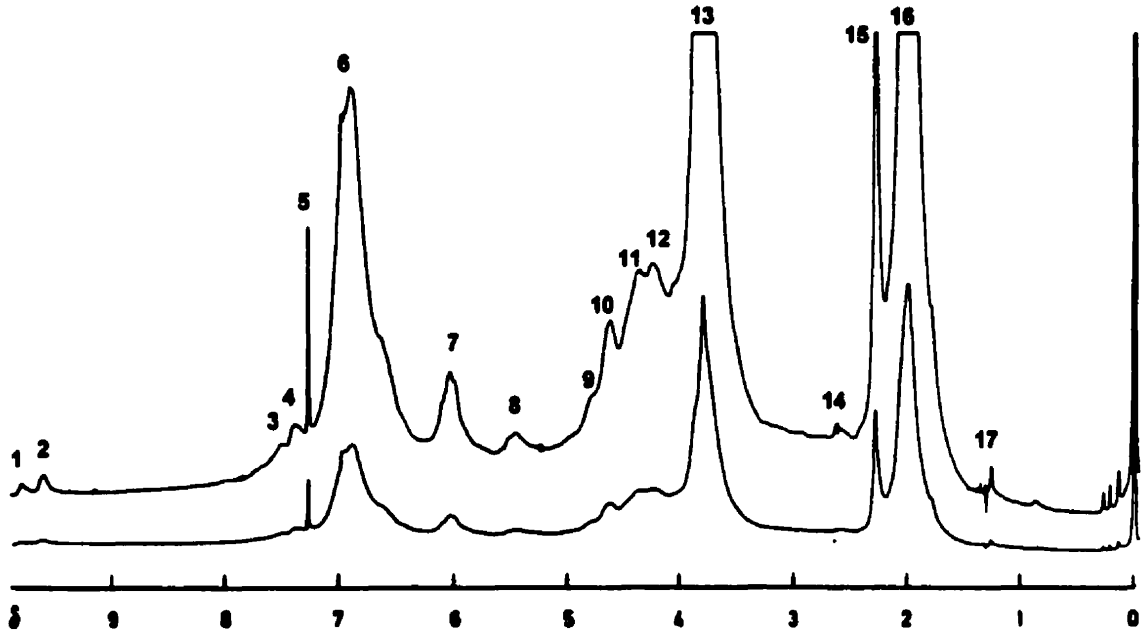

Figure 1.8. ^1H NMR (270 MHz) spectrum of acetylated milled wood lignin from black spruce[64].

Table 1.2. ^1H Chemical shifts and signal assignments for acetylated spruce lignins[64].

Signal No.	δ[a] in ppm	Assignments
1	9.84	Formyl protons in benzaldehyde units
2	9.64	Formyl protons in cinnamaldehyde units
3	7.53	Aromatic protons in benzaldehyde units
4	7.41	Aromatic protons in benzaldehyde units and vinyl protons on the carbon atoms adjacent to aromatic rings in cinnamaldehyde units
5	7.29	Chloroform ($CDCl_3$)
6	6.93	Aromatic protons (certain vinyl protons)
7	6.06	H_α in β-O-4 structures (H_α in β-1 structures, H_β in cinnamyl alcohol units)
8	5.49	H_α in β-5 structures (H_α in non-cyclic benzyl aryl ether, H_β in 2-aryloxypropiophenones)
9	4.80[b]	Inflection possibly due to H_α in pinoresinol units and H_β in non-cyclic benzyl aryl ethers (*threo* forms).
10	4.65	H_β in β-O-4 structures (methylene protons in cinnamyl alcohol units).
11	4.39	Hγ in, primary β-O-4 structures (erythro forms) and β-5 structures.
12	4.27	Hγ in several structures
13	3.81	Protons in methoxyl groups
14	2.62	Benzylic protons in β-β structures of secoisolariciresinol type, benzylic protons in 3-aryl-1-propanol units.
15	2.28	Aromatic acetate
16	2.01	Aliphatic acetate
17	1.26	Hydrocarbon contaminant

[a] Values refer to the highest point of the peak.
[b] Inflection includes contributions from unidentified signals[79].

1.3.2.2. ^{13}C NMR Spectroscopy

Carbon-13 NMR spectrometry is one of the most powerful techniques available for lignin analysis, in particular for determining minor structures not available by other techniques. ^{13}C NMR is a sensitive method for the qualitative structural analysis of lignin[80-84]. It provides detailed structural information on nearly all types of carbons including those present even in minor structures[85-89]. This is an important advantage compared to most other methods, which provide information only on specific groups.

The capacity for producing reliable quantitative analyses of functional groups in lignin is another significant feature of ^{13}C NMR[90-92] spectrometry. Methods using new pulse strategies in NMR spectrometry have opened new frontiers in the understanding of lignin structure. In the late 1970s, when ^{13}C NMR became available, about 40 signals could be distinguished in ^{13}C NMR lignin spectra using broad band proton decoupling which collapses ^{13}C multiplets and produces one sharp signal for every chemically unique carbon atom. Since carbon atoms from the backbone of organic molecules, ^{13}C NMR signal locations depend much more on the structural environment and substitution patterns than those in ^{1}H NMR; the ^{13}C spectrum contains more structural information over a much wider chemical shift range. The ^{13}C NMR spectrum of lignin can be divided into three main segments: the first (200 to 165 ppm) contains signals assigned to carbonyl carbons; the second (165 to 100 ppm) is assigned to aromatic and olefinic carbons; and the third (100 to 10 ppm) is assigned to aliphatic carbon atoms[93].

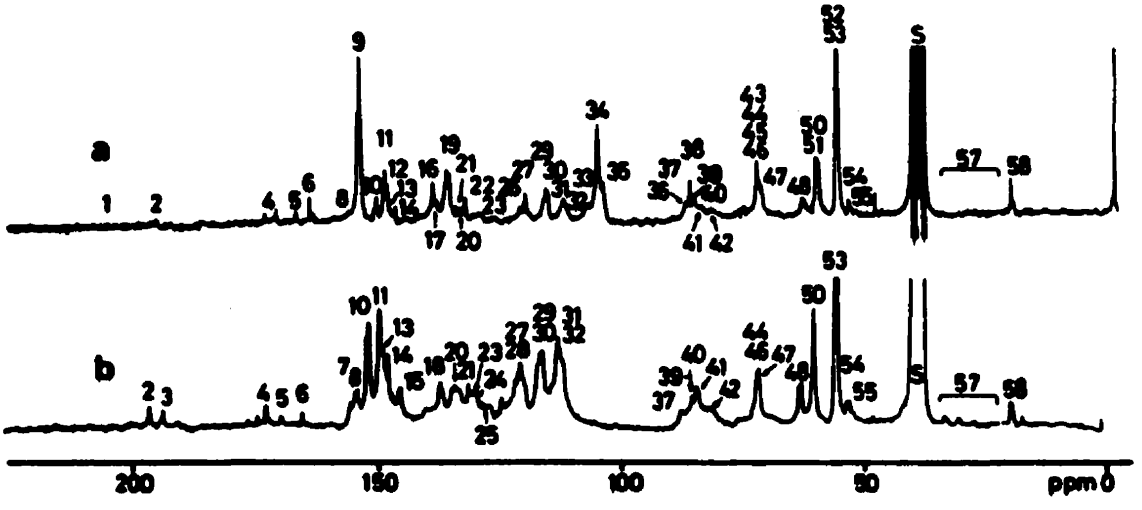

Figure 1.9. ^{13}C NMR (50.13 MHz) spectra of a: Aspen and b: Spruce milled wood lignin[93].

Table 1.3. ^{13}C Chemical shifts and signal assignments for spruce and aspen milled wood lignins[93].

Signal No.	δ in ppm/TMS	Assignments[a]
1	210-200	non-conjugated C=O in ketones
2	194	γ-CHO in cinnamaldehyde[b]
3	191.6	α-CHO in benzaldehyde
4	171-173	C=O in aliphatic R-COOR
5	165-167	αC=O in Ar-COOH
6	162	C-4 in Ar-COOH
7	152.9	C-3/C-3' in etherified 5-5 units
8	152.6	C-α in cinnamaldehyde
9	152.1	C-3/C-5 in etherified syringyl β-O-4
10	149.1	C-3 in etherified guaiacyl units
11	147.4	C-4 in etherified guaiacyl units
12	147.1	C-3/C-5 in non-etherified syringyl β-O-4
13	146.9	C-3 in non-etherified guaiacyl
14	145.3	C-4 in non-etherified guaiacyl β-O-4
15	143.4	C-4/C-4' in etherified 5-5 units
16	138	C-1 in etherified syringyl β-O-4
17	137.7	C-1 in syringyl β-β
18	135.3	C-1 in etherified guaiacyl β-O-4
19	id	C-4 in etherified and non-etherified syringyl β-O-4
20	133	C-1 in non-etherified guaiacyl β-O-4
21	132.4	C-5/C-5' in 5-5 units,C-1 non-etherified syringyl β-O-4
22	131	C-2/C-6 in p-hyrdoxyphenyl benzoate units
23	128-130	-
24	128.3-129.3	C-α and C-β in AR-CH=CH-CH_2OH
25	126.3	C-β in cinnamaldehyde
26	121.5	C-1 in p-hyrdoxyphenyl benzoate units
27	120.3	C-6 in etherified and non-etherified guaiacyl units
28	119.5	C-6 in etherified and non-etherified guaiacyl units
29	115.2	C-5 in etherified and non-etherified guaiacyl units
30	114.6	C-3/C-5 in p-hyrdoxyphenyl benzoate units
31	111.4	C-2 in guaiacyl units
32	110.9	C-2 in guaiacyl-guaiacyl stilbene units[c]
33	106.8-107	C-2/C-6 in syringyl with αC=O or αC=C
34	104.5-106.8	C-2/C-6 in syringyl in general
35	103.6	C-2/C in β-β
36	87.2	C-β in syringyl β-O-4 *threo*
37	87.2	C-α in β-5
38	86	C-β in syringyl β-O-4 *erythro*
39	85.3	C-α in β-β
40	84.5	C-β in guaiacyl β-O-4 *threo*
41	83.5	C-β in guaiacyl β-O-4 *erythro*
42	80-82	C-β and C-α in β-O-4/α-O-4 units
43	72.5	C-α in syringyl and guaiacyl β-O-4 *erythro*
44	71.8	C-α in syringyl and guaiacyl β-O-4 *erythro*
45	71.8	C-α in syringyl and guaiacyl β-O-4 *threo*

Table 1.1. Continued

Signal No.	δ in ppm/TMS	Assignments[a]
46	71.4	C-α in syringyl and guaiacyl β-O-4 *threo*
47	71.2	C-γ in β-β units
48	63	C-γ in β-5 and β-O-4 with αC=O
49	61.7	C-γ in cinnamyl alcohol units
50	60.2	C-γ in syringyl and guaiacyl β-O-4 *erythro* and *threo*
51	59.8	C-γ in syringyl and guaiacyl β-O-4 *erythro* and *threo*
52	55.7-55.9	Aromatic OCH_3 in syringyl and guaiacyl units
53	55.7-55.9	Aromatic OCH_3 in syringyl and guaiacyl units
54	53.7	C-β in β-β
55	53.1	C-β in β-5
56	-	-
57	20-40	-CH_3 and CH_2 in saturated aliphatic chain
58	20	-CH_3 in acetyl groups

[a] Solvent: DMSO-d_6
[b] Ar-CH=CH-COH
[c] Guaiacyl-CH=CH-Guaiacyl

In ^{13}C NMR studies, matching the chemical shift values of lignin and model compounds is done with spectra recorded under exactly the same conditions (solvent, temperature, and setting of the TMS δ value) to ensure valid assignments. Nevertheless, the matching technique is not completely satisfactory because the chemical shift for a specific carbon atom in a dimeric model compound is not exactly identical to those when present in a polymer[83].

The accuracy of assignments is also limited by availability of relevant model compounds for spectral measurements and by spectrometer resolution. Because of the structural heterogeneity and complexity of lignin, numerous signals are hidden in shoulders and often overlooked. In time, this difficulty can be minimized through an expanding data bank as more oligomeric lignin model compounds become available, by applying labelling techniques to lignin synthesized in vitro, and by polymerization of selectively ^{13}C-enriched coniferyl alcohol and lignin polymer (DHP) models[94, 95].

1.3.2.3. ^{31}P NMR Spectroscopy

The development of a novel NMR technique capable of determining and classifying various functional groups for both soluble[96-101] and solid lignocellulosic materials[102, 103] has been made possible by Argyropoulos et al.[96-103]. The methodology involves the selective phosphorous-tagging of a variety of functional groups present in lignin and carbohydrates, followed by solution and solid state ^{31}P NMR spectroscopies. Solution ^{31}P NMR have been used to examine soluble lignin and carbohydrate samples after phosphitylation with 2-chloro-1,3,2-dioxaphospholane. This is a novel and powerful means to determine the three principal forms of phenolic hydroxyls present in lignins i.e. *p*-hydroxyphenyl, guaiacyl, and syringyl structures. In addition, primary hydroxyls, carboxylic acids, and the two diastereomeric forms of arylglycerol-β-aryl ether units (β-O-4 structures) present in lignins can also be determined from a single ^{31}P NMR experiment. When applied to carbohydrates, the technique gave characteristic signals for the *alpha* and *beta* anomers and the epimeric forms of monosaccharides. Completely resolved ^{31}P NMR spectra were also obtained when lignin-carbohydrate model compounds were examined.

Another phosphitylation reagent namely, 2-chloro-4,4,5,5-tetramethyl-1,3,2-dioxaphospholane, have been found particularly good at resolving this region at the expense of fine resolution between the primary and secondary hydroxyls[104-106]. The ^{31}P NMR signals received due to free phenolic hydroxyls belonging to guaiacyl, syringyl, *p*-hydroxyphenyl units and most C-5 and C-6 related condensed phenolic forms are very well resolved[107]. In addition signals due to carboxylic acids are well separated from all other signals, allowing direct access to this important information related to the fundamental changes occurring within lignins during oxidative conditions[108].

1.3.2.4. Other NMR Methods

Other NMR techniques that have been used for the structural elucidation of lignins, are acetylation, silylation, and fluorination aimed at derivatizing the labile protons in lignins, followed by ^{13}C, ^{29}Si, and ^{19}F NMR spectroscopies, respectively. Acetylation of lignins is relatively simple to achieve under well established and mild

conditions. It have been used to estimate the total hydroxyl content in various lignin preparations from proton and ^{13}C NMR spectra. The ^{13}C NMR spectra may also reveal other structural features of lignins. These spectra permit the distinction to be made between aromatic and aliphatic hydroxyls, and may reveal the primary and secondary character of aliphatic hydroxyls.

Efforts to overcome some of the limitations imposed by proton and ^{13}C NMR spectroscopies have prompted the examination of other NMR-active nuclei which when covalently linked to lignin by appropriate derivatization procedures may provide additional structural information for these heterogeneous biopolymers. Early attempts examined the potential of silylation followed by silicon NMR for the determination of hydroxyl groups in kraft lignin and related model compounds[109, 110]. The ^{29}Si NMR spectra of silicon derivatives of lignins contain features that may distinguish between aromatic and aliphatic hydroxyls and carboxylic protons. The method, however, requires large sample concentrations and long instrument times. This is due to the relatively low natural abundance of the silicon-29 nuclei (4.7%), their low magnetic moment, and their high relaxation time. In order to increase the sensitivity of the experiment, the INEPT (Insensitive Nuclei Enhanced by Polarization Transfer)[111-113] pulse sequence is used, and introduces a variety of uncertainties in quantitatively interpretating the spectra.

^{19}F NMR have also been proposed as a mean of detecting different functional groups in lignins[114, 115]. The 100% natural abundance of the ^{19}F nucleus, resulting in high sensitivity during an NMR experiment, is among the advantages of fluorine NMR spectroscopy. Although the potential of this technique has been applied for detection of hydroxyl[114] and carbonyl groups[115], the major limitation of this technique is incomplete fluorine-derivatization of these functional groups in lignins.

1.4. SCOPE and AIM of this THESIS

Although the structure of lignin is considered to be adequately defined, it is certainly not perfectly refined. For this reason, it is imperative that analytical methods suitable for the fine structural characterization of solid wood and soluble lignins be developed.

The primary objective of the research presented in this thesis is focused on developing and investigating the application of novel NMR spectroscopic techniques toward studying and elucidating the role of different structural units in lignin.

Solid state ^{13}C CP/MAS was employed to measure proton spin-lattice relaxation times (T_{1H}) for several samples of softwood, lignin, and cellulosic materials as a function of pH (Chapter 2). This was done to investigate the ionization of various functional groups on the molecular mobilities of carbohydrates and lignin in order to arrive at a better understanding of their molecular connectivities and their physico-chemical properties in wood during various stages of pulping and bleaching processes.

During chemical pulping lignin in wood undergoes degradation reactions. It is clear that in most cases lignin also undergoes condensation reactions, which work against the degradation. In chapters 3 and 4 the application of quantitative ^{31}P NMR spectroscopy is implemented for determining the thermodynamic parameters governing the cleavage of arylglycerol-β-aryl ether linkages of lignins and the formation of condensed structures under kraft pulping conditions.

The carbonyl groups present in wood and pulps play an important role in determining the reactivity of lignin structures toward the yellowing of paper and the bleaching of pulp. The low contents of these groups in wood, in pulp and in paper have made the elucidation of their role rather elusive. Therefore, the necessity to obtain essential information toward understanding the reactivity of lignin structures during yellowing and pulp bleaching, initiated efforts at developing a novel method for the fine structural elucidation and quantification of the various carbonyl groups present in lignin. The development of this technique is described in chapters 5 and 6.

Despite significant recent advancements in technical and instrumental fronts,

lignin chemists are still challenged with the need to develop and apply improved methodologies in search for solutions to both fundamental and applied lignin-related problems.

1.5. REFERENCES

1. Browning, B. L., The chemistry of wood., Interscience publisher, John Wiley & Sons, New York, Chapter 1, pp. 1-6, 1963.

2. Rowell, R., The chemistry of solid wood., American chemical society, ACS., Washington, D. C. , Chapter 1, pp. 3-56, 1984.

3. Fengel, D., and Wegener, G., Wood; chemistry, ultrastructire, reactions., Walter de Gruyter, Berlin, New York, pp. 6-7, 1983.

4. Preston, R. D., The molecular architecture of plant cell walls., Chapman and Hall, Londond, 1952.

5. Wardrop, A. B., The structure and formation of the cell wall in xylem., In the formation of wood in forest trees, Ed. M. H. Zimmerman, Academic Press, New York, pp. 87-134, 1964.

6. Liese, W., The warty layer., In cellular ultrastructure of woody plants, Ed. W. A. Côté, Syracuse University Press, New York, pp. 251-269, 1965.

7. Côté, W. A., Wood ultrastructure., University of Washington Press, Syracuse, New York, 1967.

8. Bolker, H. I., Encyclopedia of chemical technology., Interscience publisher, John Wiley & Sons, New York, Vol. 5, p. 75, 1979.

9. Esau, K., Plant Anatomy., Interscience publisher, John Wiley & Sons, New York, 1965.

10. Jane, F. W., The Structure of Wood., Black, London, 1970.

11. Panshin, A. J., and de Zeeuw, C., Textbook of Wood Technology., McGraw Hill, New York, 1970.

12. Carlquist, S., Comparative Plant Anatomy., Holt, Rinehart and Winston, New York, 1961.

13. Esau, K., The Anatomy of Seed Plants., Interscience publisher, John Wiley & Sons, New York, 1960.

14. Ilvessalo, P., Wood Chemistry; The Structure of Wood., Jensen, W., Ed., Vol. 1(B1), pp. 1-50, 1967.

15. Fengel, D., and Wegener, G., Wood; Chemistry, Ultrastructure, Reactions., Walter de Gruyter, Berlin, New York, p. 33, 1983.

16. Narayanamurti, D., Die Bedeutung der Holzextraktstoffe., Holz Roh-u. Werkstoff, 15, 370-380, 1957.

17. Fengel, D., and Wegener, G., Wood; Chemistry, Ultrastructure, Reactions., Walter de Gruyter, Berlin, New York, p. 106, 1983.

18. Timell, T. E., Recent Progress in the Chemistry and Topochemistry of Compression Wood*., Wood Sci. Technol., 16, 83-122, 1982.

19. Sjöström, E., Wood chemistry: Fundamentals and applications., Second edition, Academic Press, Chapter 3, p. 65, 1993.

20. Smook, G. A., Handbook for Pulp and Paper Technologists., Second edition, Angus wilde publications, Vancouver, Chapter 1, p. 5, 1992.

21. Hergert, H. L., Infrared soectra. In: Lignins. Occurrence, Formation, Structure and reactions., Sarkanen, K. V. and Ludwig, C. H., Eds., Interscience publisher, John Wiley & Sons, New York, pp. 267-297, 1971.

22. Neish, A. C., Monomeric intermediates in the biosynthesis of lignin. In: Constitution and biosynthesis of lignin, Freudenberg, K., and Neish, A. C., Eds., Springer-Verlag, Berlin, pp. 5-43, 1968.

23. Wardrop, A. B., Occurrence and formation in plants. In: Lignins occurrence, formation, structure and reactions., Sarkanen, K. V. and Ludwig, C. H., Eds., Interscience publisher, John Wiley & Sons, New York, pp. 19-41, 1971.

24. Venverloo, C. J., The Lignin of *Populus nigra* L. cv. 'Italica' and Some Other *Salicaceae*., Holzforschung, 25, 18-24, 1971.

25. Howard, E. T., Physical and Chemical Properties of Slash Pine Tree Parts., Wood Sci. Technol., 5(4), 312-317, 1973.

26. Miksche, G. E., and Yasuda, S., Über die Lignine der Blätter und Nadeln einiger Angiospermen und Gymnospermen*., Holzforschung, 31, 57-59, 1977.

27. Luger, F., and Gampe, S., Potential forstlicher reststoffe (waldabfälle), Vol. 2, Bericht Forstl. Fak., Universität München, pp. 84-158, 1978.

28. Fyfe, C. A., Solid State NMR for Chemists , C.F.C. Press, Guelph, Ontario, Canada, Chapter 7, pp. 440-442, 1983.

29. Brauns, F. E., and Brauns, D. A., The chemistry of lignin., supplement volume. Academic press, New York, 1960.

30. Neish, A. C., Cinnamic acid derivatives as intermediates in the biosynthesis of lignin and related compounds. In: The formation of wood in forest trees., Zimmerman, M. H., Eds., Academic press, New York, pp. 219-239, 1964.

31. Freudenberg, K., The formation of lignin in the tissue and in vitro. In: The formation of wood in forest trees., Zimmerman, M. H., Eds., Academic press, New York, pp. 203-218, 1964.

32. Schubert, W. J., Lignin Biochemistry., Academic press, New York, 1965.

33. Pearl, I. A., The chemistry of lignin., Marcel Dekker Inc., New York, 1967.

34. Gross, G. G., Biosynthesis of lignin and related monomers. In: The structure, biosynthesis and degradation of wood. Recent Adv. in phytochem. 11., Loewus, F. A., and runeckles, V. C., Eds., Plenum press, New York, pp. 141-184, 1977.

35. Glasser, W. G., and Glasser, H. R., The evaluation of lignin's chemical structure by experimental and computer simulation techniques., Pap. Puu., 63, 71-83, 1981.

36. Erickson, M., Larsson, S., and Miksche, G. E., Gas-chromatographic analysis of lignin oxidation products. VII. An improved characterization of lignins.through methylation and oxidative decomposition., Acta Chem. Scand., 27, 127-140, 1973.

37. Nimz, H., Beech lignin- Proposal of a constitutional scheme., Angew. hem. Int. Ed. Engl., 13, 313-321, 1974.

38. Freudenberg, K., Entwurf eines Konstitutionsschemas für das Lignin der Fichte., Holzforschung, 18, 3-9, 1964.

39. Freudenberg, K., The constitution and biosynthesis of lignin. In: Constitution and biosynthesis of lignin., Freudenberg, K. and Neish, A. C., Eds., Spinger verlag Berlin, Heidelberg, New York, pp. 47-122, 1968.

40. Adler, E., Lignin chemistry- past, present and future., Wood Sci. Technol., 11, 169-218, 1977.

41. Sakakibara, A., Structural model of softwood lignin., Wood Sci. Technol., 14, 89-100, 1980.

42. Bolker, H.I. Natural and Synthetic Polymers., New York, Marcel Dekker, Chapter 12, 1974, .

43. Snyder, J., Breuning, R., Derguini, F., Nakanishi, K., Fractionation and proof of structure of natural products, In: Lowe, J. W., Eds., Natural products of woody plants I. Chemicals extraneous to the lignocellulosic cell wall. Springer Series in wood science, Springer, Berlin, Heidelberg, New York, Tokyo, 60-84, 1989.

44. Levy, G. C., Lichter, R. L., Nelson, G. L., Carbon-13 nuclear magnetic resonance spectroscopy., Second edition, Interscience publisher, John Wiley & Sons, New York, Chapter 10, 1980.

45. Schaefer, J., and Stejskal, E. O., Carbon-13 nuclear magnetic resonance of polymers spinning at the magic angle., J. Am. Chem. Soc., 98, 1031-1032, 1976.

46. Hall, L. D., and Yalpani, Determination of the primary structure of polysaccharides and their derivatives by solid-state carbon-13 n.m.r. spectroscopy., M., Carbohydr. Res., 91, C1-C4, 1981.

47. Saito, H., and Tabeta, R., ^{13}C Chemical shifts of solid (1→4)-α-D-glucans by cross polarization/magic angle spinning (CP/MAS) spectroscopy. Conformation-dependent ^{13}C chemical shifts as a reference in determining conformation in aqueous solution., Chem. Lett. Chem. Soc. Japan, 713-716, 1981.

48. Fyfe, C. A., Stephenson, P. J., Tylor, M. G., Bluhm, T. L., Deslandes, Y., and Marchersault, R. H., Macromolecules, 17, 501-502, 1984.

49. Saito, H., and Tabeta, R., and Hirano, S., Conformation of chitin and N-acyl chitosans in solid state as revealed by ^{13}C cross polarization/magic angle spinning (CP/MAS) NMR spectroscopy., Chem. Lett. Chem. Soc. Japan, 1479-1482, 1981.

50. Raymond, L., Morin, F. G., Marchersault, R. H., Degree of deacetylation of chitosan using conductometric titration and solid-state NMR., Carbohyr. Res., 246, 331-336, 1993.

51. Maciel G. E., O'Donnell, D. J., Ackerman, J. J. H., Hawkins, B. H., and Bartuska, V. J., A ^{13}C NMR study of four lignins in the solid and solution state., Makromol. Chem., 182, 2297, 1981.

52. Schaefer, J., Sefcik, M. D., Stejskal, E. O., McKay, R. A., Hall, P. L., Characterization of the catabolic transformation of lignin in culture using magic-angle carbon-13 NMR., Macromolecules, 14, 557-559, 1981.

53. Ludwig, C. H., Nist, B. J., McCarthy, J. L., Lignin. XII. The high resolution nuclear magnetic resonance spectroscopy of protons in compounds related to lignin., J. Am. Chem. Soc., 86, 1186-1196, 1964.

54. Ludwig, C. H., Nist, B. J., McCarthy, J. L., Lignin. XIII. The high resolution nuclear magnetic resonance spectroscopy of protons in acetylated lignin., J. Am. Chem. Soc., 86, 1196-1202, 1964.

55. Ludwig, C. H., Magnetic resonance spectra. In: Lignins, occurrence, formation, structure and reactions., Sarkanen, K. V., Ludwig, C. H., Eds., Interscience publisher, John Wiley & Sons, New York, 299-344, 1971.

56. Šutý, L., Golis, E., Chemical structure of beech lignin and its changes during water hydrolysis., Cellul. Chem. Technol., 6, 485-491, 1972.

57. Košiková, B., Polčin, J., Joniak, D., NMR studies of lignin-carbohydrate complexes., Holzforschung, 27, 59-64, 1973.

58. Faix, O., Schweers, W., Vergleichende untersuchungen an polymermodellen des lignins (DHP's) verschiedener zusammensetzungen., Holzforschung, 28, 179-185, 1974.

59. Simionescu, C. I., Dragovova, R., Kusmanova, D., NMR-spektroskopische untersuchungen von dioxanligninfraktionen., Cellul. Chem. Technol., 15, 455-464, 1981.

60. Bland, D. E., Menshun, M., The composition and reactive groups of the lignin of Eucalyptus regnans., Appita, 23, 427-433, 1970.

61. Gagnaire, D., Robert, D., A polymer model of lignin (DHP) ^{13}C selectively labelled at the benzylic positions: synthesis and NMR study., Makromol Chem., 178, 1477-1495, 1977.

62. Lundquist, K., NMR studies of lignins. 2. Interpretation of the ^{1}H NMR spectrum of acetylated brich lignin., Acta. Chem. Scand., B33, 27-30, 1979.

63. Lundquist, K., NMR studies of lignins. 3. ^{1}H NMR spectroscopic data for lignin model compounds. Acta. Chem. Scand., B33, 418-420, 1979.

64. Lundquist, K., NMR studies of lignins. 4. Investigation of spruce lignin by ^{1}H NMR spectroscopy., Acta. Chem. Scand., B34, 21-26, 1980.

65. Lundquist, K., NMR studies of lignins. 5. Investigation of non-derivatized spruce and birch lignin by ^{1}H nuclear magnetic resonance spectroscopy., Acta. Chem.

Scand., B35, 497-501, 1981.

66. Marchessault, R. H., Coulombe, S., Morikawa, H., Robert, D., Characterization of aspen exploded wood lignin. Can. J. Chem. 60, 2372-2382, 1982.

67. Hawkes, G. E., Smith, C. Z., Utley, J. H. P., Chum, H. L., Key structural features of acetone-soluble phenol-pulping lignins by ^{1}H and ^{13}C NMR spectroscopy., Holzforschung Suppl., 40, 115-123, 1986.

68. Gellerstedt, G., Gierer, J., The reactions of lignin during acidic sulphite pulping., Svensk. Papperstidn., 74, 117-127, 1971.

69. Johansson, B., Miksche, G. E., Über die benzyl-arylätherbindung im lignin II. Versuche an modellen., Acta Chem. Scand., 26, 289-308, 1972.

70. Glasser W. G., Gratzl, J. S., Collins, J. J., Forss, K., McCarthy, J. L., Lignin. XVI. Synthesis, nuclear magnetic resonance and mass spectroscopy of several monomeric and dimeric lignin-like sulfonates., Macromolecules, 6, 114-128, 1973.

71. Sarkanen, K. V., Wallis, A. F. A., Oxidative dimerization of (E)- ans (Z)-isoeugenol (2-methoxy-4-propenylphenol) and (E)- and (Z)-2,6-dimethoxy-4-propenylphenol., JCS. Perkin I., 1869-1878, 1973.

72. Nakatsubo, F., Higuchi, T., Synthesis of 1,2-diarylpropane-1,3-diols and determination of their configurations., Holzforschung, 29, 193-198, 1975.

73. Gellerstedt, G., Gierer, J., Pattersson, E. L., Szabo-Lin, I., Über die reaktionen des lignins während der neutralsulfitkochung, VI. Reaktionen von zwischenprodukten des stilbentyps., Liebigs Ann. Chem., 2021-2036, 1976.

74. Lundquist, K., Olsson, T., NMR studies of lignins. 1.Signals due to protons in formyl groups., Acta. Chem. Scand., B31, 788-792, 1977.

75. Ralph, J., Young, R. A., Stereochemical aspects of lignin model β-aryl ether quinone methide reactions., J. Wood Chem. Technol., 3, 161-182, 1983.

76. Hauteville, M., Lundquist, K., von Unge, S., NMR studies of lignins. 7. ^{1}H NMR spectroscopic investigation of the distribution of *erythro* and *threo* forms of β-O-4 structures in lignins., Acta. Chem. Scand., B40, 30-35, 1986.

77. Ralph, J., Ede, R. M., Robinson, N. P., Main, L., Reactions of β-aryl lignin model quinone methides with anthrahydroquinone and antranol., J. Wood Chem. Technol., 7, 133-160, 1987.

78. Brunow, G., Sipilä, J., Mäkelä, T., On the mechanism of formation of non-cyclic benzyl ethers during lignin biosynthesis., Holzforschung, 43, 55-59, 1989.

79. Ede, R. M., Brunow, G., Simola, L. K., Lemmetyinen, J., Two-dimentional ^{1}H-^{1}H chemical shift correlation and J-resolved NMR studies on isolated and synthetic lignins., Holzforschung, 44, 95-101, 1990.

80. Bardet, M., Gagnaire, D., Nardin, R., Robert, D., Vincendon, M., Used ^{13}C enriched wood for structural NMR investigation of wood and wood components, cellulose, and lignin., Holzforschung Suppl., 40, 17-24, 1986.

81. Chua, M. G. S., Chen, C. L., Chang, H. M., Kirk, T. K., ^{13}C NMR spectroscopic study of spruce lignin degraded by Phanerochaete chrysoporium II. New structures., Holzforschung, 36, 165-172, 1982.

82. Gellerstedt, G., Robert, D., Quantitative ^{13}C NMR analysis of kraft lignins. Acta Chem. Scand., B41, 541-546, 1987.

83. Kringstad, K. P., Mörck, R., ^{13}C NMR spectra of kraft lignins., Holzforschung, 37, 237-244, 1983.

84. Lapierre, C., Monties, B., Guittet, E., Lallemand, J. Y., Photosynthetically ^{13}C labeled poplar lignins: ^{13}C NMR experiments., Holzforschung, 38, 333-342, 1984.

85. Hassi, H. Y., Chen, C. L., Gratzl, J. S., Carbon 13 NMR characterization of lignosulfonates., Proc. Tappi Research and Development Conference, Appleton, WI., 249-260, 1984.

86. Obst, J. R., Landucci, L. L., Quantitative ^{13}C NMR of lignins. Methoxyl: aryl ratio., Holzforschung Suppl., 40, 87-92, 1986.

87. Ralph, J., Stereochemical aspects of addition reactions involving lignin model quinonemethides., J. Wood Chem. Technol., 3, 161-181, 1983.

88. Robert, D., Bardet, M., Lundquist, K., von Unge, S., ^{13}C NMR spectroscopic studies of the distribution of *erthro* and *threo* forms of various types of β-O-4 structures in lignins., Tappi Proc. Int. Symp. Wood pulp Chem., Raleigh, NC., Tappi Press, Atlanta, 217-219, 1989.

89. Robert, D., Brunow, G., Quantitative estimation of hydroxyl groups in milled wood lignin from spruce and in a dehydrogenation polymer from coniferyl alcohol using ^{13}C NMR spectroscopy., Holzforschung, 38, 85-90, 1984.

90. Landucci, L., Quantitative C-13 NMR characterization of lignin. A methodology for high precision., Holzforschung, 39, 355-359, 1985.

91. Lapierre, C., Monties, B., Guittet, E., Lallemand, J. Y., Quantitative measurements in hardwood lignin ^{13}C NMR spectra., Holzforschung, 39, 367-368, 1984.

92. Robert, D., Gagnaire, D., Quantitative analysis of lignins by ^{13}C NMR spectroscopy., Proc. The Ekman Days Int. Symp. Wood pulp Chem., Stockholm, 1, 86-88, 1981.

93. Nimz, H., Robert, D., Faix, O., Nemr, M., C-13 NMR spectra of lignin 8. Structural differences between lignins of hardwoods, softwoods, and compression wood., Holzforschung, 35, 16-26, 1981.

94. Gagnaire, G., Robert, D., A polymer model of lignin (DHP) ^{13}C selectively labeled at the benzylic positions: synthesis and NMR study., Makromol. Chem., 178, 1477-1495, 1977.

95. Haider, K. Kern, H. W., Ernst, L., Intermediate steps of microbial lignin degradation as elucidated by ^{13}C NMR spectroscopy of specifically ^{13}C enriched DHP lignins., Holzforschung, 39, 23-32, 1985.

96. Archipov, Y., Argyropoulos, D. S., Bolker, H. I. and Heitner, C., ^{31}P NMR spectroscopy in wood chemistry. Part I, Model Compounds., J. Wood Chem. Technol., 11 (2), 137-157, 1991.

97. Archipov, Y., Argyropoulos, D. S., Bolker, H. I. and Heitner, C., ^{31}P NMR spectroscopy in wood chemistry. Part II, Phosphite derivatives of carbohydrates., Carbohydrate Research, 220, 49-61, 1991.

98. Argyropoulos, D. S., Archipov, Y., Bolker, H. I. and Heitner, C., ^{31}P NMR spectroscopy in wood chemistry. Part IV, Lignin models: Spin-lattice relaxation times and solvent effects in ^{31}P NMR., Holzforschung, 47(1), 50-56, 1992.

99. Argyropoulos, D. S., Bolker, H. I., Heitner, C. and Archipov, Y., ^{31}P NMR spectroscopy in wood chemistry. Part V, Qualitative analysis of lignin functional groups., J. Wood Chem. Technol., 13(2), 187-212, 1993.

100. Argyropoulos, D. S., Quantitative Phosphorus-31 NMR analysis of lignins. A new tool for the lignin chemist., J. Wood Chem. Technol., 14(1), 45-63, 1994.

101. Argyropoulos, D. S., Quantitative Phosphorus-31 NMR analysis of six soluble lignins., J. Wood Chem. Technol., 14(1), 65-82, 1994.

102. Argyropoulos, D. S., Heitner, C., and Morin, F., ^{31}P NMR spectroscopy in wood chemistry. Part III. Solid state ^{31}P NMR of trimethyl phosphite derivatives of chromophores in mechanical pulp., Holzforschung, 46, 211-218, 1992.

103. Argyropoulos, D. S., Heitner, C., ^{31}P NMR spectroscopy in wood chemistry. Part VI. Solid state ^{31}P NMR of trimethyl phosphite derivatives of chromophores and carboxcylic acids present in mechanical pulps; a method for the quantitative determination of *ortho*-quinones., Holzforschung, 48, 112-116, 1994.

104. Fillppov, V., Archipov, Y., Argyropoulos, D. S., 4,4,5,5-tetramethyl-1,3,2-dioxaphospholanyl chloride-derivatization reagent for lignin functional group analysis materials., 7th Int. Conf. Young Scientists, Riga, Latvia, 1991.

105. Kostukevich, N. G., Fillppov, V. A., and Archipov, Y., Determination of the hydroxyl containing functional groups of the oxygen-acetic acid lignins by ^{31}P NMR spectroscopy, 7th Int. Sym. on Wood and Pulping chemistry, Beijing, China, 503-507, 1993.

106. Granata, A. and Argyropoulos, D. S., 2-Chloro-4,4,5,5-tetramethyl-1,3,2-dioxaphospholane a reagent for the accurate determination of the uncondensed and condensed phenolic moieties in lignins., J. Agri. Food Chem., 43, 1538-1544, 1995.

107. Jiang, Z. H., Argyropoulos, D. S., and Granata, A., Correlation analysis of ^{31}P NMR chemical shifts with substituent effects of phenols., Mag. Res. Chem., 33, 375-382, 1995.

108. Sun, Y., Argyropoulos, D. S., Fundamental of high pressure oxygen and low pressure oxygen-peroxide (Eop) delignification of softwood and hardwood kraft pulps; A comparison., J. Pulp and Pap. Sci. 21, 185-190, 1995.

109. Brezny, R., and Schraml, J., Silicon-29 NMR spectral studies of kraft lignin and related model compounds., Holzforschung, 41, 293-298, 1987.

110. Nieminen, O. J., Pulkkinen, E., and Rahkamaa, E., Determination of hydroxyl groups in kraft pine lignin by Silicon-29 NMR spectroscopy., Holzforschung, 43, 303-307, 1989.

111. Morris, G. A., Freeman, R., Enhancement of nuclear magnetic resonance signals by polarization transfer., J. Am. Chem. Soc., 101, 760-762, 1979.

112. Barum, D. P., Ernst, R. R., Net polarization transfer via a *J*-ordered state for signal enhancement of low-sensitivity nuclei., J. Mag. Res., 39, 163-167, 1980.

113. Doddrell, D. M., Pegg, D. T., Assignment of proton-decoupled carbon-13 spectra of complex molecule by using polarization transfer spectroscopy. A superior method to off-resonance decoupling., J. Am. Chem. Soc., 102, 6388-6390, 1980.

114. Barrelle, M., A new method for the quantitative ^{19}F NMR spectroscopic analysis of hydroxyl groups in lignins., Holzforschung, 47, 261-267, 1993.

115. Lachenal, D., Fernandes, J. C., and Froment, P., Behaviour of residual lignin in kraft pulp during bleaching., J. Pulp and Pap. Sci., 21, 173-177, 1995.

Chapter 2

Proton Spin-Lattice Relaxation Time Measurements of Solid Wood and its Constituents as a Function of pH

2.0. ABSTRACT

By measuring the proton spin-lattice relaxation times (T_{1H}) in the solid-state, for black spruce softwood, the molecular mobilities of carbohydrates and lignin have been evaluated as a function of pH. Furthermore, in an effort to examine for possible macromolecular connectivities between lignin and cellulose, similar measurements were carried out on isolated cellulose and cuoxam lignin. These studies have shown that the mobility of the polymeric constituents of wood is affected by the ionization of the different functional groups, at different pH's (2-13). The analyses of the proton spin-lattice relaxation time data at constant humidity revealed that the maximum T_{1H} for both carbohydrates and lignin occurs at about neutrality while it was found to be depressed at the two extremes of the pH range. By treating a wood sample with propylene oxide, the esterification of the acid groups was affected, thus deactivating the ionization process and their contribution to T_{1H}. The experimental T_{1H} values for cellulose and lignin after the esterification were significantly decreased at pH 6 confirming that their ionization plays a very significant role in determining chain mobility. To further substantiate our findings, two additional sets of experiments were conducted which involved the determination of T_{1H} values for isolated fully bleached cellulose and cuoxam lignin as a function of pH. The measured T_{1H} values as a function of pH when combined mathematically were found to semiquantitatively describe the pH dependence of cellulose and lignin present in solid wood in the pH range 5 to 10.

2.1. INTRODUCTION

Pulping is essentially the process of fiberizing wood[1]. The bonds which hold fibres together in wood must be broken to such an extent that individual fibres can be liberated from the wood structure. Interfibre bonds can be weakened to the point of fibre liberation using chemical, thermal and mechanical treatments. These treatments can be applied individually or in combination to produce a pulp of desired yield and quality. In all cases, an important step is the disruption of the lignin present in the middle lamella. This may be achieved by softening the lignin in the middle lamella, thermally and/or mechanically, or by degrading the lignin chemically[2].

The process by which lignin is broken down and dissolved during pulping is referred to as delignification. The ultimate goal of various delignification processes is the production of high yield pulp with superior physical and chemical properties. However, the efficient production of bright and stronger pulp at lower cost is not an easy task. This may involve a combination of various chemical and thermal treatments. For example, it has been shown that chemical pretreatment is more effective than presteaming in promoting interfiber bonding but less effective in preserving fiber length[3].

A number of studies have shown that mild sulphite treatments with sodium acid sulphite[3], sodium bisulphite[4], sodium sulphite-bisulphite[5] and sodium sulphite[6, 7], do indeed produce chemimechanical (CMP)[3-6], and chemithermomechanical (CTMP)[3, 7], pulps with strength properties superior to those of the corresponding refiner mechanical (RMP) and thermomechanical (TMP) pulps. These sulphite treatments change the polymeric properties of the wood biopolymers with concomitant increase in the strength of CMP and CTMP pulps, produced from them. Sulphonation is known to cause progressive and irreversible softening of the lignin and this effect has been held primarily responsible for the strength increases exhibited by CMP and CTMP[8]. However, no generally accepted relationship has been established between the polymeric properties of treated softwoods and pulp strength.

An important aspect in the various pulp treatments is the role of pH. The process of fibre softening by sulphonation at several pH values has been examined[9-11] and has been attributed mainly due to the disruption of the surface charges of fibres and their

affinity toward various chemical additives during pulping, bleaching and paper-making processes[12]. Proper pH control during the various stages of mechanical pulp production is an important issue since the chemical properties of papers are significantly affected by process history and the type and amount of the non-fibrous additives.

Understanding the molecular origin of the macroscopic behaviour of such pulps may lead the way to further advances in both process and properties of such materials. It is here that solid-state nuclear magnetic resonance techniques could make notable contributions toward comprehending the various morphological domains and the way in which they influence the overall macroscopic properties of the different biopolymers present in wood pulps. Indeed, recently developed techniques give promise to an increasing role for NMR.

The introduction of cross-polarization[13] (CP) and magic angle spinning[14] (MAS) were brought together by Schaefer and Stejskal[15] in carbon-13 CP/MAS NMR spectroscopy. These techniques paved the way for obtaining high resolution spectra of solid wood samples with well resolved signals for cellulose[16-18], hemicellulose and lignin[19-21], for different wood samples[22-25].

The observations made in these studies contributed a considerable body of knowledge on a variety of issues. For example, the analyses of ^{13}C CP/MAS spectra have clearly demonstrated that the grinding of wood has no influence on the crystallinity of cellulose, whereas ball milling converts "crystalline" cellulose to its amorphous form[22]. On another front, Maciel et al.[26, 27] have succeeded in assigning the most prominent signals of CP/MAS spectral of various lignins specific functional groups.

Interest in NMR relaxation parameters has shown a dramatic increase in the past 20 years. This interest has developed for a number of reasons, probably the most important being that it is essential for one to have a knowledge of nuclear relaxation rates in order to use efficiently a pulse Fourier transform NMR spectrometer. Furthermore, it is relatively easy to measure NMR relaxation parameters using such a spectrometer. The ease with which relaxation parameters can be measured has enabled spectroscopists to demonstrate and, to some extent, rediscover that these parameters are capable of providing important dynamic information such as (i) molecular rotational and angular-

momentum correlation times, τ_2 and τ_c, respectively, (ii) translational diffusion constants, and (iii) inter- and intramolecular exchange rates. The dependence of some relaxation parameters on nuclear-nuclear separations (bond lengths) allows one to use these parameters to assist in the determination of molecular structure.

The most commonly measured NMR relaxation parameters are the spin-lattice relaxation time T_1, the spin-spin relaxation T_2, the spin-lattice relaxation time in the rotating frame $T_{1\rho}$, and the nuclear Overhauser enhancement factor. The longitudinal (spin-lattice) relaxation time represents a measure of the time required for energy to pass from the spin system to other degrees of freedom. The transverse (spin-spin) relaxation time refers to thermal equilibrium within the spin system itself. According to the theory of nuclear magnetic relaxation of Solomon[28], T_1 and T_2 are functions of a correlation time τ_c. The correlation time is the time a molecule takes to turn through a radian or to move through a distance comparable to its own dimensions. The main advantage of these spectroscopic techniques is that it provides a detailed analysis of molecular motion at molecular level.

In recent years considerable effort has been devoted to the study of macromolecular dynamics as determined from nuclear magnetic relaxation parameters for probing molecular motion[29-32] and miscibility[33, 34] of polymeric blends. The examination of epoxy polymers[35-37], polyesters[36, 38-40], polycarbonates[41, 42], polyphenylenes[43], polyphenylene oxides[29], polyphenylene sulfones[29], polyphenylene sulfides[38], polystyrene[35, 42], polyimides[42] and heteroaromatic polymers[44] are just a few examples of such applications.

The advent of these applications has provided a novel approach toward investigating the polymeric components of solid wood[19, 23, 25, 45-52] in a nondestructive manner. Techniques such as proton and carbon spin-lattice (T_{1H}, T_{1C}), spin-spin (T_2) and spin-lattice in a rotating frame ($T_{1\rho}$), relaxation measurements were implemented for elucidating microstructural details of lignin-carbohydrate linkages[25, 45-50] which were otherwise impossible with solution NMR spectroscopy. Consequently, solid-state NMR techniques have opened up new avenues for studying the various morphological and structural features of wood.

2.1.1. Effect of Moisture on Spin-Lattice Relaxation Parameters of Wood

Wood normally contains water. The amount of water can reach levels such that it dominates the proton NMR signal. Early NMR studies conducted on water in wood[53, 54] and in cellulosic gels[55, 56] reported a multi-exponential behaviour of relaxation times. These studies concluded that such behaviour of relaxation was due to part of the water being intimately associated to the cell wall components, while another part was present in the cell lumen and free to diffuse. The presence of water is known to plasticize wood components[57]. Plasticization increases the mobility of the wood polymers and consequently may reduce the cross polarization (CP) efficiency at room temperature[52]. Newman[50, 51], Willis and Herring[23] have noted that spin relaxation parameters may be affected by the amount of water present on a wood sample. In addition, Newman[51] has shown that T_{1H} values were much longer for dry wood than for wet wood. On the other hand, Willis and Herring[23] reported that moisture is known to enhance signal to noise and improve the resolution of a ^{13}C CP/MAS NMR spectrum in comparison to a dry sample. They concluded[23] that hydration has an effect on both the carbohydrate and the lignin components of wood. However, the effect of hydration for aliphatic carbons of the carbohydrates and lignin is more augmented than the aromatic carbons of lignin present within a solid wood sample.

The actual chemical shift values also give indications regarding the effect of water on cellulose[38]. By increasing the moisture of cellulose from 0.5 to 16% the principle signals of cellulose shift a few ppm to higher field. A similar, but much smaller shift was also observed for cellulose acetate. The spin-lattice relaxation time (T_1) for C1, C2, C3, and C4 diminish with increased moisture contents. However, for the case of C6 there is no significant change. For cellulose acetate, qualitatively a similar behaviour was observed[38].

An important recommendation[50] therefore emerges on reporting proton spin relaxation times i.e. the water content of the sample in question needs to be specified.

2.1.2. Effect of Paramagnetic Metals on Spin-Lattice Relaxation Parameters of Wood

Another factor which may seriously affect the magnitude of proton T_1 values in wood and pulp samples is the presence of paramagnetic impurities[58] such as Fe, Mg, Cu, Mn, etc. The influence of paramagnetic impurities on nuclear relaxation takes place via interactions with the fluctuating magnetic fields. The interaction of the unpaired spins of paramagnetic impurities with the protons of carbohydrates and lignin can cause fluctuation of the magnetic intensity. Any fluctuation of magnetic intensity at a nucleus can cause spin transition if it has components of a suitable frequency. Since the magnetic moment of the electron is much larger (650 times) than that of the nucleus, even small traces of paramagnetic species in the sample can dramatically reduce the measured relaxation times. Before measuring relaxation times care must be taken to remove these impurities from wood or pulps since wood is known to contain a number of such paramagnetic centers[59].

In actual fact the dependency of proton spin-lattice relaxation times for lignin and carbohydrates as a function of total ionic contents, for a series of sulphonated pulp samples were measured and quantified by Argyropoulos and Morin[60]. They observed that after removal of the paramagnetic metal ion impurities from wood and pulp samples, the proton T_1 values were significantly decreased.

2.1.3. Effect of Static Magnetic Field on Spin-Lattice Relaxation Parameters of Wood

The field of a spectrometer can also affect the relaxation parameters of many nuclei in a complex way (apart from modifications resulting from changing the second order nature of the spectrum), once the extreme narrowing limit is exceeded. This occurs once the Larmor frequency of the nucleus being detected, or any nucleus to which it is spin coupled, e.g. ^1H, approaches or exceeds the reciprocal of the molecular correlation time. Under these conditions, which are increasingly encountered as magnet fields increase, relaxation characteristics change, the NOE decreases, and can even invert in sign[61], T_1 will exceed T_2 and consequently the efficiency of NMR decreases.

Argyropoulos et al.[62] have measured the proton spin-lattice relaxation parameters of the two principle biopolymers of wood at different magnetic fields (at 100 and 300 MHz). They concluded that a three fold increase in the static magnetic field caused an increase in the T_1 values. However, the difference in proton spin-lattice relaxation time values for both carbohydrates and lignin within the two fields, remains the same.

2.1.4. Effect of Temperature on Spin-Lattice Relaxation Parameters of Wood

Temperature can also influence the magnitude of spin relaxation measurements. Several studies have shown that the T_1 minimum is close to room temperature, while at above and below room temperature T_{1H} values raised[62, 63]. Nevertheless, if the spin-lattice relaxation time is studied as a function of temperature, a T_1 minimum occurs for each temperature where a particular process (e.g., side group motion) has $\omega_0\tau_c \sim 1$[64].

In light of the above considerable efforts to avoid any unqualified contributions to the spin-lattice relaxation times were made during our measurements.

In this chapter we document our measurements of proton spin-lattice relaxation times for wood, isolated cellulose and lignin as a function of pH. This was done in an effort to obtain further information into the structure of wood and the effect of pH on it. The derived information is discussed in terms of the macromolecular connectivities that exist between cellulose and lignin in wood and the effect of ionization of the various functional groups on its physico-chemical properties.

2.2. EXPERIMENTAL

2.2.1. Materials and Methods

2.2.1.1. Preparation

A trunk section of a black spruce (*Picea mariana*) tree was pulverized into sawdust. The sawdust was suspended in acetone three times to eliminate the water. Only the sample was then allowed to dry under ambient conditions and finally subjected to Wiley-milling to 20 mesh.

Cellulose

The cellulosic material was provided by Dr. T. Scallan of PAPRICAN. The cellulose (Q90) was commercially prepared i.e., from fully bleached black spruce kraft pulp. The letter "Q" is an abbreviation for the Quevillon mill in northern Québec, and the number "90" is the brightness of the sample.

Cuoxam Lignin

In an attempt to isolate intact lignin, wood meal from a selected spruce log was extracted for 48 hours with hot benzene-alcohol (1:1). The wood meal was then degummed by treating it twice with 5% sodium hydroxide for 24 hours and washing it successively with water, dilute acetic acid, and again with water. To remove the easily hydrolysed carbohydrates, such as pentosans and hemicelluloses, the wood meal was refluxed for 1-2 hours with 1% sulfuric acid, washed, and dried in the air. The wood meal thus prepared was then shaken for 12 hours with Schweizer's reagent $[Cu(NH_3)_4](OH)_2$, using 750 mL for 50 g wood meal. The lignin was separated by centrifuging and washed in the centrifuge jar successively with Schweizer's reagent, concentrated ammonia, water, and dilute sulfuric acid (1% w/v, 2L). It was then filtered and washed with water. The hydrolysis with 1% sulfuric acid and the extraction with cuprammonium hydroxide were repeated five times. The isolated insoluble lignin was a light yellow-brown powder. The lignin thus obtained is referred to in the literature as "Freudenberg", "cuproxam", or "cuoxam" lignin[65].

Preparation of buffer solutions and sample treatments

A wide range of buffer solutions at pH values 2, 4, 6, 8, 10, 11, and 13 was used. All buffer solutions were purchased form Fisher Ltd. with the exception of buffer solution 13 which was prepared by mixing 25 mL of 0.2 molar KCl with 66 mL of 0.2 molar NaOH[66].

2.02 g of softwood, cellulose and 0.9 g of cuoxam lignin were suspended in the 50 mL and 22.3 mL of the desired buffer solution, at room temperature under constant stirring for 24 hours. The samples were then filtered and thoroughly washed with deionized water. The samples were then dried at room temperature and kept in a desiccator under reduced pressure for a period of three weeks. This was followed by conditioning them at $45 \pm 5\%$ humidity prior to any spin relaxation measurements.

Sample conditioning and moisture control

All samples were kept in a desiccator under reduced pressure for a period of one week in the presence of drierite (calcium sulfate, anhydrous). All the samples were then exposed to 45% humidity next to 100 mL of a solution with aqueous tension of 10.69. This solution was prepared according to Lange's Handbook of Chemistry where all concentrations are expressed as percentages of anhydrous solute by weight[67]. The dry samples were kept in the desiccator next to the solution for a period of three weeks prior to any measurements. Each sample was weighed before and after each measurement.

2.2.1.2. Reactions

The removal of paramagnetic metal ion impurities from cuoxam lignin, cellulose (Q90), and softwood samples

Approximately 3 g (on oven dry basis) of wood dust were dispersed in 300 mL of a 0.2% (w/v) diethylenetriaminepentaacetic acid (DTPA) solution prepared in deionized water. The dispersion was then stirred at 60 °C for 1 hour. The filtered dust was then washed with deionized water and dispersed in 600 mL of a solution of sulphuric acid (1.1 mL/L) where it was kept under mild agitation at room temperature for 2 hours. Finally, the sample was filtered and washed three times with deionized water. This

procedure was used for all the samples examined in this work. The only exception was cuoxam lignin where sulphuric acid was replaced with 0.2% (v/v) nitric acid aimed at removing copper ions more effectively.

Determination of carbohydrate composition of extractive-free samples

The isolated filtrates from sawdust, cellulose (Q90), and cuxoam lignin after being suspended in the wide range of buffer solutions, were isolated and analyzed for the presence of various sugars and in particular, arabinose, xylose, galactose, and glucose by mean of gas chromatography. This was carried out for all treated samples. The only sugar detected was xylan for the treatment of black spruce softwood dust at pH 13 as a concentration of 116 mg/L.

Esterification of carboxylic acid groups in softwood sample with propylene oxide[108]

The acid groups of approximately 2-3 g (oven dry weight) of the sawdust sample were first exchanged to their acidic forms by suspending the sample at 1% consistency in 0.1 N HCl solution under gentle agitation for 1.0 hour. The sample was filtered and the procedure repeated. After thorough washing with deionized water, the sample was dispersed in 400 mL of a 37%-by-weight solution of propylene oxide in water[68], and allowed to react for 7 days at room temperature. Excess propylene oxide was removed by washing the sample with deionized water.

2.2.1.3. Instrumentation

^{13}CP MAS NMR and proton T_1 measurements

All samples were conditioned at 45±5% relative humidity prior to any measurements, so as the effect of moisture content on the measured parameters was eliminated. Proton spin-lattice relaxation time measurements were carried out via carbon. On a Chemagnetics M-100 spectrometer operating at a ^{13}C frequency of 25.12 MHz. All CP/MAS experiments were performed with a spinning rate of 4 kHz, a contact time of 1 ms and proton $\pi/2$ pulses of 4.5-5.0 μs duration.

The proton spin-lattice relaxation times were measured from the ^{13}C cross-

polarized spectra immediately after the application of a π-τ-$\pi/2$ pulse sequence to the proton spins. The T_1 data was fitted to the following three parameter equation:

$$M_\tau = M_{\tau=\infty} = [1 - (1+\alpha)\ \exp(-\tau/T_{1H}] \qquad [2.1]$$

where T_{1H} is the proton spin-lattice relaxation time $M_{\tau=\infty}$ is the equilibrium magnetization and α is the inversion efficiency of the proton π pulse. For perfect inversion $\alpha=1.0$; the values of α ranged between 0.80 and 0.90 s. In all relaxation experiments, recycle times of at least 5 x T_1 were used, typically with 9 different τ values. In order to reduce errors due to instrument drift (variations in amplifier output etc.), the order of the τ values was scrambled. In addition, the data were collected in blocks, i.e., 1000 transients with the first τ value, then 1000 with the second and so on through to the last value. The experiment then returned to the beginning of the list and 1000 more transients were added to the corresponding data set previously accumulated. The list was run through in this manner until an adequate signal to noise ratio was reached (usually 4000-8000 transients in total for each τ value). Spectra were obtained on 7 different τ values prior to the application of equation 2.1. The proton spin-lattice relaxation values for carbohydrates and lignin were derived by measuring the intensity of the signals at 72.4 and 148.2 ppm respectively[60, 62]. Similar measurements were also carried out for isolated cellulose (Q90) and cuoxam lignin.

2.3. RESULTS and DISCUSSION

Prior to the proton spin-lattice measurements (T_{1H}), all samples were treated under similar protocols. These measures were followed to avoid any unqualified contribution to T_{1H} which involved the removal of paramagnetic impurities and regulating the amount of moisture. Table 2.1 shows the metal ion profile before and after their removal by thorough chelating and acid washing. This procedure was very effective in removing and/or reducing their concentration significantly.

Table 2.1. Paramagnetic metal ion contents measured by atomic absorption before and after washing of softwood sawdust, cellulose and lignin.

Sample	Before washing (ppm)			After washing (ppm)		
	Fe	**Mn**	**Cu**	**Fe**	**Mn**	**Cu**
Softwood	123	142	3.3	8.7	< D.L.	1.4
Cellulose	8.4	6.5	1.1	4.4	< D.L.	0.9
Cuoxam lignin	99.6	5.0	405	< D.L.	< D.L.	9.0

D.L. = Detectiom limit

The presence of water in a wood sample or its exposure to ambient moisture can also affect the T_{1H} measurements. High moisture content contributes to the mobility of the polymer chains, resulting in lower T_{1H} values[60]. Under these conditions, the proton spin-lattice measurements (T_{1H}) of the two biopolymers of softwood were investigated. More specifically, a series of softwood samples were suspended in various buffer solutions ranging from acidic (pH 2) to alkaline (pH 13). Table 2.2 shows the magnitude of T_{1H} values for the carbohydrates and lignin polymers present in softwood.

These data were then employed to examine the relaxation behaviour of carbohydrates and lignin as a function of pH. Figure 2.1 demonstrates that the pH treatment of softwood over a wide range has significantly affected the mobilities of these biopolymers as reflected in their T_{1H} values. As the pH was varied from acidic to near neutrality (2 → 6), the T_{1H} values of both carbohydrates and lignin increased. Under

alkaline conditions the opposite was apparent. As the pH changed from near neutrality toward alkalinity (6 → 13), the T_{1H} values decreased. The maximum T_{1H} values were obtained at about neutrality, i.e. pH 6. However, a striking feature of these data is that the T_{1H} values of these biopolymers qualitatively follow each other as a function of pH. This trend is similar to that reported by Argyropoulos et al.[60, 62] and may be indicative of the presence of molecular connectivities between the lignin and carbohydrates.

Table 2.2. Spin-lattice relaxation time for cellulose and lignin signal for softwood sawdust as a function of pH.

Entry	pH	Spin-lattice relaxation time (T_{1H}) (ms)	
		Cellulose[(1)]	Lignin[(2)]
I	2	393 ± 16	377 ± 20
II	4	412 ± 4	391 ± 26
III	6	777 ± 19	661 ± 43
IV	8	576 ± 15	515 ± 46
V	10	482 ± 36	476 ± 26
VI	11	285 ± 5	317 ± 13
VII	13	299 ± 12	296 ± 22

(1) Measured via the C-13 signal at 72.4 ppm

(2) Measured via the C-13 signal at 148.2 ppm

The observed variation in the T_{1H} values as a function of pH could be attributed to the modification of the macromolecular structure of the wood components. Large variations in pH may affect the functional groups of the individual wood components by inducing diople-dipole, ion-dipole, or hydrogen-bonding interactions. The formation of hydrogen bonds by free OH groups[69], ionization of various functional groups attached to the macromolecular network[70] and the formation of ionic aggregates[58, 71] can all alter the physical and dynamic mechanical properties[72] of wood and their proton spin relaxation values. Lindberg et al.[73] have actually documented the variation of spin-lattice relaxation values for a number of chemically modified wood samples. Their measurements provided information regarding small changes in the composition of carbohydrates and lignin as caused by various chemical agents. However, the most significant account on the effect

of pH on wood pulps was presented by Lindström and Carlsson[74]. They clearly showed that the swelling of wood pulps is maximum at about neutrality and is depressed at low and high pH values similar to the trends reported in Figure 2.3. Considering the Donnan[75, 76] theory, the relaxation behaviour of carbohydrates and lignin as a function of pH, one may attempt to rationalize the ionization process for these biopolymers as follows: Under acidic conditions the extent of ionization of the various functional groups is low. However, as the pH shifts toward neutrality the extent of hydrogen bonding increases, resulting in higher T_{1H} values. As the pH shifts further to alkaline values, the opposite occurs, i.e. the ionization increases causing repulsive forces to set in, between the polymer chains (this effect is highest at pH values > than 10). Electrostatic repulsive forces may cause rupture of hydrogen bonds increasing the mobility of the polymeric chains, resulting in faster relaxation and consequently lower T_{1H} values.

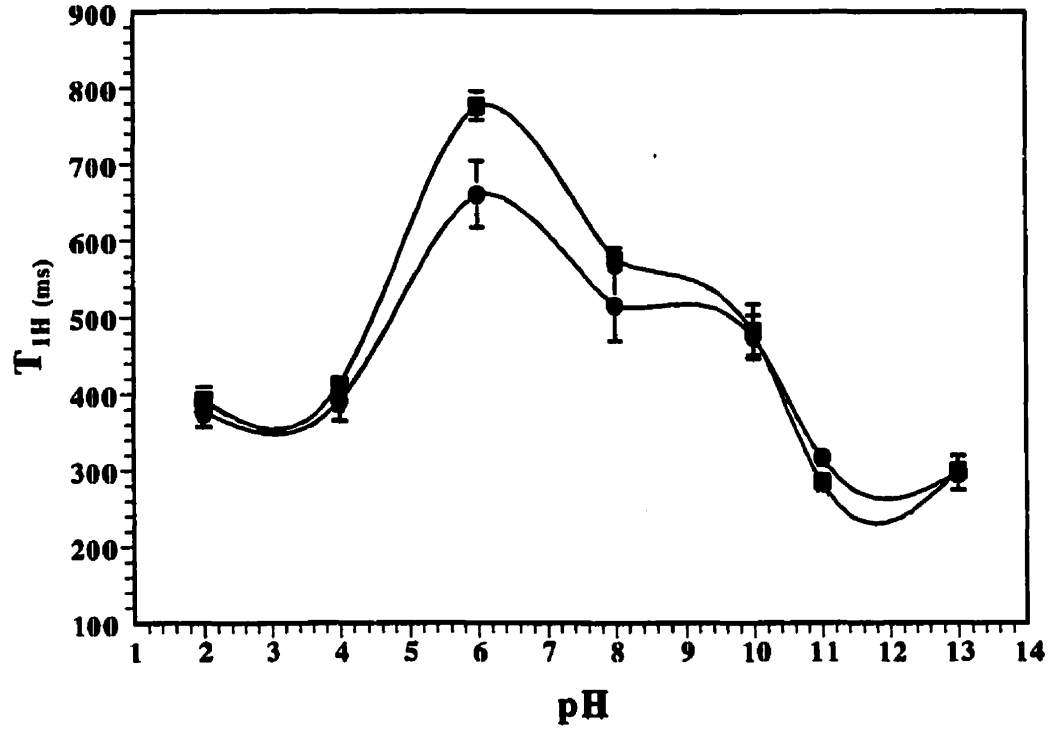

Figure 2.1. The dependence of proton spin-lattice relaxation times for lignin (●) and carbohydrates (■) in softwood sawdust as a function of pH.

Acidic groups such as carboxyl, phenolic and even enolic hydroxyl groups present within the lignocellulosic matrix can be ionized at pH values greater than 10[77]. Primary and secondary carbohydrate hydroxyl groups[78] may only partially ionize in alkaline solutions due to their weakly acidic nature[79-83].

As previously mentioned, the longest T_{1H} values for carbohydrates and lignin were observed at pH 6. At this pH, the difference in T_{1H} values between these two polymeric components of wood were augmented. A number of literature accounts have provided further support on the significance of pH near neutrality for chemically modified wood samples. Rowell et al.[84] have reported that the acetyl groups of acetylated wood is most stable at pH 6 while Farrer and Neale[85] have considered the carboxylic acid groups to be the active species affecting swelling near neutrality. The contribution of carboxylic acid groups toward dynamic relaxation was examined by Nakano as a function of pH's. They concluded that the side-chains of succinylated wood ionize in solutions above pH 5[86]. For these reasons, during this effort greater attention was paid on the role of carboxylic acid groups at pH 6. By treating a wood sample with propylene oxide[68], the esterification of the acid groups was affected; thus deactivating the ionization process and their contributions to T_{1H}. In addition, the carboxylic protons were displaced with longer propylene groups. Both of these are expected to increase the mobility of the polymer chains allowing for faster relaxation. Indeed the experimental T_{1H} values for cellulose and lignin after the esterification were significantly decreased at pH 6. Table 2.3 and Figure 2.2 shows the magnitude of these relaxation times and compares them at pH 6 before and after esterification.

In an effort to ascertain and further substantiate our T_{1H} measurements, four samples of softwood sawdust were exposed at various pH's and their T_{1H} values were measured at 45% moisture. This set of experiments assured that the reproducibility of our data was adequate for the purposes of this work. The aforementioned reproducibility data is presented in Table 2.4 showing an excellent agreement to that of Table 2.2.

Table 2.3. Spin-lattice relaxation time data for cellulose and lignin signals for softwood sawdust at pH 6 before and after esterification of carboxylic acids.

Entry	pH	Spin-lattice relaxation time (T_{1H}) (ms)	
		Cellulose	Lignin
I	6	777 ± 19	661 ± 43
II*	6	597 ± 24	509 ± 64

*Measurements after esterification

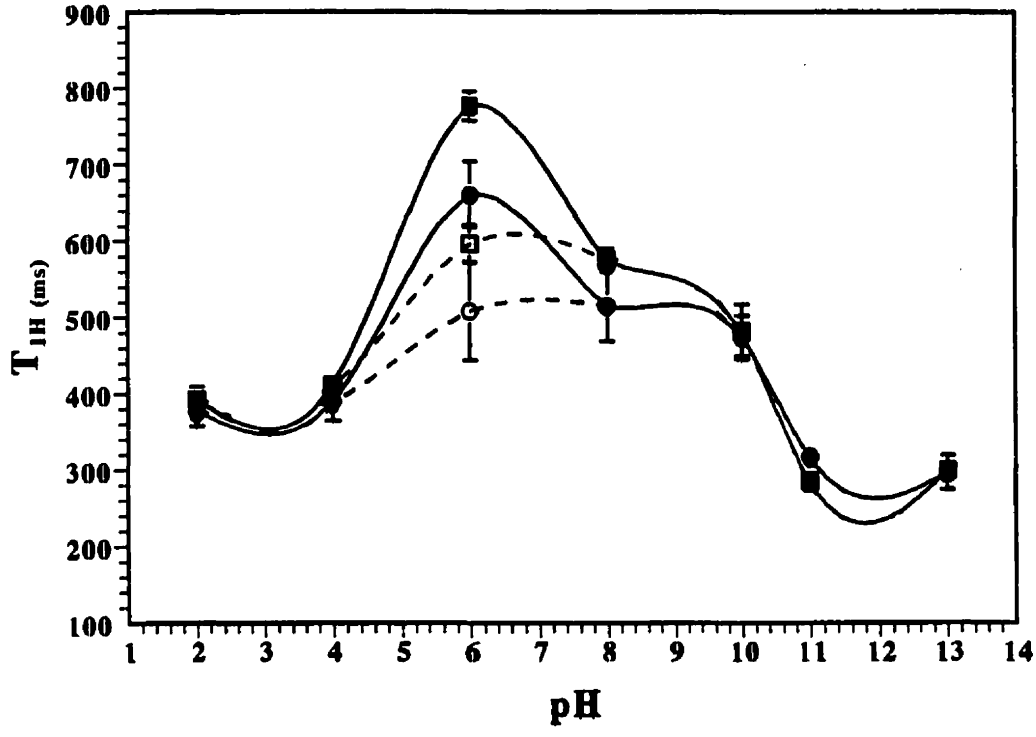

Figure 2.2. The dependence of proton spin-lattice relaxation times for lignin (●) and carbohydrates (■) in softwood sawdust before and after (---) esterification at pH 6.

Table 2.4. Evaluation of spin-lattice relaxation time for cellulose and lignin in softwood sawdust as a function of pH, at 45% relative humidity.

Entry	pH	Spin-lattice relaxation time (T_{1H}) (ms)	
		Cellulose[1]	Lignin[2]
I	2	391 ± 6	366 ± 17
II	4	404 ± 6	393 ± 22
III	10	488 ± 12	475 ± 28
IV	13	300 ± 4	300 ± 31

(1) Measured via C-13 signal at 72.4 ppm

(2) Measured via C-13 signal at 148.2 ppm

In an effort to further substantiate and comprehend our findings, two additional sets of experiments were conducted. These involved the determination of T_{1H} values of isolated fully bleached cellulose and cuoxam lignin as a function of pH. These measurements were carried out in exact analogy to the experimental protocols followed for softwood sawdust. These studies were so designed as to provide the contributions of the individual components to the overall relaxation behaviour of softwood[87-92].

2.3.1. Cellulose (Q90)

In nature, cellulose exists as microfibrils of varying dimensions[93, 94]. These are aggregates of parallel chains of cellulose macromolecules which are held together by hydrogen bonding. However, as in all crystalline polymers, there are amorphous regions within cellulose. These regions occur when the chains are not oriented parallel to each other.

Horii et al.[95] have shown that carbon-13 spin-lattice relaxation times (T_{1C}) are longer for crystalline than non-crystalline cellulose. In the crystalline regions of cellulose the chains are held together by cellulose-cellulose hydrogen bonds. This interchain bonding would result in rigidity of the crystalline regions which would not permit partial rotation of the anhydrocellulose rings without breaking hydrogen bonds. However, in the

amorphous regions of the polymer, the decreased packing density of the chains probably permits the cellulose rings to undergo partial rotation[63].

Other observations on various material characteristics of cellulose hydrogels, such as dynamic mechanical[96], mechanical and swelling[97-103], thermoelasticity[99] and swelling kinetics[100] have been studied by means of NMR and Raman spectroscopy. However, the effect of ionization on T_{1H} for cellulose as a function of pH has not been examined before.

The surface charge of cellulose arises from the dissociation of acidic group and this depends on pH[104]. At high pH's, the acidic groups exist in their dissociated salt form and the surface charge is substantially negative, whereas at low pH's, the acid groups exist in a largely undissociated form and the surface charge is closer to zero (the isoelectric point) or it may even become slightly positive.

. The proton spin-lattice relaxation times for a series of cellulose samples (Q90) were measured as a function of pH. These data are depicted in Figure 2.3 indicating that the T_{1H} values increased as the pH was changed from acidic to neutral, reaching its maxima at pH 6. Above this pH the T_{1H} was reduced up to pH 10, then increased again for pH 11 and 13. The T_{1H} relaxation behaviour of isolated cellulose is very similar to the corresponding carbohydrate measurements for softwood. The only significant difference was observed beyond pH 10. The T_{1H} values of cellulose were found to be higher by 400 and 500 ms at pH 11 and 13 respectively when compared to the T_{1H} measurements of the carbohydrate component in softwood.

Neale[79-81] considered the hydroxyl groups as very weak acids capable of forming sodium salts. Because of the very low dissociation constants of the hydroxyl groups, conversion to the sodium salt and subsequent swelling by necessity occurs at very high alkalinities. For example, he calculated an ionization constant of $Ka=1.84x10^{-14}$ (pKa= 13.74 at 25 °C) assuming that only one hydroxyl group per anhydroglucose unit is ionized, below 20% NaOH. In this case Ka represents the sum of the ionization constants for three hydroxyls per anhydroglucose unit. Neale[79-81] also concluded that the glucose units in cellulose behave like weak acids with an approximate pKa value of 13.7. An approximation of pKa values for a number of functional groups associated in cellulosic

materials have been reported[105, 106].

Table 2.5. Spin-lattice relaxation time for isolated cellulose (Q90) and cuoxam lignin as a function of pH.

Entry	pH	Spin-lattice relaxation time (T_{1H}) (ms)	
		Cellulose (Q90)[(1)]	Cuoxam Lignin[(2)]
I	2	700 ± 13	315 ± 15
II	4	841 ± 15	328 ± 25
III	6	849 ± 29	353 ± 12
IV	8	781 ± 9	366 ± 4
V	10	688 ± 5	375 ± 7
VI	11	693 ± 24	346 ± 19
VII	13	791 ± 14	232 ± 14

(1) Measured via C-13 signal at 72.4 ppm

(2) Measured via C-13 signal at 148.2 ppm

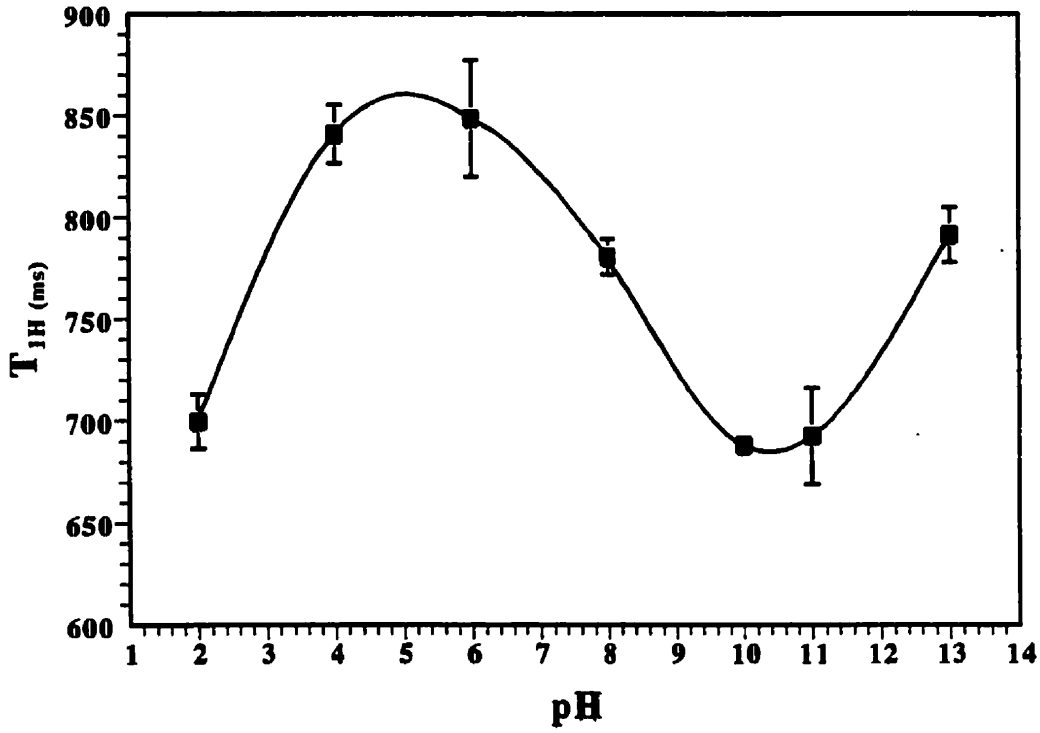

Figure 2.3. The dependence of proton spin-lattice relaxation times for isolated cellulose (■) as a function of pH.

Carboxylic acid groups which are present in the pectic components and in 4-O-methyl-glucuronic acid units of xylan hemicelluloses, have an approximate pKa value of 4.5 ($Ka=3.16x10^{-5}$)[105]. Furthermore, the dissociation constants of the primary and secondary hydroxyl groups of carbohydrates were found to be $0.93x10^{-14}$ and $0.025x10^{-14}$ respectively[106]. Considering these data an attempt was made to rationalize the impact of ionization of the different functional groups of cellulose on the behaviour of T_{1H} as a function of pH. Figure 2.4 shows the calculated degrees of ionization as a function of pH for the different functional groups of cellulose. Therefore, it is not surprising to see that the T_{1H} values in Figure 2.4 increased since the ionization of most cellulosic functional groups occurs at pH 11 and above. It is noteworthy to mention at this point, that after treatment of cellulose at pH 13, (66 mL 0.2M NaOH and 25 mL of 0.2M KCl) the resulting material turned to light-yellow in colour and hardened. This physical change was manifested in the increased T_{1H} values for samples exposed at this pH (Figure 2.3). The possibility of conversion of cellulose I to cellulose II under highly alkaline conditions (>3M), was also considered. However, the ^{13}C CP/MAS spectral analysis of cellulose exposed at this pH did not exhibit any additional C1 signal due to mercerization.

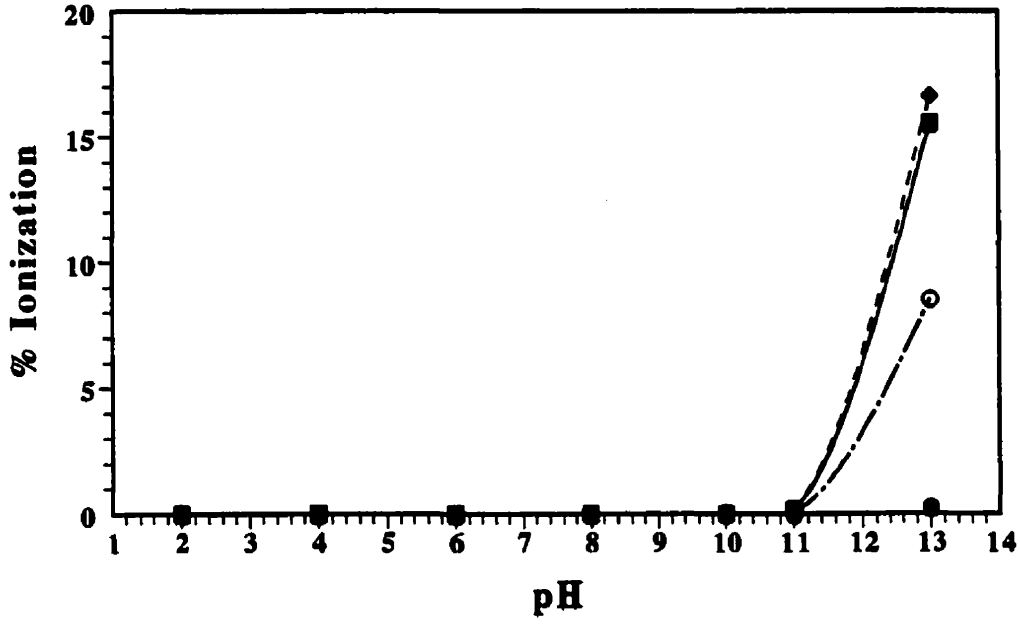

Figure 2.4. Percent ionization for cellulose (■), glucose in cellulose (♦), primary (○) and secondary hydroxyl (●) groups in cellulose.

2.3.2. Cuoxam Lignin

Unlike cellulose, the T_{1H} plots for cuoxam lignin as a function of pH did not behave in qualitative similarity to the corresponding measurements for lignin in softwood (Figure 2.5). These measurements showed that the T_{1H} values increased from pH 2 to a maximum value at pH 10. After this pH, the mobility of lignin was found to increase dramatically as evidenced by the reduced T_{1H} values. This is to be expected since the alkaline treatment of lignin is known to soften its macromolecular structure even allowing its dissolution.

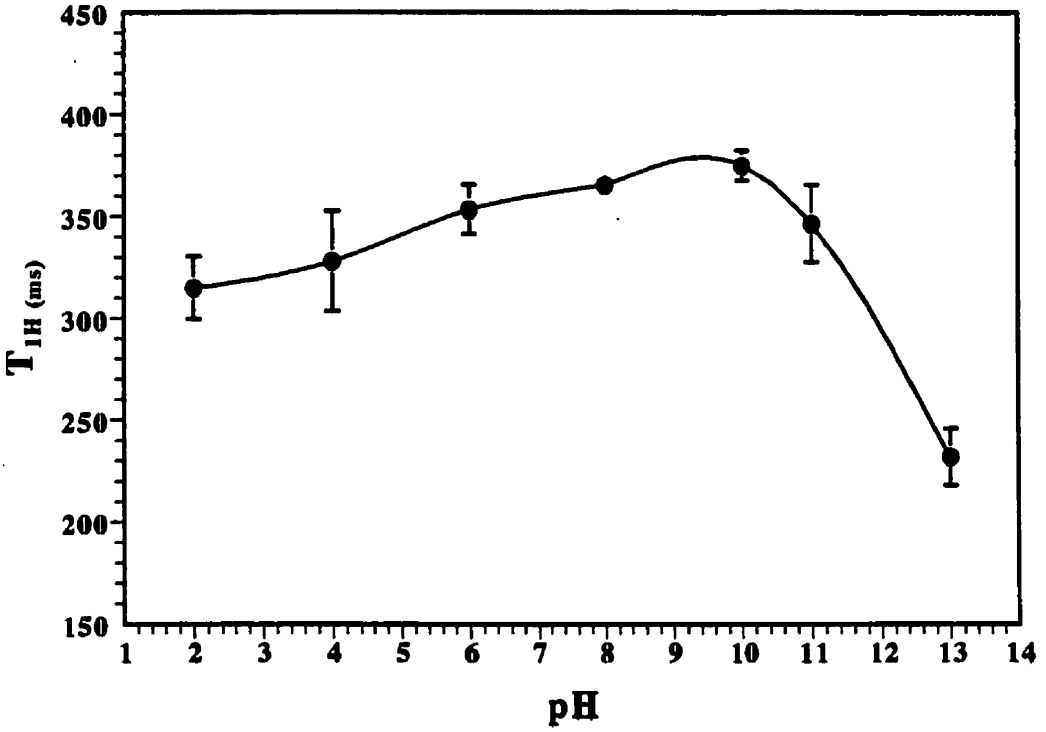

Figure 2.5. The dependence of proton spin-lattice relaxation times for isolated lignin (●) as a function of pH.

Lignin is known to behave as a spherical, amorphous macromolecule[59, 107-109] of a polydisperse molecular weight distribution. The swelling behaviour of these materials was found to be similar to that of polyelectrolyte networks[110]. Flory[111] has suggested that crosslikned polyelectrolytes swell at elevated pH's due to the effect of ionization on

conformation. The ionization effect is attributed to the presence of carboxylic acid groups which are known to form intermolecular hydrogen bonds within the lignin network structure[110] via the abundant free phenolic hydroxyl groups[112]. Consequently, the extent of ionization of these two functional groups and their contribution to T_{1H} at various pH's were examined. On the basis of approximate pKa values for carboxylic acids (pKa=4.5)[105] and free phenolic hydroxyl groups (pKa=10.21)[105] the percent ionization of these groups were calculated as a function of pH (Figure 2.6).

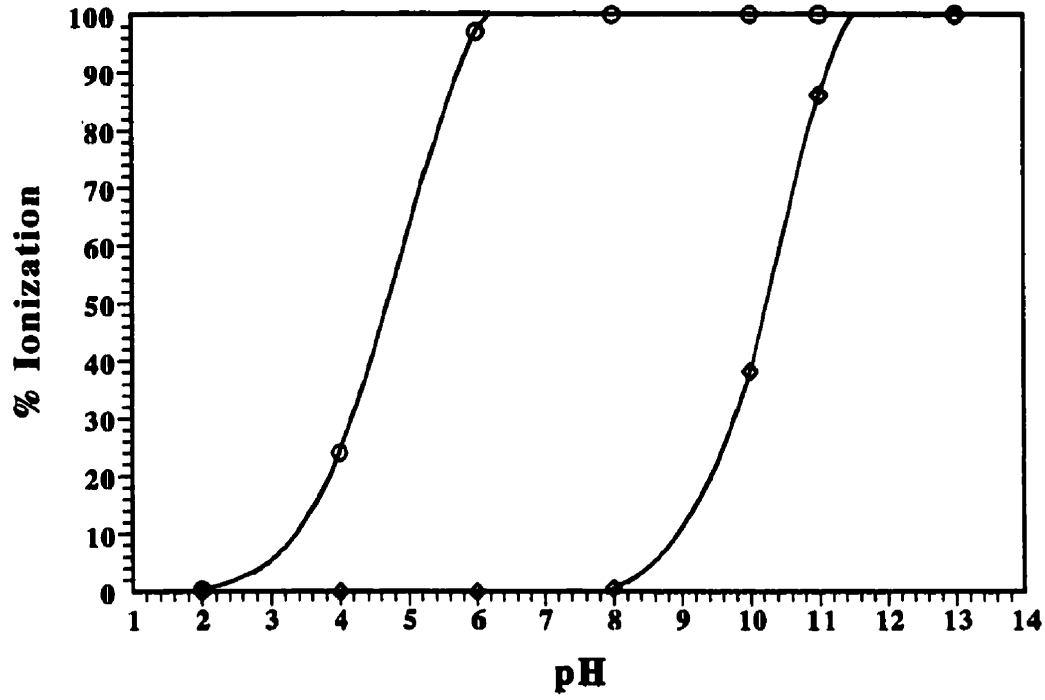

Figure 2.6. Percent ionization of carboxylic acids (○), and free phenolic hydroxyls (◇) groups in lignin.

These calculations show that the carboxylic acid groups were nearly fully ionized at pH 6. However, the free phenolic hydroxyl groups began to ionize at pH 10 (40%). At this point, the T_{1H} values started to decrease. As the ionization of these groups proceeded to maximum (pH 11 and 13), the mobility of the lignin macromolecular network increased significantly contributing to its alkaline softening.

2.3.3. Correlation of the Cellulose and Lignin T_{1H} Measurements with those of Wood

In an effort to obtain a better insight on the significance of our measurements so far and to examine for possible molecular connectivities between lignin and carbohydrates in wood, the T_{1H} data for cellulose (Q90) and cuoxam lignin as a function of pH were compared to the corresponding measurements for wood (Figure 2.7). To facilitate comparison of these data to those of softwood (Figure 2.1), they were plotted on the same scale.

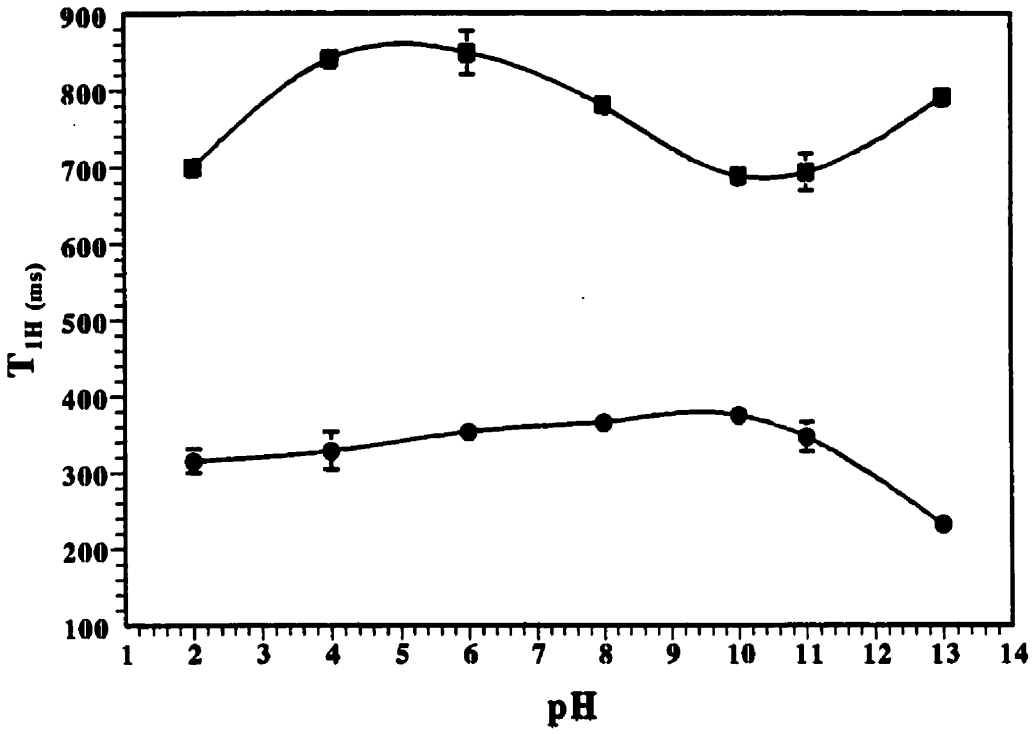

Figure 2.7. Proton spin-lattice relaxation times for isolated cellulose (■) and cuoxam lignin (●) and as a function of pH.

These data shows that the magnitude of the T_{1H} values for isolated cellulose were higher to that obtained for the carbohydrate signals in wood. Nonetheless, the trend of their relaxation behaviour seems to be very similar to that of the carbohydrates in wood. On the other hand, the T_{1H} values for cuoxam lignin was relatively close to those measured in softwood with the exception of pH's 6, 8, and 10. However, compared to

softwood, the relaxation trends as a function of pH were found to be quite different.

The comparison of the overall relaxation data has lead to another significant observation. Contrary to the overall relaxation trends observed for lignin and carbohydrates in softwood, the relaxation behaviour of cellulose did not follow by that of lignin. The main reason for such discrepancy between the two sets of data is likely attributed to the lack of molecular connectivities and the absence of hemicelluloses that may associate (i.e. lignin carbohydrate complexes)[113-115] these two polymers in wood. Supporting evidence for such observation was obtained by examining their relaxation behaviour with those of softwood, especially beyond pH 10.

The comparison of these plots shows that the T_{1H} trends for the two isolated polymers behave differently (Figure 2.7) while in the case of softwood, the lignin and carbohydrates appeared to be intimately associated with each other (Figure 2.1) since their T_{1H} values followed each other as a function of pH.

Further in our analysis, the overall average rate of T_{1H} for these independent studies was calculated in accordance to equation 2.2 and plotted in Figure 2.8.

$$\left(\frac{1}{T_{1H}}\right)_{O.A.R} = \left(\frac{Wt.Fr.}{T_{1H}}\right)_{Cellulose} + \left(\frac{Wt.Fr.}{T_{1H}}\right)_{Lignin} \qquad [2.2]$$

where; T_{1H} O.A.R= Overall average rate of proton spin-lattice relaxation time
T_{1H} Cellulose = Spin-lattice relaxation time of cellulose; Wt. Fr.= weight fraction ≈ 0.7
T_{1H} Lignin = Spin-lattice relaxation time of lignin; Wt. Fr.= weight fraction ≈ 0.3

The simulated plot of the isolated materials shows an increase in T_{1H} from acidic pH's reaching a maximum near neutrality and a decreasing trend under alkaline conditions. These data indicate that under acidic conditions the molecular rigidity increases while the mobility of these macromolecules increases under alkaline conditions. The measured T_{1H} values as a function of pH when combined mathematically were found to semiquantitatively describe the pH dependence of cellulose and lignin present in solid

wood in the pH range 5 to 10.

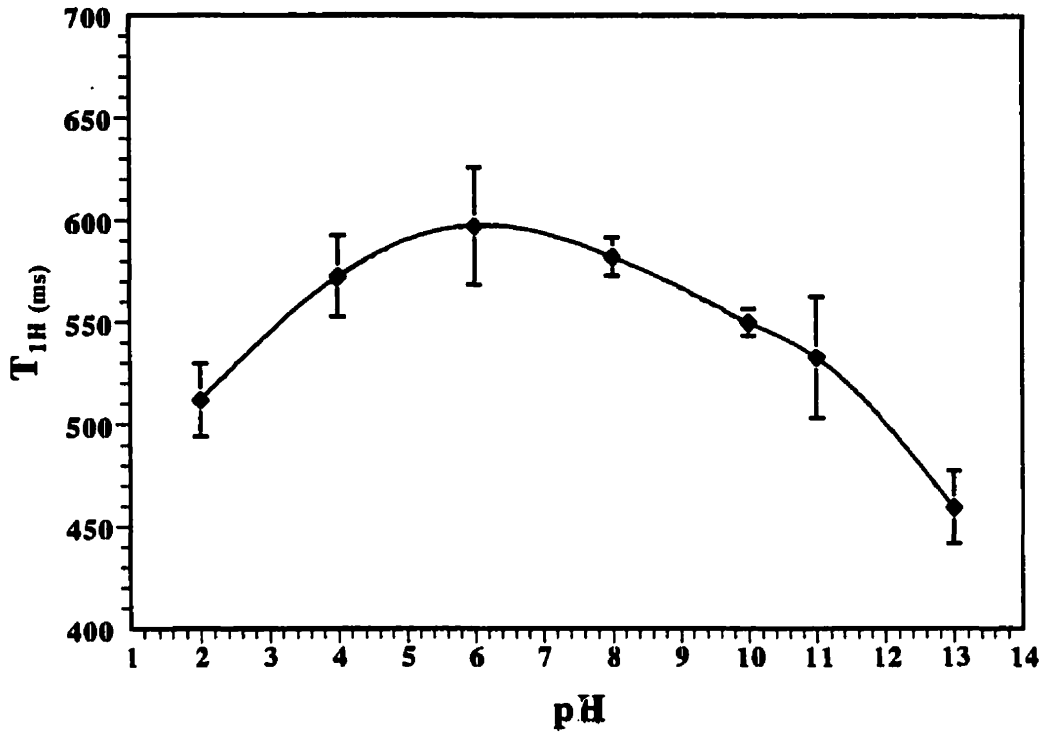

Figure 2.8. The simulated behaviour of overall proton spin-lattice relaxation times (♦) for cuoxam lignin and carbohydrates as a function of pH.

2.4. CONCLUSIONS

Solid-state proton spin-lattice relaxation measurements for carbohydrates and lignin at room temperature and constant moisture over a wide range of pH's were examined. These studies indicated that ionization of various functional groups can influence the mobility of these biopolymers and consequently their physico-chemical properties. The analyses of the T_{1H} data showed that as the pH increased from acidic to near neutrality (2 → 6), the T_{1H} values of carbohydrates and lignin increased, reaching a maximum at pH 6. However, as the pH changed from near neutrality toward alkalinity (6 → 13), the T_{1H} values decreased, promoting the softening of these biopolymers under alkaline conditions.

Having explored the effect of pH on the macromolecular properties of the constituents of wood, we now turn our attention to explore the stereoselective degradation of the arylglycerol-β-aryl ether structures in lignin under kraft pulping conditions. As opposed to the solid-state NMR work carried out in Chapter 2, Chapter 3 used quantitative solution ^{31}P NMR to probe the sought structural changes in lignin.

2.5. REFERENCES

1. Larsson, L. I., and Samuelson, O., Sugars in sulfite spent liquor., Svensk. Papperstidn., 70, 571-575, 1967.

2. Karger, B. L., Snyder, L. R., and Horvath, C., An Introduction to Separation Science., John Wiley & Sons Inc., New York, 1973.

3. Atack, D., Heitner, C., and Stationwala, M. I., Ultra high yield pulping of eastern black spruce., Svensk. Papperstidn., 81, 164-176, 1978.

4. Giertz, H. W., Papermaking properties of spruce chemimechanical pulps-an interim report., Pulp and Paper Mag. Can., 69, Nov. 1, 75-78, 1968.

5. Ford, M. J., and Gardener, P. E., Method of producing high yield chemimechanical pulps., United states Patent 4, 116, 758, Sept. 1978.

6. Ri, S., and Nakano, J., High yield pulp production by a modified sulphite process., J. Jap. Tappi, 28, 7, 38, 1974.

7. Höglund, H., and Bodin, O., Modified thermomechanical pulp., Svensk. Papperstidn., 72, 11, 343, 1976.

8. Atack, D., and Heitner, C., Dynamic mechanical properties of sulphonated Eastern black spruce., International Mechanical Pulping Conference Proceedings., Technical section, CPPA., pp. 1-12, June 1979.

9. Giertz, H. W., Chemimechanical pulping of hardwoods, Proceedings International Symposium on New Forestry Resources for the Pulp and Paper Industry., 244-276, EUCEPA, Madrid, May 1974.

10. Richardson, C. A., and Le Mahieu, J. R., Superground wood from Aspen., Tappi, 48, 6, 344, 1965.

11. Atack, D., Heitner, C., and Karnis, A., Ultra high yield pulping of eastern black spruce. Part 2*., Svensk. Papperstidn., 83, 133-141, 1980.

12. Roberts, J. C., The Chemistry of Paper., The Royal Society of Chemistry, Cambridge, UK., Chapter 6-7, pp. 89-140, 1996.

13. Hartmann, S., and Hahn, E. L., Nuclear doubleresonance spectroscopy., Bull. Am. Phys. Soc., 5, 498, 1959.

14. Andrew, E. R., Bradbury, A., and Eades, R. G., Removal of dipolar broadening of nuclear magic resonance spectra of solids by specimen rotation., Nature, 183, 1802-1803, 1959.

15. Schaefer, J., and Stejskal, E. O., Carbon-13 nuclear magnetic resonance of polymers spinning at the magic angle., J. Am. Chem. Soc., 98, 1031-1032, 1976.

16. Atalla, R. H., Gast, J. C., Sindrof, D. W., Bartuska, V. J., Maciel, G. E., ^{13}C spectra of cellulose polymorphs., J. Am. Chem. Soc., 102, 3249-3251, 1980.

17. Atalla, R. H., Vanderhart, D. J., Native cellulose: a composite of two distinct crystalline forms., Science, 223, 283-285, 1984.

18. Evans, R., Newman, R. H., Roick, U. C., Suckling, I. D., and Wallis, A. F. A., Changes in cellulose crystallinity during kraft pulping. Comparison of infrared, X-ray differaction and solid-state NMR results., Holzforschung, 49, 498-504, 1995.

19. Gerasimowicz, W. V., Hicks, K. B., Pfeffer, P. E., Evidence for the existence of associated lignin-carbohydrate polymers as revealed by carbon-13 CP/MAS solid state NMR spectroscopy., Macromolecules, 17, 2597-2603, 1984.

20. Manders, W., Solid state ^{13}C NMR determination of the syringyl/guaiacyl ration in hardwoods., Holzforschung, 41, 13-18, 1987.

21. Hatfield, G. R., Maciel, G. E., Erbatur, O., Erbatur, G., Qualitative and quantitative analysis of solid lignin samples by carbon-13 nuclear magnetic resonance spectroscopy., Anal. Chem., 59, 172-179, 1987.

22. Kolodziejski, W., Frye, J. S., Maciel, G. E., Carbon-13 nuclear magnetic resonance spectrometry with cross polarization and magic angle spinning for the analysis of lodgepole pine wood., Anal. Chem., 54, 1419-1424, 1982.

23. Willis, J. M., and Herring, F. G., Effect of water in the ^{13}C CP/MAS NMR spectrum of white spruce wood., Macromolecules, 20, 1554-1556, 1987.

24. Nimz, H. H., and Nemr, M., Carbon-13 NMR spectra of lignins, 9. Spin-lattice relaxation times (T1) and determination of interunit linkages in three hardwood lignins (Alnus Glutinsoa, Corylus Avellanus and Acer Pseudoplatanus)., J. Wood Chem. Technol., 2(4), 371-382, 1982.

25. Tekely, P., Vignon, M. R., Cross polarization/Magic angle spinning ^{13}C-NMR characterization of steam exploded poplar wood., J. Wood Chem. Technol., 7(2),

215-228, 1987.

26. Maciel, G. E., O'Donnell, D. J., Ackermann, J. J. H., Hawkins, B. H., Bartuska, V. J., A ^{13}C NMR study of four lignins in the solid and solution states., Makromol. Chem., 182, 2297-2304, 1981.

27. Bartuska, V. T., Maciel, G. E., Bolker, H. I., Fleming, B. I., Structural studies of lignin isolation procedures by ^{13}C NMR., Holzforschung, 34, 214-217, 1980.

28. Solomon, I., Relaxation processes in a system of two spins., Phys. Rev., 99, 559-565, 1955.

29. Schaefer, J., and Stejskal, E. O., Buchdahl, R., Magic-angle ^{13}C NMR analysis of motion in solid glassy polymers., Macromolecules., 10, 384-405, 1977.

30. McBriety, V., J., Douglass, D. C., Recent advances in the NMR of solid polymers., Macromolecules Rev., 16, 295-366, 1981.

31. Havens, J. R., and Koenig, J. L., Applications of high-resolution carbon-13 nuclear magnetic resonance spectroscopy to solid polymers., Appl. Spectrosc., 37(3), 226-249, 1983.

32. Cory, D. G., and Ritchey, W. M., Inversion recovery cross-polarization NMR in solid semicrystalline polymers., Macromolecules, 22, 1161-1615, 1989.

33. McBriety, V., J., Douglass, D. C., and Kwei, T. K., Compatibility in blends of poly(methyl methacrylate) and poly(styrene-co-acrylonitrile). 2. An NMR study., Macromolecules, 11(6), 126-1267, 1978.

34. Grobelny, J., Rice, D. M., Karasz, F. E., MacKnight, W. J., High-resolution solid state carbon-13 nuclear magnetic resonance study of polybenzimidazole/polyimide blends., Macromolecules, 23, 2139-2144, 1990.

35. Van der Hart, D. L., Earl, W. L., Garroway, A. N., Resolution in ^{13}C NMR of organic solids using high-power proton decoupling and magic-angle sample spinning., J. Magn. Reson., 44, 361-401, 1981.

36. Garroway, A. N., Ritchey, W. M., Moniz, W. B., Some molecular motions in epoxy polymers: A ^{13}C solid-state NMR study., Macromolecules, 15, 1051-1063, 1982.

37. Rosh, P. B., Larkey, C. S., Crawford, P. A., The use of liquid and solid state NMR study compatibility with epoxy resins., Polymer Preprints., 22, 274-275, 1981.

38. Hortling, B., Lindberg, J. J., Kanerva, A., Pellinen, J., 6th National NMR Symposium., Abstract of Papers, p. 26, Jyvaskyla 1982.

39. Jelinski, L. W., Dumais, J. J., Watnick, P. I., Bass, S. W., Shephard, L., ^{13}C-NMR of ABS in the solid state. Characterization and relaxation studies., J. Polym. Sci., Polymer Chem. Ed., 20, 3285-3296, 1982.

40. Jelinski, L. W., Chemical shift parameters and molecular motion in Poly(butylene terephthalate) and poly(butylene terephthalate)-containing polymers., Macromolecules, 14, 1341-1345, 1981.

41. Steger, T. R., Schaefer, J., and Stejskal, E. O., McKay, R. A., Molecular motion in polycarbonate and modified polycarbonates., Macromolecules, 13, 1127-1132, 1980.

42. chaefer, J., and Stejskal, E. O., Steger, T. R., Sefcik, M. D., McKay, R. A., Carbon-13 $T_{1\rho}$ experiments on solid glassy polymers., Macromolecules, 13, 1121-1126, 1980.

43. Brown, C. E., Jones, M. B., Cross polarization, magic angle ^{13}C NMR spectroscopy of poly(p-phenylene) and lower oligomers., Polymer Letters Ed., 18, 653-658, 1980.

44. Brown, C. E., Khoury, I., Bezoari, M., Kovacic, R., Characterization of aromatic polymers (Bezenoid and Heterocyclic) by cross-polarization, magic-angle ^{13}C-NMR spectroscopy., J. Polymer. Sci., Polymer Chem. Ed., 20, 1697-1707, 1982.

45. Teeäär, R., Gravitis, J., Erins, P., Pugulis., J., Kulkevics, A., Gromov, V. S., Lippmaa, E., Changes in the phase structure and conformation state of wood components during explosive autohydrolysis., Dolk. Akad. Nauk SSSR, 288(4), 932-935, Phys. Chem., 1986.

46. Teeäär, R., Lippmaa, E., Gravitis, J., Andersons, B., Erins, P., Relaxation study of the native and steam exploded wood supernetwork structure by solid-state high resolution carbon-13 NMR spectrscopy., Khim. Drev., (6), 106-107, 1985.

47. Teeäär, R., Gravitis, J., Andersons, B., and Lippmaa, E., CP/MAS NMR of steam explosion-treated wood and its major constituents., Teubner-Texte zur Physik, 9, 240-249, 1986.

48. Tekely, P., Vignon, M. R., Proton T_1 and T_2 relaxation times of wood components using 13C CP/MAS NMR., J. Polym. Lett., 25 (6), 257-261, 1987.

49. Gravitis, J., Kokorevics, A., Teeäär, R., Zharov, A., Lippmaa, E., Structural changes of wood and its components initiated by the simultaneous action of shear deformation and high pressure., J. Pulp Paper Sci., 17, J119-123, 1991.

50. Newman, R. H., Nuclear magnetic resonance study of spatial relationships between chemical components in wood cell walls., Holzforschung, 46(3), 205-210, 1992.

51. Newman, R. H., Carbon-13 nuclear magnetic resonance studies of molecular motion in wood and paper., 4th Int. Symp. Wood and Pulping Chem., 195-199, Paris, France, 1987.

52. Ni, J., Frazier, C. E., Molecular correlation to macroscopic wood performance using CP/MAS NMR., Holzforschung, 50(4), 327-334, 1996.

53. Hsi, E., Hossfeld, R., and Bryant, R. G., Nuclear magnetic resonance relaxation study of the water absorbed on milled northern white-cedar., J. Coll. Interf. Sci., 62, 389-395, 1977.

54. Riggin, M. T., Sharp, A. R., Kaiser, R., and Schneider, M. H., Transverse NMR relaxation of water in wood., J. Appl. Polym. Sci., 23, 3147-3154, 1979.

55. Carles, J. E., and Scallan, A. M., The determination of the amount of bound water within cellulosic gels by NMR spectroscopy., J. Appl. Polym. Sci., 17, 1855-1865, 1973.

56. Froix, M. F., and Goedde, A. O., The effect of temperature on the cellulose/water interaction from NMR relaxation times., Macromolecules, 9, 428-430, 1976.

57. Kelly, S. S., Rials, T. G., and Glasser, W. G., Relaxation behaviour of the amorphous components of wood., J. Mater. Sci., 22, 617-624, 1987.

58. Sivashinsky, N., and Tanny, G. B., The state of water in swollen ionomers containing sulfonic acid salts., J. Appl. Polym. Sci., 26, 2625-2637, 1981.

59. Sarkanen, K. V., and Ludwig, C. H., In Lignins: Occurrence, Formation, Structure and Reactions., Wiley-Interscience, New York, 1971.

60. Argyropoulos, D. S., Morin, F. G., Probing the macromolecular structure of wood and pulps with proton spin-lattice relaxation time measurements in the solid state., Wood Sci. Technol., 29, 19-30, 1995.

61. Noggle, J. H., and Schirmer, R. E., The Nuclear Overhauser Effect: Chemical

Applications., Academic Press, New York, 1971.

62. Argyropoulos, D. S., Morin, F. G., and Lapcik, L., Magnetic field and temperature effects on the solid state proton spin-lattice relaxation time measurements of wood and pulps., Holzforschung, 49, 115-118, 1995.

63. Froix, M. F., and Nelson, R., The interaction of water with cellulose from nuclear magnetic resonance relaxation times., Macromolecules, 8(6), 726-730, 1975.

64. Sillescu, H., Solid state NMR- A tool for studying molecular motion in polymers., Makromol. Chem., Macromol. Symp., 1, 39-49, 1986.

65. Pearl, I. A., The Chemistry of Lignin; the isolation of lignin, pp. 11-12, Marcel Dekker Inc., New York, 1967 .

66. Weast, R. C., CRC Handbook of Chemistry and Physics, CRC Press, Inc., 58th Ed., p. D-134, 1977-1978.

67. Dean, J. A., Lange's Handbook of Chemistry, McGraw-Hill book company, New York, 12th Ed., pp. 10-81 to 10-85, 1979.

68. Sjöström, E., and Enström, B., A method for the separate determination of sulpho and carboxyl groups in sulphite pulps., Svensk. Papperstidn., 15(3), 55-59, 1966.

69. Yano, S., and Hatakeyama, H., Effect of hydrogen bond formation on dynamic mechanical properties of amorphous cellulose., J. Appl. Polym. Sci., 20, 3221-3231, 1976.

70. Proctor, H. R., The equilibrium of dilute hydrochloric acid and gelatin., J. Chem. Soc., 105, 313-327, 1914.

71. Eisenberg, A., Hird, B., and Moore, R. B., A new multiplet-cluster model for the morphology of random ionomers., Macromolecules, 23(18), 4098-4107, 1990.

72. Akitsu, H., Gril, J., Morooka, T., and Norimoto, M., Dynamic mechanical properties of chemically modified wood (II)., Chemical Modification of Lignocellulosic Proc., Rotorua, New Zealand, 7-8 Nov., pp. 130-139, 1992.

73. Lindberg, J. J., Björkman, A., Salmén, L., and Soljamo, K., Chemically modified wood: Solid-State Cross-Polarization-Magic-Angle Spinning NMR Spectroscopy., Acs. Symp. Ser., No. 489, Ch. 21, pp. 320-328, 1992.

74. Lindström, T., and Carlsson, G., Proc. Eucepa Conf., Warsaw, Poland, 1978.

75. Donnan, F. G., and Harris, A. B., The osmotic pressure and conductivity of aqueous solutions of congo-red, and reversible membrane equilibria., J. Chem. Soc., 99, 1554-1577, 1911.

76. Donnan, F. G., Z. Elektrochem., Theorie der membrangleichgewichte und membranpotentiale bei vorhandensein von nicht dialysierenden elektrolyten., 17, 572-581, 1911.

77. Pu, Q., Gustafson, R., and Sarkanen, K., Donnan equilibria in wood-alkali interactions; Part 3. Theoretical modeling., J. Wood Chem. Technol., 13 (1), 1-24, 1993.

78. Nevell, T. P., and Zeronian, S. H., Cellulose Chemistry and its applications., Ellis Horwood Limited, Halsted Press, New York, p. 27, 1985.

79. Neale, S. M., The swelling of cellulose, and its affinity relations with aqueous solutions: Part I. Experiments on the behaviour of cotton cellulose and regenerated cellulose in sodium hydroxide solution, and their theoretical interpretation., J. Text. Inst., 20, T373-T400, 1929.

80. Neale, S. M., The swelling of cellulose, and its affinity relations with aqueous solutions: Part II. Acidic properties of regenerated cellulose illustrated by the absorption of sodium hydroxide and water from dilute solutions and their consequent swelling., J. Text. Inst., 21, T225, 1930.

81. Neale, S. M., The swelling of cellulose, and its affinity relations with aqueous solutions: Part III. The preferential absorption of sodium hydroxide from dilute solutions as a characteristic property of cellulose, and an indicatiopn of previous mercerisation or other swelling treatment., J. Text. Inst., 22, T320, 1931.

82. Pennings, A. J., and Prins, W., The polyelectrolytic nature of cellulose gels in alkali solutions., J. Polym. Sci., 58, 229-248, 1962.

83. Sarkanen, K. V., and Söderström, K., Studies on acidic dissociation constants of hydroxyl groups in glycosides., Proc. First Cellulose Conf., Cellulose Institute, Syracuse, New York, pp. 15-28, Apr. 1958.

84. Rowell, R. M., Lichtenberg, R. S., and Larsson, P., Stability of acetyl groups in acetylated wood to changes in pH, temperature, and moisture., Chemical Modification of Lignocellulosic Proc., Rotorua, New Zealand, 7-8 Nov., pp. 33-40, 1992.

85. Farrer, J., and Neale, S. M., The distribution of ions between cellulose and solutions of electrolyte., J. Colloid. Sci., 7, 186-195, 1952.

86. Nakano. T., Effects of ionization of side chains of partly succinylated wood on mechanical properties., Chemical Modification of Lignocellulosic Proc., Rotorua, New Zealand, 7-8 Nov., pp. 52-57, 1992.

87. Harris, E. E., A lignin-carbohydrate bond in wood., Tappi, 36(9), 402-405, 1953.

88. Glasser, W. G., Sarkanen, S., Lignin: Properties and Materials., Chapter 2. Structure and properties of the lignin-carbohydrate comples polymer as an amphipathic substance., ACS Sym. Ser., 397, Toronto, Canada, June 5-11, pp. 11-28, 1989.

89. Iversen, T., Lignin-carbohydrate bonds in a lignin-carbohydrate complex isolated from spruce., J. Wood Sci. Technol., 19, 243-251, 1985.

90. Eriksson, Ö., and Lindgren, B. O., About he linkage between lignin and hemicelluloses in wood., Svensk. Papperstidn., 2, 59-63, 1977.

91. Eriksson, Ö., and Goring, D. A. I., Structural studies on the chemical bonds between lignins and carbohydrates in spruce wood., J. Wood Sci. Technol., 14, 267-279, 1980.

92. Lundquist, K., Simonson, R., Tingsvik, K., Lignin carbohydrate linkages in milled wood lignin preparation from spruce wood., Svensk. Papperstidn., 86, 44-47, 1982.

93. Timell, T. E., Recent progress in the chemistry of wood hemicelluloses., J. Wood Sci. Technol., 1, 45-70, 1967.

94. Manley, R. St. J., Molecular morphology of cellulose., J. polym. Sci., 9(A2), 1025-1059, 1971.

95. Horii, F., Kitamaru, R., CP/MAS carbon-13 NMR study of spin relaxation phenomena of cellulose containing crystalline and non-crystalline components., J. Carbohyr. Chem., 2(4), 641-662, 1984.

96. Westman, L., Swelling and mechanical properties of cellulose hydrogels., Thesis (D. Tech.), Royal Institute of Technology, Department of Physical Technology Swedish Forest Products Research Laboratory (STFI), Stockholm, Sweden, 1980.

97. Westman, L., and Lindström, T., Swelling and mechanical properties of cellulose hydrogels. Part I. Preparation, characterization, and swelling behaviour., J. Appl. Polym. Sci., 26, 2519-2532., 1981.

98. Westman, L., and Lindström, T., Swelling and mechanical properties of cellulose hydrogels. Part II. The relation between the degree of swelling and the creep compliance., J. Appl. Polym. Sci., 26, 2533-2544., 1981.

99. Westman, L., and Lindström, T., Swelling and mechanical properties of cellulose hydrogels. Part III. Temperature effect on the swelling and compliance levels studied by dilatometry and ^{1}H-NMR spectroscopy., J. Appl. Polym. Sci., 26, 2545-2559, 1981.

100. Westman, L., and Lindström, T., Swelling and mechanical properties of cellulose hydrogels. Part IV. Kinetics of swelling in liquid water., J. Appl. Polym. Sci., 26, 2561-2572, 1981.

101. Westman, L., and Lindström, T., Swelling and mechanical properties of cellulose hydrogels. Part V. Swelling in concentrated alkaline solutions., J. Appl. Polym. Sci., Appl. Polym. Symp., 37, 363-376, 1983.

102. Brown, W., Stilbs, P., and Lindström, T., Self-diffusion of small molecules in cellulose gels using FT-pulsed field gradient NMR., J. Appl. Polym. Sci., 29, 823-827, 1984.

103. Nielsen, O. F., Lindström, T., and Lund, P. A., Low-frequency (30-400 cm^{-1}). Raman spectra of water in cellulose gels., Acta Chem. Scand., Ser. A, 36, 623-625, 1982.

104. Sandell, L. S., and Luner, P., Flocculation of microcrystalline cellulose with cationic ionene polymers., J. Appl. Polym. Sci., 18, 2075-2083, 1974.

105. Pu, Q., and Sarkanen, K., Donnan equilibria in wood-alkali interactions. Part 1. Quantitative determination of carboxyl-, carboxyl ester and phenolic hydroxyl groups., J. Wood Chem. Technol., 9(3), 293-312, 1989.

106. Pu, Q., Gustafson, R., and Sarkanen, K., Donnan equilibria in wood-alkali interactions. Part 3. Theoretical modeling., J. Wood Chem. Technol., 13(1), 1-24, 1993.

107. Gupta, P. R., Goring, D. A. I., Physicochemical studies of alkali lignins (Part I and II)., Can. J. Chem., 38, 248-258, 259-269, 1960.

108. Brauns, F. E., The chemistry of lignin., Academic Press, New York, 1952.

109. Rezanowich, A., Yean, W. Q., Goring, D. A. I., The molecular properties of milled wood and dioxane lignins: sedimentation, diffusion, viscosity, refractive index increment and UV absorption., Svensk. Papperstidn., 66(5), 141-149, 1963.

110. Lindström, T., Westman, L., The colloidal behaviour of kraft lignin. Part IV: Syneresis and hysteresis in swelling of kraft lignin gels., Colloid & polym. Sci., 260, 594-598, 1982.

111. Flory, P. J., Principle of polymer chemistry., Chap. XIII., Phase equilibria in polymer system. pp. 584-589., Cornell University Press, Ithaca, New York, 1953.

112. Akim, L. G., Fedulina, T. G., and Shevchenko, S. M., ^{13}C NMR of lignins in aqueous alkali: I. Ionisation effect on the spectra of model compounds and milled wood lignins., Holzforschung, 50, 237-244, 1996.

113. Watanabe, T., Kaizu, S., and Koshijima, T., Binding sites of carbohydrates moities toward lignin in "lignin-carbohydrate complex" from Pinus densiflora wood., Chem. Lett., Chemi. Soc., Japan., 1871-1874, 1986.

114. Watanabe, T., Ohnishi, J., Yamasaki, Y., Kaizu, S., and Koshijima, T., Binding-site analysis of the ether linkages between lignin and hemicelluloses in lignin-carbohydrate complexes by DDQ-Oxidation., Agric. Biol. Chem., 53 (8), 2233-2252, 1989.

115. Watanabe, T., and Koshijima, T., Structural features of 2,3-Dichloro-5,6-dicyano-1,4-benzoquinone-oxidized lignin acetate revealed by carbon-13 nuclear magnetic resonance spectroscopy., Mokuzai Gakkaishi., 35 (2), 130-134, 1989.

Chapter 3

Determination of Thermodynamic Parameters Governing the Stereoselective Degradation of Arylglycerol-β-aryl Ether Bonds in Milled Wood Lignin Under Kraft Pulping Conditions

3.0. ABSTRACT

During this investigation, softwood (*picea mariana*) milled wood lignin was subjected to kraft pulping conditions at the temperature range 100-160 °C, for variable lengths of time. After quantitative isolation of the treated lignins, they were subjected to ^{31}P NMR analyses which allowed the absolute rates of scission of the *erythro* and *threo* diastereomers of the arylglycerol-β-aryl ether structures present in lignin to be derived. The plots of the kinetic data revealed that two kinetic regimes operate i.e. an initial fast phase that is followed by another slower phase. In agreement with previous accounts, the rate constants for these scission reactions were found to follow a pseudo-first-order rate law, during both phases. Rate constant data obtained during this effort, invariably indicated that the *erythro* isomers of the β-O-4 units of softwood milled wood lignin cleave faster than their *threo* counterparts during both phases. At elevated temperatures (160 °C) the difference was found to be augmented. The general stability of the *threo* diastereomers toward kraft pulping seems to be the manifestation of a considerably slower reaction of the pulping reagents with the *threo* diastereomers of the β-aryl ethers. Arrhenius and Erying plots of these data supplied the complete profile of thermodynamic parameters governing this commercially important ether scission reaction.

3.1. INTRODUCTION

The degradation of lignin under kraft pulping conditions is known to be related to its reactivity[1, 2], rather than its accessibility[3] to the pulping reagents. The faster delignification rate of hardwoods compared to softwoods lends support to such observations. This is the case not only because hardwoods are of lower lignin content but also due to the presence of the syringyl units in lignin[4]. More specifically, the structural elements of the lignin in hardwoods are composed of different proportions of syringyl and guaiacyl units[5], while those in softwoods are exclusively composed of guaiacyl units. Consequently, such a variation in the arylglycerol-β-aryl ether (β-O-4) structures, which account for more than 40% of the repeating units in lignin[4, 6], plays an important role toward controlling its reactivity during kraft pulping.

In order to avoid excessive carbohydrate degradation, commercial kraft pulping protocols are typically terminated at a lignin content of 4-5% for softwoods and 3% for hardwoods. Structural studies of the residual lignin remaining with the fibre at this stage have shown that significant amounts of arylglycerol-β-aryl ether structures[7, 8] are still present. Lignin-carbohydrate linkages[9-12], lignin condensation reactions[13-15], aryl group migration reactions[16, 17], and stereochemical and thermodynamic considerations affecting the stability of the β-O-4 bonds[10, 14, 16] are all factors that need to be explored in detail if we are to arrive at a comprehensive description of the chemistry of the process.

The presence of two asymmetric carbon centres within the arylglycerol-β-aryl ether moieties in lignin, allows for the existence of *erythro* and *threo* diastereoisomers. Softwood lignins have been shown to contain equal amounts of *erythro* and *threo* diastereomers[18-22], while the *erythro* diastereomers predominate in hardwood lignins. The reason for the predominance of the *erythro* diastereomers in hardwoods has been rationalized on the basis of the extensive content of syringyl units in such species which exist preferentially in their *erythro* forms[19, 23-25]. Consequently, the efficiency of a delignification reaction is governed by the chemical and stereochemical considerations that affect the scission of the predominant arylglycerol-β-aryl ether (β-O-4) structures of lignin.

The *erythro* and *threo* forms of the arylglycerol-β-aryl ether structures of lignin and several model compounds have been investigated by using a variety of techniques, such as X-ray crystallography[26], ozonation[21, 27, 28], and a variety of one- and two-dimensional nuclear magnetic resonance spectroscopic methods[19, 20, 22, 29, 30].

In particular, ozonation has been proved[21] to be a powerful means to obtain reliable values of *erythro/threo* ratios for insoluble samples such as wood meal, pulps, or Klason lignins. Unlike other oxidative degradation methods used in lignin chemistry, such as nitrobenzene and permanganate oxidations, which shorten the lignin side chain to an aldehyde or a carboxylic acid group, ozonation provides a significant amount of information about the side chain structures[31] of lignin. Extensive ozonation of lignin destroys its aromatic moieties, but preserves the side chains in the form of identifiable mono- and dicarboxcylic acids. More specifically, the side chains of the arylglycerol-β-aryl ether moieties, after saponification with aqueous alkali, can be recovered and quantified in the form of erythronic and threonic acids according to the reaction sequence of Figure 3.1. Using this technique Taneda et al.[27] have monitored the relative changes of the *erythro/threo* ratios of residual lignin at different extents of lignin degradation under kraft pulping conditions. They reported that the *threo* isomers can exist longer during the delignification treatment.

This method has been used successfully for the determination of *erythro/threo* ratios of a variety of lignocellulosic materials and lignins of different botanical origin (Table 3.1)[31, 32].

Proton-NMR spectroscopy has also been used for the determination of the distribution of the *erythro* and *threo* diastereomers in β-O-4 structures. Ralph and Helm[30] have demonstrated that such a method can be applied with precision on a series of lignin model compounds, while, Hauteville et al.[20] used proton NMR spectroscopy to examine the stereochemical features of β-O-4 structures of spruce and birch lignins. The latter investigators reported that the *erythro/threo* ratio of these structures in spruce lignin exist in equal amounts, while the *erythro* diastereomers predominated in birch lignin.

Robert et al.[29] have paved the way in using ^{13}C NMR spectroscopy for the same

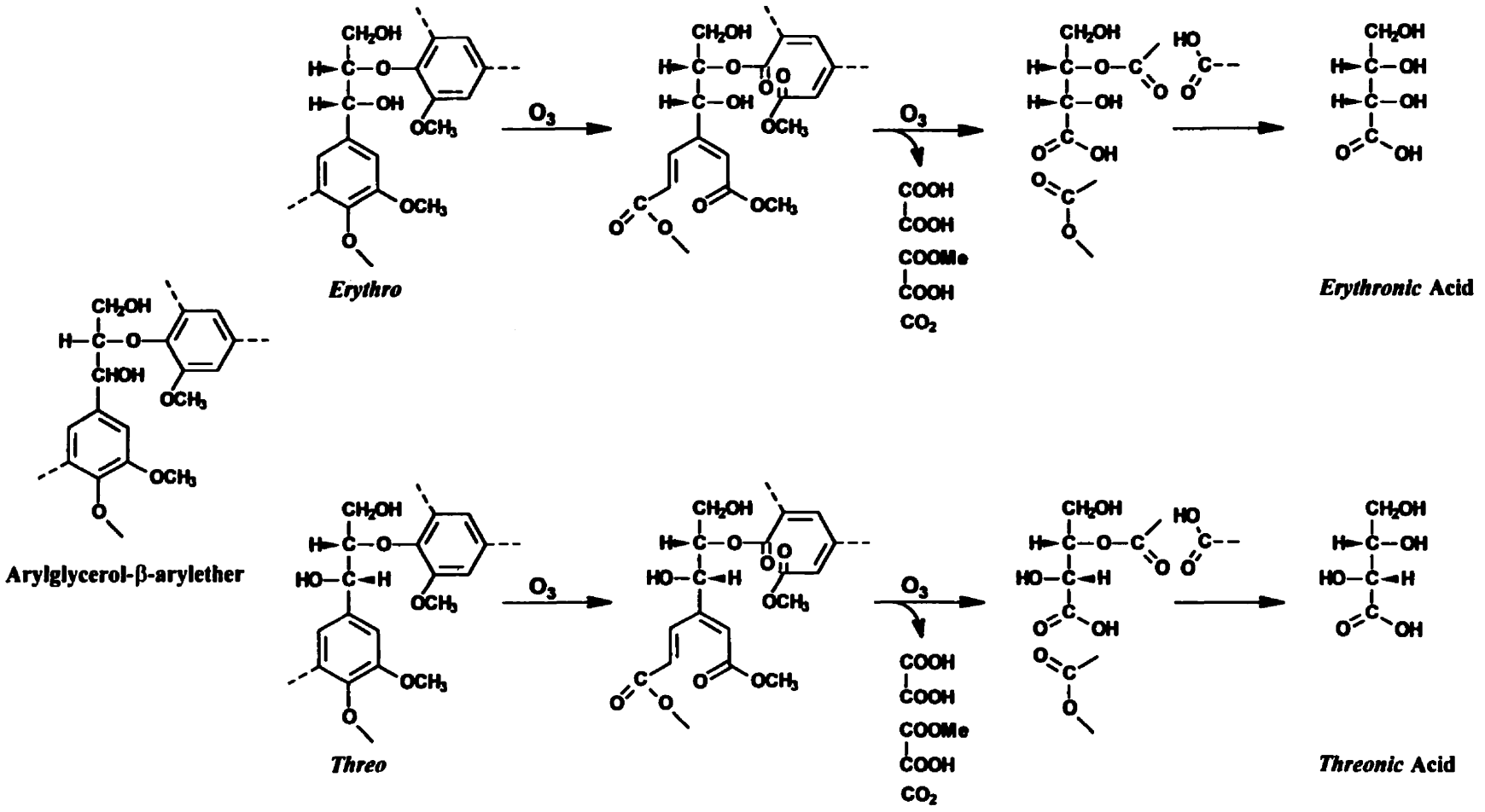

Figure 3.1. Reaction sequences operating during the ozonation of arylglycerol-β-O-4 structures. The amounts of *erythronic* and *threonic* acids provide valuable information on the abundance of the two diastereomers in the sample.

Table 3.1. *Erythro/threo* ratios for various isolated and *in situ* lignins determined by ozonation[32].

Substrate	Ozonation time (min)	E/T ratio
Lignins		
Kraft lignin	6	0.75
Klason lignin *Tsuga heterophylla*	18	0.76
Klason lignin *Populus deltoides*	18	0.78
Soda lignin *P. deltoides*	6	1.94
Native spruce Lignin	6	0.79
Native spruce Lignin	18	0.88
Native spruce Lignin	40	0.82
MWL *Corchorus capsularis fiber*	6	2.18
MWL *C. capsularis wood*	6	1.84
C.capsularis fiber lignin (enzymatic)	6	2.00
C.capsularis wood lignin (enzymatic)	6	2.06
Wood meals		
Norway spruce	40	1.05
Norway spruce (ozon. in gl. acetic acid)	40	1.03
Tsuga heterophylla	30	1.02
Tsuga heterophylla	40	1.27
Tsuga heterophylla	60	1.01
Tsuga hetcrophylla (compression wood)	40	1.36
Pseudotsuga menziesii	40	1.01
Populus deltoides	20	2.72
Populus deltoides	40	3.03
Arbutus menziesii tension sapwood	40	3.69
Liquidambar styraciflua	40	2.86
Eucalyptus gummifera	40	2.60
E. grandis	40	2.45
Corchorus capsularis fiber	40	2.41
C. capsularis wood	40	2.02
Grasses		
Bagasse	40	1.92
Wheat straw	40	1.88
Wheat straw (saponified)	40	1.94
Pulps		
Soda pulp (cottonwood)	40	3.05
Bagasse pulp (1st stage delignif.)	40	1.94
Wheat straw pulp (1st stage delignif.)	40	2.25

purpose. This was accomplished by examining several lignin model compounds and the two-dimensional (INADEQUATE) spectra of aspen milled wood lignin. Nimz et al.[19] also used ^{13}C NMR spectroscopy to probe the same stereochemical details in beech lignins. Their results implied that in beech lignin the *erythro* β-O-syringyl ethers are by far more predominant. Kringstad and Mörk[33], also using ^{13}C NMR spectroscopy, reported that the dissolved kraft lignin from spruce wood contained higher amounts of *threo* than *erythro* units.

In recent years a new form of spectroscopy has emerged that allows, amongst others, the quantitative routine determination of the absolute amounts of the *erythro* and *threo* units in soluble lignin preparations[34-38]. This is achieved by the quantitative phosphitylation of all -OH groups in lignin followed by quantitative ^{31}P acquisition.

The overall phosphitylation reaction of labile protons used is depicted as follows:

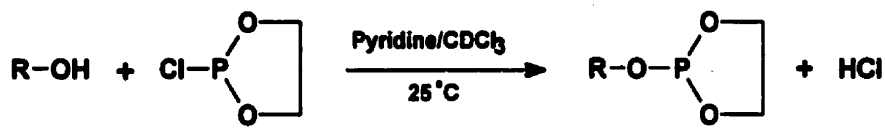

Where R = Residues of Phenols, Alcohols
Aldehydes, Sugars, Carboxylic Acids
and other hydroxyl containing lignin moieties

Figure 3.2. The derivatization reaction of 1, 3, 2-dioxaphospholanyl chloride (I) with compounds containing labile hydrogens.

Quantitative ^{31}P NMR offers this facility with significant advantages over ^{1}H and ^{13}C NMR spectroscopies, including excellent signal dispersion, rapid acquisition protocols and most significantly, precise quantitative information due to the use of internal standards[34-38]. This novel and quantitative tool has been employed for the quantitative determination of lignin functional groups[37], i.e. the three principal forms of phenolic hydroxyl groups, *p*-hydroxyphenyl, guaiacyl, and syringyl, primary hydroxyls, carboxylic acids, and the two diastereomeric forms of arylglycerol-β-arylether units. All these

moieties present in lignins can be determined from a single quantitative ^{31}P NMR experiment after derivatization with appropriate phosphitylating reagents.

A typical quantitative ^{31}P NMR spectrum and signal assignment of softwood milled wood lignin phosphitylated with (I) is shown in Figure 3.3;

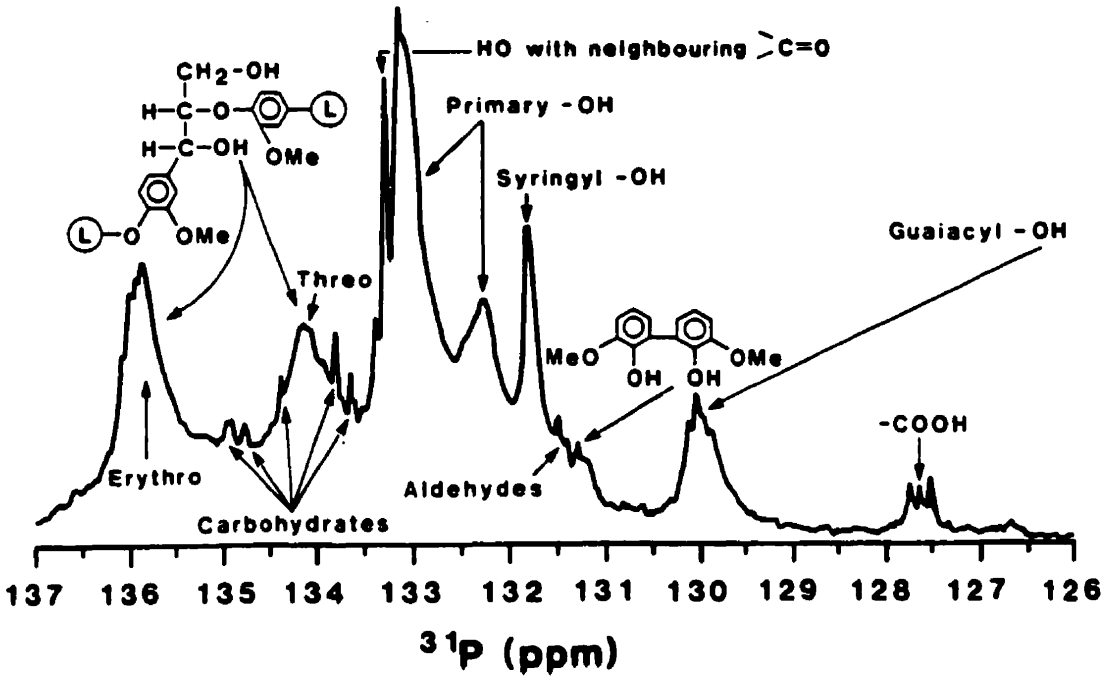

Figure 3.3. Quantitative ^{31}P NMR spectrum and signal assignment of birch dioxane lignin after derivatization with (I)[37].

The signals due to the *erythro* and *threo* forms of the β-O-4 units for isolated softwood and hardwood lignins[39] and model compounds[34] have been carefully assigned. Further evidence substantiating these assignments was sought by specifically alkylating[37] these positions in lignin. More specifically, the methylation of the *alpha* hydroxyl groups in β-O-4 structures (proposed by Adler et al.[40]) caused the complete elimination of two ^{31}P NMR signals at 135.0 and 134.2 ppm attributed to the *erythro* and *threo*

configurations of the arylglycerol-β-arylether structures respectively.

A number of applications of this technique toward studying specific details of lignin structure have appeared in the recent literature. Jiang and Argyropoulos[41] have used this form of spectroscopy to study the stereospecificity of the degradation of the β-O-4 bonds, while Froass et al.[42] used the technique to unravel salient features of the degradation of β-O-4 bonds under conventional and modified pulping protocols. This methodology was used extensively by Saake et al.[43] to determine the *erythro* to *threo* ratios for a series of synthetic lignins as a function of their molar mass.

The numerous advantages offered by quantitative ^{31}P NMR have paved the way toward detailed enquiries, which involve large arrays of repetitive kinetic experiments. As such, the kinetics of scission of β-O-4 bonds under commercial kraft pulping conditions can now be investigated by using milled wood lignin and this novel form of spectroscopy. More specifically, in this effort we will discuss our measurements of the absolute rates of scission of the *erythro* and *threo* diastereomers of the β-O-4 structures in milled wood lignin, as a function of time and temperature. These studies allowed the determination of the fundamental thermodynamic parameters governing the stereoselective degradation of these highly abundant structural elements in lignin.

3.2. EXPERIMENTAL

3.2.1. Materials and Methods

3.2.1.1. Preparation

Isolation of Milled Wood Lignin

The extraction and purification of milled wood lignin was carried out according to the Björkman method[44]. Initially 150-200 g of wood chips were pulverized to 100 mesh and then subjected to ball milling (3 weeks) using a porcelain ball mill. The wood meal was then dispersed in 3L of dioxane containing 4.0% water. The suspension was stirred with a magnetic bar for 3 weeks. The wood meal was then separated and discarded from the dioxane solution by centrifugation. The dioxane solution was evaporated under reduced pressure. The resulting residue was dissolved in acetic acid (20 mL per gram of lignin) containing 10% water. This solution was then added to water (250 mL per gram of lignin) while stirring. This material was then washed by centrifugation with occasional shaking of the vessel to distribute the lignin. After evaporating the water with a stream of air, the isolated residue was dissolved in (2:1 v/v) 1,2-dichloroethane/ethanol (20 mL per gram of lignin). This solution was added dropwise to diethyl ether (250 mL per gram of lignin). The material was then centrifuged and washed after decanting the ether. This step was repeated 2-3 times in which, each washing was allowed to stand overnight. The final products were washed once with hexane and the precipitate was first dried in air and then over drierite in vacuo. The elemental analysis of the resulting material was carbon 60.86%, hydrogen 5.71%, and methoxyl 15.45%.

3.2.1.2. Reactions

Treatment of Milled Wood Lignin Under Kraft Pulping Conditions

Initially, a white liquor solution was prepared containing 5.43 g of sodium hydroxide (NaOH as Na_2O) and 1.6 g of sodium sulphide (Na_2S as Na_2O) per 100 mL deionized water with active alkali and sulfidity of 70.38 g/L and 22.92%, respectively. This solution was then mixed with an equal volume of pure dioxane. During a typical

experiment, the softwood milled wood lignin (0.1 g) was dissolved in 1.33 g of the above solution (approximately simulating a liquor/wood ratio of 4/1). The reaction was carried out in a 10 mL stainless steel bomb whose air was displaced by nitrogen. The kraft cooking was simulated by heating and occasionally shaking the bomb in an oil bath preheated to the desired temperature for a specific time. At the end of the reaction period, the bomb was cooled with cold water and its contents were acidified to pH 2 using dilute hydrochloric acid (0.2M HCl). The precipitate was allowed to settle overnight. It was then collected by centrifugation and washed with acidified water to remove the inorganic salts. The precipitated degraded lignin was then freeze dried and brought to constant weight at room temperature under reduced pressure. This material accounted for approximately 80% of the total weight.

However, in an effort to isolate the rest 20%, the solution containing the water soluble low molecular weight lignin, resulting from the first aqueous acidic precipitation, was allowed to dry at room temperature. The remaining low molecular weight lignin was extracted by the addition of 10-15 mL of high purity tetrahydrofuran. This was followed by evaporation of the solvent to a fine viscous residue, and dropwise addition to 20 mL of diethyl ether.

This step was repeated 2-3 times allowing the collection of more lignin, free from inorganic salts. Finally, the diethyl ether was evaporated and the remaining lignin was freeze dried. These samples after being brought to constant weight under reduced pressure accounted for almost 16% of the starting lignin. The two sets of the degraded lignin samples collected, were then mixed thoroughly prior to subsequent analyses and accurately weighted. The ^{31}P NMR data collected was converted from mol/g to mol/L by using the relation below:

$$\frac{[\textit{Functional group determined by } ^{31}P \textit{ NMR (mol/g)}] \; X \; [\textit{Amount of isolated lignin (g)}]}{[\textit{Volume of initial cooking liquor (L)}]}$$

3.2.1.3. Instrumentation

Quantitative ^{31}P NMR Spectroscopy

1,3,2 dioxaphospholanyl chloride was used as the phosphitylation reagent. Approximately 30.0 mg of dry lignin was weighed into a 2 mL volumetric flask. Then, 800μL of a solvent mixture containing pyridine and $CDCl_3$ at a volume ratio of 1.6/1 were added. The mixture was stirred with a magnetic bar until the lignin was fully dissolved. Following the addition of 100 μL of a solution containing both bisphenol-A as the internal standard, and chromium acetylacetonate as the relaxation reagent were added. Finally, 100μL of 1,3,2 dioxaphospholanyl chloride were added and the flask was sealed and shaken to ensure thorough mixing. The ^{31}P NMR spectra were obtained by using inverse gated decoupling on a Varian XL-300 FT-NMR spectrometer operating at 121.5 MHz. The internal deuterium lock was provided by the deuterium atoms present in the deuterated chloroform, used as the solvent. The external standard was 85% H_3PO_4. All downfield shifts from H_3PO_4 were considered positive. A sweep width of 10000 Hz was observed and spectra were accumulated with a time delay of 10 sec between successive pulses. Pulse width corresponding to a 45° flip angle and a line broadening of 2 Hz was used for acquiring the processing of the spectra. For the 45° flip angle a series of experiments showed that there was no further increase in signal intensity after a 7 sec pulse delay was applied. All chemical shifts reported are relative to the dimeric model compound with water which has been observed to give a sharp ^{31}P signal at 121.1 ppm[38].

3.3. RESULTS and DISCUSSION

During this investigation softwood (*picea mariana*) milled wood lignin was subjected to kraft pulping conditions at a temperature range varying from 100-160 °C, for variable lengths of time. Each isothermal set of measurements involved eight samples of milled wood lignin being exposed at the set temperature for variable lengths of time. Since the rate of most chemical reactions increase as the temperature rises, the actual reaction times were shortened as the temperature was increased. This was done in order to avoid excessive lignin degradation at the high end of the temperature range. Efforts at quantitatively isolating the lignin after the reaction were also made in order to ensure that most of the degraded low molecular weight fragments were included in the quantitative ^{31}P NMR analyses that followed. Care was also exercised to integrate all NMR spectra acquired at precisely identical chemical shift ranges (126-138 ppm) so that the derived information will be free of artifacts introduced from such variations.

The kinetic data describing the actual consumption of both stereoisomers for the arylglycerol-β-aryl ethers in milled wood lignin under kraft pulping conditions is tabulated in Table 3.2. The isothermal kinetic data (at 100 °C) has been plotted in Figure 3.4. A closer examination of these plots reveals that for the actual process of scission of these ether bonds two kinetic regimes operate. An initial fast phase that is followed by another slower phase. We have termed these two phases as "initial" and "bulk" in accordance with the terminology used to describe the kinetics of pulping processes.

These data were then fitted to different kinetic expressions in order to determine the sought rate constants. As such, the rate constants (k) for the reaction describing the cleavage of arylglycerol-β-aryl ether linkages during both stages were found (on the basis of correlation coefficients) to follow a pseudo-first-order rate law, in agreement with the accounts of Gierer and Ljunggren[45].

Table 3.2. Kinetic data obtained by quantitative ^{31}P NMR spectroscopy for the concentration of *erythro* and *threo* units as a function of different treatment intensities.

Temp. °C	Reaction time $_{(min)}$	*Erythro* x 10^2 $_{(mol/L)}$	*Threo* x 10^2 $_{(mol/L)}$	E/T ratio
25	-----	8.79	8.66	1.02
	120	8.09	8.16	0.99
	150	7.46	7.80	0.96
100	15	7.00	7.16	0.98
	30	6.18	6.81	0.91
	45	5.48	6.44	0.85
	60	4.77	6.11	0.78
	75	4.43	6.03	0.73
	150	4.37	6.05	0.72
	225	4.30	6.07	0.71
	300	4.22	6.10	0.69
120	10	5.95	6.82	0.87
	20	5.11	6.29	0.81
	30	4.40	5.78	0.76
	40	3.81	5.29	0.72
	60	3.61	5.20	0.69
	120	3.43	5.14	0.67
	180	3.25	5.08	0.64
	240	3.09	5.00	0.62
140	5	5.69	6.20	0.92
	10	4.95	5.80	0.85
	20	3.90	4.90	0.80
	30	3.13	4.08	0.77
	45	3.02	4.30	0.70
	90	2.55	3.99	0.64
	135	2.27	3.55	0.64
	180	1.94	3.26	0.59
160	5	3.39	5.37	0.63
	10	2.67	4.44	0.60
	15	2.15	3.68	0.58
	20	1.82	3.26	0.56
	30	1.59	2.50	0.63
	60	1.14	1.86	0.61
	90	0.77	1.39	0.55
	120	0.49	0.96	0.51

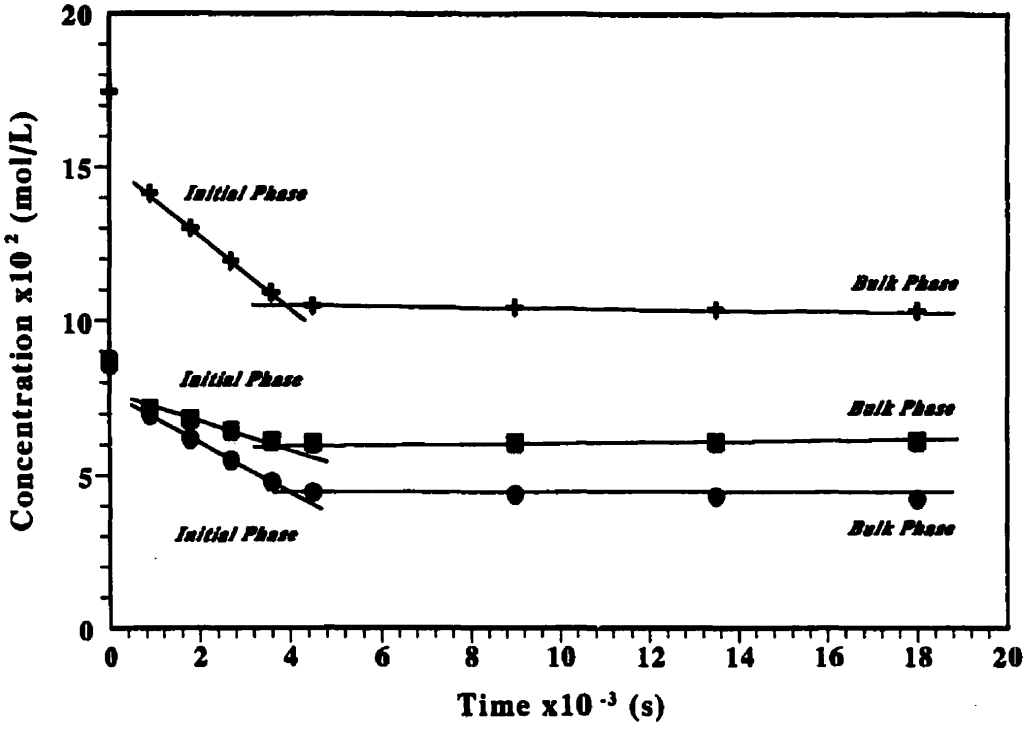

Figure 3.4. The plot of concentration vs. time describing the degradation of *erythro*(●) and *threo*(■) isomers, and the overall arylglycerol-β-ether(+) structures in milled wood lignin under homogeneous kraft pulping conditions at 100°C.

Subsequently, by plotting ln k versus 1/T, the energy of activation was calculated on the basis of the Arrhenius equation [3.1].

$$k = A\, e^{\left(\frac{-E_a}{RT}\right)} \qquad [3.1]$$

where:

A= *Pre-exponential factor*
E_a= *Activation energy*
R= *Gas constant*

This equation relates the rate constant k of a chemical reaction to the absolute temperature T (in K). It describes the behaviour of a vast number of chemical reactions amazingly well, particularly over a fairly small temperature range, but in some instances

over as large a range as 100 degrees[46, 47]. Thus the plot of ln k vs T^{-1} is linear, with slope $-E_a/R$ and intercept ln$A$.

A similar relationship is also derived by the absolute reaction rate theory, which is used almost exclusively toward understanding, the kinetics of reactions in solution[48]. The activated complex in the transition state is reached by reactants in the initial state as the highest point of the most favourable reaction path on the potential energy surface.

The formation of the activated complex may be regarded as an equilibrium process involving an "almost" normal molecule (almost, since it is short by one mode of vibrational energy). The free energy of activation $\Delta G^{1/T}$ can therefore be defined as in normal thermodynamics,

$$\Delta G^{\frac{1}{T}} = -RT\, lnK^{\frac{1}{T}} = \Delta H^{\frac{1}{T}} - T\Delta S^{\frac{1}{T}} \qquad [3.2]$$

leading to

$$k = \frac{\kappa T}{h} \exp\left(\frac{-\Delta G^{\frac{1}{T}}}{RT}\right) = \frac{\kappa T}{h} \exp\left(\frac{-\Delta H^{\frac{1}{T}}}{RT}\right) \exp\left(\frac{\Delta S^{\frac{1}{T}}}{R}\right) \qquad [3.3]$$

where:

$\Delta H^{1/T}$ = *Enthalpy of activation*
$\Delta S^{1/T}$ = *Entropy of activation*
κ = *Boltzmann's constant*
h = *Planck's Constant*

Equation **[3.3]** dictates that a plot of ln(k/T) against 1/T is linear, with a slope, $-\Delta H^{1/T}/R$ and an intercept (ln κ/h + $\Delta S^{1/T}/R$)=(23.8 + $\Delta S^{1/T}/R$). This is sometimes referred to as the Eyring relationship. When applied, both Arrhenius and Eyring plots are known to give very similar results.

Most investigators are content to use the best linear plots of ln$k$ or ln(k/T) vs T^{-1} in estimating E_a or $\Delta H^{1/T}$ values, and to assume that these are constant over a narrow

temperature range[49].

These equations were thus employed for obtaining the energy of activation, enthalpy, entropy, and Gibbs free energy of activation for the reaction pathways of the *erythro* and *threo* cleavage of the arylglycerol-β-aryl ether structures present in softwood milled wood lignin during both initial and bulk phase.

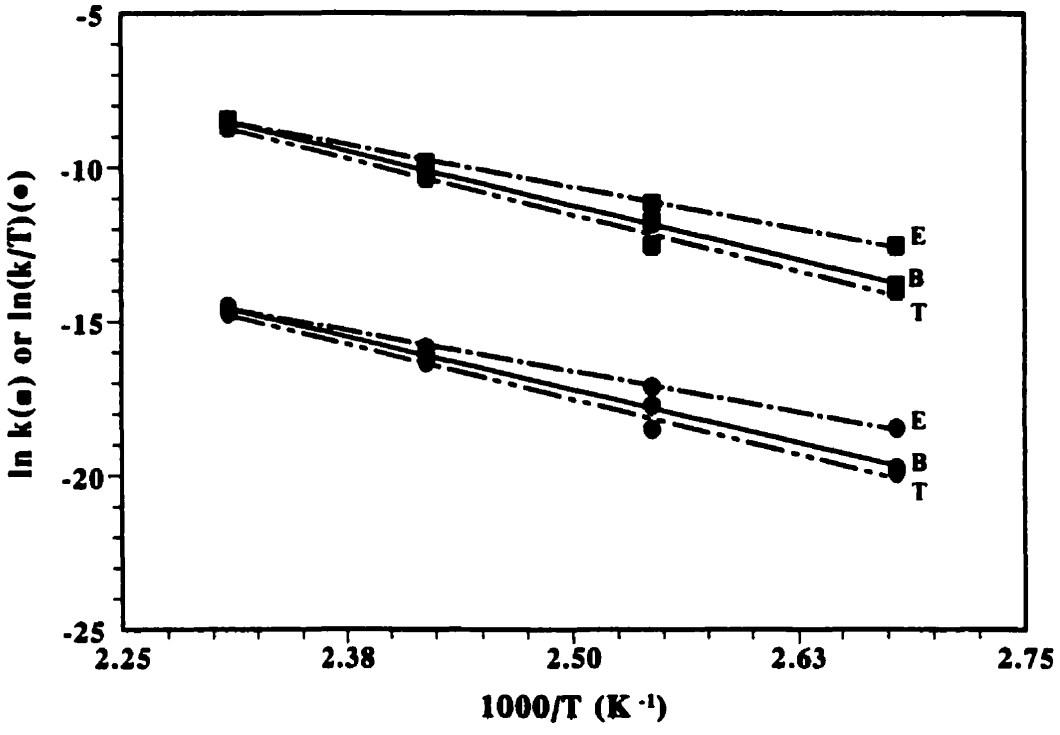

Figure 3.5. Arrhenius(■) and Eryring (●) plots for the determination of the energy of activation, enthalpy of activation, and entropy of activation governing the cleavage of *erythro* (E) and *threo*(T) isomers and the overall arylglycerol-β-aryl ether structures (B) in milled wood lignin under homogeneous kraft pulping conditions during the bulk phase.

Experiments with both phenolic and non-phenolic β-aryl ether model compounds have shown how lignin structures may fragment in alkali, with the subsequent generation of new phenolic hydroxyl groups[50]. For example, in Figure 3.6, the non-phenolic β-aryl ether structure (IA) undergoes hydrolysis in alkali if it contains a free α- or γ- hydroxyl groups (R=OCH_3), or if the α position bears a carbonyl group[51]. The mechanism of this

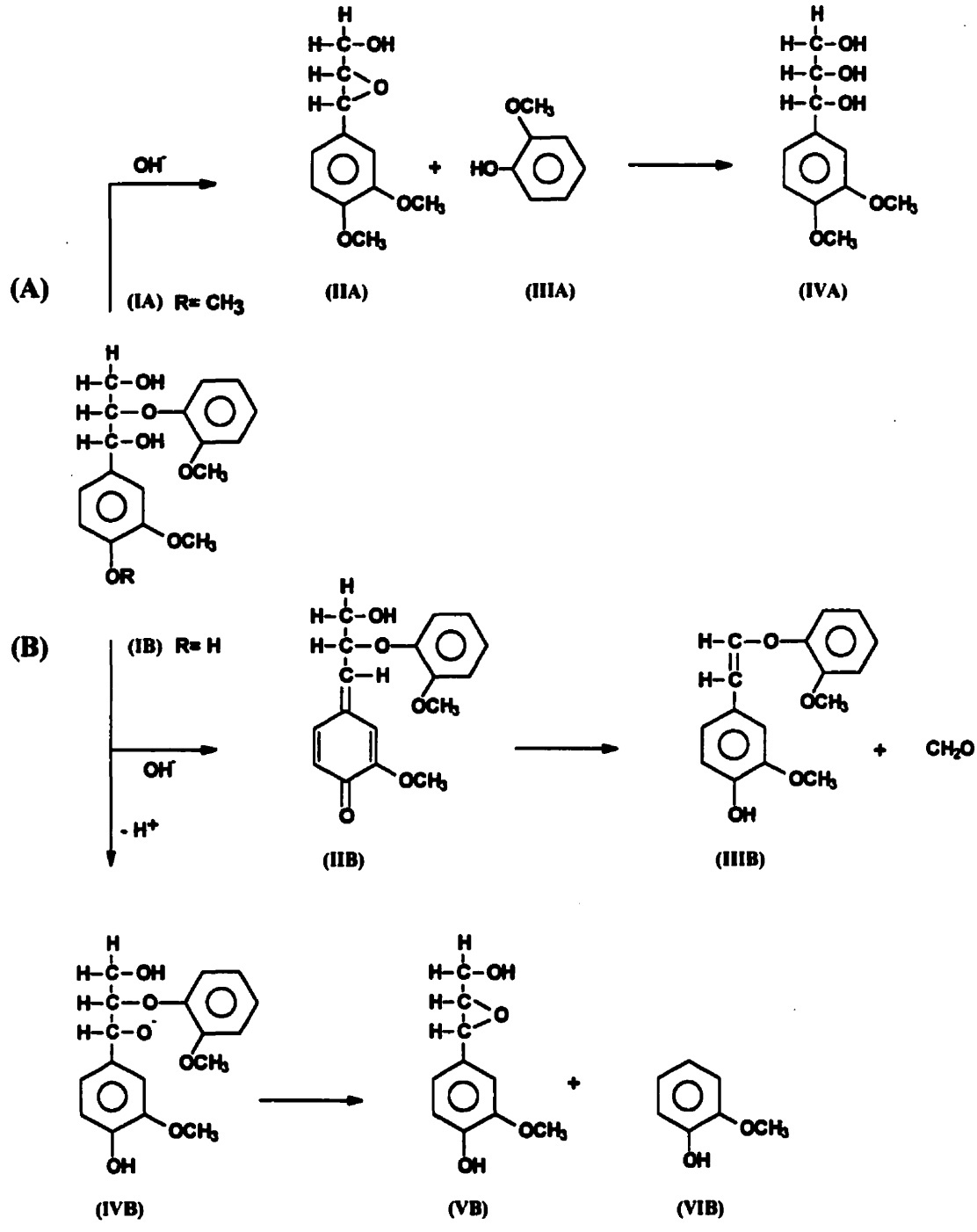

Figure 3.6. The various reactions that are thought to occur in phenolic (B:bottom) and non-phenolic (A:top) lignin arylglycerol-β-aryl ether units under kraft pulping conditions[32].

cleavage[52, 53] is thought to include a nucleophilic attack of the neighbouring hydroxyl group on the β carbon.This results in the formation of an epoxide (IIA) and liberation of a phenoxide ion (IIIA). This mechanism is supported by the observation that compound (IA) can be made stable to alkaline hydrolysis by methylation of the α and γ hydroxyls so that the epoxide can no longer be formed.

The phenolic β-ether structure (IB, R=OH) also undergoes alkaline hydrolysis, involving a somewhat more complex set of reactions [54-56]. Initially the quinonemethide (IIB) is thought to be formed, which subsequently eliminate formaldehyde yielding the comparatively stable enol aryl ether structure (IIIB). Cleavage of the β-aryl ether takes place only as a side reaction, yielding guaiacol (VIB) and the epoxide (VB).

In the light of the above description of events, that have been documented to occur under kraft pulping conditions[32], we are now to examine certain aspects of our data in order to further comprehend its significance.

Brunow et al.[57] who have examined the pH dependency of water addition to quinonemethides (structure IIB, Figure 3.6) for various arylglycerol-β-aryl ether lignin model compounds, have concluded that the distribution of the *erythro* and *threo* diastereomers in such compounds depends upon the kinetics of this addition. In actual fact, acidified water addition to such quinonemethides caused the predominancy of *erythro* isomers over it's *threo* counterparts. As such, it was thought appropriate to examine if such an occurrence is applicable under the conditions of the present experiments for softwood lignin. More specifically, since at the end of the various kinetic kraft pulping experiments, the pH of the degraded milled wood lignin was above 11.5-12.0, the question is whether or not acidification of this mixture could increase the formation of the *erythro* isomer, and if such predominancy would occur, how could this have affected our kinetic measurements?

In an effort to address the above concerns, experiments were carried out in duplicate. Two samples of milled wood lignin were treated at room temperature for a period of 2 and 2.5 hours with the same reagents that were used during the actual kinetic measurements. The alkaline mixtures were then acidified with 0.2 M HCl to a pH value of 2. The resulting suspensions were then kept for a period of 27 hours simulating the

actual isolation conditions used during our kinetic work providing enough time for possible reaction involving alterations between the two diastereomers.The isolated products were then subjected to quantitative ^{31}P NMR spectroscopy and the *erythro* and *threo* contents of the β-O-4 units were measured.

The *erythro* to *threo* ratio of the softwood milled wood lignin used in this effort was determined to be equal to one (Table 3.2). Similar values have also been reported by Taneda et al.[58], Jiang and Argyropoulos[41], Froass et al. [42] and other investigators[18-22]. Our analyses showed no indication, of even a minor increase, in the *erythro* diastereomer over it's *threo* counterpart. In fact, the *erythro/threo* ratio was determined to be slightly lower than unity. Not surprisingly, the data of Table 3.2 suggests that this treatment caused partial cleavage of the ether bonds in lignin since lignin has been shown to undergo a series of minor reactions in the presence of white liquor at room temperature[59, 60]. Contrary to our working hypothesis, the *erythro* diastereomers of the β-O-4 units were found to cleave somewhat more than their *threo* counterparts during this treatment. This caused the E/T ratio to become slightly lower than unity.

The rate constants data of Table 3.3 invariably indicates that the *erythro* isomers of the overall β-O-4 units of softwood milled wood lignin cleave faster than their *threo* counterparts during both the initial and the bulk phase. These data also reveals that at elevated temperatures the difference is augmented. For example at 160 °C the rate constant for the cleavage of the *erythro* isomer increases by almost a factor of 1.2, resulting in significantly lower E/T values (Table 3.2). Miksche[61] who studied the degradation kinetics of a veratrylglycerol-β-guaiacyl ether model compound under alkaline pulping conditions has shown that the β-aryl ether bond of the *erythro* isomer is cleaved approximately four times faster than the *threo* isomer. A similar result has also been reported by Obst[62]. As such, the rate data set obtained for softwood milled wood lignin under homogeneous kraft pulping conditions should not be surprising.

On a different front Jiang and Argyropoulos[41] who monitored the stereoselective degradation of β-O-4 structures in model compounds, milled wood lignin and residual and dissolved kraft lignins have reported that the *erythro* isomers are less stable than their

Table 3.3. Kinetic data describing the degradation of the erythro and threo isomers and the overall arylglycerol-β-aryl ether units in milled wood lignin under homogeneous kraft pulping conditions.

Temp.°C		Rate Constant (k x 10^5) s^{-1}		Correlation coefficient	
		Initial	Bulk	Initial	Bulk
100	*Erythro* isomer	14.1 ± 0.3	0.36 ± 0.0	0.999	0.994
	Threo isomer	5.9 ± 0.0	0.08 ± 0.0	0.999	0.982
	Overall β-O-4	9.7 ± 0.1	0.10 ± 0.0	0.999	0.996
120	*Erythro* isomer	24.7 ± 0.2	1.43 ± 0.0	0.999	0.999
	Threo isomer	14.2 ± 0.2	0.36 ± 0.0	0.999	0.999
	Overall β-O-4	18.8 ± 0.0	0.79 ± 0.0	0.999	0.999
140	*Erythro* isomer	39.6 ± 1.2	5.38 ± 0.3	0.998	0.995
	Threo isomer	28.1 ± 1.0	3.50 ± 0.2	0.998	0.994
	Overall β-O-4	33.3 ± 0.1	4.24 ± 0.0	0.999	0.999
160	*Erythro* isomer	69.1 ± 4.0	21.7 ± 1.0	0.993	0.996
	Threo isomer	56.4 ± 4.0	17.5 ± 0.7	0.990	0.997
	Overall β-O-4	61.1 ± 4.0	19.0 ± 0.8	0.992	0.997

threo counterparts under kraft pulping conditions. In addition, Taneda et al.[58] who have used ozonolysis to determine the *erythro/threo* ratios in a series of residual kraft lignins, have attributed their findings of consecutively lower ratios (as a function of degree of delignification) to the lower reactivity of the *threo* isomer of the non-phenolic β-O-4 lignin structures. Taneda et al.[58] postulated that the actual reactivities of the *erythro* and *threo* diastereomers, toward scission of the arylglycerol-β-arylether bond, is governed by steric factors. An examination of the two possible conformations of the β-aryl ether structures reveals that the formation of the epoxide intermediate is less favoured in the case of the *erythro* diastereomer (Figure 3.5).

Therefore, the rate data of Table 3.3 is further substantiated with literature efforts on model compounds, isolated lignins and actual dissolved and residual lignin analyses. The general stability of the *threo* diastereomers toward kraft pulping seems to be the manifestation of a considerably slower reaction of the pulping reagents with the *threo* diastereomers of the β-aryl ethers.

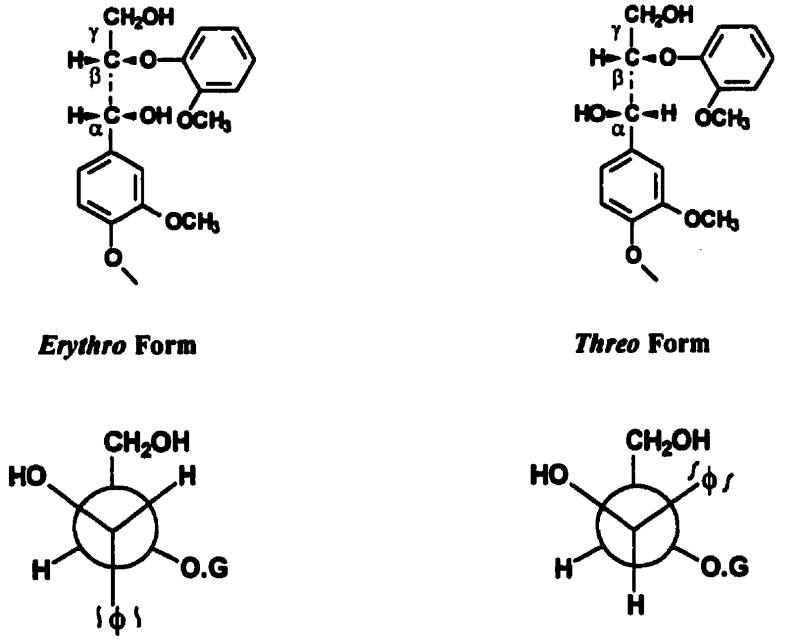

Figure 3.7. The possible conformations of arylglycerol-β-aryl ether structures[58].

Table 3.4. Activation energies, enthalpies, entropies, and Gibbs free energies governing the degradation of the erythro and threo isomers and the overall arylglycerol- β-aryl ether structures in milled wood lignin under homogeneous kraft pulping conditions.

Degradation phase		From Arrhenius plot		From Erying plot			Gibbs free energy
		E_a kJmol^{-1}	*R^2	$\Delta H^{\ddagger}_{T}$ kJmol^{-1}	$\Delta S^{\ddagger}_{T}$ JK^{-1}mol^{-1}	*R^2	$\Delta G^{\ddagger}_{T}$ kJmol^{-1}
Initial							
	Erythro isomer	35.2 ± 1.3	0.997	31.8 ± 1.3	-235.3 ± 0.7	0.997	102.0 ± 1.0
	Threo isomer	50.2 ± 1.0	0.999	46.8 ± 1.0	-202.1 ± 0.6	0.999	107.1 ± 1.0
	Overall β-O-4	40.9 ± 0.9	0.999	37.5 ± 0.9	-223.1 ± 0.5	0.999	104.0 ± 1.0
Bulk							
	Erythro isomer	91.5 ± 3.0	0.998	88.2 ± 3.0	-115.3 ± 1.6	0.998	122.6 ± 3.0
	Threo isomer	122.3 ± 8.9	0.990	119.0 ± 9.0	-46.0 ± 5.0	0.989	133.0 ± 9.0
	Overall β-O-4	117.5 ± 2.4	0.999	114.2 ± 2.5	-55.2 ± 1.4	0.999	130.7 ± 2.5

*R^2 = Correlation coefficient

The Arrhenius plot of the data describing the initial phase (Table 3.3) indicates that the cleavage of the *erythro* isomers required lower activation energy compared to their *threo* counterparts. The difference between these activation energies was found to be equal to 15 ± 1.6 kJmol^{-1}. Miksche's[63] kinetic studies have also shown that the *erythro* form of a arylglycerol-β-(2-methoxyphenyl)-ether model compound is about 2.1 kcal (8.8kJmol^{-1}) more stable than its *threo* counterpart. The qualitative proximity of the two sets of data is actually notable when one considers that Miksche[63] examined model compounds while this effort is focused on actual isolated lignin. The Arrhenius plot (Figure 3.5) for the accumulated data during the bulk phase (Table 3.3) showed that the *erythro* isomers required higher activation energy to be cleaved than their *threo* counterparts. The difference between these activation energies was found to be equal to 30.8 ± 9.4 kJmol^{-1}.

In an effort to rationalize for the observed two kinetic phases the data of Figure 3.2 was examined as follows. The actual reduction in the concentration of β-aryl ether (specially for experiments conducted at lower temperatures) at the end of the initial phase was correlated to the total amount of guaiacyl phenolic units present in the original milled wood lignin. For example, at the end of the initial phase and for the isothermal data set obtained at 100 °C the amount of β-aryl ethers were reduced by 5.9×10^{-2} mol/L. By considering that the total amount of guaiacyl phenolic hydroxyl groups, determined on the original milled wood lignin sample, was 8.8×10^{-2} mol/L, then one realizes that during the initial phase, the β-aryl ethers bearing free phenolic groups would preferentially cleave, followed by those whose phenolic groups are etherified[64].

Obviously, in the data of Figure 3.2, the distinction between the etherified and the non-etherified β-aryl ethers that can be made for the data set obtained at 100 °C, becomes less accessible at higher temperatures. During the bulk phase of each isothermal kinetic run, non-phenolic β-aryl ethers, and newly formed phenolic groups associated with α- and β-aryl ether structures undergo further degradation[64]. Miksche has shown that model compounds possessing phenolic hydroxyl groups react at different rates depending on their substitution patterns and stereochemistry[63]. For example under alkaline

conditions, the formation of a quinonemethide from a model compound possessing a γ-primary hydroxyl group i.e. 1A-(*erythro*) and 1B-(*threo*) proceeds approximately twice as fast as the formation of quinonemethide from a compound whose γ- carbon does not posses a hydroxyl group i.e. 2A-(*erythro*) and 2B-(*threo*) (Figure 3.8).

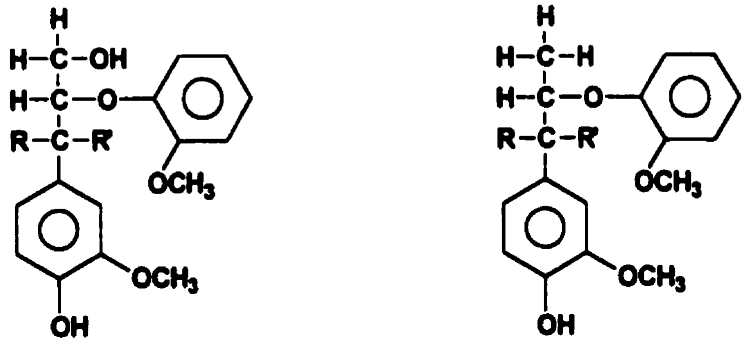

1A: R=H, R'=OH (*erythro*)
1B: R=OH, R'=H (*threo*)

2A: R=H, R'=OH (*erythro*)
2B: R=OH, R'=H (*threo*)

Figure 3.8. Arylglycerol-β-aryl ether model compounds containing free phenolic hydroxyl groups examined by Miksche[63].

It is not, therefore, surprising that during the bulk phase, any residual non-etherified β-aryl ethers may also cleave slower than those cleaved during the initial phase compared to the cleavage of etherified β-aryl units during the initial phase[64].

The calculated values for the enthalpy, entropy and Gibbs free energy governing the scission of the two diastereomers of the arylglycerol-β-arylether structures of lignin, were found to be relatively close (Table 3.4). The Gibbs free energies for the scission of both diastereomers were found to be somewhat higher for the *threo* isomers during the initial phase. The positive sign of the Gibbs free energies, determined for both stages, implies that the cleavage of the β-O-4 moieties in lignin is a non-spontaneous process at room temperature. The entropy signs describing the scission of both isomers were found to be negative. This is a common characteristic in reactions involving polymers as reactants[65]. The enthalpy of activation for the cleavage of the *erythro* and *threo* isomers were found to be positive, pointing to the endothermic nature of the reaction during both stages.

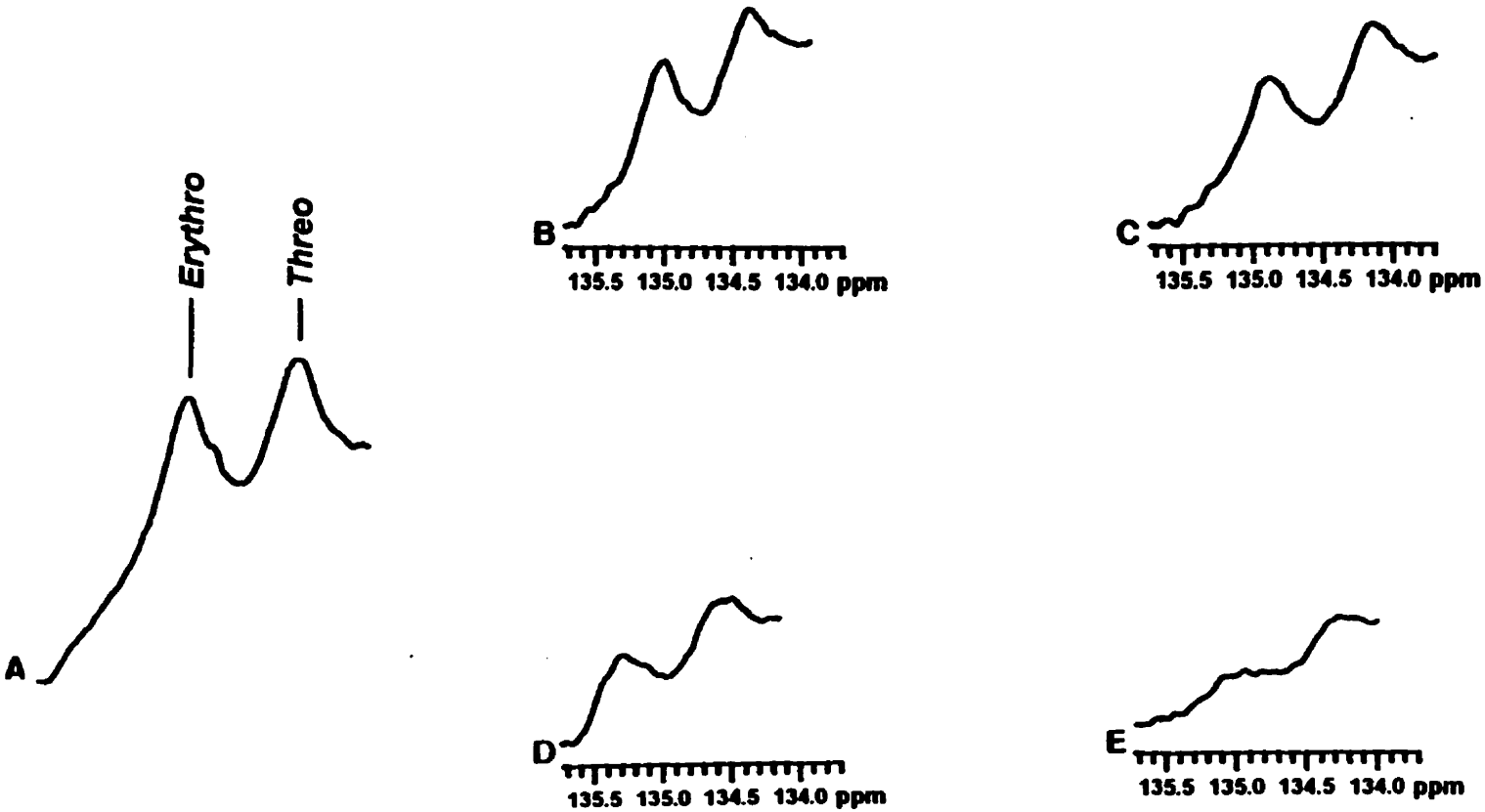

Figure 3.9. Quantitative ^{31}P NMR spectra of *erythro/threo* ratios of milled wood lignins at various times and temperatures under homogeneous kraft pulping conditions.(**A**: Starting material at 25°C, **B**: 225 min at 100°C, **C**: 180 min at 120°C, **D**: 90 min at 140°C, **E**: 90 min at 160°C).

3.4. CONCLUSIONS

The kinetics of the stereoselective degradation of arylglycerol-β-aryl ether linkages present in softwood milled wood lignin were investigated by using quantitative ^{31}P NMR spectroscopy. The overall reaction involving the cleavage of these structures followed a pseudo-first order rate law. The E/T ratio of the starting milled wood lignin was found to be 1.02 and decreased to 0.51 after 2 hours of cooking at 160 °C. The activation energy of the *erythro* isomer was found to be always lower than its counterpart for both the initial and the bulk phases of delignification.

Having explored the stereoselective degradation of the arylglycerol-β-aryl ether bonds using quantitative solution ^{31}P NMR, we then turn our attention at better defining the formation of condensed structures during kraft pulping. While in Chapter 3, we followed an ether scission reaction, in chapter 4 we are following a carbon-carbon bond formation as a side-reaction.

3.5. REFERENCES

1. Fergus, B. J., and Goring, D. A. I., The topochemistry of delignification in kraft and neutral sulphite pulping of birch wood., Pulp Paper Mag. Can., 19, T315-320, 1969.

2. Procter, A. R., Yean, W. Q., and Goring, D. A. I., The topochemistry of delignification in kraft and sulphite pulping of spruce wood., Pulp Paper Mag. Can., 17, T445-453, 1967.

3. Chiang, V. L., Puumala, R. J., Takeuchi, H., and Eckert, R. C., Comparison of softwood and hardwood kraft pulping., Tappi, 71(9), 173-176, 1988.

4. Sarkanen, K. V., Precursors and their polymerization. in: lignin: occurrence, formation, structures, and reactions., Eds. by Sarkanen, K. V., and Ludwig, C. H., Wiley-Interscience, New York, Chapter 4, pp. 95-163, 1971.

5. Chang, H-M. and Sarkanen, K. V., Species variation in lignin: Effect of species on the rate of kraft delignification., Tappi, 56(3), 132-134, 1973.

6. Adler, E., Lignin chemistry: past, present, and future., J. Wood Sci. Technol., 11, 169-218, 1977.

7. Nimz, H., Tschirner, U. and Roth, M., Mild hydrolysis of β-0-4 linkages in lignin., 2nd Int. Symp. on Wood Pulping Chem., Tsukuba Science City, Japan, 1, 90-94, 1983.

8. Gellerstedt, G., Lindfors, E.-L., Lapierre, C. and Monties, B., Structural changes in lignin during kraft cooking. Part 2. Characterization by acidolysis., Svensk. Papperstidn., 87(9), R61-R67, 1984.

9. Yamasaki, T., Hosoya, S., Chen, C-L., Gratzl, J. and Chang, H-M., Characterization of residual lignin in kraft pulp., 1st Int. Symp. on Wood Pulping Chem., Stockholm, Sweden, 2, 34-42, 1981.

10. Taneda, H., Hosoya, S., Nakano, J. and Chang, H-M., Behaviour of lignin-hemicellulose linkages in chemical pulping., 6th Int. Symp. on Wood Pulping Chem., Melbourne, Australia, 1, 117-118, 1991.

11. Jiang, J., Chang, H-M., Bhattacharjee, S.S. and Kwoh, D. L. W., Characterization of residual lignin isolated from unbleached and semibleached softwood kraft pulps., J. Wood Chem. Technol., 7(1), 81-96, 1987.

12. Minor, J. L., Chemical linkage of polysaccharides to residual lignin in

loblolly pine kraft pulps., J. Wood Chem. Technol., 6(2), 185-201, 1986.

13. Gierer, J., Imsgard, F. and Pettersson, I., Possible condensation and polymerization reactions of lignin fragments during alkaline pulping processes., Appl. Polym. Symp., 28, 1195-1211, 1976.

14. Chiang, V. L., Kalppo, K., Stokke, D. and Funaoka, M., Structural changes of lignin in kraft and acid sulphite delignification of western hemlock., 5th Int. Symp. Wood Pulping Chem., Raleigh, NC, 593-597, 1989.

15. Hortling, B., Turunen, E. and Sundquist, J., Investigation of residual lignin in chemical pulps. Part 2. Purification and characterization of residual lignin after enzymatic hydrolysis of pulps., Nord. Pulp Pap. Res. J., 7(2), 1-8, 1992.

16. Gierer, J., Aryl migrations during pulping., J. Wood Chem. Technol., 12(4), 367-386, 1991.

17. Gierer, J., and Nelson, C. R., Mechanism of aryl group migration in the formation of stilbenes from, 1,1-bis (*p*-hydroxyaryl)ethane 2-0-aryl ethers., J. Org. Chem., 43(21), 4028-4032, 1978.

18. Lundquist, K., NMR studies of lignins. 4. Investigation of spruce lignin by ^{1}H NMR spectroscopy., Acta Chem. Scand., B34, 21-26, 1980.

19. Nimz, H. H., Tschirner, U., Stähle, M., Lehmann, R., Schlosser, M., Carbon-13 NMR spectra of lignin. 10. Comparison of structural units in spruce and beech lignin., J. Wood Chem. Technol., 4, 265-284, 1984.

20. Hauteville, M., Lundquist, K., von Unge, S., NMR studies of lignins. 7. ^{1}H NMR spectroscopic investigation of the distribution of *erythro* and *threo* from β-O-4 structures in lignins., Acta Chem. Scand., B40, 31-35, 1986.

21. Matsumoto, Y., Ishizu, A., Nakano, J., Studies on chemical structure of lignin by ozonation., Holzforchung Suppl., 40, 81-85, 1986.

22. Ede, R. M., Brunow, G., Simola, L. K., Lemmetyinen, J., Two dimentional ^{1}H-^{1}H chemical shift correlation and *J*-resolved NMR studies on isolated and synthetic lignins., Holzforchung, 44, 95-101, 1990.

23. Lundquist, K., von Unge, S., NMR studies of lignins. 8. Examination of pyridine-d_5 solutions of acetylated lignins from birch and spruce by ^{1}H NMR spectroscopy., Acta Chem. Scand., B40, 791-797, 1986.

24. Bardet, M., Gagnaire, D., Nardin, R., Robert, D., Vincendon, M., Use of ^{13}C

enriched wood for structural NMR investigation of wood and wood components, cellulose and lignin in solid and in solution., Holzforchung Suppl., 40, 17-24, 1986.

25. Bardet, M., Lundquist, K., Robert, D., von Unge, S., ^{13}C NMR spectroscopic studies of the distribution of *erythro* and *threo* forms of various types of β-O-4 structures in lignins., 1989 Proc. Int. Symp. on Wood Pulping Chem., Raleigh, U.S.A., May 22-25, 217-219, 1989.

26. Lundquist, K. and Stomberg. R., Stereochemistry of the structural elements in lignins., 5th Int. Symp. Wood Pulping Chem., Raleigh, NC, 659-662, 1989.

27. Taneda, H., Habu, N. and Nakano, J., Ratio of *erythro* and *threo* isomers in lignin., 4th Int. Symp. Wood Pulping Chem. Paris, France, 2, 175-178, 1987.

28. Matsumoto, Y., Ishizu, A. and Nakano, J., Studies on chemical structures of lignin by ozonation., 2nd Int. Symp. Wood Pulping Chem., Tsukuba Science City, Japan, 4, 68-71, 1983.

29. Robert, D., Bardet, M., Lundquist, K. and von Unge, S., ^{13}C NMR spectroscopic studies of the distribution of *erythro* and *threo* forms of various types of β-O-4 structures in lignins., 5th Int. Symp. on Wood Pulping Chem., Raleigh, NC, 217-219, 1989.

30. Ralph, J., and Helm, R. F., Rapid proton-NMR method for determination of *threo*:*erythro* ratios in lignin model compounds and examination of reduction stereochemistry., 6th Int. Symp. Wood and Pulp Chem., Vol. 2, Melbourne, 345-350, 1991.

31. Tsutsumi, Y., Islam, A., Anderson, C. D., Sarkanen, K. V., Acid permanganate oxidations of lignin and model compounds: comparison with ozonolysis., Holzforchung, 44, 59-66, 1990.

32. Sarkanen, K. V., Islam, A., Anderon, C. D., In: Methods in lignin chemistry: Ozonation., Eds. by Lin, S. Y., and Dence, C. W., Springer-Verlag Berlin, Heidelberg, Chapter 6, pp. 387-404, 1971.

33. Kringstad, K. P. and Mörck, R., 13C-NMR Spectra of kraft lignins., Holzforschung, 37, 237-244, 1983.

34. Archipov, Y., Argyropoulos, D. S., Bolker, H. I. and Heitner, C., ^{31}P NMR spectroscopy in wood chemistry. Part I, Model compounds., J. Wood Chem. Technol., 11(2), 137-157, 1991.

35. Archipov, Y., Argyropoulos, D. S., Bolker, H. I. and Heitner, C., ^{31}P NMR spectroscopy in wood chemistry. Part II, Phosphite derivatives of carbohydrates., Carbohydr. Research, 220, 49-61, 1991.

36. Argyropoulos, D. S., Archipov, Y., Bolker, H. I. and Heitner, C., ^{31}P NMR spectroscopy in wood chemistry. Part IV, Lignin models: spin-lattice relaxation times and solvent effects in ^{31}P NMR., Holzforschung, 47(1), 50-56, 1992.

37. Argyropoulos, D. S., Bolker, H. I., Heitner, C. and Archipov, Y., ^{31}P NMR spectroscopy in wood chemistry. Part V, Qualitative analysis of lignin functional groups., J. Wood Chem. Technol., 13(2), 187-212, 1993.

38. Argyropoulos, D. S., Quantitative phosphorus-31 NMR analysis of lignins, A new tool for the lignin chemist., J. Wood Chem. Technol., 14(1), 45-63, 1994.

39. Argyropoulos, D. S., Quantitative phosphorus-31 NMR analysis of six soluble lignins., J. Wood Chem. Technol., 14(1), 65-82, 1994.

40. Adler, E., Brunow, G., and Lundquist, K., Investigation of the acid-catalysed alkylation of lignins by means of NMR spectroscopic methods., Holzforchung, 41, 199-207, 1987.

41. Jiang, Z.-H., Argyropoulos, D. S., The stereoselective degradation of arylglycerol-β-aryl ethers during kraft pulping., J. Pulp Pap. Sci., 20(7), J183-187, 1995.

42. Froass, P. M., Ragauskas, A. J., and Jiang, J. E., Chemical structure of residual lignin from Kraft Pulp., J. Wood Chem. Technol., 16(4), 347-365, 1996.

43. Saake, B., Argyropoulos, D. S., Beinhoff, O., and Faix, O., A comparison of lignin polymer models (DHPs) and Lignins by ^{31}P NMR spectroscopy., Phytochemistry, 43, 499-507, 1996.

44. Björkman, A. Studies on finely divided wood. Part 1. Extraction of lignin with neutral solvents., Svensk. Papperstidn., 59, 477-485, 1956.

45. Gierer, J., and Ljunggren, S., The reaction of lignins during sulfate pulping: Part 16. The kinetics of the cleavage of β-aryl ether linkages in structures containing carbonyl groups., Svensk. papperstidn., 82, 71-81, 1979.

46. Merbach, A. E., Moore, P., Howarth, O. W., and Mcteer, C. H., Stopped-flow Fourier-transform NMR and NMR line broadening studies of the rates of dimethyl sulphoxide exchange with the hexakis (dimethylsulphoxide) complexes

of Aluminium(III), Gallium(III) Ions in nitromethane solution., Inorg. Chim. Acta., 39, 129-136, 1980.

47. Beitz, J. V., Miller, J. R., Cohen, H., Wieghardt, K., and Meyerstein, D., Activation energies for an intramolecular electron transfer reaction., Inorg. Chem., 19, 966-968, 1980.

48. Glasstone, S., Laidler, K. J., and Erying, H., The theory of rate processes., McGraw- Hill, New York, Kreevoy, M. M., and Truhlar, D. G., Chap. 1, 1941.

49. Kohnstam, G., Heat capacities of activation and their uses in mechanistic studies., Adv. Phy. Org. Chem., 5, 121-172, 1967.

50. Marton, J., Lignins: Occurrence, formation, structure and reactions., Eds. by Sarkanen, K. V., and Ludwig, C. H., Wiley-Interscience, New York, Ch. 16, p. 639, 1971.

51. Gierer, J., Lenz, B., Norén, I., and Söderberg, S., Reactions of lignin during sulfate cooking III. The splitting of aryl-alkyl ether bonds in milled wood lignin by alkali., Tappi, 47(4), 233-239, 1964.

52. Gierer, J., and Kunze, I., Zur Spaltung von β-Hydroxy-alkyl-aryläthern durch Alkali., Acta Chem. Scand., 15, 803-807, 1961.

53. Gierer, J., and Norén, I., Zur Spaltung von β-Hydroxy-alkyl-aryläthern durch alkali. II. Der stereochemische verlauf., Acta Chem. Scand., 16(8), 1976-1988, 1962.

54. Adler, E, Chim., Biochim., Lignin, Cellulose et Hemicelluloses., Grenoble, p. 73, 1964.

55. Adler, E., Falkehag, I., Marton, J., and Halvarson, H., The behaviour of lignin in alkaline pulping Part 2; Model experiments with arylalkyl-β-aryl ether., Acta Chem. Scand., 18, 1313-1314, 1964.

56. Gierer, J., Lenz, B., and Wallin, N.-H., The Reaction of lignin during sulphate cooking. Part V.* Model experiments on the splitting of aryl-alkyl ether linkages by 2N sodium hydroxide and by white liquor**., Acta Chem. Scand., 18, 1469-1476, 1964.

57. Brunow, G., Karlsson, O., Lundquist, K. and Sipilä, J., On the distribution of the diastereomers of the structural elements in lignins: The steric course of reactions mimicking lignin biosynthesis., J. Wood Sci. Technol., 27, 281-286, 1993.

58. Taneda, H., Habu, N., and Nakano, J., Characterization of the side chain steric structures in the various lignins., Holzforschung, 43, 187-190, 1989.

59. Miksche, G. E., Lignin reactions in alkaline pulping processes (Rate processes in soda pulping)., Chemistry of delignification with oxygen, ozone, and peroxides. UniPublishers Co., LTD. Tokyo, Japan, pp. 107-120, 1980.

60. Lundquist, K., On the degradation of lignin during pulping conditions., Chemistry of delignification with oxygen, ozone, and peroxides. Uni Publishers Co., LTD. Tokyo, Japan, pp. 121-135, 1980.

61. Miksche, G.E., Zum Alkalischen Abbau der Alkoxyarylglycerin-β-Arylätherstrukturen der Lignins., Versuche mit *Erythro*-Veratryiglycerin-β-Guajacyläther., Acta Chem. Scand., 26(8), 3275-3281, 1972.

62. Obst, J. R., Kinetics of alkaline cleavage of β-Aryl ether bonds in lignin models: Significance to delignification., Holzforschung, 37, 23-28, 1983.

63. Miksche, G. E., Über das verhalten des lignins bei der alkalikochung., VIII. Isomerisierung der phenolatanionen von *erythro*- und *threo*- isoeugenolglykol-β-(2-methoxyphenyl)-äther über ein chinonmethid., Acta Chem. Scand., 26, 4137-4142, 1972.

64. Ljunggren, S., The significance of aryl ether cleavage in kraft delignification of softwood., Svensk. Papperstidn., 13, 363-369, 1980.

65. Moore, J. W., and Pearson, R. G., Kinetics and Mechanism., Third edition. A Wiley-Interscience Publication, New York, p. 180, 1981.

Chapter 4

On the Formation of Diphenylmethane Structures in Lignin Under Kraft, EMCC® and Soda Pulping Conditions

4.0. ABSTRACT

This chapter describes our efforts focused at defining the formation of diphenylmethane moieties in lignin during conventional kraft and soda pulping conditions. This objective was realized by confirming initially the assignment of a ^{31}P NMR signal as being due exclusively to the presence of phosphitylated diphenylmethane (DPM) phenolic hydroxyl groups. More specifically, softwood milled wood lignin (*picea marianna*) was subjected to kraft pulping conditions in the presence and absence of varying amounts of formaldehyde. After quantitative recovery of the lignin, the ^{31}P NMR spectra were recorded and the spectra revealed selective signal growth in the region confined between 142.8-144.3 ppm, in accordance with previous model compound work and detailed calculations based on the Hammett principles. To further substantiate our conclusions we also carried out two series of isothermal (120 °C) kraft and soda pulping experiments followed by quantitative determinations of the DPM moieties and correlated our findings with the differences in chemistry known to occur between the two processes. Finally, diphenylmethane phenolic moieties were determined in isolated residual lignins from two western hemlock kraft pulp samples produced via an EMCC® mill protocol and a laboratory batch digester, respectively. These structures prevailed amongst the condensed phenolic units of the conventional pulp, providing additional evidence supporting the fact that modern modified pulping technologies alter the structure of residual kraft lignin beneficially.

4.1. INTRODUCTION

While the ether bonds of lignin cleave efficiently under alkaline pulping conditions, the formation of condensed structures decreases its reactivity and diminishes the solubility of the residual lignin[1]. This phenomenon seriously interferes with the complete removal of lignin and the rate of delignification, especially during the final stages of most pulping processes.

During the past several years a number of modifications have been proposed for the conventional kraft pulping process aimed at enhancing delignification[2-5]. Rapid displacement heating (RDH)[6-9] and modified continuous cooking (MCC)[10-13] are two examples of these processes. In addition, the use of pulping additives such as polysulfide[14-16] and anthraquinone[16-18] have also been advocated.

Amongst the reactions that are known to interfere with the process of alkaline delignification are those involving the formation of carbon-carbon bonds. Formaldehyde is known to be liberated[19] as early as 100 °C, as a result of C_γ elimination from phenylcoumaran[20, 21] and from guaiacylglycerol-β-aryl ether structures, both abundant in native lignin[22-24]. The released formaldehyde is known to cause the substitution of hydroxymethyl groups at positions *ortho* to the phenolate moieties[22]. This potentially represents a very important reaction since one-third of the phenolic nuclei in softwood kraft lignin[25] and about one-half of the phenolic and non-phenolic units in softwood milled wood lignin contain free C5 positions[23]. The methylolated phenols may undergo further reaction to yield diphenylmethane moieties[1, 26, 27].

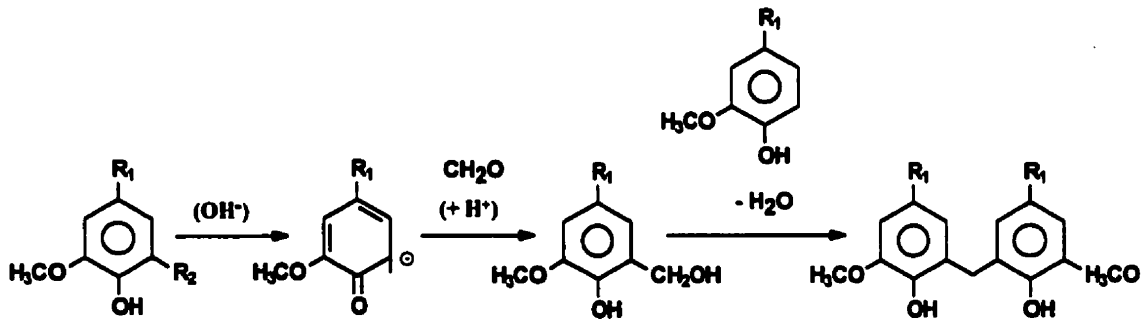

Figure 4.1. Formation of a typical diphenylmethane moiety[1].

A number of these structures (I-IV) have been suggested[28-31]. Another condensation reaction caused by the liberation of formaldehyde during alkaline hydrolysis is Tollen's reaction[1]. This reaction involves the substitution of hydroxymethyl groups at side-chain positions provided activating carbonyl groups are present[1, 25].

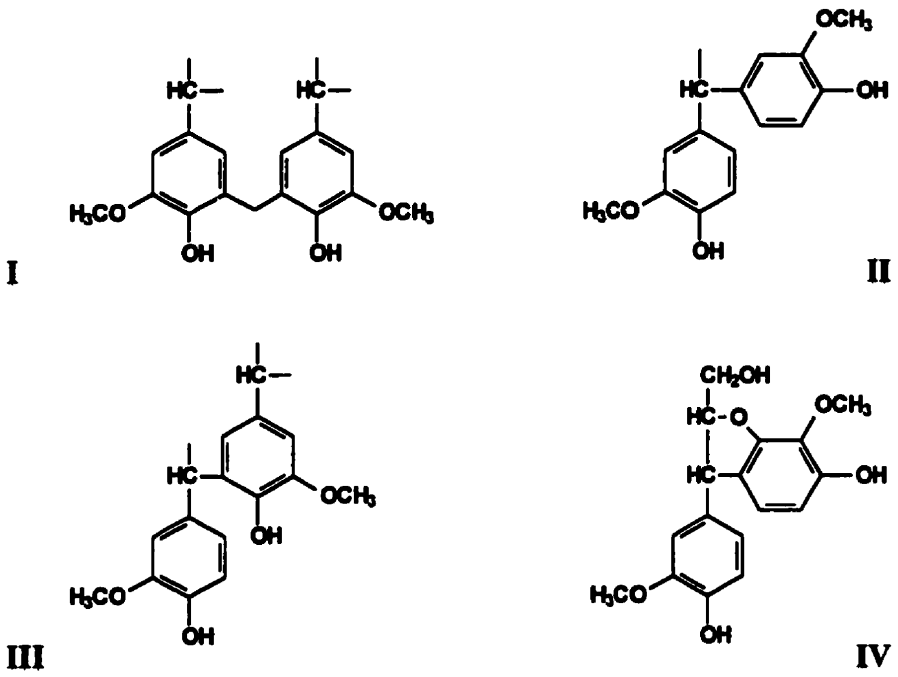

Figure 4.2. Chemical structure of different diphenylmethane moieties in lignin.

Although several studies by Chiang and Funaoka[32-34] have claimed to show convincing qualitative and quantitative evidence for the presence of diphenylmethanes in residual kraft lignin, a number of questions in relation to the method of detection have recently surfaced[35]. Since the development of ^{31}P NMR spectroscopy[36-40] for probing lignin structure, the technique has been successfully implemented for the absolute determination of the various phenolic and non-phenolic structures in several native and technical lignins[41-44]. The availability of a phosphitylating reagent[40] that permits excellent resolution, and the quantitative spectroscopic detection of several phenolic moieties with varying substitution patterns[44-46], provides an excellent opportunity for systematically exploring the complex reactions that occur in lignin during alkaline pulping. For

example, such an effort has already lead to the definition of the fundamental thermodynamic parameters that govern the stereoselective degradation of the arylglycerol-β-aryl ether bonds in milled wood lignin under kraft pulping conditions[47].

As mills move toward elemental chlorine free bleaching (ECF) the negative impact of condensed lignin structures on final pulp brightness ceiling provides additional incentives to minimize condensation reactions from occurring in the digester and during oxygen delignification. The precise identification of such structures and their formation kinetics could be a major step forward toward understanding and minimizing their detrimental effects.

In this paper we aim to describe our efforts that are focused at defining the formation of diphenylmethane moieties in lignin during conventional kraft and soda pulping conditions. This objective was realized by initially confirming the assignment of a ^{31}P NMR signal as being due exclusively to the presence of phosphitylated diphenylmethane phenolic hydroxyl groups. The overall phosphitylation reaction of labile protons is depicted as follow;

Figure 4.3. The derivatization reaction of 2-chloro-4,4,5,5-tetramethyl-1,3,2-dioxaphospholane with compounds containing labile hydrogens.

We then accumulated kinetic data for the formation of these species under soda and kraft pulping conditions and correlated this information to known chemistry.

4.2. EXPERIMENTAL

4.2.1. Materials and Method

4.2.1.1. Preparation

Isolation of Milled Wood Lignin

The extraction and purification of milled wood lignin was carried out according to the Björkman method[44]. Initially 150-200 g of wood chips were pulverized to 100 mesh and then subjected to ball milling (3 weeks) using a porcelain ball mill. The wood meal was then dispersed in 3L of dioxane containing 4.0% water. The suspension was stirred with a magnetic bar for 3 weeks. The wood meal was then separated and discarded from the dioxane solution by centrifugation. The dioxane solution was evaporated under reduced pressure. The resulting residue was dissolved in acetic acid (20 mL per gram of lignin) containing 10% water. This solution was then added to water (250 mL per gram of lignin) while stirring. This material was then washed by centrifugation with occasional shaking of the vessel to distribute the lignin. After evaporating the water with a stream of air, the isolated residue was dissolved in (2:1 v/v) 1,2-dichloroethane/ethanol (20 mL per gram of lignin). This solution was added dropwise to diethyl ether (250 mL per gram of lignin). The material was then centrifuged and washed after decanting the ether. This step was repeated 2-3 times in which, each washing was allowed to stand overnight. The final products were washed once with hexane and the precipitate was first dried in air and then over drierite in vacuo. The elemental analysis of the resulting material was carbon 60.86%, hydrogen 5.71%, and methoxyl 15.45%.

Preparation of Kraft Pulps and Residual lignin Isolation

A conventional western hemlock kraft pulp was prepared at Paprican in a laboratory batch digester using conditions described previously[46]. The western hemlock EMCC® (extended modified continuous cooking) pulp was supplied by a Canadian mill. The isolation of residual lignin was carried out from pre-extracted pulp meal following a procedure[46] described previously.

4.2.1.2. Reactions

Treatment of milled wood lignin under homogeneous kraft or soda pulping conditions

Initially, a white liquor solution was prepared containing 7.0 g of sodium hydroxide (0.175 mole NaOH) and 6.2 g of sodium sulphide (0.026 mole $Na_2S.9H_2O$) per 100 mL deionized water. For the case of the soda "cooks" the molar amount of sodium sulphide ($Na_2S.9H_2O$) used for the kraft pulping experiments was substituted with sodium hydroxide dissolved in 200 mL of deionized water and dioxane (1:1 v/v). This solution was then mixed with an equal volume of dioxane. During a typical experiment, 0.1 g of softwood milled wood lignin prepared according to the Björkman procedure[47, 48] and having the following elemental composition: 60.86% carbon, 5.71% hydrogen, and 15.45% methoxy, was used. This lignin was dissolved in 1.33 g of the previously described white liquor (the ratio of liquor:lignin was 4:1). The reaction was carried out in a 10 mL stainless steel bomb whose air was displaced by nitrogen. The kraft cooking was simulated by heating and occasionally shaking the bomb in an oil bath preheated to the desired temperature and for specific time intervals. At the end of the reaction period, the bomb was cooled with cold water and its contents were acidified to pH 2 using dilute hydrochloric acid (0.2M HCl). The precipitate was allowed to settle overnight. It was then collected by centrifugation and washed with acidic water to remove the inorganic salts. The precipitated degraded lignin was then freeze dried and brought to constant weight at room temperature under reduced pressure. This material accounted for approximately 80% of the initial weight of lignin used. In an effort to isolate the remaining 20%, the solution containing the water soluble low molecular weight lignin resulting from the first aqueous acidic precipitation was allowed to dry at room temperature. The remaining low molecular weight lignin was extracted by addition of 10-15 mL high-grade tetrahydrofuran. This was followed by evaporation of the solvent to a fine viscous residue, and dropwise addition to 20 mL of diethyl ether. This step was repeated 2-3 times allowing the collection of more lignin, free from inorganic salts. Finally, the diethyl ether was evaporated and the remaining lignin was freeze dried. The samples, after being brought to constant weight under reduced pressure, accounted for almost 16% of the starting lignin. The two sets of degraded lignin samples collected,

were then mixed thoroughly prior to subsequent analyses.

Addition of formaldehyde to milled wood lignin followed by homogeneous kraft pulping

100 mg of milled wood lignin were placed in a 10 mL stainless steel bomb. The lignin was then dissolved by the addition of 1.33 g of white liquor solution, prepared by dissolving 7.0 g of sodium hydroxide (NaOH) and 6.2 g of sodium sulphide ($Na_2S.9H_2O$) in 200 mL solution of deionized water and absolute dioxane (1:1 v/v). Two separate sets of experiments were carried out 120 °C in which the amount of formaldehyde added was varied. For the first series of experiments 11.1 μL of a 30% formaldehyde solution, accounting for 50% of the total β-aryl ether bonds, was added to each sample, while for the second series, 22.2 μL (representing 100% of the total β-aryl ether bonds) were added. After replacing the air with nitrogen, each bomb was sealed. Four reaction bombs (each containing the above mixture) were then placed in a preheated oil bath and after occasional shaking they were removed after 1, 2, 3, and 4 hours of treatment. The isolation and purification procedure were conducted in a manner identical to those discussed in the previous section.

4.2.1.3. Instrumentation

Quantitative ^{31}P NMR spectroscopy

The derivatizing reagent 2-chloro-4,4,5,5-tetramethyl-1,3,2-dioxaphospholane was synthesized[40] and used as the phosphitylation reagent. Approximately 30 mg of dry lignin was added to 800 μL of a solvent mixture containing pyridine and $CDCl_3$ at a volume ratio of 1.6/1. The mixture was stirred with a magnetic bar until the lignin was fully dissolved. This was followed by the addition of 100 μL of a solution containing both (11 mg/mL) cyclohexanol, used as the internal standard, and (5 mg/mL) chromium acetylacetonate, used as the relaxation reagent. Finally, 100 μL of 2-chloro-4,4,5,5-tetramethyl-1,3,2-dioxaphospholane, was added and the flask was sealed and shaken to ensure thorough mixing. The ^{31}P NMR spectra were obtained by using inverse gated decoupling on a Varian XL-300 FT-NMR spectrometer at 121.5 MHz. The obtained spectra were integrated 3 times in separate occasions and the resulting data were

averaged out as reported here. Further details dealing with acquisition and spectral processing have been described elsewhere[40, 49].

4.3. RESULTS AND DISCUSSION

In our earlier work the phosphorus NMR spectra of solubilized kraft lignin contained, amongst others, a signal centered around 143.5 ppm[40]. On the basis of model compound work and calculations based on the Hammett principles[50], this signal was tentatively assigned to be due to diarylmethane structures possessing free phenolic hydroxyl groups[40]. In an effort to confirm the validity of our earlier work, the interaction of milled wood lignin with formaldehyde under kraft pulping conditions was clarified by conducting experiments in which different amounts of formaldehyde were introduced in the reaction mixture prior to the cook. More specifically, two different sets of experiments were carried out with four samples of milled wood lignins being subjected to kraft pulping at 120 °C with the addition of formaldehyde accounting for 50 and 100% of the total aryl ether units of lignin, respectively[51]. After quantitative recovery of the lignin, the ^{31}P NMR spectra were recorded and the spectra critically examined. Figure 4.4 shows a representative series of such spectra.

A comparison of the ^{31}P NMR spectra of milled wood lignin (A) to those treated under kraft pulping conditions without (B) and with (C & D) the addition of formaldehyde, reveals substantial signal growth (Table 4.1) at around 143.5 ppm. Indeed the area under the broad signal (142.8-144.3 ppm), labelled DPM, was increased in spectra C and D where significant amounts of formaldehyde have been added (Table 4.1). In addition, one observes that the spectra of the samples in which formaldehyde has been added display a new signal at 147.01 ppm which appears in the aliphatic OH region. In accordance with the chemistry of the formaldehyde/phenol interaction, that is known to occur under alkaline conditions[19, 20], it is very likely that this signal is due to the aliphatic primary hydroxyl group of methylolated aromatic rings.

When the ^{31}P NMR signal in the region 142.8-144.3 ppm, was integrated, the determination of the actual concentrations of diphenylmethane structures in milled wood lignin in the presence and absence of formaldehyde under kraft pulping conditions as a function of reaction time at 120 °C was made possible (Table 4.1).

The quantitative data thus collected revealed that under isothermal conditions (120 °C) the addition of formaldehyde to the kraft reaction medium causes the build up of

DPM structures within lignin, while in the absence of externally added formaldehyde, these structures predominate after three to four hours of reaction. It is also interesting to note that when a large excess of formaldehyde was added (amounting to 100% of the total aryl ethers) the amount of DPM structures reached a value of 0.4 mmoles/g within 60 minutes at 120 °C remaining approximately constant beyond this point.

Table 4.1. Showing the actual amounts of DPM(1) structures present in MWL(2) before and after the addition of formaldehyde(3) under homogeneous kraft pulping conditions(4).

Reaction Time (min)	DPM x 10^4 (mol/g)		
	Control Kraft	50%(3)	100%(3)
60	0.83	1.60	4.0
120	1.41	2.20	4.2
180	2.41	3.00	4.4
240	4.10	4.10	4.6

(1) Diphenylmethane structures
(2) Milled wood lignin (softwood, *Picea mariana*)
(3) Amount of formaldehyde added, expressed as %of the total amount of aryl ethers present in MWL
(4) The temperature of the kraft pulping experiment was set at 120 °C

In an effort to further substantiate our conclusions we then carried out two series of isothermal (120 °C) kraft and soda pulping experiments followed by quantitative determinations of the DPM moieties and correlated our findings with the differences in chemistry known to occur between the two processes.

The data of Table 4.2 clearly demonstrates that the formation of diphenylmethane moieties is a considerably more facile reaction under soda pulping conditions than under kraft pulping conditions. Sulphide ions present in kraft liquors are responsible for promoting and accelerating lignin fragmentation reactions as well as suppressing undesirable condensation reactions[1, 52, 53].

The presence of sulfide ions within sulfate liquors has been suggested to preclude the liberation of formaldehyde from the lignin biopolymer[19]. Alternatively, the absence of sulfide, i.e. soda pulping, allows the intermediate quinonemethides (Figure 4.5) to lose formaldehyde, causing the formation of undesirable alkaline stable enol ethers[1, 54].

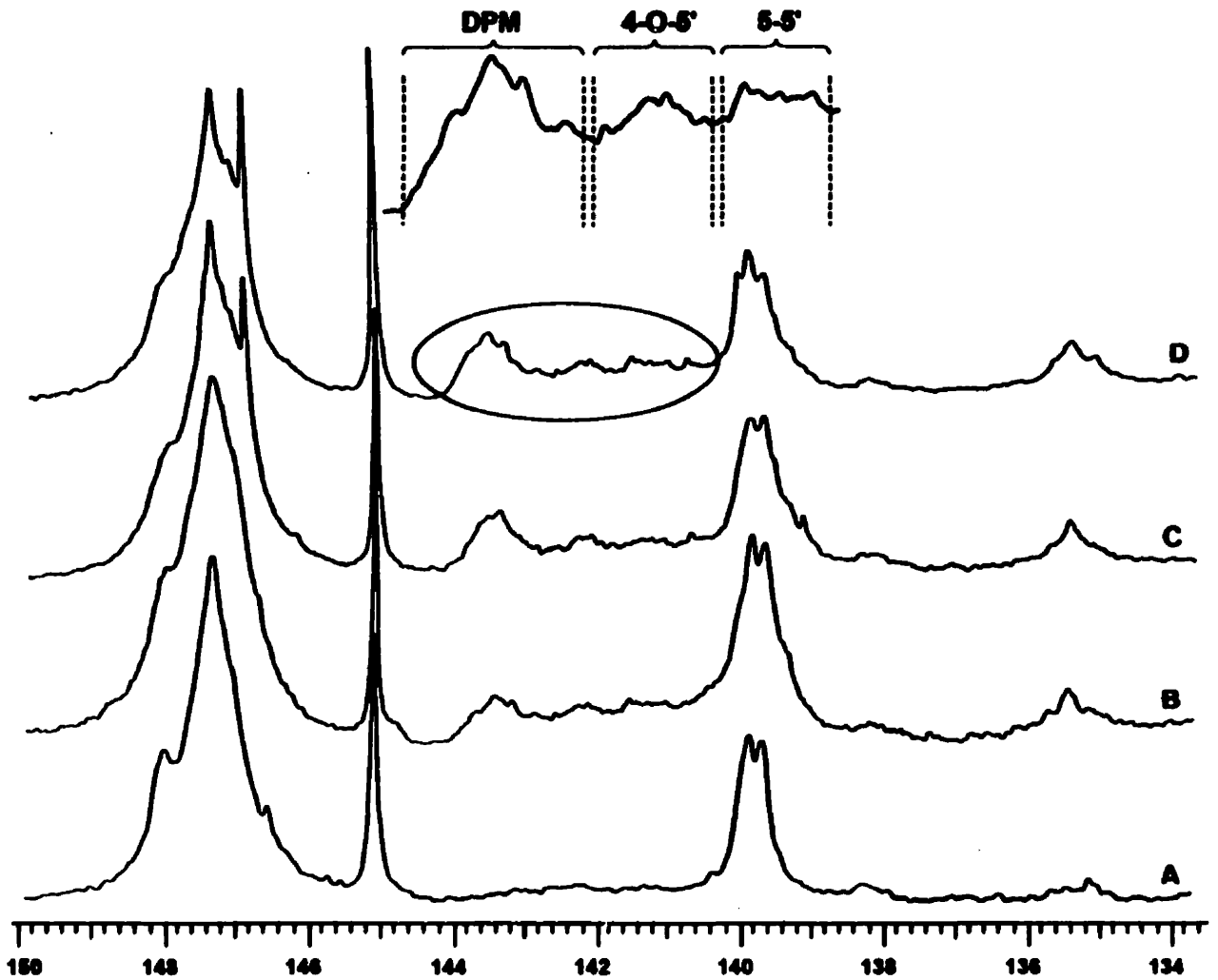

Figure 4.4. Quantitative ^{31}P NMR spectra of milled wood lignin before and after being subjected to isothermal (120 °C, 3 h) homogeneous kraft pulping conditions; (A) blank, (B) control kraft pulping, (C) with the addition of 11μL and (D) 22μL formaldehyde corresponding to 50% and 100% of the aryl ether structures in lignin.

Table 4.2. Showing the actual amounts of DPM[1] structures present in MWL[2] under homogeneous kraft and soda[3] pulping conditions[4].

Reaction Time (min)	DPM x 10^4 (mol/g)	
	Kraft pulping	Soda pulping
60	0.83	1.60
120	1.41	2.20
180	2.41	3.10
240	4.10	4.30

(1) Diphenylmethane structures.
(2) Milled wood lignin (softwood, *Picea mariana*).
(3) Amount of sodium sulphide was replaced with sodium hydroxide.
(4) The temperature of the pulping experiments was set at 120 °C.

The rate data of Table 4.2 clearly demonstrates the efficiency of formation of diphenylmethanes under soda pulping conditions especially early in the process. Therefore, it is not surprising that bleaching a soda-AQ pulp is more difficult compared to a kraft pulp of a similar kappa number[55].

Amongst the various principles that operate during modified pulping, the control of alkalinity is of prime importance. Maintaining hydroxide concentration at a uniformly low level offers distinct advantages as far as carbohydrate degradation is concerned. In this context, maintaining a uniformly low alkalinity may also have an impact on the actual amount of diphenylmethane structures that form within the residual kraft lignin. For this reason residual lignin was isolated from two hemlock kraft pulp samples (kappa number 26.0) produced via an EMCC® mill protocol and a laboratory batch digester, respectively. The data of Table 4.3 is in accord with the previous observations. While in the conventional kraft pulp the overall amount of C-5 substituted phenolic environments is higher by 11%, the diarylmethane structures prevail amongst them by 37%. This data coupled with the earlier account of Froass et al.[43] provides convincing evidence supporting the fact that modern modified cooking technologies alter the structure of lignin beneficially.

The region of the ^{31}P NMR spectra assigned to the overall condensed phenolic units (140.2-144.3 ppm), in addition to the diphenylmethane moieties, also includes phenolic hydroxyl groups belonging to 4-O-5′ and 5,5′ structures.

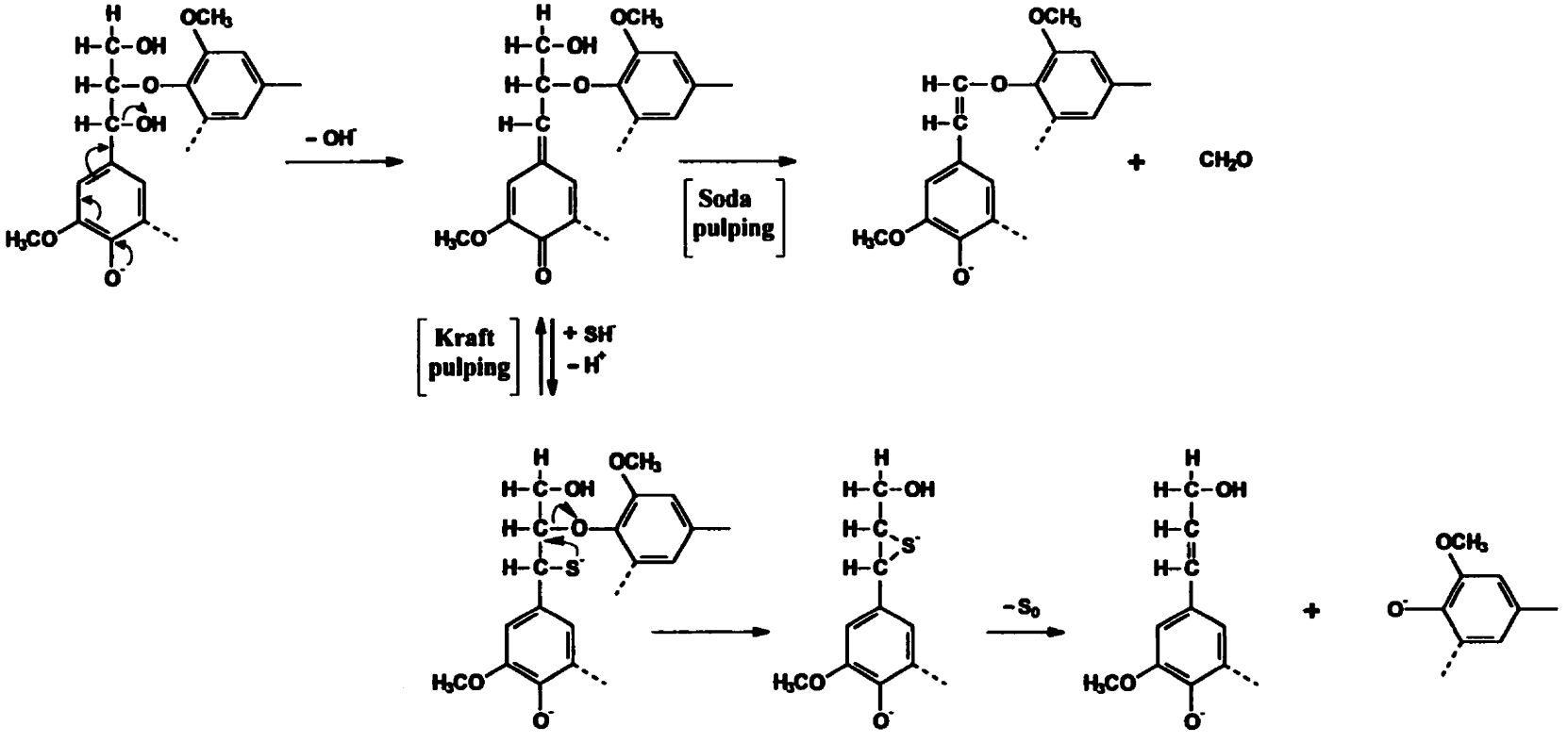

Figure 4.5. The cleavage of β-aryl ether bonds in kraft and soda pulping[54].

More specifically, on the basis of model compound work and detailed calculations these structures have been assigned to the signals ranging between 142.8-141.7 ppm and 141.7-140.2 ppm respectively[40, 50] (Figure 4.4). This assignment was also confirmed by the efforts of Smit and co-workers[44]. In 1995, Brunow's group announced the discovery of the dienzodioxocin bonding patterns as being prevalent in softwoods lignins[56, 57]. This involves the formation of α, β ethers on the same 5-5′ biphenyl structure. The new moiety when subjected to soda pulping conditions was shown to release significant amounts of structures bearing 5,5′ biphenolic hydroxyl groups[58]. Therefore, under kraft pulping conditions it is likely that similar reactions will occur releasing 5,5′ biphenolic hydroxyl groups. The data of Figure 4.6 shows that indeed such structures are released in very significant amounts after 4 hours at 120 °C (about 1.5 mmole/g are formed within milled wood lignin). As anticipated, the presence of formaldehyde does not seem to affect the rate of formation of 5,5′ biphenolic hydroxyl groups or the concentration of dibenzyl ether (4-O-5′) structures.

Table 4.3. Showing the actual distribution of condensed and diphenylmethane structures present in conventional and EMCC® kraft pulps of similar kappa number.

Pulp sample identity	Total Concentration x 10^4 (mol/g)	
	Condensed units[1]	DPM units[2]
Conventional kraft (k=26.8)[3]	17.0	3.0
EMCC® kraft (k=26.0)[3]	15.0	2.0

(1) Total condensed phenolic structures.
(2) Diphenylmethane phenolic OH structures.
(3) Kappa number.

Finally, the formation of diphenylmethane structures under kraft and soda pulping conditions were found to follow pseudo-first-order kinetics with rate constants $14.8 \times 10^{-5} \pm 2.2 \times 10^{-7} s^{-1}$ and $9.2 \times 10^{-5} \pm 8.8 \times 10^{-7} s^{-1}$, respectively.

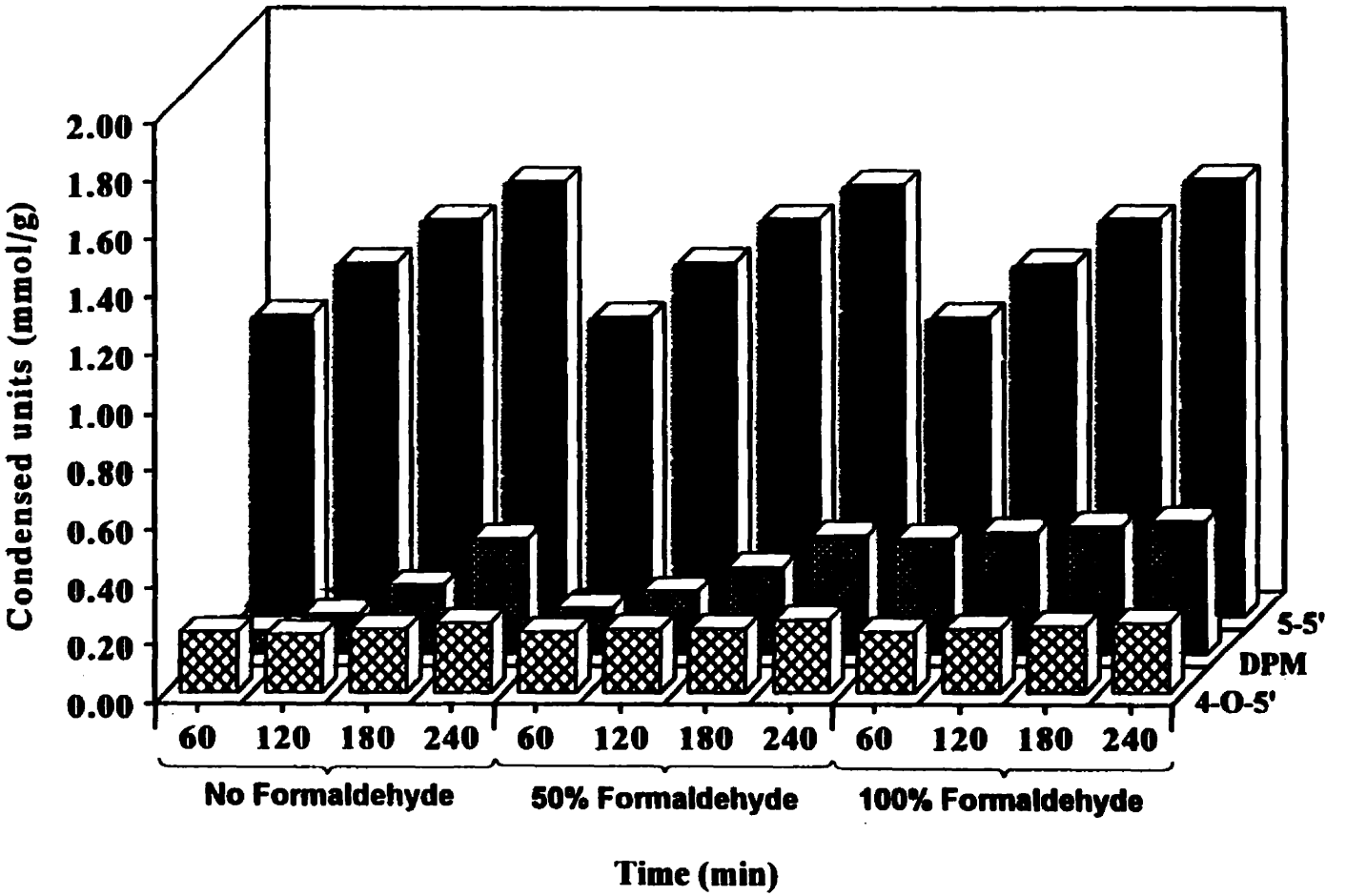

Figure 4.6. Kinetic data showing the development of the actual amounts of 4-O-5', 5,5' biphenolic and diphenylmethane phenolic hydroxyl structures on softwood milled wood lignin under homogeneous kraft pulping conditions at 120 °C in the presence and absence of formaldehyde. The amount of formaldehyde added is expressed as %of the total amount of aryl ethers present in MWL.

4.4. CONCLUSIONS

By using quantitative ^{31}P NMR spectroscopy it is possible to identify, quantify and follow the formation of phenolic hydroxyl groups that belong to diphenylmethane units under kraft and soda pulping conditions. These units exhibit a ^{31}P chemical shift signal that is confined between 142.8 to 144.3 ppm. Data derived during the course of this work implied that diphenylmethanes are formed in higher quantities during a conventional pulping as opposed to its EMCC® counterpart, at the same kappa number.

Having explored the formation of condensed structures in kraft lignin, which seriously affect its subsequent reactivity, we now turn our attention at another functional group which when present on the lignins side-chain dramatically affects its reactivity; this is the carbonyl group. Chapter 5, using model compounds explores the fundamentals of a novel NMR-based technique for the detection of minute amounts of carbonyl groups in lignin.

4.5. REFERENCES

1. Marton, J., Reactions in alkaline pulping., In Lignins: occurrence, formation, structure, and reactions., Eds., K. V. Sarkanen, C. H. Ludwig, Wiley Interscience, New York, pp. 639-694, 1971.

2. Johansson, B., Mjöberg, J., Sandström, P., and Teder, A., Modified continuous kraft pulping-now a reality., Svensk. Papperstidn., 10, 30-35, 1984.

3. Backlund, A., Extended delignification of softwood kraft pulp in a continuous digester., Tappi, 67, 62-65, 1984.

4. Teder, A., and Sandström, P., Pulp yield in continuous kraft pulping with a modified alkali profile., Tappi, 1, 68, 94-95, 1985.

5. Mera, F. E., Chamberlin, J. L., Extended delignification, an alternative to conventional kraft pulping., TAPPI Pulping Conf. Proceed., Washington, DC, pp. 459-465, 1987.

6. Swift, L. K., Dayton, J. S., RDH pulping process, impact on the mill energy balance., CPPA Energy Management Conf. Toronto, ON, pp. 31-37, 1987.

7. Tikka, P. O., Virkola, N. E., Pursiainen, S. A., Hamala, I. T., The process chemistry and the control of an RDH-digester house., TAPPI Pulping Conf. Proceed., Washington, DC, pp. 635-645, 1987.

8. Barrat, K. B., Kraft pulping for the environment of the 90's., TAPPI Annual Meeting Proceed., TAPPI PRESS, Atlanta, GA, pp. 95-102, 1990.

9. Shin, N. H., Sundaram, V. S. M., Jameel, H., Bleaching of softwood RDH pulps with low/no chlorine bleaching sequence., TAPPI Annual Meeting Proceed., TAPPI PRESS, Toronto, ON, pp. 817-828, 1990.

10. Dillner, B., Larsson, L. O., and Tibbling, P., Nonchlorine bleaching of pulp produced by the modified continuous cooking process., Tappi, 73, 167-172, 1990.

11. Whitley, D. L., Zierdt, J. R., and Lebel, D. J., Mill experience with conversion of a Kamyr digester to modified continuous cooking., Tappi, 73, 103-108, 1990.

12. Stromberg, B., Modified continuous cooking-an update., TAPPI Pulping Conf. Proceed., Washington, DC, pp. 453-458, 1987.

13. Prasad, D. Y., Gnanasekaran, A., and Mohan Rao, N. R., Modified kraft

hardwood pulp yields high brightness and high strength., Tappi, 77, 141-147, 1994.

14. Jiang, J. E., Extended modified cooking of southern pine with polysulfide: effects on pulp yield and physical properties., Tappi, 77, 120-124, 1994.

15. Mao, B., and Hartler, N., Improved modified kraft cooking; Part 3: Modified vapor-phase polysulfide cooking., Tappi, 77, 149-153, 1994.

16. Jmeel, H., Gratzl, J., Prasad, D. Y., and Chivukula, S., Extending delignification with AQ/polysulfide., Tappi, 78, 151-160, 1995.

17. Blain, T. J., Anthraquinone pulping: fifteen years later., Tappi, 76, 137-146, 1993.

18. Sturgeoff, L. G., and Pitl, Y., Low-kappa pulping without capital investment: using anthraquinone for low-kappa pulping., Tappi, 77, 95-100, 1994.

19. Ekman, K. H., Formaldehyde obtained by alkaline hydrolysis of wood and lignin., Tappi, 84, 398-402, 1965.

20. Adler, E., Marton, J., Falkehag, S. I., The behaviour of lignin in alkaline pulping, I. Model experiments with phenylcoumarans., Acta Chem. Scand., 18, 1311-1312, 1964.

21. Gierer, J., Söderberg, S., Über die carbonylgruppen des lignins., Acta Chem. Scand., 13, 127-137, 1959.

22. Adler, E., Falkehag, S. I., Marton, J., and Halvarson, H., The behaviour of lignin in alkaline pulping, II. Model experiments with arylalkyl-β-aryl ethers*., Acta Chem. Scand., 18, 1313-1314, 1964.

23. Adler, E., Lundquist, K., Estimation of "Uncondensed" phenolic units in spruce lignin., Acta Chem. Scand., 15, 223-234, 1961.

24. Gierer, J., Lenz, B., and Wallin, N. H., The splitting of aryl-alkyl ether bonds in milled wood lignin by white liquor. Part VII. Reaction of lignin during sulfate cooking., Tappi, 48, 402-405, 1965.

25. Marton, J., Marton, T., and Falkehag, S. I., Alkali-catalyzed reactions of formaldehyde with lignins., Adv. Chem. Ser., 59, 125-144, 1966.

26. Chirkin, G., and Tishschenko, D., Oxidation reduction in alkaline pulping., Zhurn. Priklad. Khim., 35, 153-159, 1962.

27. Harkin, J. M., o-Quinonemethides as tentative structural elements in lignin., Adv. Chem. Ser., 59, 65-74, 1966.

28. Gierer, J., Chemistry of delignification. Part 1: General concept and reactions during pulping., J. Wood Sci. Technol., 19, 289-312, 1985.

29. Brunow, G., Miksche, G. E., Some reactions of lignin in kraft and polysulfide pulping., Appl. Polym. Symp., 28, 1155-1168, 1976.

30. Gierer, J., Imsgard, F., and Pettersson, I., Possible condensation and polymerization reactions of lignin fragments during alkaline pulping processes., Appl. Polym. Symp., 28, 1195-1211, 1976.

31. Johansson, B., and Miksche, G. E., Über das verhalten des lignin bei der alkalikochung. IV., Acta Chem. Scand., 23, 824-930, 1969.

32. Chiang, V. L., and Funaoka, M., The formation and quantity of diphenylmethane type structures in residual lignin during kraft delignification of Douglas-Fir., Holzforchung, 42, 385-391, 1988.

33. Chiang, V. L., and Funaoka, M., The dissolution and condensation reactions of guaiacyl and syringyl units in residual lignin during kraft delignification of sweetgum., Holzforchung, 44, 147-155, 1990.

34. Chiang, V. L. and Funaoka, M., The difference between guaiacyl and guaiacyl-syringyl units in their responses to kraft delignification., Holzforchung, 44, 309-313, 1990.

35. Chan, F. D., Nguyen, K. L., and Wallis, A. F. A., Estimation of the aromatic units in lignin by nucleus exchange- Areassessment of the method., J. Wood Chem. Technol., 15, 473-491, 1995.

36. Archipov, Y., Argyropoulos, D. S., Bolker, H. I., and Heitner, C., ^{31}P NMR spectroscopy in wood chemistry. Part I. Model compounds, J. Wood Chem. Technol., 11, 137-157, 1991.

37. Archipov, Y., Argyropoulos, D. S., Bolker, H. I., and Heitner, C., ^{31}P NMR spectroscopy in wood chemistry. Part II. Phosphite derivatives of carbohydrates., Carbohyd. Research, 220, 49-61, 1991.

38. Argyropoulos, D. S., Archipov, Y., Bolker, H. I., and Heitner, C., ^{31}P NMR spectroscopy in wood chemistry. Part IV. Lignin models: Spin-lattice relaxation times and solvent effects in ^{31}P NMR., Holzforschung 47, 50-56, 1992.

39. Argyropoulos, D. S., Bolker, H. I., Heitner, C., and Archipov, Y., ^{31}P NMR spectroscopy in wood chemistry. Part V. Qualitative analysis of lignin functional groups., J. Wood Chem. Technol., 13, 187-212, 1993.

40. Granata, A., Argyropoulos, D. S., 2-chloro-4,4,5,5-tetramethyl-1,3,2-dioxaphospholane a reagent for the accurate determination of the uncondensed and condensed phenolic moieties in lignin., J. Agric. Food Chem., 43, 1538-1544, 1995.

41. Argyropoulos, D. S., Sun, Y., Mazur, M., Milox pulping: Lignin characterization by ^{31}P NMR spectroscopy and oxidative degradation., Nord. Pulp Pap. Res., 10, 68-73, 1995.

42. Sun, Y., and Argyropoulos, D. S., Fundamentals of high pressure oxygen and low pressure oxygen-peroxide (Eop) delignification of softwood and hardwood kraft pulps; A comparison., J. Pulp Paper Sci., 21, 185-190, 1995.

43. Froass, P. M., Ragauskas, A. J., and Jiang, J., Chemical structure of residual lignin from kraft pulp., J. Wood Chem. Technol., 16, 347-365, 1996.

44. Smit, R., Suckling, I. D., and Ede, R. M., A new method for the quantification of condensed and uncondensed softwood lignin structures., The 9th Int. Symp. Wood and Pulp. Chem., Montréal, Canada, Oral presentations volume, L4-1 to L4-6, 1997.

45. Jiang, Z. H., Argyropoulos, D. S., The application of the Mannich reaction toward the quantitative analysis of lignins., The 8th Int. Symp. Wood and Pulp. Chem., Helsinki, Finland, Vol. I, 511-518, 1995.

46. Jiang, Z. H., Argyropoulos, D. S., Isolation and characterization of residual lignins in kraft pulps., The 9th Int. Symp. Wood and Pulp. Chem., Montréal, Canada, Oral presentations volume, J2-1 to J2-6, 1997.

47. Ahvazi, B. C., Argropoulos, D. S., , Thermodynamic parameters governing the stereoselective degradation of arylglycerol-β-aryl ether bonds in milled wood lignin under kraft pulping conditions., Nord. Pulp Pap. Res. J., 12, 282-288, 1997.

48. Björkman, A., Studies on finely divided wood. Part 1. Extraction of lignin neutral solvents. Svensk. Papperstidn., 59, 477-485, 1956.

49. Argyropoulos, D. S., Quantitative phosphorus-31 NMR analysis of lignin; A new tool for the lignin chemist., J. Wood Chem. Technol., 14, 45-63, 1994.

50. Jiang, Z. H., Argyropoulos, D. S., and Granata, A., Correlation of ^{31}P NMR Chemical shifts with substituent effects of phenols, Mag. Res. Chem., 33, 375-382, 1995.

51. Adler, E., Lignin chemistry-past, present and future., J. Wood Sci. Technol., 11. 169-218, 1977.

52. Hägglund, E., Sulphidity in the sulphate process., Tappi, 32, 241-245, 1949.

53. Enkvist, T., and Hägglund, E., Studien über den zusammenhang zwischen sulfidierung, Methylierung und sulfitierung von lignin., Svensk. Papperstidn., 53, 85-93, 1950.

54. Gierer, J., Chemical aspects of kraft pulping., J. Wood Sci. Technol., 14, 267-279, 1980.

55. Parthasarathy, V. R., Grygotis, R. C., Wahoske, K. W., and Bryer, D. M., A sulfur-free, chlorine-free alternative to kraft pulping., Tappi, 79, 189-198, 1996.

56. Karhunen, P., Rummakko, P., Sipilä, J., Brunow, G., and Kilpeläinen, I., Dibenzodioxocins; A novel type of linkages in softwood lignins., Tetrahedron Lett., 36, 169-170, 1995.

57. Karhunen, P., Rummakko, P., Sipilä, J., Brunow, G., and Kilpeläinen, I., The formation of Dibenzodioxocin structures by oxidative coupling. A model reaction for lignin biosynthesis., Tetrahedron Lett., 36, 4501-4504, 1995.

58. Karhunen, P., Mikkola, J., Brunow, G., The behaviour of dibenzodioxocin structures in lignin during alkaline pulping processes., The 9th Int. Symp. Wood and Pulp. Chem. Montréal, Canada, Oral presentations volume, R1-3 to R1-3, 1997.

Chapter 5

^{19}F Nuclear Magnetic Resonance (NMR) Spectroscopy for the Elucidation of Carbonyl Groups in Lignin Model Compounds

5.0. ABSTRACT

A new method for the detection of different classes of carbonyl groups in a series of carbonyl-containing lignin-like model compounds has been developed. The method is based on the selective fluoride-induced trifluoromethylation of carbonyl groups with trifluoromethyltrimethylsilane (TMS-CF_3) in the presence of tetramethylammonium fluoride (TMAF), followed by hydrolysis with aqueous HF or TMAF in the case of quinones. In this study a series of ketones, aldehydes, quinones, and dimeric-lignin model compounds, were quantitatively trifluoromethylated followed by ^{19}F NMR spectral analyses of the resulting fluorine-containing derivatives, allowing for a thorough understanding of their structure/^{19}F chemical shift relationships. These studies have shown that the ^{19}F-NMR chemical shifts of the trifluoromethyl groups vary significantly and consistently for various classes of carbonyl groups which may be present in complex lignocellulosic materials. These studies are to form the basis for the development of a novel and sensitive method that can be used to obtain quantitative information on the various carbonyl groups present in such materials.

5.1. INTRODUCTION

The carbonyl groups present in wood and pulps play an important role in determining the reactivity of lignin structures toward the yellowing of paper and the bleaching of pulp[1-4]. The low contents of these groups in wood, in pulp and in paper have made the elucidation of their role rather elusive. Detecting and determining these groups will pave the way toward arriving at new conclusions in relation to a variety of pressing issues as far as the yellowing of paper and the bleaching of chemical and mechanical pulps are concerned. Therefore, the necessity to obtain essential information toward understanding the reactivity of lignin structures during yellowing and inhibition, initiated efforts at developing a novel method for the fine structural elucidation and quantification of the various carbonyl groups present in lignin.

The presence of carbonyl groups in lignin was first postulated by Klason[5] as early as 1922. However, Adler et al.[6-8] and Pew[9] were the first to obtain reliable direct evidence for the presence of conjugated carbonyl groups, in particular coniferyl aldehyde-type structures in spruce lignin. In 1979, further investigations by Geiger and Fuggerer[10] resulted in the detection of cinnamaldehyde-type structures of conjugated carbonyls in milled wood lignin. Additional experimentation suggested the presence of other types of conjugated and possibly non-conjugated carbonyls (α-carbonyl) structures [Figure 5.1(a, b)] in lignin. These structures, including trace amounts of quinone ketals[11, 12] [Figure 5.1(d)] have been recognized to be a portion of the total carbonyl content present in milled wood lignins. However, different lignin isolations may contain a variety of other possible carbonyl containing structures. For instance, technical lignins and in particular, alkali lignins, contain appreciable amounts of α-carbonyl groups in addition to benzaldehydes- and *o*-quinones. Nevertheless, investigations in this area have continued to grow aimed at the identification of these groups and elucidating their role in lignin reactivity. Recent studies by Panchapakesan[13] provided evidence and new information on such deactivating groups in lignin.

These studies have shown that the presence of carbonyl groups in lignins, in particular those present as *o*- and *p*-quinonoids, quinonemethides, and other extended conjugate enone systems, are not only contributors to the color observed in lignified plant

tissues[14, 15], but also sensitizers in the photo-yellowing of lignocellulosics[16, 17]. Oxidation of lignins with reagents such as molecular oxygen, hydrogen peroxide, and chlorine may further increase their carbonyl content[18]. The *o*- and *p*-quinone structures so generated in residual lignins of pulps may further alter the color of the pulps and promote their capacity to be photosensitized[13, 19].

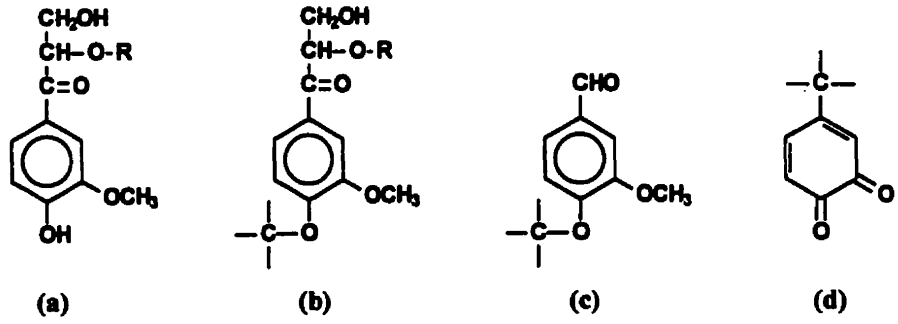

Figure 5.1. Structures of lignin moieties with carbonyl groups.

Two methods have been proposed for the determination of the carbonyl content in lignin preparations. These methods are based on the oximation[20, 21] and reduction[22] of the carbonyl groups in lignins.

The first method involves the reaction of carbonyl groups with hydroxylamine hydrochloride at room temperature. This is a relatively simple procedure, since hydroxylamine hydrochloride reacts with almost all types of carbonyl groups, including those of diketones[20] and *o*- and *p*-quinones. In general, the carbonyl group of an aldehyde or ketone condenses with hydroxylamine hydrochloride, forming an oxime with the liberation of hydrochloric acid:

$$\diagdown\!\!\diagup C{=}O + NH_2OH \cdot HCl \longrightarrow \diagdown\!\!\diagup C{=}NOH + H_2O + HCl \qquad [5.1]$$

Using this procedure, the total carbonyl content of a lignin preparation can be conveniently determined by titration of the liberated hydrochloric acid, since one

carbonyl group quantitatively liberates one mol of hydrochloric acid.

Alternatively, the total carbonyl content of a lignin preparation can be determined by reduction with either sodium or potassium borohydride.

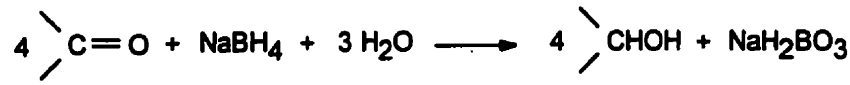

$$4\ \diagdown\!\!\diagup C{=}O + NaBH_4 + 3\,H_2O \longrightarrow 4\ \diagdown\!\!\diagup CHOH + NaH_2BO_3 \qquad [5.2]$$

$$NaBH_4 + H_2SO_4 + 3\,H_2O \longrightarrow NaHSO_4 + H_3BO_3 + 4\,H_2 \qquad [5.3]$$

Carbonyl groups in a lignin preparation are reduced with an excess of sodium borohydride in an alkaline solution [Equation 5.2]. After the reaction, the excess sodium borohydride is decomposed by the addition of a solution of dilute sulfuric acid [Equation 5.3]. The volume of molecular hydrogen liberated is then measured volumetrically. The same experiment is repeated in the absence of the lignin sample (blank test). Since each mole of hydrogen consumed corresponds to a mole of carbonyl group, the total carbonyl content in lignin is determined from the difference in the volumes of hydrogen liberated in the presence and absence of lignin.

According to these methods, the total amount of carbonyl groups in Björkman lignin has been found to vary between 0.22-0.24 mol CO/OCH_3 via oximation and 0.41-0.44 mol CO/OCH_3 via reduction, respectively. The discrepancies between these methods have been rationalized by Gierer and Söderberg[23]. They suggested that the reaction of the carbonyl groups in lignin and hydroxylamine hydrochloride is incomplete, while their reduction by borohydride goes to completion. For example, certain α-aryl-ketones were found to react very slowly[24] with hydroxylamine hydrochloride but rapidly with borohydride. They also imply that a certain fraction of the carbonyl groups in lignin is present in a "masked" form, e.g., as hemiacetals, which are unreactive towards hydroxylamine but reducible by borohydride.

Despite the knowledge aimed at understanding and elucidating the role of the carbonyl groups in lignins, there are still no fundamental techniques available for classifying these groups. The objective of this study is to identify and determine all distinct classes of carbonyl groups in lignin by implementing an innovative method.

The strategy followed toward the development of such a method was as follows: various carbonyl groups present in lignins and several model compounds were to be quantitatively derivatized with a reagent which readily reacts with carbonyls and which contains an NMR sensitive heteroatom. Next, the structure/chemical shift relations must be evaluated in order to allow for the precise qualification of the different classes of carbonyls in complex mixtures. Therefore, according to these criteria, Ruppert's reagent [trifluoromethyltrimethylsilane (TMS-CF_3)] was chosen for the selective and quantitative fluoride-induced trifluoromethylation of carbonyl groups. This was followed by ^{19}F NMR spectroscopy aimed at probing the resulting fluorine-containing derivatives.

The ^{19}F nucleus has several advantages over other NMR-active nuclei:

i) ^{19}F and ^{1}H are the easiest isotopes to study since both have 100% natural abundance causing them to have greater receptivity than any other nuclei.

ii) The ^{19}F nucleus is of a low spin lattice relaxation time, and it's sensitivity is greater than ^{13}C and ^{29}Si.

iii) ^{19}F and ^{1}H have spins of one half which means zero quadrupolar moments, resulting in sharp, narrow line widths, and well resolved NMR signals.

These factors make ^{19}F NMR a superior tool over other NMR nuclei. Accordingly, ^{19}F NMR was selected as the most appropriate instrument for the analysis of carbonyl groups in lignins.

The introduction of trifluoromethyl groups into organic molecules and macromolecules has been the subject of significant interest by both synthetic and medicinal chemists[25]. These compounds have been examined for their potential as biologically active drugs and agrochemicals[26]. Trifluoromethyl-substituted compounds often exhibit significant effects in their physical and chemical properties. This is mainly due to the following considerations:

i) Fluorine and hydrogen atoms are comparable in size. Their van der Waal's radii are 1.35 and 1.20 Å respectively, making a molecule and its fluoro analogues almost indistinguishable to a guest molecule.

ii) The C-F bond energy is about 485 kJ/mol. Such high bond energies leads to increased thermal stability of fluoro analogues.

iii) Fluorine-containing molecules often show different chemical properties. These differences are attributed to the high electronegativity of fluorine.

Table 5.1. Properties of some common elements. [a]

Element	Covalent radius (Å) [b]	van der Waals radius (Å)	C-X bond energy (kcal/mol)	Electronegativity [c]
I	1.33	2.5	57.4	2.5
Br	1.14	1.95	65.9	2.8
Cl	0.99	1.8	78.5	3.1
F	0.64	1.35	105.5	4.0
H	0.30	1.20	98.9	<0.5
C	0.77	2.0 [d]	83.1	2.6

[a] Values from Pauling (1967), and Holland et al. (1964)

[b] Single bond covalent radii for iodine, bromine, chlorine, fluorine, hydrogen, and carbon, taken from Pauling (1967)

[c] Electronegativities based on the Pauling scale (Pauling 1967)

[d] van der Waals radius of CH_3 is given

In 1989 Prakash and co-workers[27] reported the efficient and selective fluoride-induced trifluoromethylation of carbonyl compounds with trifluoromethyltrimethylsilane ($TMS\text{-}CF_3$)[28]. The work of this group has been focused at developing new synthetic methods for introducing perfluoroalkyl groups into different classes of carbonyl compounds by using efficient nucleophilic trifluoromethylating agents. Various carbonyl containing compounds when reacted with ($TMS\text{-}CF_3$) in the presence of a catalytic amount of *tetra*-n-butylammonium fluoride (TBAF) have been shown to undergo such reaction. This reaction works equally well for different classes of carbonyl groups, such as aldehydes, ketones, enones, carboxylic acid, and even ketoesters[29] without being affected by moisture.

Table 5.2. NMR properties of some common magnetic nuclei.

Nucleus	Spin	γ	Natural [a] Abundance	Sensitivity		Chemical shift range (ppm) [d]	Reference Substance
				Relative [b]	Absolute [c]		
^{1}H	1/2	26725	99.98	1	1	10	$(CH_3)_4Si$
^{2}H	1	4117	1.5×10^{-2}	9.6×10^{-3}	2×10^{-6}	10	$(CD_3)_4Si$
^{13}C	1/2	6726	1.1	1.5×10^{-2}	2×10^{-4}	340	$(CH_3)_4Si$
^{15}N	-1/2	-2711	0.4	1.0×10^{-3}	3×10^{-6}	620	$NH_3(l)$
^{17}O	-5/2	-3627	3.7×10^{-2}	2.9×10^{-2}	3×10^{-6}	850	H_2O
^{19}F	1/2	25167	100	0.83	0.83	700	CCl_3F
^{31}P	1/2	10829	100	6.6×10^{-2}	7×10^{-2}	960	H_3PO_4 (85%)

[a] Values from Gerig (1978)

[b] Relative sensitivity based on constant number of each nuclide

[c] Absolute sensitivity based on natural abundance of each nuclide

[d] Values from Gerig (1978); and Jardetzky & Roberts (1981)

In this work a series of organic compounds containing different classes of carbonyl groups were subjected to the proposed chemical reaction and their carbonyl groups were converted to their trifluoro analogues according to the following schematic reaction mechanism.

Finally, the resulting fluorine-containing derivatives were examined by ^{19}F NMR spectroscopy. As a result, numerous signals, due to the different classes of carbonyl groups, were detected and studied.

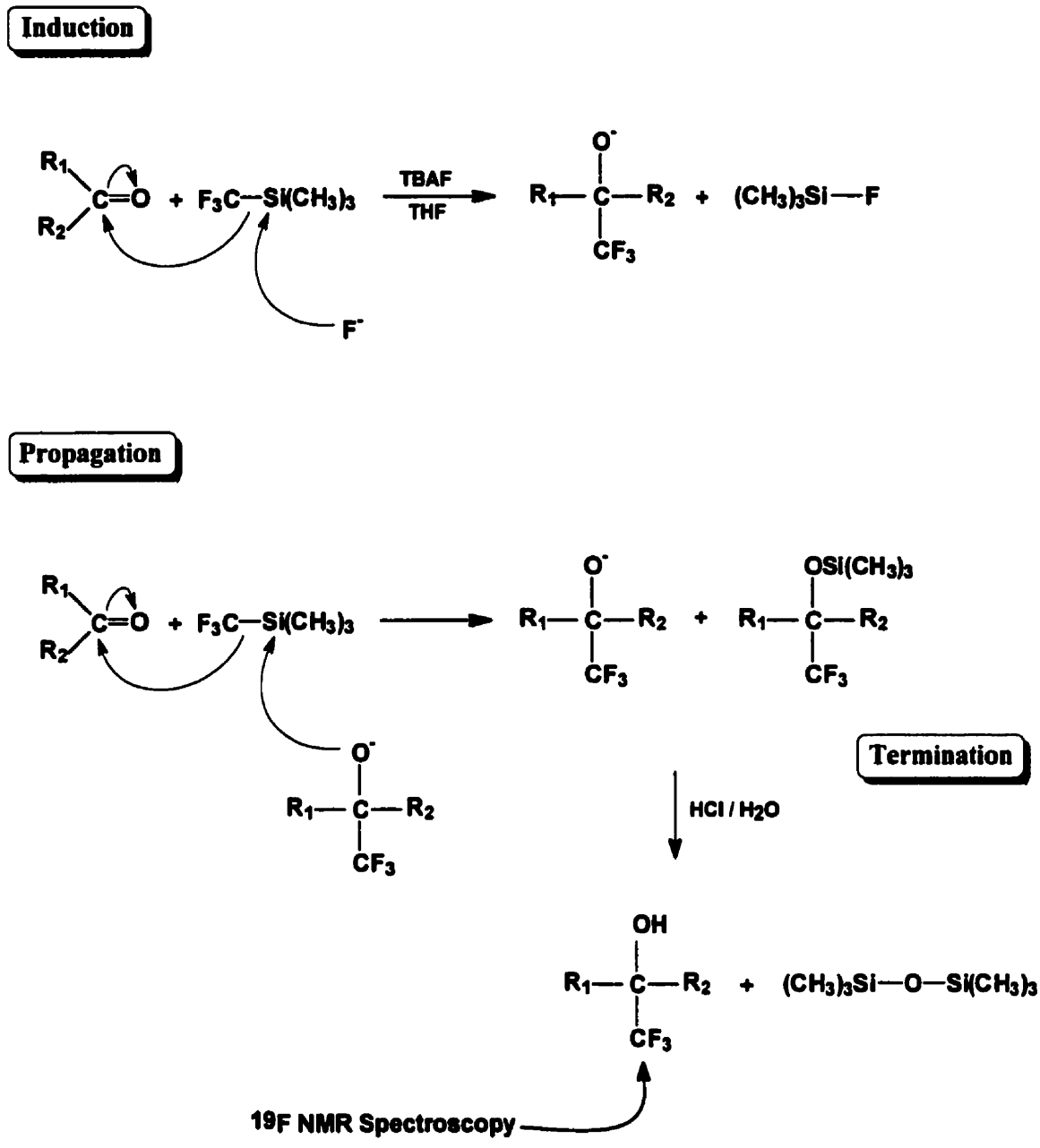

Figure 5.2. The mechanistic reaction pathway for trifluoromethylation of carbonyl groups[27].

5.1.1. The Chemistry of Carbonyl Compounds

The carbon-oxygen double bond of carbonyl groups is similar in many respects to the carbon-carbon double bond of alkenes (Figure 5.3). The carbonyl carbon atom is sp^2 hybridized and forms three sigma (δ) bonds. The fourth valence electron remains in a carbon p orbital and forms a pi (π) bond to oxygen by overlapping with an oxygen p orbital. The oxygen atom also has two non-bonding pairs of electrons, which occupy its remaining two orbitals. Thus, the carbonyl carbon and the three atoms attached to it, lie in the same plane. The bond angles between the three attached atoms are approximately 120°, making a trigonal coplanar structure (Figure 5.4). The carbon-oxygen double bond is both shorter (1.22 Å versus 1.43 Å) and stronger [175 kcal/mol (732 kJ/mol) versus 92 kcal/mol (385 kJ/mol)] than a normal carbon-oxygen single bond.

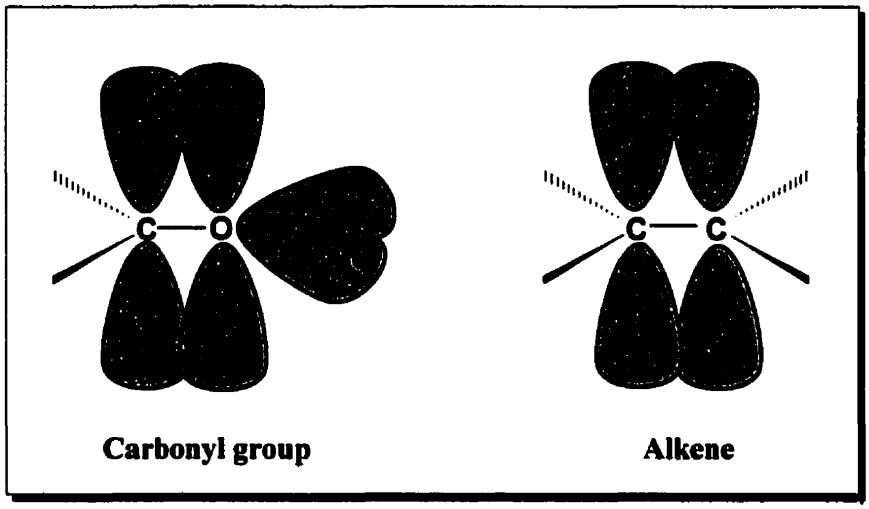

Figure 5.3. Electronic structure of the carbonyl group.

Carbon-oxygen double bonds are polarized because of the high electronegativity of oxygen relative to carbon. Hence, all types of carbonyl compounds have substantial dipole moments.

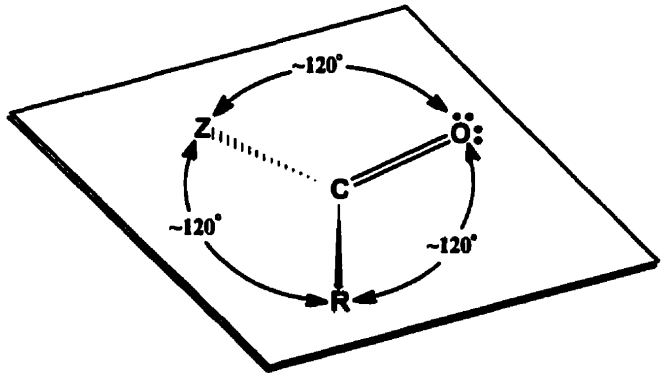

Figure 5.4. Geometric structure of the carbonyl group.

The most important consequence of carbonyl-group polarization is the chemical reactivity of the carbon-oxygen double bond. Since the carbonyl carbon carries a partial positive charge, it is an electrophilic site and is attacked by nucleophiles. Conversely, the carbonyl oxygen carries a partial negative charge and is a nucleophilic site.

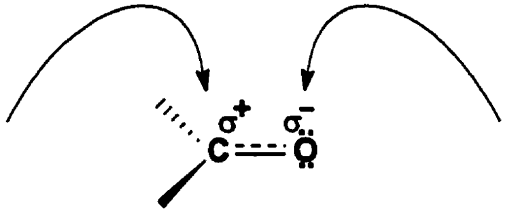

This charge distribution arises from two effects: the inductive effect of the electronegative oxygen and the resonance contribution of the second structure shown below.

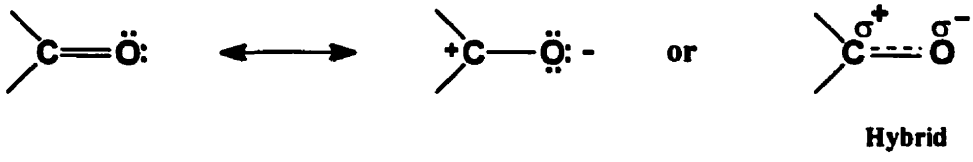

Resonance of hybrid structures for the carbonyl group

One highly characteristic reaction of aldehydes and ketones is the nucleophilic addition to the carbon-oxygen double bond. Aldehydes and ketones are especially susceptible to nucleophilic addition because of the structural features mentioned above. The trigonal coplanar arrangement of groups around the carbonyl carbon implies that the carbonyl carbon is relatively open to attack from above or below. The positive charge on the carbonyl carbon suggests that it is especially susceptible to attack by a nucleophile. The negative charge on the carbonyl oxygen indicates that nucleophilic addition is susceptible to acid catalysis. The nucleophilic addition to the carbon-oxygen double bond can be visualized as taking place in two general path ways; as illustrated in Figure 5.5.

5.1.1.1. For particularly strong nucleophiles

The nucleophile uses its electron pairs to form a bond to the carbonyl carbon. As this happens, an electron pair from the carbon-oxygen π bond shifts out to the carbonyl oxygen and the hybridization state of the carbon changes from sp^2 to sp^3. The important feature of this step is the ability of the carbonyl oxygen to accommodate the electron pair of the carbon-oxygen double bond. In the second step, the oxygen associates with an electrophile (usually a proton). This happens because the oxygen is now much more basic; it carries a full negative charge, and it resembles the oxygen of an alkoxide ion. (In some reactions the oxygen of the carbonyl group actually becomes the oxygen of an alkoxide ion.)

5.1.1.2. An acid-catalyzed mechanism

This mechanism operates when carbonyl compounds are treated with reagents that are strong acids but weak nucleophiles. In the first step the acid attacks an electron pair of the carbonyl oxygen: the resulting protonated carbonyl compound is highly reactive toward nucleophilic attack at the carbonyl carbon (in a second step) because of the contribution made by the second resonance structure below:

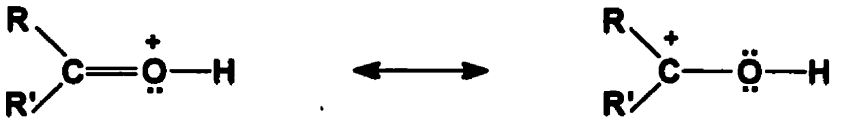

The general nucleophilic addition to the carbon-oxygen double bond can be illustrated as follows:

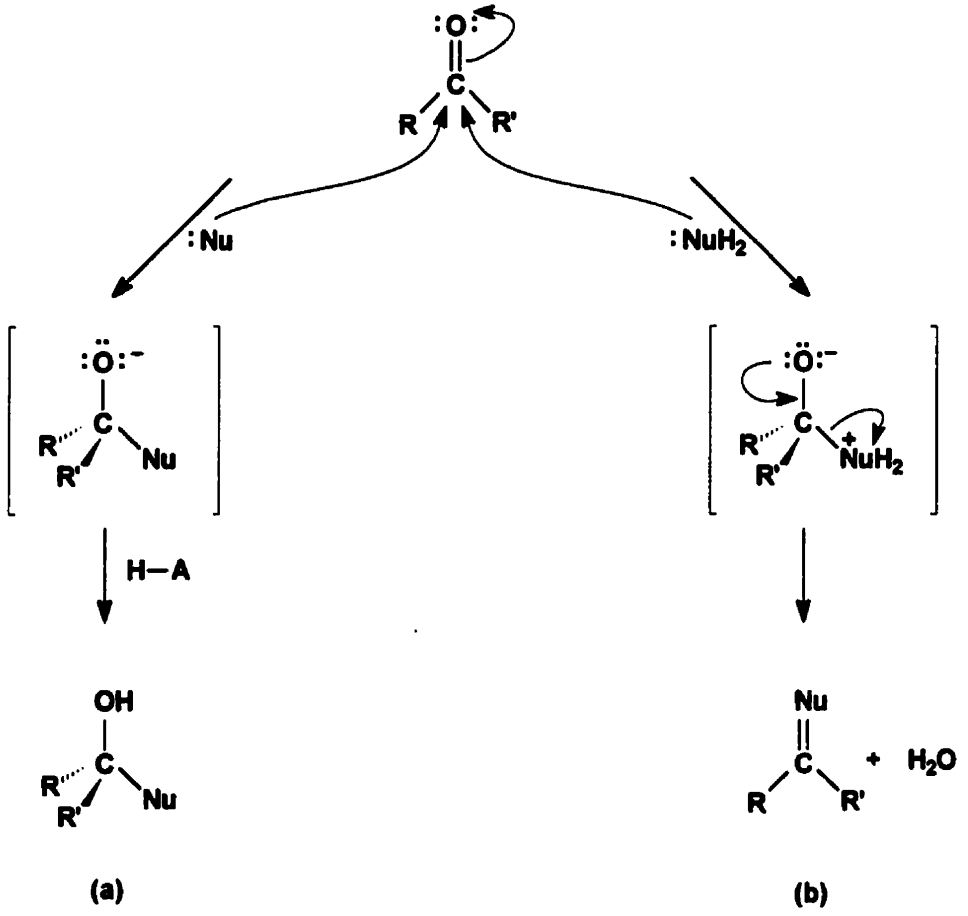

Figure 5.5. The addition of a nucleophile to a ketone or aldehyde.

Typically, trifluoromethylation of carbonyl groups follows the (a) reaction pathway with the trifluoromethyl group acting as a nucleophile, bearing substantial negative charge. The intermediate trifluoromethylated siloxy compound is then hydrolyzed to the corresponding alcohol with aqueous hydrochloric acid (1M HCl).

5.1.2. Fluorine-19 NMR Spectroscopy

In recent years, there has been much progress in lignin structure determination using NMR spectroscopy.

^{1}H would seem to be the nucleus of choice because of its high sensitivity to detection and its natural presence in lignin. However, ^{1}H-NMR studies of lignins involves acetylation or other derivatization procedures which cause unwanted chemical modification of the lignin samples.

Another difficulty with using ^{1}H-NMR is the relatively narrow spectral dispersion of chemical shifts, typically 10-12 ppm in the absence of paramagnetic species. The slower tumbling associated with larger macromolecules causes broad NMR linewidths and a loss of both signal intensity and spectral resolution.

^{13}C-NMR is a sensitive method for the qualitative structural analysis of lignin. It provides detailed structural information on nearly all types of carbons including those in minor structures. However, the capacity for producing reliable quantitative analysis of carbonyl groups in lignin is limited by its inability to differentiate the presence of different classes of carbonyls.

Studies of carbonyl groups in lignin by ^{1}H and ^{13}C-NMR have been limited due to those problems[30].

As an alternative to ^{1}H and ^{13}C, other NMR detectable nuclei may be used to obtain structural details for large macromolecular complexes. For example, ^{31}P NMR spectroscopy has been used successfully for the quantitative determination of different classes of hydroxyl groups in lignins[31-34].

An NMR observable nucleus should ideally allow: a high sensitivity of detection that is comparable to ^{1}H, a large chemical shift range like that of ^{31}P or ^{17}O, and the ability to incorporate the label into biomolecules for NMR observations. Table 1.2 shows that the fluorine-19 nucleus offers high sensitivity and a large chemical shift dispersion. Its sensitivity is only 17% lower than proton and, fluorine, in all its chemical forms gives rise to a spectral dispersion of more than 700 ppm[35]. While ^{13}C, ^{15}N, ^{17}O, and ^{31}P also provide wide chemical shift ranges, their lower natural abundance or gyromagnetic ratios cause their sensitivity of detection to be inferior to ^{19}F. The detection of these other

nuclei can be improved by (expensive) isotopic enrichment, increased sample concentrations, or indirect detection.

There are several limitations associated with the use of ^{19}F-NMR for obtaining structural information. First, one must prove that the fluorine substitution does not alter the structure and function of the system in which it is incorporated. Second, ^{19}F-NMR does not provide complete structural information in the way that ^{1}H-NMR and x-ray crystallography can. Rather, only limited information can be obtained concerning fluorine environment within a macromolecule. Finally, there is no quantitative method for interpreting fluorine chemical shifts unambiguously in terms of structural details. Although this problem is to a large extent associated with all NMR observable nuclei, much progress has been made in identifying shielding contributions that affect fluorine chemical shifts.

5.1.2.1. Fluorine Shielding Constant

Since nuclear shielding constants are not measurable directly, it is necessary to measure shielding[36-39], σ_C, relative to some reference resonance, σ_R; the differences are known as chemical shifts, δ:

$$\delta = \sigma_R - \sigma_C \qquad [5.4]$$

δ is negative if the reference compound is less shielded than the sample. Both internal and external referencing are used with different reference compounds. Trifluoroacetic acid (TFA) has been used extensively, particularly as external reference. However, TFA is not satisfactory for correlating chemical shift measurements due to the bulk susceptibility corrections that must be applied. Because of the magnitude of ^{19}F shifts, these corrections are not very important. Several other reference standards are often used[40] (Table 5.3).

The most common reference compound is $CFCl_3$. Evaluating σ requires some detailed knowledge of the excited-state wave functions of the molecule, which is rarely available. Following an oversimplified picture it is possible and useful to write σ as a

sum of local effects and long-range or molecular effects (Equation 5.5).

$$\sigma = \sigma_d(local) + \sigma_p(local) + \sigma_m + \sigma_r + \sigma_e + \sigma_s \quad [5.5]$$

Where;

σ_m = neighbour anisotropy effect
σ_r = ring current effect
σ_e = electric field effect
σ_s = solvent effect

This scheme is arbitrary but useful. σ_d (local) and σ_p (local) are the diamagnetic and paramagnetic local terms of Ramsey's equation for nuclear shielding due to electrons closely associated with the nucleus. The chemical shift of the fluorine nucleus is dominated by σ_p (local). For instance the ^{19}F resonance of F_2 occurs about 625 ppm to low field of that for HF. The difference in σ_d can be estimated to be about 20 ppm. σ_p is zero for spherically symmetric species such as an atom or an ion, like F^-, whereas it is appreciable for an asymmetric distribution of *p* electrons such as covalently bonded fluorine. The discrepancy between experimental and calculated values is due to the partial ionic character of the bond in F_2 which reduces σ_p considerably from its calculated value. σ_m is related to the anisotropy in the diamagnetic susceptibilities, Δx, of a certain group of electrons. The magnitude of this contribution depends only on the magnitude of Δx and the geometry of the molecule.

This means that σ_m should be equal for the ^{19}F and ^1H resonances, and typically of the order of 1 ppm. The magnitude of σ_r and its effect on nuclear shielding should again be independent of the nucleus and hence the magnitude of this term should be typically about 1ppm. The σ_e term is related to the intramolecular electric fields arising from charges remote from the shielded nucleus. The σ_e term for the fluorine resonance is more important than σ_m and σ_r, and can be considered to be made up of three contributions. When the fluorine is in an axially symmetric environment the first contribution to σ_e may simply be related to drift of electrons along the bond direction, and the second contribution to the distortion of the electronic charge distribution in a direction perpendicular to the bond direction. The third contribution is due to time dependent electric dipoles mutually induced between bonds in the molecule and the bond

to the shielded nucleus. Such dipoles give a nonzero average value of E^2, written $<E^2>$.

$$\sigma_e = -AE_z - BE^2 - B_1\langle E^2\rangle \qquad [5.6]$$

$$\langle E^2\rangle = \sum_i \frac{3P_iI_i}{R_i^6} \qquad [5.7]$$

This is the so called van der Waals contribution, σ_w, for which P_i and I_i are the polarizability and first ionization potential of the electron group (bond). Experimental estimates of the constants A, B, and B´ have shown that they are quite large for fluorine and that A is negative. Typical values are A=about -10×10^{-12} e.u.s., B≃B_1 $20\div40\times10^{-18}$ e.u.s. σ_s contains contributions of the same type as σ_m, σ_r, and σ_e, but they are of intermolecular origin.

5.1.2.2. Fluorine Coupling Constants

^{19}F chemical shifts are extended over a much wider ppm range than that found with the ^1H. The intrinsic sensitivity of a given nucleus to its environment is determined by the density, distribution, and symmetry of the orbital electrons surrounding the nucleus. In hydrogen, only the *s*-electron exerts an orbital magnetic field at the nucleus. However, in covalently bound fluorine, with a valency shell containing unequal populations in its three 2 *p*-orbitals, the fluorine chemical shift tensor is quite large and orientation sensitive[41,42]. As a result, the ^{19}F-NMR observed peak positions are highly dependent on the micro-environment of the fluorine nucleus.

Spin coupling between nuclei is mediated by shared electrons involved in chemical bonding. Table 5.4 shows the magnitudes of coupling constants for F-F and F-H spin-spin interactions. The geminal coupling constants for H-F (40-80 Hz) or F-F (150-300 Hz) are larger than those for H-H (12-15 Hz).

5.1.2.3. Relaxation and ^{19}F-NMR Linewidths

The mechanism of relaxation derives from the action of local fluctuating fields on

nuclear magnetic moment. There are three relaxation pathways associated with a ^{19}F nucleus placed inside a molecule. The first is dipolar coupling between ^{19}F and its neighboring spins (i.e ^{1}H). A second pathway is that of chemical shift anistropy (CSA) where both the overall and the internal motions of a fluoro-substituted macromolecule contribute to the averaging of the orientation-dependent chemical shift. A third mechanism arises from spin-rotation, where a fluctuating field is produced by the rotational motion of a molecule's electron cloud. Spin rotation contributes to relaxation only for small symmetric molecules, and has minimal contribution in larger macromolecules[43-45].

While the large anisotropy of the ^{19}F chemical shift has the advantage of providing a wide spectral distribution for ^{19}F-NMR peaks, it has one important drawback. At higher fields, the observed line broadening ($1/\pi\ T_2$) increases with the squared frequency of resonance. As a result, the increase in resolution that one expects in going to higher fields (which scales linearly with ω) is offset by CSA relaxation[46]. Narrower ^{19}F-NMR linewidths have been observed at lower fields from alkaline phosphatase and dihydrofolate reductase.

Table 5.3. Some F-19 NMR reference standards [39].

Compound	$\sigma_{(ppm)}$ [a]
$CFCl_3$	0.00
CF_3COOH (int.)	-76.55
CF_3COOH (ext.)	-78.90
CF_3CCl_3	-82.20
$CFCl_2.CFCl_2$	-67.80
$CF_2Cl.CCl_3$	-65.10
C_4F_8	-135.15
C_6F_{12}	-133.23
C_6F_6	-164.90

[a] Shifts upfield from $CFCl_3$ are negative.

Table 5.4. Fluorine coupling constants. [a]

Group	H-F coupling constant (Hz)	Group	H-F coupling constant (Hz)
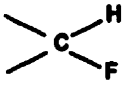	44 - 81	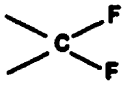	150 - 300
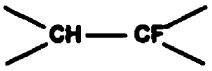	7 - 31	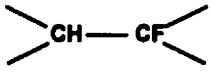	7 - 31
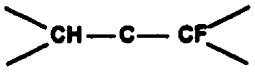	~0	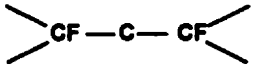	0 - 18
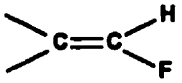	72 - 81	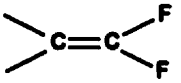	7 - 87
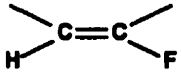	1 - 8	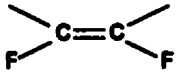	109 - 131
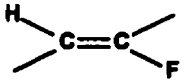	12 - 40	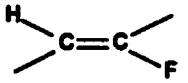	~20
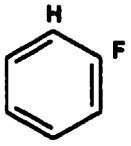	6 - 10	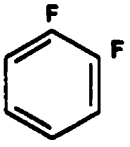	0 - 7
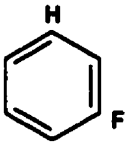	6 - 9	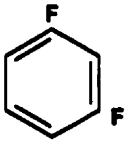	0 - 15
	~2		~2

[a] data from Freeny (1967)

Table 5.5. Contributions of dipolar interactions and chemical shift anisotropy to fluorine relaxation.

	Dipolar Interaction [a]	Chemical Shift Anisotropy [b]
Dominates [c] Linewidth	molecular weight <20 Kd and magnetic fields <300 MHz	molecular weight >20 Kd and magnetic fields >300 MHz
H	$\gamma_1\gamma_2 h^2 I_1(\frac{1}{r^3_{12}} - \frac{3r_{12}\cdot r_{12}}{r_{12}})I_2$	$\gamma h I_1 \delta H_o$
T_1^{-1}	$\gamma_1^2\gamma_2^2 h^2 I_2(I_2+1)[\frac{1}{12}J^o(\omega_1-\omega_2) + \frac{3}{2}J^1(\omega_1)+J^2(\omega_1+\omega_2)]$	$\frac{6}{40}\omega_1^2\delta_x^2(1+\frac{\eta^2}{3})J(\omega_1)$
T_2^{-1}	$\gamma_1^2\gamma_2^2 h^2 I_2(I_2+1)[\frac{1}{6}J^o(0) + \frac{1}{24}J^o(\omega_1-\omega_2)+J^1(\omega_1) + \frac{3}{2}J^1(\omega_2)+\frac{3}{8}J^2(\omega_1+\omega_2)]$	$\frac{1}{40}\omega_1^2\delta_x^2(1+\frac{\eta^2}{3})[4J(0) + 3J(\omega_1)]$
$J(\omega)$ [d] isotropic	$\frac{\tau_c}{(1+\omega^2\tau_c^2)}$	$\frac{2\tau_c}{(1+\omega^2\tau_c^2)}$

[a] Two non-identical spin interaction between spins 1 and 2 with respective gyromagnetic ratios I in hamiltonians (H) refer to the spin z component angular momentum operator and otherwise refers to the spin angular momentum. The vector distance separation is given by r, and the in the spectral density functions $J(\omega)$ is the rotational correlation time constant.

[b] The δ and η are the anisotropy and asymmetry of the fluorine chemical shift tensor

[c] From Hull & Sykes (1947); Hardin & Horowitz (1987); and Gerig (1989)

[d] The spectral density functions for other motions are described by Hardin & Horowitz (1987)

5.2. EXPERIMENTAL

5.2.1. Materials and Methods

5.2.1.1. Reactions

Acetylation of Lignin Model Compounds

Carbonyl containing compound (~ 200 mg) was acetylated with 2-4 mL of acetic anhydride/pyridine (1:1, v/v) at room temperature overnight in a 100-mL flask. Ethanol (50 mL) was added, and, after 30 min, the solvents were removed by film evaporation. Repeated addition and removal (film evaporation) of ethanol (five to ten times) resulted in the removal of acetic acid and pyridine from the sample. The acetate was dried in vacuo over KOH and P_2O_5 or purified as described below prior to drying.

Trifluoromethylation Procedure

Carbonyl containing model compound (10 mmol) was dissolved in 3 mL of high purity tetrahydrofuran (THF). To this solution an excess (15 mmol) of trifluoromethyltrimethylsilane (TMS-CF_3) was added. The mixture was then treated with a catalytic amount (20 mg) of tetramethylammonium fluoride (TMAF) under constant stirring at 0°C for 0.5 hours. It was then brought to room temperature and continued to completion (TLC). The intermediate siloxy adducts were hydrolysed by the addition of aqueous hydrofluoric acid (10% HF). Finally, the hydrolysed mixture was extracted with chloroform (3x15 mL) and dried over anhydrous magnesium sulphate. The hydrolysis of all the quinones were accomplished by replacing HF with TMAF. The isolated products were characterized by ^{19}F, ^{1}H NMR and GC-MS.

5.2.1.2. Instrumentation

^{19}F NMR Spectroscopy

All spectra were recorded on a Varian Unity 500 FT-NMR spectrometer at an operational frequency of 470.3 MHz. The model compound derivatives were dissolved in deuterated chloroform (10-20 mg/1.0 mL $CDCL_3$) using fluorotrichloromethane ($CFCl_3$) as internal reference. The measurements were carried out in a 5 mm tube at

room temperature. The acquisition time of 0.64 sec was used followed by the relaxation delay of 2 sec. The number of scans acquired was 8 per measurement. Pulse widths corresponding to a 45° flip angle and a line broadening of 1 Hz was used during acquisition and processing of the spectra.

^{1}H NMR Spectroscopy

The NMR spectra were recorded at a proton operating frequency of 200.1, 299.9 and 499.8 MHz on Varian XL-200 FT-NMR, Varian XL-300 FT-NMR and Varian unity 500 spectrometer respectively. The model compounds containing carbonyl groups and their derivatives were dissolved in deuterated chloroform (30 mg/1.0 mL $CDCL_3$) using tetramethylsilane (TMS) as internal reference. The measurements were carried out in a 5 mm tube at room temperature. No relaxation delay was used. The acquisition time for Varian XL-200 FT-NMR, Varian XL-300 FT-NMR and Varian unity 500 spectrometer were 3.752, 2.496, and 1.892 sec respectively. The number of scans for the acquisition of the ^{1}H NMR signals were 128.

^{13}C NMR Spectroscopy

The model compounds containing carbonyl groups and their derivatives were dissolved in deuterated chloroform (30 mg/1.0 mL $CDCL_3$) and quantitative ^{13}C NMR spectra were obtained on both Varian XL-300 FT-NMR and Varian Unity 500 spectrometer operating at 75.4 and 125.7 MHz respectively. The internal reference was tetramethylsilane (TMS). The measurements were carried out in a 5 mm tube at room temperature with heteronuclear-decoupling. No relaxation delay was used. The acquisition time on Varian XL-300 FT-NMR and Varian Unity 500 spectrometer were 0.970 and 1.083 sec respectively. The number of scans ranged between 65000 to 80000.

^{31}P NMR Spectroscopy

The ^{31}P NMR spectra were obtained by using inverse gated decouling on a Varian XL-300 FT-NMR spectrometer at 121.5 MHz. The internal deuterium lock was provided by the deuterium atoms present in the deuterated chloroform, used as the solvent. The

external standard was 85% H_3PO_4. All downfield shifts from H_3PO_4 were considered positive. A sweep width of 10000 Hz was observed and spectra were accumulated with a time delay of 10s between successive pulses. Pulse width corresponding to a 45° flip angle and a line broadening of 2 Hz was used for the processing of the spectra. For the 45° flip angle a series of experiment showed that there was no further increase in signal intensity after a 7s pulse delay was applied. All chemical shifts reported are relative to the dimeric model compound with water which has been observed to give a sharp ^{31}P signal at 121.1 ppm[31-34].

Gas Chromatography/Mass Spectrometry

GC-MS analyses were carried out a Hewlett Packard 5972 mass spectrometer interfaced to a Hewlett Packard 5890A gas chromatograph with a 30m x 0.25mm packed silica capillary column. The injection port temperature was 280 °C and the oven temperature was varied from 100 °C to 250 °C, with a gradient of 5 °C/min. The CF_3-containing lignin model compounds were analyzed after silylation.

5.2.2.3. Characterization of trifluoromethylated compounds

1. ^1H NMR ($CDCl_3$)(TMS) δ: 1.77 (s, 3H); 2.60 (s, 1H); 7.37-7.46 (m, 3H); 7.56-7.61 (m, 2H) ppm. ^{19}F NMR ($CDCl_3$)($CFCl_3$) δ: -81.35 (s) ppm. MS *m/z* 190 (M^+), 151, 127, 121, 105, 91, 77, 51. Anal. Calcd for $C_9H_9F_3O$: C, 56.84; H, 4.77; F, 29.97. Found: C, 56.92; H, 4.69; F, 29.92. 96% yield.

2. ^1H NMR ($CDCl_3$)(TMS) δ: 1.74 (s, 3H); 2.35 (s, 1H); 5.67 (s, 1H); 6.829 (d, 2H, J=8.78 Hz); 7.432 (d, 2H, J=8.58 Hz) ppm. ^{19}F NMR ($CDCl_3$)($CFCl_3$) δ: -81.76 (s) ppm. MS *m/z* 206 (M^+), 188, 167, 149, 137, 119, 107, 91. Anal. Calcd for $C_9H_9F_3O_2$: C, 52.43; H, 4.40; F, 27.65. Found: C, 52.48; H, 4.49; F, 27.67. 98% yield.

3. ^1H NMR ($CDCl_3$)(TMS) δ: 1.74 (s, 3H); 2.90 (s, 1H); 3.879 (d, 3H, J=6.64 Hz); 5.84 (s, 1H); 6.86-7.13 (m, 3H) ppm. ^{19}F NMR ($CDCl_3$)($CFCl_3$) δ: -81.60 (s) ppm. MS *m/z* 236 (M^+), 197, 167, 151, 124. 110, 69, 51. Anal. Calcd for $C_{10}H_{11}F_3O_3$: C, 50.85; H, 4.69; F, 24.13. Found: C, 50.91; H, 4.68; F, 24.19. 96% yield.

4. ^{1}H NMR ($CDCl_3$)(TMS) δ: 1.73 (s, 3H); 2.54 (s, 1H); 3.879 (d, 6H, J=10.26 Hz); 6.78 (s, 2H); 7.22 (s, 1H) ppm. ^{19}F NMR ($CDCl_3$)($CFCl_3$) δ: -81.47 (s) ppm. MS *m/z* 266 (M^+), 227, 197, 181, 155, 123, 93, 69. Anal. Calcd for $C_{11}H_{13}F_3O_4$: C, 49.63; H, 4.92; F, 21.41. Found: C, 49.69; H, 4.85; F, 21.35. 95% yield.

5. ^{1}H NMR ($CDCl_3$)(TMS) δ: 1.73 (s, 3H); 2.72 (s, 1H); 3.841 (d, 6H, J=2.16 Hz); 6.825 (d, 1H, J=8.48 Hz); 7.03-7.11 (m, 2H) ppm. ^{19}F NMR ($CDCl_3$)($CFCl_3$) δ: -81.56 (s) ppm. MS *m/z* 250 (M^+), 211, 181, 139, 124, 107, 95, 77. Anal. Calcd for $C_{11}H_{13}F_3O_3$: C, 52.80; H, 5.24; F, 22.78. Found: C, 52.85; H, 5.28; F, 22.80. 95% yield.

6. ^{1}H NMR ($CDCl_3$)(TMS) δ: 2.93 (s, 1H); 7.34-7.38 (m, 6H); 7.47-7.52 (m, 4H) ppm. ^{19}F NMR ($CDCl_3$)($CFCl_3$) δ: -74.79 (s) ppm. MS *m/z* 252 (M^+), 233, 213, 183, 165, 127. 105, 77. Anal. Calcd for $C_{11}H_{13}F_3O_3$: C, 66.67; H, 4.40; F, 22.60. Found: C, 66.71; H, 4.32; F, 22.66. 94% yield.

7. ^{1}H NMR ($CDCl_3$)(TMS) δ: 3.22 (s, 1H); 3.84 (s, 6H); 6.87-7.03 (m, 4H); 7.03-7.47 (m, 4H) ppm. ^{19}F NMR ($CDCl_3$)($CFCl_3$) δ: -75.11 (s) ppm. MS *m/z* 312 (M^+), 273, 243, 212, 168, 135, 108, 77. Anal. Calcd for $C_{16}H_{15}F_3O_3$: C, 61.54; H, 4.84; F, 18.25. Found: C, 61.56; H, 4.88; F, 18.17. 96% yield.

8. ^{1}H NMR ($CDCl_3$)(TMS) δ: 2.60 (s, 1H); 4.989 (q, 1H, J=6.60 Hz); 7.38-7.48 (m, 5H) ppm. ^{19}F NMR ($CDCl_3$)($CFCl_3$) δ: -78.848 (d, J_{F-H}=6.1 Hz) ppm. MS *m/z* 176 (M^+), 159, 127, 107, 89, 79, 51. Anal. Calcd for $C_8H_7F_3O$: C, 54.55; H, 4.01; F, 32.36. Found: C, 54.58 H, 3.99; F, 32.40. 97% yield.

9. ^{1}H NMR ($CDCl_3$)(TMS) δ: 2.59 (s, 1H); 3.89 (s, 3H); 4.925 (q, 1H, J=6.78 Hz); 5.72 (s, 1H); 6.947 (d, 3H, J=13.93 Hz) ppm.^{19}F NMR ($CDCl_3$)($CFCl_3$) δ: -78.981 (d, J_{F-H}=6.1 Hz) ppm. MS *m/z* 222 (M^+), 205, 183, 153, 125, 93, 65, 51. Anal. Calcd for $C_9H_9F_3O_3$: C, 48.66; H, 4.08; F, 25.65. Found: C, 48.70; H, 4.11; F, 25.69. 95% yield.

10. ^{1}H NMR ($CDCl_3$)(TMS) δ: 2.18 (s, 1H); 3.85 (s, 6H); 4.924 (q, 1H, J=6.58 Hz); 6.68 (s, 2H) ppm. ^{19}F NMR ($CDCl_3$)($CFCl_3$) δ: -78.890 (d, J_{F-H}=6.1 Hz) ppm. MS *m/z* 252 (M^+), 205, 183, 167, 155, 140, 123, 95. Anal. Calcd for $C_{10}H_{11}F_3O_4$: C, 47.63; H, 4.40; F, 22.60. Found: C, 47.62; H, 4.42; F, 22.58. 98% yield.

11. ^{1}H NMR ($CDCl_3$)(TMS) δ: 2.50 (s, 1H); 3.87 (s, 6H); 4.943 (q, 1H, J=6.64 Hz); 6.841 (t, 1H, J=4.88 Hz); 6.976 (d, 2H, J=3.42 Hz) ppm.^{19}F NMR ($CDCl_3$)($CFCl_3$) δ: -

78.916 (d, J_{F-H}=6.1 Hz) ppm. MS *m/z* 236 (M^+), 219, 197, 167, 139, 124, 108, 96. Anal. Calcd for $C_{10}H_{11}F_3O_3$: C, 50.85; H, 4.69; F, 24.13. Found: C, 50.92; H, 4.66; F, 24.11. 99% yield.

12. ^1H NMR ($CDCl_3$)(TMS) δ: 2.97 (s, 1H); 4.58-4.66 (m, 1H); 6.20 (q, 1H, J=9.46 Hz); 6.842 (d, 1H, J=15.93 Hz); 7.31-7.44 (m, 5H) ppm. ^{19}F NMR ($CDCl_3$)($CFCl_3$) δ: -79.458 (d, J_{F-H} =6.1 Hz) ppm. MS *m/z* 202 (M^+), 184, 165, 133, 115, 91, 77, 55. Anal. Calcd for $C_{10}H_9F_3O$: C, 59.41; H, 4.49; F, 28.19. Found: C, 59.45; H, 4.52; F, 28.17. 99% yield.

13. ^1H NMR ($CDCl_3$)(TMS) δ: 2.25 (s, 1H); 3.84 (s, 3H); 4.531 (t, 1H, J=13.19 Hz); 5.65 (s, 1H); 5.961 (q, 1H, J=9.12 Hz); 6.689 (d, 1H, J=15.73 Hz); 6.82-6.88 (m, 3H) ppm. ^{19}F NMR ($CDCl_3$)($CFCl_3$) δ: -79.607 (d, J_{F-H} =6.1Hz) ppm. MS *m/z* 248 (M^+), 219, 199, 179, 161, 147, 119, 91. Anal. Calcd for $C_{11}H_{11}F_3O_3$: C, 53.23; H, 4.47; F, 22.96. Found: C, 53.28; H, 4.44; F, 22.97. 99% yield.

14. ^1H NMR ($CDCl_3$) δ: 0.091 (s, 18H); 6.16 (s, 4H) ppm. ^{19}F NMR($CDCl_3$)($CFCl_3$) δ: -80.51 (s) ppm. MS *m/z* 323 (M^+ - CF_3), 307, 285, 265, 254, 223, 219, 189.

15. ^1H NMR ($CDCl_3$) δ: 2.42 (br, 4H); 6.19 (s, 4H,); 6.27 (s, 4H,) ppm. ^{19}F NMR ($CDCl_3$)($CFCl_3$) δ: -80.81 (s); -80.75 (s) ppm. MS *m/z* 179 (M^+ - CF_3), 159, 143, 110, 83, 69, 53. Anal. Calcd for $C_8H_6F_6O_2$: C, 38.73; H, 2.44; F, 45.94. Found: C, 38.75; H, 2.49; F, 45.96. 96% yield.

16. ^1H NMR ($CDCl_3$) δ: 0.08-0.09 (d, 18H, J=2.5 Hz); 1.93-1.94 (d, 3H, J=1.26 Hz); 5.85-5.86 (d, 1H, J=1.18 Hz); 6.16 (s, 2H) ppm. ^{19}F NMR ($CDCl_3$)($CFCl_3$) δ: -80.67 (s); -77.03 (s) ppm. MS *m/z* 337 (M^+ - CF_3), 321, 268, 229, 203, 175, 147, 127.

17. ^1H NMR ($CDCl_3$) δ: 2.02-2.03 (d, 3H, J=1.16 Hz); 2.30 (br, 2H); 5.98-5.99 (d, 1H, J=1.72 Hz); 6.24-6.25 (t, 2H, J=2.16 Hz) ppm. ^{19}F NMR ($CDCl_3$)($CFCl_3$) δ: -81.21 (s); -77.25 (s) ppm. MS *m/z* 193 (M^+ - CF_3), 173, 145, 124, 69, 51. Anal. Calcd for $C_9H_8F_6O_2$: C, 41.24; H, 3.08; F, 43.48. Found: C, 41.27; H, 3.15; F, 43.50. 95% yield.

18. ^1H NMR ($CDCl_3$) δ: -0.137- -0.125 (d, 18H, J=2.38 Hz); 1.36-1.39 (d, 9H, J=5.30 Hz); 7.45-7.51 (m, 3H); 7.80-7.95 (m, 4H) ppm. ^{19}F NMR ($CDCl_3$)($CFCl_3$) δ: -78.56 (s); -78.55 (s) ppm. MS *m/z* 479 (M^+ -CF_3), 441, 410, 372, 344, 301, 267, 233.

19. ^{1}H NMR ($CDCl_3$) δ: 1.37-1.41 (d, 9H, J=8.60 Hz); 3.19-3.30 (d, 2H, J=21.23 Hz); 7.52-7.60 (m, 3H); 7.89-8.03 (m, 4H) ppm. ^{19}F NMR ($CDCl_3$)($CFCl_3$) δ: -78.61 (s); -78.29 (s) ppm. MS *m/z* 335 (M^+ - CF_3), 320, 266, 251, 209, 181, 152, 112. Anal. Calcd for $C_{20}H_{18}F_6O_2$: C, 59.41; H, 4.49; F, 28.19. Found: C, 59.38; H, 4.46; F, 28.22. 94% yield.

20. ^{1}H NMR ($CDCl_3$) δ: 0.021 (s, 18H); 1.03 (s, 9H); 1.20 (s, 9H); 5.39 (s, 1H); 6.01 (s, 1H) ppm. ^{19}F NMR ($CDCl_3$)($CFCl_3$) δ: -68.84 (s); -74.89 (s) ppm. MS *m/z* 504 (M^+ - CF_3), 489, 435, 399, 379, 327, 285, 259.

21. ^{1}H NMR ($CDCl_3$) δ: 1.05 (s, 9H); 1.25 (s, 9H); 2.45 (s, 1H); 3.05 (s, 1H); 5.19 (s, 1H); 6.06 (s, 1H) ppm.^{19}F NMR ($CDCl_3$)($CFCl_3$) δ: -69.59 (s); -75.87 (s) ppm. MS *m/z* (silylated) 504 (M^+ - CF_3), 489, 399, 379, 327, 285, 259, 239. Anal. Calcd for $C_{16}H_{22}F_6O_2$: C, 53.33; H, 6.15; F, 31.63. Found: C, 53.40; H, 6.10; F, 31.59. 89% yield.

22. ^{1}H NMR ($CDCl_3$) δ: 0.042 (s, 18H); 7.22-7.31 (m, 3H); 7.36-7.61 (m, 4H); 7.76-7.83 (m, 3H) ppm. ^{19}F NMR ($CDCl_3$)($CFCl_3$) δ: -74.52 (s) ppm. MS *m/z* 247 (M^+ - $C_{11}H_{14}F_3OSi$), 213, 181, 165, 135, 105, 77, 51.

23. ^{1}H NMR ($CDCl_3$) δ: 4.75 (s, 2H); 7.25-7.34 (m, 2H); 7.41-7.55 (m, 6H); 7.67-7.72 (t, 2H, J=7.32 Hz) ppm. ^{19}F NMR ($CDCl_3$)($CFCl_3$) δ: -73.55 (s) ppm. MS *m/z* 175 (M^+ - $C_8H_6F_3O$), 152, 105, 77, 51. Anal. Calcd for $C_{16}H_{12}F_6O_2$: C, 54.87; H, 3.45; F, 32.54. Found: C, 54.91; H, 3.50; F, 32.58. 98% yield.

25. ^{1}H NMR ($CDCl_3$)(TMS) δ: 3.63 (s, 1H); 3.78 (s, 3H); 3.863 (d, 6H, J=5.40 Hz), 4.07-4.12 (m, 2H); 4.449(t, 1H, J=1.80 Hz); 5.57 (s, 1H); 6.692 (q, 1H, J=3.60 Hz); 6.77-6.83 (m, 2H); 6.865 (d, 1H, J=5.10 Hz); 6.95-6.99 (m, 1H); 7.193 (d, 1H, J=4.80 Hz); 7.294 (d, 1H, J=1.2 Hz) ppm. ^{13}C NMR ($CDCl_3$)(TMS) δ: 55.85; 56.04; 56.17; 61.36; 79.59 (q, $J_{C\text{-}CF}$=26.4 Hz); 82.64; 109.87; 110.48; 112.07; 118.25; 120.72; 121.66; 124.62; 124.97 (q, $J_{C\text{-}F}$=286.59 Hz); 128.93; 146.18; 148.56; 148.89; 151.53 ppm. ^{19}F NMR ($CDCl_3$)($CFCl_3$) δ: -75.53 (s) ppm. MS *m/z* (silylated) 402 (M^+), 302, 278, 248, 235, 221, 181, 165. Anal. Calcd for $C_{19}H_{21}F_3O_6$: C, 56.72; H, 5.26; F, 14.16. Found: C, 56.74; H, 5.29; F, 14.22. 95% yield.

27. ^{1}H NMR ($CDCl_3$)(TMS) δ: 3.84 (s, 3H); 3.87 (s, 3H); 3.90 (s, 3H), 3.93 (d, 1H, J=3 Hz); 4.24 (d, 1H, J=12 Hz); 4.640 (d, 1H, J=12 Hz); 5.865 (d, 1H, J=3 Hz); 6.84-7.12 (m, 6H) ppm. ^{13}C NMR ($CDCl_3$)(TMS) δ: 56.11; 56.19; 56.64; 71.68; 75.62 (q,

$J_{C\text{-}CF}$=27.9 Hz); 108.78; 110.06; 111.44; 113.40; 120.41; 121.80; 122.95; 125.60 (q, $J_{C\text{-}F}$=286.59 Hz); 127.88; 147.37; 148.68; 149.16; 149.95 ppm. ^{19}F NMR ($CDCl_3$)($CFCl_3$) δ: -77.63 (s) ppm. MS *m/z* 372 (M^+), 303, 248, 235, 217, 189, 180. Anal. Calcd for $C_{18}H_{19}F_3O_5$: C, 58.06; H, 5.14; F, 15.31. Found: C, 58.21; H, 5.20; F, 15.29. 96% yield.

29. ^{1}H NMR ($CDCl_3$)(TMS) δ: 2.25 (s, 3H); 3.75 (s, 1H); 3.79 (s, 3H), 3.88 (s, 3H); 3.935 (d, 1H, J=9 Hz); 4.12 (d, 1H, J=5.99 Hz); 4.33 (s, 1H); 5.60 (s, 1H,); 5.70 (s, 1H); 6.55-6.64 (m, 3H); 6.94 (d, 1H, J=5.40 Hz); 7.10 (d, 1H, J=4.80 Hz); 7.311 (d, 1H, J=1 Hz) ppm. ^{13}C NMR ($CDCl_3$)(TMS) δ: 21.19; 55.88; 55.93; 61.31; 79.85 (q, $J_{C\text{-}CF}$=28.9 Hz); 82.64; 109.59; 112.95; 113.93; 118.43; 121.01; 122.19; 125.07 (q, $J_{C\text{-}F}$=286.59 Hz); 128.71; 134.83; 143.81; 145.62; 146.35; 151.36 ppm. ^{19}F NMR ($CDCl_3$)($CFCl_3$) δ: -75.48 (s) ppm. MS *m/z* (silylated) 618 (M^+), 480, 451, 411. 365, 343, 323, 271. Anal. Calcd for $C_{19}H_{21}F_3O_6$: C, 56.72; H, 5.26; F, 14.16. Found: C, 56.78; H, 5.19; F, 14.18. 93% yield.

5.3. RESULTS & DISCUSSION

Initially a series of model compounds containing carbonyl groups, including various quinones, were trifluoromethylated and their ^{19}F NMR spectra were examined. This was done in order to understand the relationships between the chemical environment of CF_3-containing derivatives and their ^{19}F NMR chemical shifts. Detailed work with carbonyl containing arylglycerol β-O-4 ether model compounds followed, aimed at understanding the trifluoromethylation reaction so that it can eventually be applied to lignins, solid wood and paper samples.

Prior to commencing the discussion, an examination of the ^{19}F chemical shifts of fluorine-containing compounds is described. Such data was obtained on four different monofluorinated organic compounds in order to commence accumulating information on the structure versus ^{19}F chemical shift relationships. Monofluorinated aromatic compounds exhibited a single ^{19}F NMR signal upfield from $CFCl_3$.

Furthermore, in order to examine the chemical shifts of monofluorinated-organic compounds containing carbonyl group, *p*-fluorobenzaldehyde was trifluoromethylated. The resulting fluorine-containing derivatives featured two major ^{19}F NMR signals. One at -103.26 ppm due to the original aromatic fluorine and a new signal (a doublet) due to the trifluoromethyl group present on the carbon atom of the former carbonyl group in benzaldehyde, i.e. at -79.122 and -79.144 ppm (Table 5.6).

In general the chemical shifts of the aromatic fluorine atoms occur within the range δ=-130 to -180 ppm (upfield from $CFCl_3$). Fluorine chemical shift (δ_F) of substituted compounds generally decrease in the order *ortho* > *para* > *meta*. The shifts of fluorine nuclei *meta* or *para* to a substituent can be successfully correlated with their π-electron charge densities and bond orders as calculated by the Hückel MO method. For example, substituents such as $-NH_2$ and -OH, which produce an increase in the π-electron density at the *para* carbon atom, produce an increase in the shielding of the *para* fluorine atoms and substituents such as $-NO_2$ and -CHO, which decrease the π-electron density, decrease the fluorine shielding. However, for fluorine nuclei in a position *ortho* to a substituent, large deviations are always found. This is the so-called "ortho effect":

whenever two fluorine atoms are in *ortho* positions to each other an upfield shift of about 20 ppm is apparent. This effect is found to be a feature of all the fluorobenzene shifts and is additive. In fact such an effect was observed in the ^{19}F NMR analysis of *o*- and *p*-fluoroaniline. The ^{19}F chemical shift of *o*-fluoroaniline was observed upfield to that of *p*-fluoroaniline by approximately 8 ppm (Table 5.6).

Table 5.6. F-19 NMR signals of some monofluorinated organic compounds.

Compound	Chemical Structure	^{19}F NMR (ppm)
Fluoro benzene		**-113.5**
***o*-Fluoro aniline**	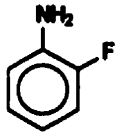	**-135.6**
***p*-Fluoro aniline**		**-127.3**
***p*-Fluoro benzaldehyde**	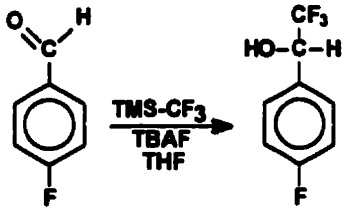 (A) (B)	**-103.2 (A)** **-103.2, -79.133 (B)** **(d, J_{F-H}=6.2 Hz)**

Such ortho effects can be accounted for satisfactorily in terms of intramolecular electric field contributions. Differences in δ_F in substituted aromatic compounds can be reasonably predicted according to the following relation[47]:

$$\Delta\sigma = \Delta\sigma_{electronic} + \Delta\sigma_{electric} \qquad [5.8]$$

where $\Delta\sigma_{electronic}$ takes into account differences in π-electron charge distribution and $\Delta\sigma_{electric}$ is the difference in the resultant electric fields at fluorine nuclei.

This demonstrates that the chemical shift of ^{19}F is quite sensitive to environment[48] and therefore ^{19}F spectroscopy would be useful tool for measuring and probing different classes of compound containing fluorine and fluorine-derivatives.

5.3.1. Aromatic Compounds Containing Carbonyl Groups

Various organic compounds containing carbonyl groups in different chemical environments were subjected to the described trifluoromethylation reaction. This eventually allowed for the correlation of trifluoromethylated structures to their ^{19}F resonance for carbonylic environments that may likely be present in lignins. These studies indicated that the ^{19}F NMR chemical shifts vary significantly for several classes of carbonyl groups. For example, the ^{19}F NMR signal of various trifluoromethylated ketones, such as acetophenone (1) was observed at -81.35 ppm distinguishing it from that of *p*-hydroxyacetophenone (2) recorded at -81.76 ppm upfield from $CFCl_3$. Such variations of ^{19}F chemical shifts were also apparent for different aldehydes.

The ^{19}F NMR chemical shift of trifluoromethylated benzaldehyde (8) was recorded (doublet) at -78.848 ppm while the ^{19}F NMR signals moved progressively downfield with the addition of different substituents on the benzene ring. This demonstrates that the chemical shift of ^{19}F is quite sensitive to environment[48] and therefore ^{19}F spectroscopy would be useful tool for measuring and probing different classes of compounds containing fluorine and fluorine-derivatives.

It is well known that the fluorine (^{19}F) nucleus has similar magnetic properties to those of the proton, and may be coupled not only with each other, but also with protons. Absorption by fluorine does not appear in the proton NMR spectrum since it appears far off the proton observation scale, but fluorine splitting of proton signals can be seen. This was evident for all the trifluormethylated aldehyde derivatives examined during this work. All the aldehydes were found to have the same splitting (6.1 Hz), while they exhibited different ^{19}F NMR chemical shifts due to different chemical substituents present on their benzene rings.

Another significant observation during this phase of our work showed that all ^{19}F NMR signals of the various trifluoromethylated ketones appeared at a region distinct to those of aldehydes. For example, different trifluoromethylated aldehydes exhibited signals at about -79 ppm, while trifluoromethylated ketones gave ^{19}F signals at about -81 ppm. This is a very significant feature of this work since it can be used for the classification of the different carbonyl environments that may be present in lignin (Table 5.7 and 5.8).

The introduction of a trifluoromethyl group onto the carbon atom of ketone or aldehyde may alters the chemical properties of almost all the starting ketones[1] and aldehydes to chiral compounds. This may allow the compounds to exhibit optical activity, and manifest enantiomeric properties. Furthermore, Norgai et al.[49] have also concluded that a trifluoromethyl group " behaves as a substitutent as large as a cyclohexyl group and a little smaller than a *sec*-butyl group". The observed ^{19}F chemical shift variations therefore, are not surprising.

5.3.1.1. Salient Features of the Reaction

The trifluoromethylation of most of the examined organic compounds was first carried out in the presence of catalytic amounts of tetra-n-butylammonium fluoride (TBAF) acting as an initiator for the reaction. Although this salt was quite effective on the series of chain reactions required, other catalysts were also investigated since the reaction yields were consistently low. Potassium *tert*-butoxide and *tetra*-n-butylammonium iodide (TBAI) have been used with success as initiators for the trifluoromethylation of acetophenone[50]. In comparison to tetra-n-butylammonium fluoride (TBAF), both work equally well. In fact the final yields of the reaction increased to about 88% when potassium *tert*-butoxide was employed. However, there are some drawbacks associated with the use of such initiators, restricting their use in trifluoromethylating lignins.

In general the treatment of carbonyl-containing compounds with Ruppert's reagent in the presence of TBAF only resulted in qualitatively converting these compounds to

[1] Except for benzophenone (6) and 4,4'-dimethoxybenzophenone (7).

their siloxy intermediates. The hydrolysis of trimethylsiloxytrifluoromethylated intermediates was also found to be rather inefficient when dilute HCl was used. For the case of benzophenone, the hydrolysis of the siloxy intermediates was particularly inefficient. Such problems were also observed by another group in their attempt to trifluoromethylate hindered steroidal ketones[51]. Both of these issues were found to be responsible for the low overall yields of the reaction. Such yields could not qualify this reaction as an analytical tool. Wang and Ruan succeeded in improving the yields of this reaction to quantitative levels, by using the more effective tetramethylammonium fluoride (TMAF) as an initiator.

In our work we addressed the issue of efficiently cleaving the silyl ethers by using 40% aqueous HF solution in acetonitrile (CH_3CN)[52]. After careful purification of the products, their yield was calculated and compared to those with TBAF. The combination of TMAF and 40% HF was therefore used in all subsequent efforts of trifluoromethylating the various sets of compounds discussed in this thesis[2].

5.3.2. Quinones

Another class of carbonyl-containing compounds of special interest to wood science is α,β-unsaturated ketones known as quinones. Quinones are an interesting and valuable class of compounds because of their oxidation-reduction properties. They can be easily reduced to hydroquinones by reagents like sodium borohydride ($NaBH_4$) and stannous chloride ($SnCl_2$). Alternatively hydroquinones can be easily reoxidized back to quinones by potassium nitrosodisulfonate (Fremy's salt). Since quinones are highly conjugated, they are colored; *p*-benzoquinone, for example, is yellow. In addition, due to their high degree of conjugation, quinones are energetically closely balanced against the corresponding hydroquinones. This facility of interconversion provides a convenient oxidation-reduction system that has been studied intensively.

[2] Quinones were hydrolyzed with TMAF.

Table 5.7. Fluoride ion induced trifluoromethylation of carbonyl compounds of ketones with trifluoromethyltrimethylsilane.

Entry	Precursor	Product	Reaction Conditions	Overall % Yield	^{19}F NMR$_{(ppm)}$	GC-MS m/e
1)	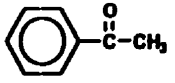	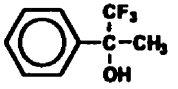	0 °C, 30 min 25 °C, 16h hydrolysis, 8h	96	-81.35	MS m/z 190 (M^+), 151, 127, 121, 105, 91.
2)	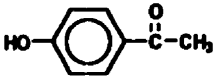	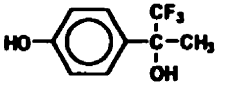	0 °C, 30 min 25 °C, 6h hydrolysis, 2h	98	-81.76	MS m/z 206 (M^+), 188, 167, 149, 137, 119.
3)	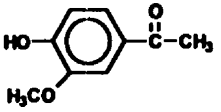	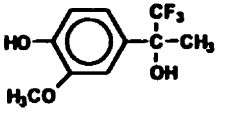	0 °C, 30 min 25 °C, 14h hydrolysis, 5h	96	-81.60	MS m/z 236 (M^+), 197, 167, 151, 124, 110.
4)	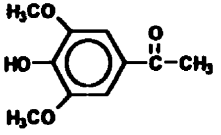	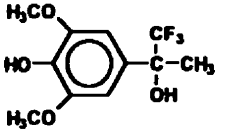	0 °C, 30 min 25 °C, 18h hydrolysis, 2h	95	-81.47	MS m/z 266 (M^+), 227, 197, 181, 155, 123.
5)	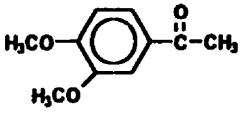	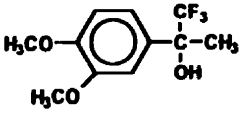	0 °C, 30 min 25 °C, 14h hydrolysis, 5h	95	-81.56	MS m/z 250 (M^+), 211, 181, 139, 124, 107.
6)	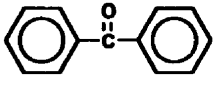	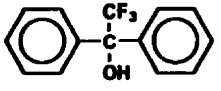	0 °C, 30 min 25 °C, 16h hydrolysis, 5h	94	-74.79	MS m/z 252 (M^+), 253, 213, 183, 165, 127.
7)	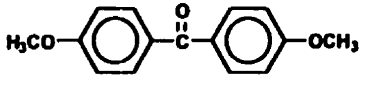	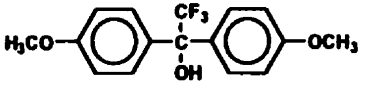	0 °C, 30 min 25 °C, 16h hydrolysis, 5h	96	-75.11	MS m/z 312 (M^+), 273, 243, 212, 135, 108.

Table 5.8. Fluoride ion induced trifluoromethylation of carbonyl compounds of aldehydes with trifluoromethyltrimethylsilane.

Entry	Precursor	Product	Reaction Conditions	Overall % Yield	^{19}F NMR(ppm)	GC-MS m/e
8)	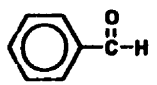	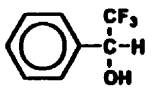	0 °C, 30 min 25 °C, 20h hydrolysis, 5h	97	-78.848 (d, J_{F-H} = 6.1 Hz)	MS m/z 176 (M^+), 159, 127, 107, 89, 79.
9)	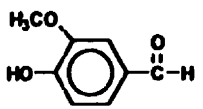	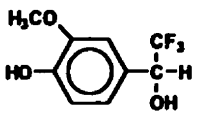	0 °C, 30 min 25 °C, 20h hydrolysis, 5h	95	-78.981 (d, J_{F-H} = 6.1 Hz)	MS m/z 222 (M^+), 205, 183, 153, 125, 93.
10)	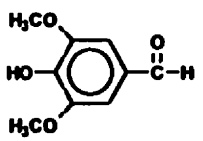	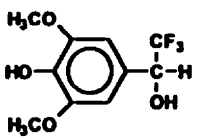	0 °C, 30 min 25 °C, 24h hydrolysis, 5h	98	-78.890 (d, J_{F-H} = 6.1 Hz)	MS m/z 252 (M^+), 205, 183, 167, 155, 140.
11)	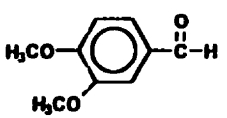	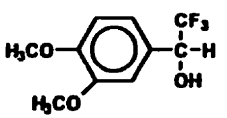	0 °C, 30 min 25 °C, 24h hydrolysis, 5h	99	-78.916 (d, J_{F-H} = 6.1 Hz)	MS m/z 236 (M^+), 219, 197, 167, 139, 124.
12)	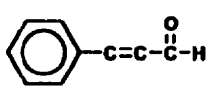	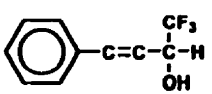	0 °C, 30 min 25 °C, 16h hydrolysis, 5h	99	-79.458 (d, J_{F-H} = 6.1 Hz)	MS m/z 202 (M^+), 184, 165, 133, 115, 91.
13,	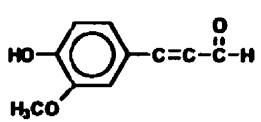	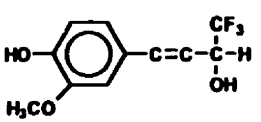	0 °C, 30 min 25 °C, 18h hydrolysis, 5h	99	-79.607 (d, J_{F-H} = 6.1 Hz)	MS m/z 248 (M^+), 219, 199, 179, 161, 147.

In many cases quinones and aromatic hydroquinones seem to take part in oxidation-reduction cycles essential to living organisms. A number of studies have shown that quinones are present, in small amounts in wood and high-yield mechanical pulps[53,54]. However, despite their low abundance, they have been held responsible as one of the significant factors for the yellowing of paper[55-60].

The trifluoromethylation of quinones by adding only to one of the carbonyl carbon atoms has been studied by Stahly and Bell[61]. However, in an effort to evaluate the reactivity of quinones (on both carbonyl carbon atoms) with Ruppert's reagent, a number of different compounds were selected and trifluoromethylated.

Initially *p*-benzoquinone was trifluoromethylated. The CF_3-containing trimethylsiloxy intermediate **(14)** was isolated and later examined by ^1H and ^{19}F NMR spectroscopies. The ^1H NMR spectrum featured two signals. One of them was very close to the signal of tetramethylsilane (TMS) internal standard, and was most likely due to the intermediate trimethylsiloxy adduct while the second signal was attributed to the four environmentally equivalent methyl protons. The upfield position of this signal in comparison to the starting material indicated the elimination of the deshielding effect of the carbonyl groups caused by the trifluoromethylation reaction. On the other hand, the ^{19}F NMR spectrum exhibited only one signal at -80.51 ppm, suggesting that both introduced trifluoromethyl groups were environmently equivalent.

After hydrolysis, the isolated compound **(15)** was subjected to ^{19}F and ^1H NMR investigations in order to assign the signals for the corresponding fluorine and alcohol groups of the derivative. The ^{19}F NMR spectrum showed two signals with equal intensity and 0.05 ppm difference in their chemical shifts (Figure 5.6). The ^1H NMR spectrum confirmed the complete hydrolysis of the silyl ethers, since the trimethylsiloxy signal disappeared completely and instead a new signal due to the hydroxyl group appeared at 2.42 ppm. In addition, two other signals corresponding to the four unsaturated protons of each stereoisomer were observed.

This data in conjunction with its GC-MS spectrum, confirmed the purity of the products. As such, the formation of two stereoisomers (***syn*** and ***anti***) as a result of trifluoromethylation and hydrolysis became evident. The absence of these geometric

isomers prior to hydrolysis can only be explained by the presence of the bulky trimethylsiloxy groups which considerably hinders the formation of the"*syn*" isomer, therefore giving rise to only one signal in the ^{19}F NMR spectrum at -80.51ppm.

Methyl-*p*-benzoquinone, being of the same class as *p*-benzoquinone, yet asymmetric, when subjected to trifluoromethylation and the products examined by ^{1}H and ^{19}F NMR spectroscopies showed that both carbonyl groups were substituted by the CF_3 groups. The ^{19}F NMR spectrum of the new compound **(16)** displayed two well resolved signals at -77.03 and -80.67 ppm. These signals were assigned to both CF_3 substituted of the former carbonyl carbons adjacent and nonadjacent to the methyl group, respectively.

In an additional effort to examine an alternative siloxy hydrolysis systems the siloxy adduct of methyl-*p*-benzoquinone was also treated with N,N´-dimethylformamide in potassium fluoride (DMF-KF). Detailed examination of the isolated products showed that such hydrolysis medium was effective at cleaving silyl ether bonds yielding the corresponding alcohols. However, the high boiling point of DMF caused difficulties during the workup.

The subsequent hydrolysis of the CF_3-containing siloxy intermediates with 40% HF solution was limited since such concentrations would result in the cleavage of several arylglycerol β-O-4 ether bonds when applied to lignins. However, lower concentration of HF (i.e. 10%) failed to cleave silyl ether bonds completely due to the low solubility of quinones in acetonitrile. This problem was resolved by the addition of tetramethylammonium fluoride (TMAF) in THF at room temperature. Such combination was able to cleave the trimethylsiloxy intermediates effectively to their corresponding alcohols, resulting in the development of a novel method of cleaving silyl ethers.

When 2-*tert*-butyl anthraquinone was subjected to trifluoromethylation, the ^{1}H NMR spectrum of the isolated intermediate **(18)** showed the presence of trimethylsiloxy groups, and its ^{19}F NMR spectrum displayed two overlapping signals seperated by 0.007 ppm. Such evidence supported the observation of two stereoisomers of derivatized *p*-benzoquinones.

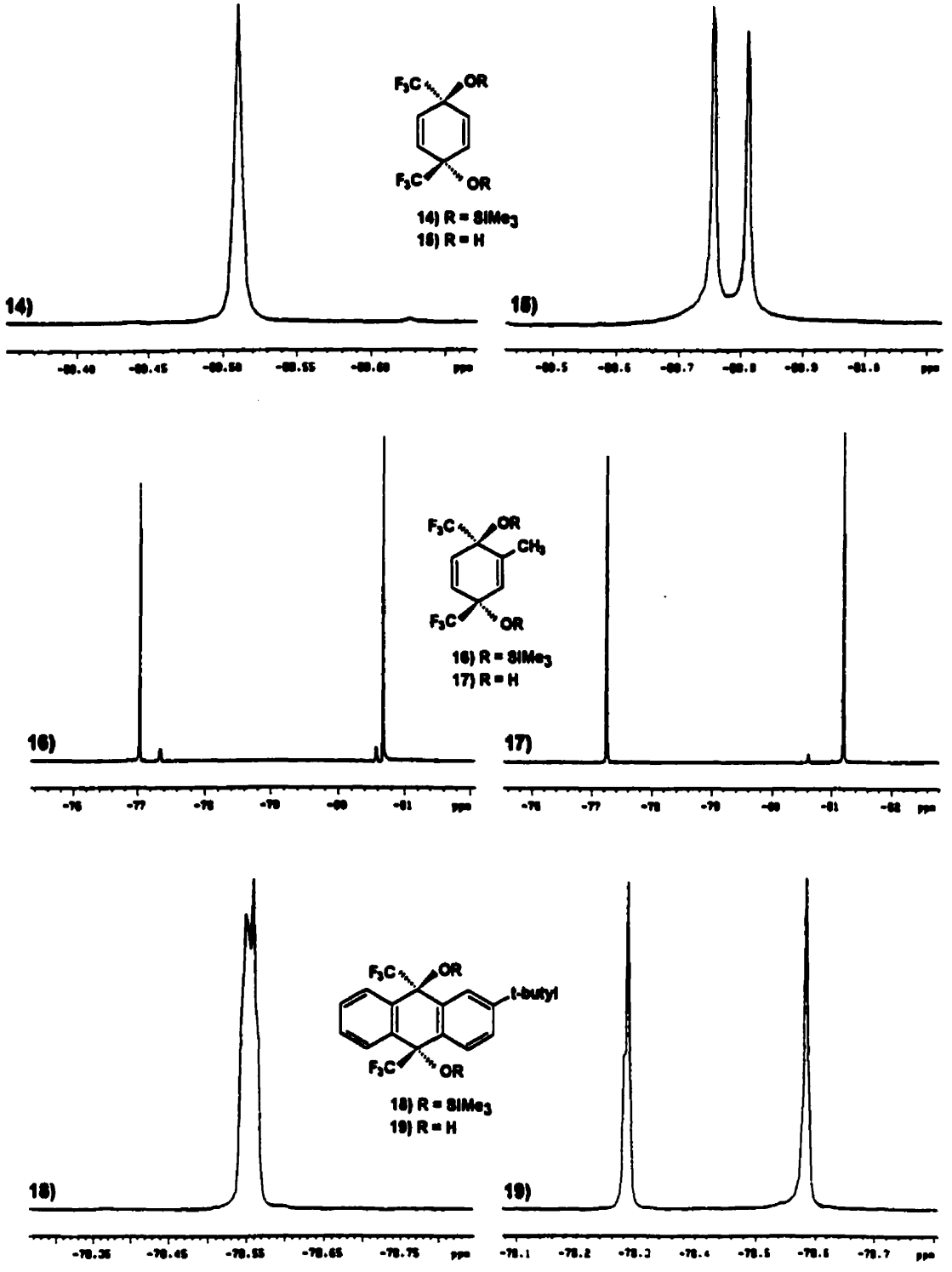

Figure 5.6. ^{19}F NMR spectra of trifluoromethylated quinones before (left) and after (right) hydrolysis.

This was concluded since the *t*-butyl group, though far removed from the carbonyl groups is less sterically hindering than the neighbouring methyl group in methyl-*p*-benzoquinone (Figure 5.6).

The ^{1}H NMR spectrum of **(19)** showed a broad signal due to the hydroxyl groups at 3.19 ppm, while its ^{19}F NMR spectrum showed two signals at -78.29 and -78.61 ppm due to the substituted CF_3 and -OH groups on both carbon atoms of the carbonyl groups.

In addition to *para* quinones, *ortho* quinones are another important class of dicarbonyl-containing compounds that may be found in lignin. *Ortho* quinones may be formed during demethylation and/or deprotonation of several guaiacyl-lignin structures as a result of various chemical reactions.

To evaluate the reactivity of *ortho* quinone with Ruppert's reagent, 3´,5´-di-*tert*-butyl-1,2 benzoquinone was trifluoromethylated and hydrolysed. The trifluoromethylated intermediates **(20)** and hydrolysed **(21)** were isolated and probed with ^{19}F, ^{1}H spectroscopies, and GC-MS. According to the obtained data, *ortho* quinones were found to undergo this process quite efficiently as shown in Table 5.9.

Furthermore, the same procedure was carried out for benzil, and the chemistry of the trifluoromethylated intermediates **(22)** and alcohols **(23)** was once again studied in detail. The ^{19}F NMR spectra of the both **(22)** and **(23)** depicted only one signal due to the symmetric structure of benzil.

5.3.3. Lignin Model Compounds

Our efforts toward examining the potential of Ruppert's reagent for the elucidation of carbonyl groups in lignins were then focused at dimeric model compounds containing carbonyl groups, resembling those present in lignins. Dimeric model compounds have often been used in NMR studies aimed at the structural elucidation of lignins[62-66].

^{31}P, ^{1}H, ^{13}C NMR spectroscopies, and GC/MS analyses were used in a manner similar to that described so far in each step of the trifluoromethylation reaction and the obtained spectra were compared to those of the starting materials aimed at monitoring all changes that took place during the course of the reaction.

Table 5.9. Fluoride ion induced trifluoromethylation of quinones with trifluoromethyltrimethylsilane.

Entry	Precursor	Product	Reaction Conditions	Overall % Yield	^{19}F NMR(ppm)	GC-MS m/e
14) 15)	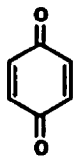	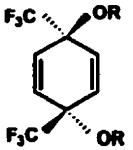 14) R = $SiMe_3$ 15) R = H	0°C, 30 min 25°C, 6h hydrolysis, 5h	96	14 {-80.51 15 {-80.75 {-80.81	MS m/z 323 (M^+- CF_3), 307, 285, 265, 254, 223. MS m/z 179 (M^+- CF_3), 159, 143, 110, 83, 69.
16) 17)	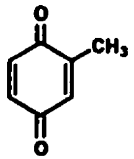	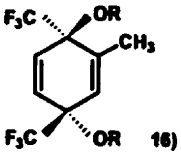 16) R = $SiMe_3$ 17) R = H	0°C, 30 min 25°C, 7h hydrolysis, 5h	95	16 {-77.03 {-80.67 17 {-77.25 {-81.21	MS m/z 337 (M^+- CF_3), 321, 268, 229, 203, 175. MS m/z 193 (M^+- CF_3), 173, 145, 124, 69, 51.
18) 19)	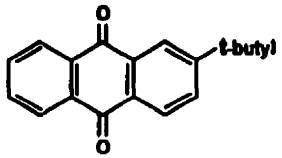	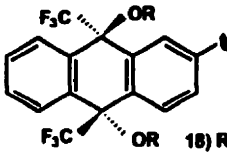 18) R = $SiMe_3$ 19) R = H	0°C, 30 min 25°C, 8h hydrolysis, 6h	94	18 {-78.55 {-78.56 19 {-78.29 {-78.61	MS m/z 479 (M^+- CF_3), 410, 372, 344, 301, 267. MS m/z 335 (M^+- CF_3), 320, 266, 251. 209, 181.
20) 21)	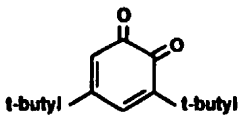	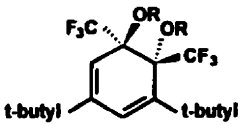 20) R = $SiMe_3$ 21) R = H	0°C, 30 min 25°C, 4h hydrolysis, 5h	89	20 {-68.84 {-74.89 21 {-69.59 {-75.87	MS m/z 504 (M^+- CF_3), 489, 435, 399, 379, 327. MS m/z 504 (silylated), (M^+ - CF_3), 489, 399, 379, 327, 285.
22) 23)	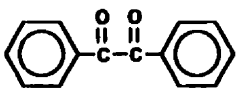	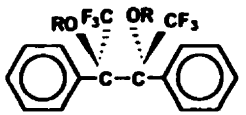 22) R = $SiMe_3$ 23) R = H	0°C, 30 min 25°C, 5h hydrolysis, 4h	98	22 {-74.52 23 {-73.55	MS m/z 247 (M^+- $C_{11}H_{14}F_3OSi$), 213, 181, 165, 135, 105. MS m/z 175 (M^+- $C_8H_6F_3O$), 152, 105, 77, 51.

Initial attempts to trifluoromethylate the α-carbonyl of dimer **(24)** [3,4-dimethoxy-α-(2-methoxy-phenoxy)-γ-hydroxy propiophenone] posed some difficulties since low yields of the trifluoromethylated products were obtained when stoichiometric amounts of TMS-CF_3 in the presence of TBAF were used. The presence of the primary γ-OH was suspected as interfering with reaction of **(24)** with TMS-CF_3.In an effort to understand the role of the γ-OH in this reaction, two avenues were followed.

The compound was acetylated prior to trifluoromethylation, thus protecting the primary γ hydroxyl groups. Following acetylation, the model compound was trifluoromethylated selectively at the carbonyl group. After hydrolysis with 1N HCl, the yield of the purified products was calculated to be 46%. Although this procedure improved the final yield to a small extent, the reaction yield was still low for using this reaction to quantitatively study lignins.

Trifluoromethylation of 3,4-dimethoxy-α-(2-methoxy-phenoxy) acetophenone **(26)** was the other approach. The overall trifluoromethylation of the α-carbonyl of **(26)** took place with somewhat more facility than that of **(24)**. Although the spectral analysis of the product **(27)** showed only one ^{19}F NMR signal at -77.63 ppm due to trifluoromethyl group, the yield of the product never exceeded 46%.

Finally the yields of these reactions were considerably improved by using tetramethylammonium fluoride (TMAF) as the initiator and 20% aqueous HF in acetonitrile as the hydrolysis medium. These modifications not only increased the reaction yields by twofold they also gave fully clean trifluoromethylated products.

The ^{19}F NMR spectrum of **(25)** showed a single signal at -75.53 ppm due to substituted CF_3, while the ^{31}P NMR spectra featured a signal at 127.4 ppm due to the formation of tertiary α-OH as a result of the hydrolysis.

The ^{13}C NMR contained a new quartet due to the CF_3 group while the complete elimination of the carbonyl signal signified the trifluoromethylation of the carbonyls (Table 5.12 and Figure 5.8). This was verified by examining the ^{1}H NMR spectrum of the compound, where a new signal at 5.57 ppm signified the formation of α-OH (Figure 5.7).

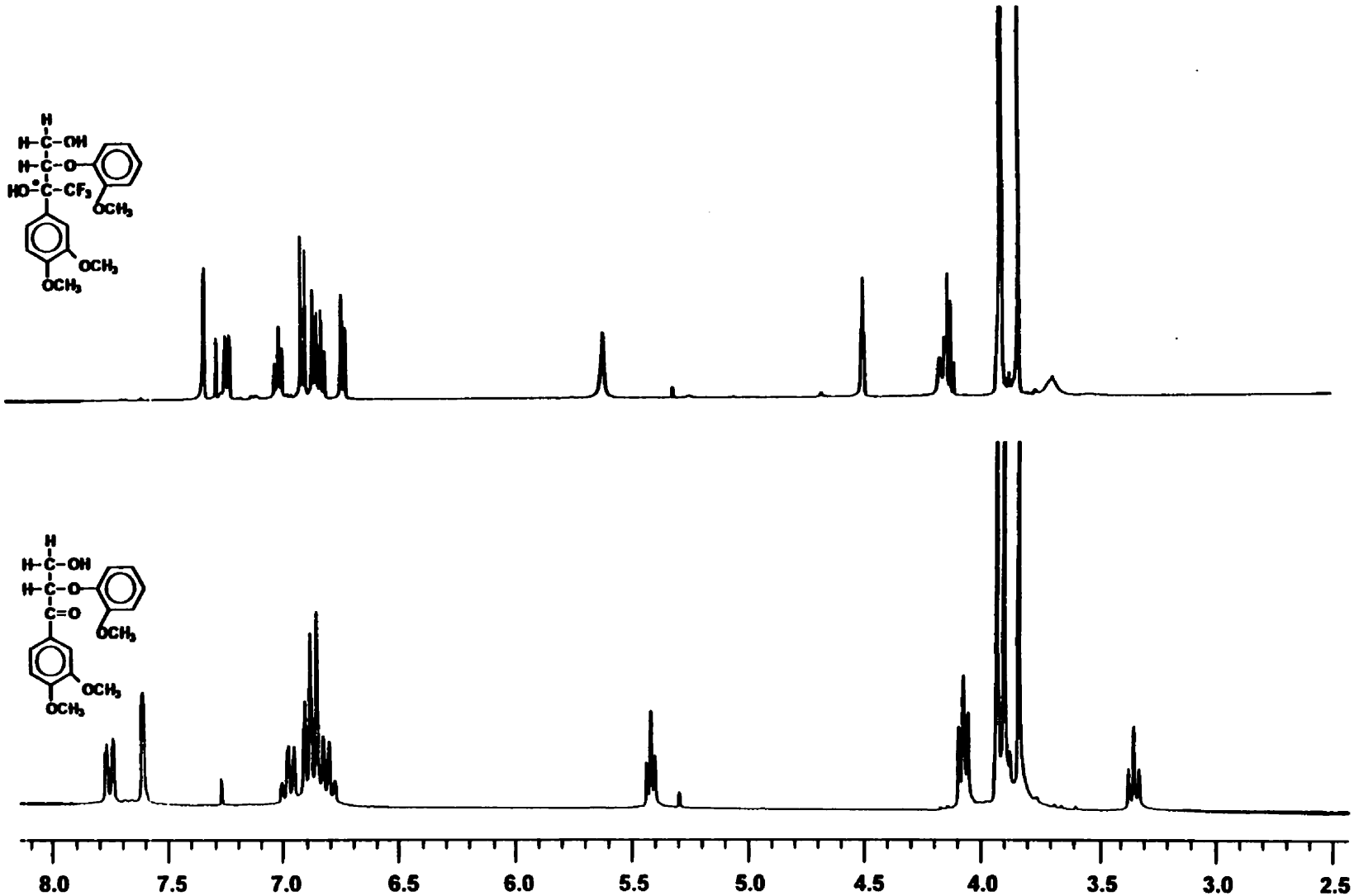

Figure 5.7. ^{1}H NMR spectra of lignin model compound, before and after trifluoromethylation.

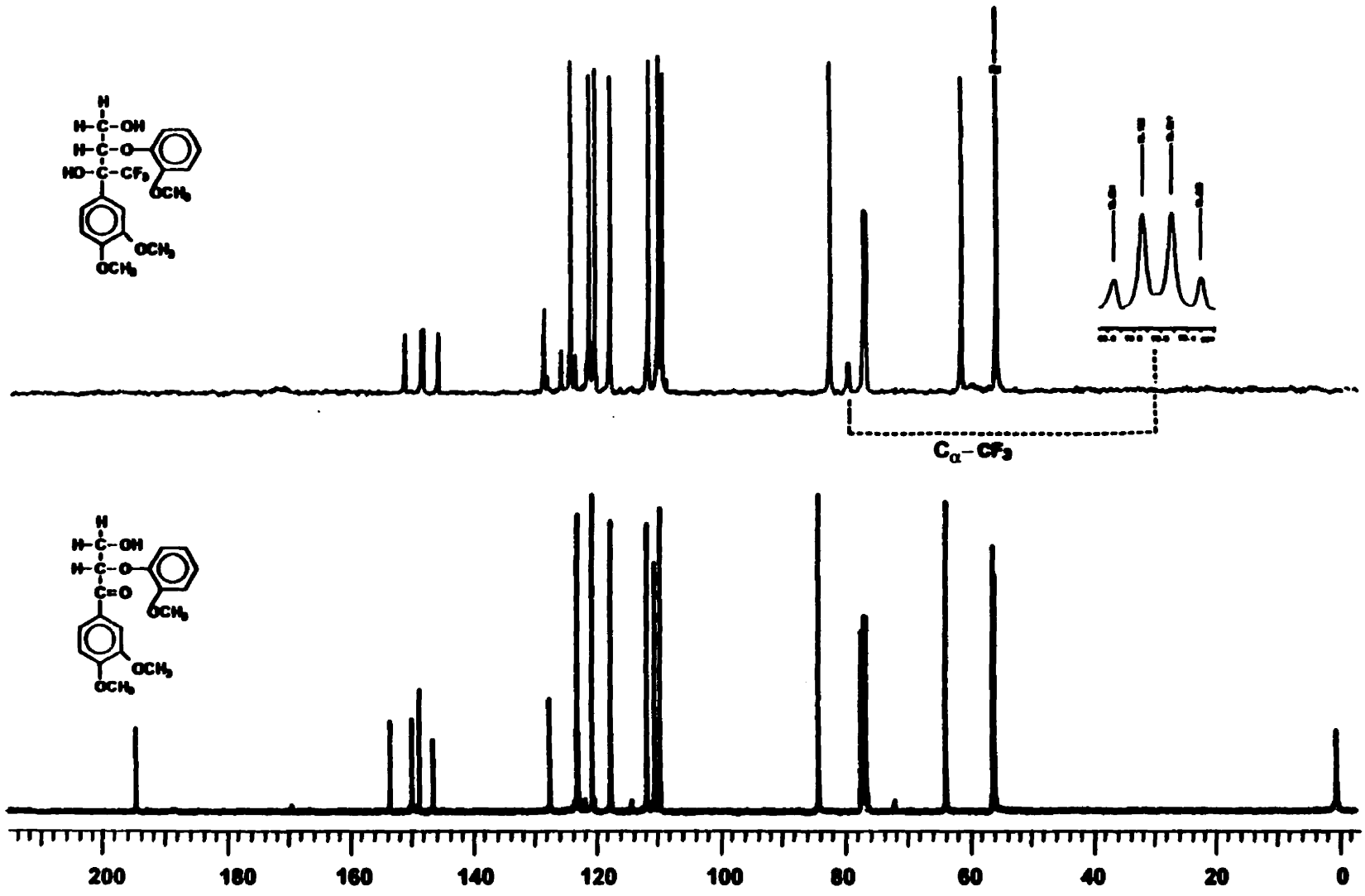

Figure 5.8. ^{13}C NMR spectra of lignin model compound, before and after trifluoromethylation.

To further confirm our findings, 3-methoxy-4-hydroxy-α-(2-methoxy-4-methyl)-γ-hydroxy-propiophenone **(28)** was trifluromethylated under the same conditions. The resulting CF_3-containing compound **(29)** was then examined by GC-mass, ^{19}F, ^{13}C and ^{1}H NMR spectroscopies. Consequently, it was demonstrated that trifluoromethylation of dimeric lignin model compounds can be quantitatively achieved with the more effective TMAF as an initiator.

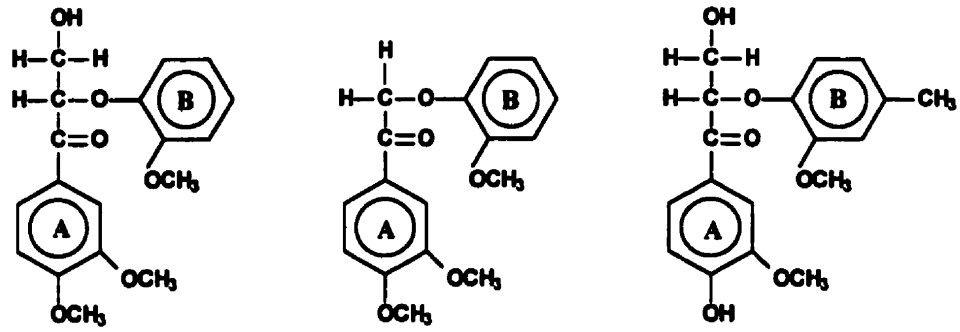

(CYI) (CYII) (CYIII)

Figure 5.9. Chemical structure of lignin model compounds.

The next issue was whether or not the trifluoromethylation reaction could result in the scission of arylglycerol β-O-4 ether bonds. This is a very important issue as far as the primary objectives of this work are concerned, since more than 40% of the structural units in lignins are believed to be linked together by β-ether bonds[67-69].

Such an event may take place due to the presence of trimethylsilyl fluoride, formed as side product in conjunction with Ruppert's reagent during the reaction. In a series of publications that address the selective cleavage of ether bonds in lignin, there is substantial evidence that trimethylsilyl iodide is capable of cleaving β-O-4 ether bonds. In fact several studies have shown that this is an effective method of cleavage the ether bonds between lignin side chains and aromatic nuclei[70-74].

Although the reaction was carried out in the absence of trimethylsilyl iodide (TMSiI), the formation of trimethylsilyl fluoride (TMSiF) during the course of the reaction was a possibility to consider since it could behave similarly to TMSiI.

Table 5.10. Fluoride ion induced trifluoromethylation of carbonyl groups with trifluoromethyltrimethylsilane.

Entry	Precursor	Product	Reaction Conditions	Overall % Yield	^{19}F NMR (ppm)	GC-MS m/e
24) 25)	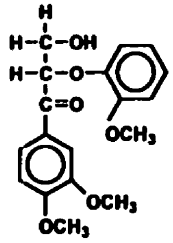	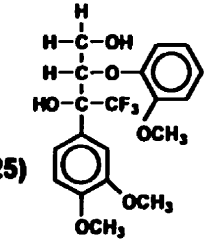	0°C, 30 min 25°C, 24h hydrolysis, 24h	95	-75.53	Ms m/z (silylated) 402, (M^+), 302, 278, 248, 235, 221.
26) 27)	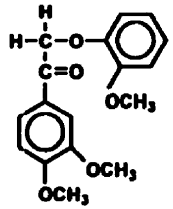	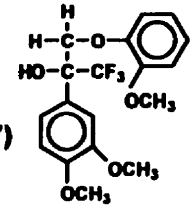	0°C, 30 min 25°C, 24h hydrolysis, 24h	96	-77.63	Ms m/z 372, (M^+), 303, 248, 235, 217, 189.
28) 29)	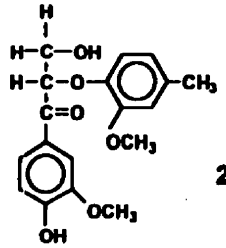	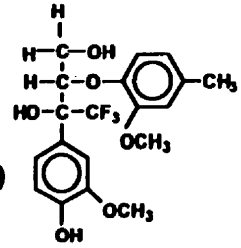	0°C, 30 min 25°C, 24h hydrolysis, 24h	93	-75.48	Ms m/z (silylated) 618, (M^+), 480, 451, 411, 365, 343.

Table 5.11. Qualitative C-13 NMR chemical shifts of dimeric lignin model compounds.

Compound	α	β	γ	C-1	C-2	C-3	C-4	C-5	C-6	Other
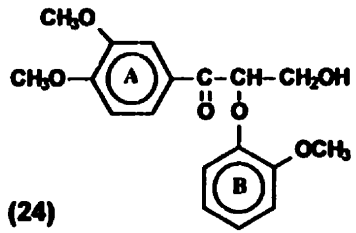 (24)	*194.97*	*84.35*	*63.67*	*128.03* *123.43*	*110.08* *112.26*	*149.14* *146.91*	*153.88* *150.32*	*110.94* *118.11*	*123.59* *121.10*	*A* *p*-OCH_3 56.03 *m*-OCH_3 55.90 *B* *o*-OCH_3 55.74
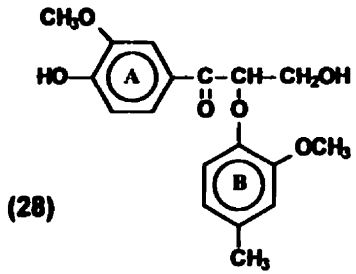 (28)	*195.02*	*84.60*	*63.65*	*133.45* *124.18*	*110.71* *114.02*	*146.80* *144.61*	*151.08* *150.06*	*113.13* *118.42*	*127.73* *121.30*	*A* *p*-OCH_3 55.99 *B* *o*-OCH_3 55.70 *p*-CH_3 21.09
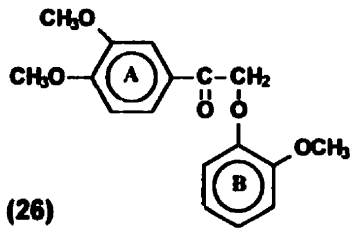 (26)	*193.18*	*71.89*	——	*127.74* *122.26*	*110.03* *112.01*	*149.12* *147.48*	*153.72* *149.61*	*110.30* *114.51*	*122.69* *120.72*	*A* *p*-OCH_3 56.34 *m*-OCH_3 55.92 *B* *o*-OCH_3 55.81

Table 5.12. Qualitative C-13 NMR chemical shifts of dimeric lignin model compounds after trifluoromethylation. .

Compound	α	β	γ	CF_3	C-1	C-2	C-3	C-4	C-5	C-6	Other
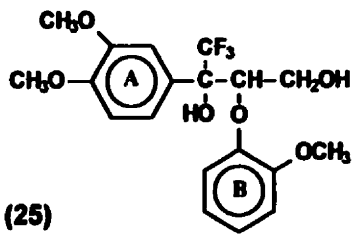 (25)	79.27 79.48 79.70 79.92	82.64	61.36	128.39 126.11 123.83 121.55	128.93 121.66	109.87 112.07	148.56 146.18	151.53 148.89	110.48 118.25	124.62 120.72	Phenyl Unit A Phenyl Unit B
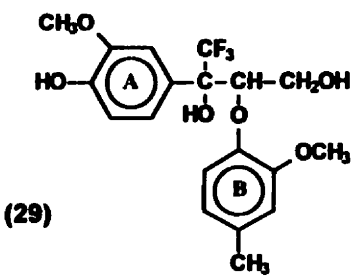 (29)	79.52 79.73 79.96 80.17	82.64	61.31	128.49 126.21 123.93 121.65	134.83 122.19	109.59 113.93	145.62 143.81	151.36 146.35	112.95 118.43	128.71 121.01	Phenyl Unit A Phenyl Unit B
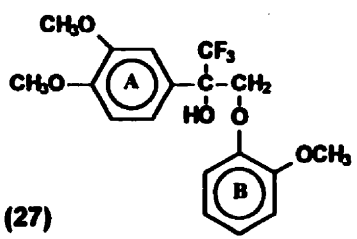 (27)	75.05 75.43 75.80 76.18	71.68	____	129.02 126.74 124.46 122.18	127.88 120.41	108.78 111.44	148.68 147.37	149.95 149.16	110.06 113.40	122.95 121.80	Phenyl Unit A Phenyl Unit B

For this reason, gas-chromatography was employed to evaluate the integrity of alkyl-aryl ether bonds of the lignin model compounds **(24 and 26)** before and after the reaction. It was confirmed that under the conditions employed in this work, the formation of trimethylsilyl fluoride (TMSiF) did not cleave the β-ether bonds of the models used. Tetrabutylammonium iodide can not be used as an initiator for the reaction, since it would result in the formation of trimethylsilyl iodide (TMSiI) which will in return cleave the alkyl-aryl ether bonds in dimeric model compounds and lignin. Pottasium *tert*-butoxide, was found to be a very effective initiator of trifluoromethylation for a series of monomeric model compounds. Its strongly basic character, however, poses the danger of structural alterations to the delicate and complex nature of lignin. The trifluoromethylation reaction in the presence of *tetra*-n-butylammonium fluoride (TBAF) resulted in low yields, precluding this procedure from becoming a tool for the quantitative analysis of carbonyl groups in lignins.

5.4. CONCLUSIONS

The quantitative trifluoromethylation of carbonyl groups for a series of carbonyl-containing lignin-like model compounds has been accomplished. This was achieved by using trifluorotrimethylsilane (Ruppert's reagent) in the presence of TMAF. This reagent was found to be an efficient nucleophilic trifluoromethylating agent for derivatizing a variety of carbonyl-containing compounds. Although their ^{19}F NMR signals were well resolved, allowing differentiation amongst the various classes of carbonyl groups, the chemical shifts of trifluoromethylated quinones occupied a wide range, overlapping with those of ketones.

Having established the precise conditions required for the trifluoromethylation reaction so as to qualify as an analytically reliable reaction. In Chapter 6 we turn our attention on actual lignin samples.

5.5. REFERENCES

1. Heitner, C. and Schmidt, J., Light-induced yellowing of wood-containing papers-A review of fifty years of research., Proc. 6th. Int. Symp. on Wood and Pulping Chem., 1, 131-149, 1991.

2. Schmidt, J. A. and Heitner, C. E., Light-induced yellowing of mechanical and ultra-high yield pulps. Part 3. Radical-induced cleavage of etherified guaiacylglycerol-β-arylether groups in the main degradative pathway., J. Wood Chem. Technol., 13, 309-325, 1993.

3. Schmidt, J. A. and Heitner, C. E., Light-induced yellowing of mechanical Pulp: effect of methylation, $NaBH_4$ reduction and ascorbic acid on chromophore formation., J. Wood Chem. Technol., 11, 397-418, 1991.

4. Leary, G. J., Recent progress in understanding and inhibiting the light-induced yellowing of mechanical pulps., J. of Pulp and Paper Sci., 20 (6), 154-160, 1994.

5. Klason, P., Beitrag zur Kenntnis der Konstitution des Fichtenholz-Lignins(II). Ber Dtsch. Chem. Ges., 55, 448-455, 1922.

6. Adler, E., Björkqvist K. J., Häggroth, S., Über die Ursache der Farbreaktionen des Holzes., Acta Chem. Scand., 2, 93-94, 1948.

7. Adler, E. and Ellmer, L., Coniferylaldehydgruppen im Holz und in isolierten Ligninpraparaten., Acta Chem. Scand., 2, 836-840, 1948.

8. Adler, E., Sulfite pulping properties of spruce wood from unpeeled, floated logs. Part 1. Catechol tannins in the surface layer of the sapwood., Svensk. Papperstidn., 54, 445-450, 1951.

9. Pew, J. C., Structural aspect of the color reaction of lignin with phenols., J. Am. Chem. Soc., 73, 1678-1685, 1951.

10. Geiger, H. and Fuggerer, H. Über den Chemismus der Wiesener-Reaktion auf Lignin., Z. Natuforsch., 34b, 1471-1472, 1979.

11. Adler, E. and Marton, J., Zur Kenntnis der Carbonylgruppen im Lignin. I. Acta Chem. Scand., 13, 75-96, 1959.

12. Larsson, S. and Miksche G. E., Gaschromatographische Analyse von Ligninoxidations-produkten. VI. 4,4-Bis-aryloxy-cyclohexa-2,5-dienonestrukturen im Lignin., Acta Chem. Scand., 26, 2031-2038, 1972.

13. Panchapakesan, B. Photo-induced reactions of lignin and lignin fragments: Photo-oxidation of chlorinated organics in bleach plant effluents and brightness stability of high yield pulps. Ph. D. Thesis, North Carolina State University, Raleigh, North Carolina, USA. 1990.

14. Hon, D. N. S. and Glasser, W. On possible chromophore structures in wood and pulps- a survey of the present state of knowledge., Polym-Plast Technol. Eng., 12, 157-179, 1979.

15. Lebo, S. Y., Lonsky, W. F. W., McDonough, T. J., Medvecz, P.J., The occurrence and light induced formation of *ortho*-quinonoid lignin structures in white spruce refiner mechanical pulps., Proct. Int. Pulp Bleach Conf., Orlando, FL, June 6-9, 277-251, 1988.

16. Brunow, G. and Eriksson, B., α-Carbonyl groups as sensitizers in the photo-dehydrogenation of phenolic structures in lignin., Acta Chem. Scand., 25, 2779-2781, 1971.

17. Lin, S. Y. and Kringstad, K. P., Photosensitive groups in lignin and lignin model compounds., Tappi, 53, 658-663, 1970.

18. Chang, H. M. and Allen, G. G., Oxidation. In: Lignins. Occurrence, formation, structure and reactions., Eds. Sarkanen, K.V., and Ludwig, C.H., Wiley-Interscience, New York, 433-485, 1971.

19. Gierer, J. and Lin, S. Y., Photodegradation of lignin. A contribution to the mechanism of chromohore formation., Svensk. Papperstidn., 75, 233-239, 1972.

20. Heuser, E., Analytik der Carbonylgruppe. In: Müller E, Bayer O, Meerwein H, Ziegler K (eds.) Methoden der organischen Chemie (Houben-Weyl) 4. Aufl., Bd II Analytische Methoden., George Thieme, Stuttgart, Federal Republic of Germany, 434-472, 1953.

21. Heuser, E., Analytik von Chinonen. In: Müller E, Bayer O, Meerwein H, Ziegler K (eds.) Methoden der organischen Chemie (Houben-Weyl) 4. Aufl., Bd II Analytische Methoden. George Thieme, Stuttgart, Federal Republic of Germany, 434-472, 1953.

22. Lindberg, B. and Misiorny, A., Quantitative analysis of reducible carbohydrates by means of sodium borohydride., Svensk. Papperstidn., 55, 13-14, 1952.

23. Gierer, J. and Söderberg, S., Über die Carbonylgruppen des Lignins., Acta Chem. Scand., 13, 127-137, 1959.

24. Adler, E. and Marton, J. Acta Chem. Scand., 13, 75, 1959. [Preliminary report, Marton, J. Proc. IVth Intern. Congr. Biochem., Vienna 1958, vol. II, 154, 1959].

25. Liebman, J. F., Greenberg, A., Dolbier, W. R., Jr., Eds. VCH: Fluorine-containing molecules, structure, reactivity, synthesis, and applications., New York, 1988.

26. Banks, R. E. Ed., Organofluorine compounds and their industrial applications., Ellis Horwood Ltd., Chichester, 1979.

27. Prakash, G. K. S.; Krishnamurti, R.; Olah, G. A., Fluoride-induced trifluoromethylation of carbonyl compound with trifluoromethyltrimethylsilane(TMS-CF_3). A trifluoromethide equivalent., J. Am. Chem. Soc., 111, 393-395, 1989.

28. Ruppert, I., Schlich, K., Volbach, W., Die Ersten CF_3-Substituierten Organyl(chlor)Silane., Tetrahedron Lett., 25, 2195-2198, 1984.

29. Prakash, G. K. S. and Pichika, R., Direct trifluoromethylation of α-keto esters to β,β,β-trifluorolactic acid derivatives using trifluoromethyltrimethylsilane., Synlett., 9, 643-644, 1991.

30. Lundquist, K., and Robert, D., Proton(^{1}H) and Carbon-13 nuclear magnetic resonance spectroscopy. In: Method in lignin chemistry., Eds. Dence, C. W. and Lin, S. Y., Berlin, Ch. 5.3 and 5.4., pp. 242-273, 1992.

31. Archipov, Y., Argyropoulos, D. S., Bolker H. I. and Heitner, C., ^{31}P NMR spectroscopy in wood chemistry. Part I. Lignin model compounds., J. Wood Chem. Technol., 11(2), 137-157, 1991.

32. Archipov, Y., Argyropoulos, D. S., Bolker, H. I., and Heitner, C., ^{31}P NMR spectroscopy in wood chemistry. Part II. Phosphite derivatives of carbohydrates., Carbohydr. Research., 220, 49-61, 1991.

33. Argyropoulos, D. S., Archipov, Y., Bolker, H. I., and Heitner, C., ^{31}P NMR spectroscopy in wood chemistry. Part IV. Spin-lattice relaxation times & solvent effects in ^{31}P NMR., Holzforschung, 47, 50-56, 1993.

34. Argyropoulos, D. S., Bolker, H. I., Heitner, C. and Archipov, Y., ^{31}P NMR spectroscopy in wood chemistry. Part V. Qualitative analysis of lignin functional groups., J. Wood Chem. Technol., 13, 187-212, 1993.

35. Jenkins, B. G., Detection of site-specific binding and co-binding of ligands to macromolecules using fluorine-19 NMR., Life Sci., 48, 1227-1240, 1991.

36. Emsley, J. W. and Phillips, L., The effect of solvents on the chemical shift of fluorine nuclei in aromatic compounds., Mol. Phys., 11, 437-456, 1966.

37. Emsley, J. W. and Phillips, L., Chemical shifts of fluorine nuclei in some fluorinated pyridines., J. Chem. Soc., B434-439, 1969.

38. Mooney, E. F., An Introduction to ^{19}F NMR spectroscopy., Heyden/Sadler, 1970.

39. Emsley, J. W. and Phillips, L., Fluorine chemical shifts in NMR spectroscopy., J. W. Emsley, J. Feeney, and L. H. Sutcliffe, Eds., Pergamon Press, Oxford, 1971.

40. Dungan, C. H. and Van Wazer, J. R., Compilation of reported ^{19}F NMR chemical shifts., Wiley-Interscience, New York, 1970.

41. Feeney, J., NMR studies of nuclei other than hydrogen., Nuclear magnetic resonance of organic chemists., D. W. Mathieson, ed., New York, Academic Press, pp. 151-158. 1967.

42. Gerig, J. T., Fluorine nuclear magnetic resonance of fluorinated ligands., Methods Enzymology., 177B, 3-23, 1989.

43. Jardetzky, O. and Roberts, G. C. K., NMR in molecular biology., New York, Academic Press, 1981.

44. Gerig, J. T., Fluorine nuclear magnetic resonance in biochemistry., Biol. Magn. Reson., L. Berliner & Reuben, J., ed. New York, Plenum Press, 139-203, 1978.

45. Hull, W. E., Sykes, B. D., Dipolar spin relaxation of fluorine-19 in multispin system., Application to fluorine-19 labeled proteins., J. Chem. Phys., 63, 867-880, 1975.

46. Sykes, B. D., and Weiner, J. H., Biosynthesis and ^{19}F NMR characterization of fluoroamino acid containing proteins., Magnetic resonance in Biology., J. S. Cohen, ed. New York, John Wiley & Sons. 171-196. 1980.

47. Boden, N., Emsley, J. W., Feeney, J. and Sutcliffe, L. H., The effect of π-electron distribution and intramolecular electric fields on the ^{19}F NMR shielding in substituted perfluorobenzene., Mol. Phys., 8, 133-149, 1964.

48. Gerig, J. T., In: Biological magnetic resonance., Vol. 1., Berliner, L. G. and Reubens, J., Eds. Plenum, New York, Chapter 4., 1978.

49. Nagai. T., Nishioka. G., Koyama. M., Ando. A., Takuichi. M., and Kumadaki, I., Reactions of trifluoromethyl ketones. IX. Investigation of the steric effect of a trifluoromethyl group based on the stereochemistry on the dehydration of trifluoromethyl homoallyl alcohols., J. of Fluorine Chem., 57, 229-237, 1992.

50. Prakash, G. K. S., Krishnamurti, R., Olah, G. A., Fluoride-induced trifluoromethylation of carbonyl compound with trifluoromethyltrimethylsilane(TMS-CF_3). A trifluoromethide equivalent., J. Am. Chem. Soc., 111, 393-395, 1989.

51. Wang, Z., and Ruan, B., Trifluoromethylation of steroidal ketones., J. of Fluorine Chem., 69, 1-3, 1994.

52. Greene, T. W., and Wuts, P. G. M., Protective groups in organic synthesis., second edition, New York, John Wiley & Sons Inc., 71, 1991.

53. Argyropoulos, D. S., Heitner, C. and Morin, F. G., ^{31}P NMR spectroscopy in wood chemistry. Part III. Solid state ^{31}P NMR of trimethyl phosphite derivatives of chromophores in mechanical pulp., Holzforschung, 46, 211-218, 1992.

54. Argyropoulos, D. S., and Heitner, C., ^{31}P NMR spectrocopy in wood chemistry. Part VI. Solid state ^{31}P NMR of trimethyl phosphite derivatives of chromophores and carboxcylic acids present in mechanical pulps: A method for the quantitative determination of *ortho*-quinones., Holzforschung Suppl., 48, 112-116, 1994.

55. Lin, S. Y., and Kringstad, K. P., Some reactions in the photoinduced discoloration of lignin., Norsk. Skiksind., 25, 252-256, 1971.

56. Kringstad, K. P., Some possible reactions in the light-induced degradation of high-lignin-containing high-yield pulps., Papier., 27(10A), 462-466, 1973.

57. Forsskåhl, I., and Janson, J., The irradiation of mechanical pulps with monochromatic light at selected wavelenghts., Proc. 6th Int. Symp. of Wood and Pulping Chem., Melbourne, Australia, 1, 255-263, 1991.

58. Castellan, A., Nourmamode, A., Jeager, C. and Forsskåhl, I., Photochemistry of lignocellulosic materials., Eds. Heitner, C. and Scaiano, J. C., ACS Symp. Ser., 531, pp. 60-76, 1993.

59. Gellersted, G. and Pattersson, E. L., Light-induced oxidation of lignin. Part 2. The oxidative degradation of aromatic rings., Svensk. Papperstidn., 80, 15, 1977.

60. Lebo, S. E., Lonsky, W. F. W., McDonough, T. J., Medvecz, P. J., and Dimmel, D. R., The occurrence of light-induced formation of *ortho*-quinoid lignin structures in white spruce refiner mechanical pulp., J. Pulp and Paper Sci., 16(5), J139-143, 1990.

61. Stahly, P. G., Bell, R. D., A new method for synthesis of trifluoromethyl-substituted phenols and anilines., J. Org. Chem., 54, 2873-2877, 1989.

62. Adler, E., Brunow, G., Lundquist, K., Investigation of the acid-catalysed alkylation of lignin by means of NMR spectroscopic methods., Holzforschung, 41, 199-207, 1987.

63. Lundquist, K., NMR studies of lignins. 4. Investigation of spruce lignin by ^{1}H NMR spectroscopy., Acta Chem. Scand., B34, 21-26, 1980.

64. Lundquist, K., and Olsson, T., NMR studies of lignin. 1. Signal due to proton in formyl groups., Acta Chem. Scand., B31, 788-792, 1977.

65. Brunow, G., Lundquist, K., Comparison of a synthetic dehydrogenation polymer of coniferyl alcohol with milled wood lignin from spruce using ^{1}H NMR spectroscopy, Pap. Puu., 11, 669-672, 1980.

66. Lundquist, K., NMR studies of lignins. 5. Investigation of non-derivatized spruce and birch lignin by ^{1}H NMR spectroscopy., Acta Chem. Scand., B35, 497-501, 1981.

67. Lai, Y. Z., Sarkanen, K. V.; In: Lignins. Occurrence, formation, structure and reactions., Eds. Sarkanen, K.V., and Ludwig, C.H., Wiley-Interscience, New York, pp. 226-228, 1971.

68. Erickson, M., Larsson, S., and Miksche, G. E., Gas chromatographic analysis of lignin oxidation products. VIII. The structure of lignin of spruce., Acta Chem. Scand., 27, 903-914, 1973.

69. Matsumoto, Y., Ishizu, A., and Nakano, J., Selective cleavage of arylglycerol-β-aryl ether type structures in Lignin I., Mokuzai Gakkaishi., 26(12), 806-810, 1980.

70. Matsumoto, Y., Ishizu, A., Iiyama, K., and Nakano, J., Selective cleavage of arylglycerol-β-aryl ether type structures in lignin I., Mokuzai Gakkaishi., 28(4), 249-254, 1982.

71. Makino, S., Meshitsuka, G., and Ishizu, A., Selective cleavage of ether bonds in lignin by trimethylsilyl iodide., J. Wood and Pulp. Chem., 275-277, 1989.

72. Makino, S., Meshitsuka, G., and Ishizu, A., Selective cleavage of ether bonds in lignin by trimethylsilyl iodide., Mokuzai Gakkaishi., 36(6), 460-465, 1990.

73. Fujino, K., Meshitsuka, G., and Ishizu, A., Selective cleavage of ether bonds in lignin by trimethylsilyl iodide II., Mokuzai Gakkaishi., 38(10), 956-962, 1992.

74. Ho, T. L., and Olah, G., Cleavage of esters and ethers with iodotrimethylsilne., Angew. Chem., Int. Ed. Engl., 15(12), 774-775, 1976.

Chapter 6

^{19}F Nuclear Magnetic Resonance (NMR) Spectroscopy for the Quantitative Detection and Classification of Carbonyl Groups in Lignins

6.0. ABSTRACT

A novel method that permits the quantitative detection and classification of various carbonyl groups in lignins has been developed. The proposed method was optimized with the quantitative trifluoromethylation of a series of carbonyl-containing lignin-like model compounds. This effort was followed by ^{19}F NMR spectral analyses of the resulting fluorine derivatives allowing for a thorough understanding of their structure/^{19}F chemical shift relationships. The various carbonyl groups present in lignins were also investigated by trifluoromethylating them in the presence of catalytic amounts of tetramethylammonium fluoride (TMAF), followed by hydrolysis with TMAF in THF. By using a variety of selective reactions it became possible to assign a number of prominent ^{19}F NMR signals to a variety of carbonyl groups present in lignins. Our studies demonstrated that the proposed method can be applied toward the quantitative determination of carbonyl groups that are present in soluble native and technical lignins.

6.1. INTRODUCTION

Lignin is a complex phenylpropanoid biopolymer formed by an enzyme initiated radical polymerization of cinnamyl alcohols[1]. Due to the random nature of its formation, lignin does not posses regularity in its repeating units[2-4]. This peculiarity makes the characterization of its structure a challenging task.

A number of studies have demonstrated the presence of small amounts of carbonyl groups in lignins[5-8]. In particular milled wood lignins have been reported to contain conjugated cinnamaldehyde structures and α-carbonyl groups[9]. Other investigations have shown that technical lignins contain appreciable amounts of α-carbonyl groups in addition to benzaldehyde and quinones[10, 11]. The presence of carbonyl groups in lignins, in particular those present as *o*- and *p*-quinonoids, quinonemethides, and other extended conjugated enone systems, are not only responsible for the color of lignified plant tissue[12, 13] but also sentisizing centres in the photoyellowing of lignocellulosic materials[14]. In general, the low content of these groups in lignins has made the elucidation of their role rather elusive. For example, quinones, which are present in wood and high-yield mechanical pulps[15, 16] in rather low amounts, only recently have been unequivocally shown to be responsible for the yellow colour of photochemically reverted papers[15-20].

Several methods for determining the carbonyl groups in lignins are available[21-25]. Amongst these, the most effective and simple is the one that utilizes the reaction of carbonyl groups with hydroxylamine hydrochloride forming an oxime and hydrochloric acid. Subsequent titration of the hydrochloric acid provides an estimation of the amount of carbonyl groups in a sample[8, 25]. A modification of this technique, claiming greater reproducibility, has been described by Zakis[26]. The modified procedure calls for the use of triethanolamine to function as the acid acceptor followed by a back titration. A technique that attempts the distinction of α-carbonyl groups to those of conjugated aldehydes is also available[22, 23], based on sample reduction (sodium borohydride) followed UV spectroscopic measurements. The latter method requires the use of appropriate lignin model compounds that serve as standards for determining the changes in molar absorbitivity of the absorption bands that are caused by the reduction of a particular carbonyl group to the corresponding benzylic alcohol.

Infrared spectroscopy has been also used for investigating various structures in lignin[27-29] inculding carbonyls[30]. Recently, Hortling et al.[31] reported a semiquantitative technique for the determination of carboxylic and non-conjugated carbonyl groups by IR spectroscopy. However, the application of these techniques were not widespread since their precision is limited and the various classes of carbonyl moieties can not be differentiated.

NMR is rapidly becoming a powerful analytical tool in the hands of wood chemists aimed at providing answers in relation to the structure of lignins. However, the complex structure of these materials has imposed some serious challenges and limitations, even in the application and use of NMR[32]. Efforts to overcome some of the limitations imposed by proton[33-35] and ^{13}C-NMR spectroscopies[36-38] have prompted the examination of other NMR-active nuclei. These efforts have provided additional tools for obtaining fine structural details for these heterogeneous biopolymers. The determination of a variety of labile protons in lignins has been carried out by ^{29}Si-, ^{31}P- and ^{19}F- based NMR methods, for suitably silylated[39, 40], phosphitylated[41-48] and fluorinated[49, 50] lignins respectively. Furthermore, Lebo et al.[13] and recently, Argyropoulos et al.[51] have reported the detection of *ortho* quinones in mechanical pulps. In particular, the latter group has actually managed to follow their formation during the process of light-induced yellowing using solid-state ^{31}P-NMR spectroscopy[51].

The ^{19}F nucleus is 100% naturally abundant and its high gyromagnetic ratio makes its NMR sensitivity nearly the same as that of proton. Its chemical shift extends over a wide range providing adequate signal dispersion that may reduce signal overlap and aid interpretation. Attempts at determining the carbonyl content of lignin by ^{19}F-NMR have actually been made previously after *p*-fluorobenzylation[52] of the lignin or its derivatization with *p*-fluorophenylhydrazine[53]. In both cases the ^{19}F-NMR signals received were found to overlap over a relatively narrow range thus diminishing the quantitative reliability of the techniques. Furthermore, the proposed methods were not capable to distinguish amongst the different classes of carbonyl groups present in lignin.

In a previous effort, our attention was focused at the development of an ^{19}F-based novel magnetic resonance method aimed at expanding the frontiers of application of

NMR for the analysis of carbonyl groups in lignin[54]. For this purpose a selective and quantitative trifluoromethylation reaction was developed for tagging the carbonyl groups in various lignin model compounds, using trifluoromethyltrimethylsilane (TMS-CF_3) in the presence of tetramethylammonium fluoride (TMAF). More specifically, a series of ketones, aldehydes, quinones and dimeric lignin model compounds were quantitatively trifluoromethylated, followed by ^{19}F NMR spectral analyses of the resulting fluorine derivatives. This effort allowed for a thorough understanding of the various structure/^{19}F chemical shifts relationships[55] that operate for lignin-like moieties.

The present effort attempts to expand the application of quantitative trifluoromethylation to lignins, aimed at elucidating the nature and the quantity of the various carbonyl groups present in them.

6.2. EXPERIMENTAL

6.2.1. Materials and Methods

6.2.1.1. Reactions

Trifluoromethylation

The following trifluoromethylation procedure was developed and applied to all lignin samples. 100 mg of lignin were dissolved, under constant stirring, in 10 mL of dry tetrahydrofuran (THF) at room temperature. After 10 min of stirring, 600 μL of trifluoromethyltrimethylsilane (TMS-CF_3) were added. The mixture was cooled at 0 °C for 10 min followed by the addition of catalytic amount (15 mg) of tetramethylammonium fluoride (TMAF) acting as the initiator. The reaction mixture continued to be stirred at 0 °C for 30 min and then at room temperature for 24 hours. The intermediate trifluoromethylated siloxy adducts were then hydrolysed by the addition of (50 mg) of tetramethylammonium fluoride (TMAF) at room temperature for 24 hours in THF. After evaporating the THF under reduced pressure, the residue was washed and centrifuged thoroughly by 3x50 mL water. Finally, the isolated materials were dissolved in a mixture of dioxane/water (25:5, v/v) and freezed dried under reduced pressure.

Sodium Borohydride Reduction

Lignin (200 mg) was dissolved into 25 mL of a solution composed of (60:40:50, v/v) 2-methoxyethanol, isopropanol, and water respectively. This was followed by the addition of 3 mL of a solution composed of 0.01N sodium hydroxide and 100 mg of sodium borohydride and stirred at 40 °C for 24 hours. The reaction mixture was then acidified to pH 3-4 with dilute (10%) sulfuric acid. The organic solvents were evaporated under reduced pressure and the lignin was precipitated with the addition of water. The precipitated lignin was then washed and centrifuged 3 times, dissolved in a mixture of dioxane/water (25:5, v/v) and freeze dried.

Dakin Reaction

Lignin (200 mg) was suspended in a solution of 6.5 mL of n-propanol and 7.5 mL

of water under constant stirring for 15 min. To this mixture 5 drops of a 0.5M sodium hydroxide solution was added causing the complete dissolution of the lignin. This was followed by the addition of 702 μL of 30% hydrogen peroxide. After adjusting the pH of the mixture to 10.6, the reaction mixture was stirred at 50 °C for 4 hours. Then the reaction was neutralized by the addition 1-2 drops of 25% sulfuric acid to pH 4.7. After evaporating the organic solvent under reduced pressure, the lignin was precipitated by addition of water. The precipitated lignin was washed with water and centrifuged 3 times with 15 mL of water. The isolated lignin was then dissolved in a mixture of dioxane/water (25:5, v/v) and freeze dried.

Sodium Hydrosulphite Reduction of Lignin Model Compounds

Selected lignin model compounds (200 mg) were dissolved in 5 mL of dioxane and a slow stream of nitrogen was bubbled through the solution for about 30 minutes. To this solution 200 mg of sodium hydrosulphite ($Na_2S_2O_4$) dissolved in 5 mL of water were added. After various reaction times (15, 60, and 240 min), a 1 mL aliquot of the mixture was withdrawn, acidified by the addition of 1M HCl, and extracted with ethylacetate. The organic solvent was then evaporated under reduced pressure and the residue was analyzed by GC-MS chromatogram.

Sodium Hydrosulphite Reduction of Lignin

Lignin (200 mg) were dissolved in 5 mL of dioxane and a slow stream of nitrogen was bubbled through the solution for about 30 minutes. To this mixture, a solution composed of 200 mg of sodium hydrosulfite in 5 mL of water was added and the reaction mixture was kept under stirring at room temperature for 1 hour. The mixture was then freeze dried and the residue was washed with small aliquots of water followed by centrifugation (x3). Finally, the reduced lignin was dissolved in a mixture of dioxane/water (25:5, v/v) and freeze dried.

6.2.1.2. Instrumentation

Gas Chromatography/Mass Spectrometry

GC-MS analyses were carried out on a Hewlett Packard 5972 mass spectrometer interfaced to a Hewlett Packard 5890A gas Chromatograph with a 30m x 0.25 mm packed silica capillary column. The injection port temperature was 280 °C and the oven temperature increase profile was from 100 °C to 250 °C, with a gradient of 5 °C/min.

^{19}F NMR Spectroscopy

All spectra were recorded on a Varian Unity 500 FT-NMR spectrometer at an operational frequency of 470.3 MHz. The derivatized trifluoromethylated lignin were dissolved in 800 μL of a solvent mixture composed of pyridine and deuterated chloroform (15-20 mg/0.8 mL) at a volume ratio of 1.6:1, v/v. The mixture was stirred with a magnetic bar until the lignin was fully dissolved. To this mixture, 100 μL of an internal standard solution were added (i.e 1.69 g/mL 1.6:1 v/v pyridine/$CDCl_3$ of 3,3'-bis(trifluoromethyl)benzophenone; whose chemical shift was referenced to fluorotrichloromethane. Quantitative acquisitions were carried out in 5 mm tubes at room temperature with acquisition times of 0.64 sec followed by a relaxation delay of 10 seconds. The number of scans acquired was 1000 per measurement. Pulse widths corresponding to a 45° flip angle and a line broadening of 2 Hz were used during acquisition and processing of the spectra.

Two-Dimensional NMR Spectroscopy (HMQC)

Such spectra were acquired using 10-30 mg of sample dissolved in 0.6 mL $CDCl_3$ or DMSO-D_6 or acetone-D_6 on a Varian Unity 500 NMR spectrometer using a 5 mm inverse detection probe (DHP). The chemical shifts were referenced to Me_4Si and $CFCl_3$ for ^{13}C and ^{19}F respectively. HMQC spectra were acquired over a 30 ppm window in F_2 (^{19}F) and 190 ppm in F_1 (^{13}C) with GARP-1 decoupling. The value of the coupling constant was adjusted to the estimated value for the ^2J C-F of 30 Hz. 2K x 256 increments were acquired. After F_1 zero-filling, Fourier transformation, and squared cosine bell apodization, the transformed data matrix was 1024 (F_2) x 512 (F_1) real points.

6.2.1.3. Characterization

6.2.1.3.1. Characterization of Trifluoromethylated Model Compounds

1. ^{1}H NMR ($CDCl_3$)(TMS) δ: 1.77 (s, 3H); 2.60 (s, 1H); 7.37-7.46 (m, 3H); 7.56-7.61 (m, 2H) ppm. ^{19}F NMR ($CDCl_3$/pyridine)($CFCl_3$) δ: -80.30 (s) ppm. MS *m/z* 190 (M^+), 151, 127, 121, 105, 91, 77, 51. Anal. Calcd for $C_9H_9F_3O$: C, 56.84; H, 4.77; F, 29.97. Found: C, 56.92; H, 4.69; F, 29.92. 96% yield.

2. ^{1}H NMR ($CDCl_3$)(TMS) δ: 1.74 (s, 3H); 2.35 (s, 1H); 5.67 (s, 1H); 6.829 (d, 2H, J=8.78 Hz); 7.432 (d, 2H, J=8.58 Hz) ppm. ^{13}C NMR ($CDCl_3$)(TMS) δ: 23.85; 74.54 (q, $J_{C\text{-}CF}$=29.1 Hz); 115.11; 155.83; 129.36 (q, $J_{C\text{-}F}$= 284.9 Hz); 155.83. ^{19}F NMR ($CDCl_3$/pyridine)($CFCl_3$) δ: -80.57 (s) ppm. MS *m/z* 206 (M^+), 188, 167, 149, 137, 119, 107, 91. Anal. Calcd for $C_9H_9F_3O_2$: C, 52.43; H, 4.40; F, 27.65. Found: C, 52.48; H, 4.49; F, 27.67. 98% yield.

3. ^{1}H NMR ($CDCl_3$)(TMS) δ: 1.74 (s, 3H); 2.90 (s, 1H); 3.879 (d, 3H, J=6.64 Hz); 5.84 (s, 1H); 6.86-7.13 (m, 3H) ppm. ^{19}F NMR ($CDCl_3$/pyridine)($CFCl_3$) δ: -80.38 (s) ppm. MS *m/z* 236 (M^+), 197, 167, 151, 124. 110, 69, 51. Anal. Calcd for $C_{10}H_{11}F_3O_3$: C, 50.85; H, 4.69; F, 24.13. Found: C, 50.91; H, 4.68; F, 24.19. 96% yield.

4. ^{1}H NMR ($CDCl_3$)(TMS) δ: 1.73 (s, 3H); 2.54 (s, 1H); 3.879 (d, 6H, J=10.26 Hz); 6.78 (s, 2H); 7.22 (s, 1H) ppm. ^{19}F NMR ($CDCl_3$/pyridine)($CFCl_3$) δ: -80.28 (s) ppm. MS *m/z* 266 (M^+), 227, 197, 181, 155, 123, 93, 69. Anal. Calcd for $C_{11}H_{13}F_3O_4$: C, 49.63; H, 4.92; F, 21.41. Found: C, 49.69; H, 4.85; F, 21.35. 95% yield.

5. ^{1}H NMR ($CDCl_3$)(TMS) δ: 1.73 (s, 3H); 2.72 (s, 1H); 3.841 (d, 6H, J=2.16 Hz); 6.825 (d, 1H, J=8.48 Hz); 7.03-7.11 (m, 2H) ppm. ^{19}F NMR ($CDCl_3$/pyridine)($CFCl_3$) δ: -80.42 (s) ppm. MS *m/z* 250 (M^+), 211, 181, 139, 124, 107, 95, 77. Anal. Calcd for $C_{11}H_{13}F_3O_3$: C, 52.80; H, 5.24; F, 22.78. Found: C, 52.85; H, 5.28; F, 22.80. 95% yield.

6. ^{1}H NMR ($CDCl_3$)(TMS) δ: 2.93 (s, 1H); 7.34-7.38 (m, 6H); 7.47-7.52 (m, 4H) ppm. ^{19}F NMR ($CDCl_3$/pyridine)($CFCl_3$) δ: -73.39 (s) ppm. MS *m/z* 252 (M^+), 233, 213, 183, 165, 127. 105, 77. Anal. Calcd for $C_{11}H_{13}F_3O_3$: C, 66.67; H, 4.40; F, 22.60. Found: C, 66.71; H, 4.32; F,22 .66. 94% yield.

7. ^{1}H NMR ($CDCl_3$)(TMS) δ: 3.22 (s, 1H); 3.84 (s, 6H); 6.87-7.03 (m, 4H); 7.03-7.47 (m, 4H) ppm. ^{19}F NMR ($CDCl_3$/pyridine)($CFCl_3$) δ: -73.76 (s) ppm. MS *m/z* 312 (M^+), 273, 243, 212, 168, 135, 108, 77. Anal. Calcd for $C_{16}H_{15}F_3O_3$: C, 61.54; H, 4.84; F, 18.25. Found: C, 61.56; H, 4.88; F, 18.17. 96% yield.

8. ^{1}H NMR ($CDCl_3$)(TMS) δ: 2.60 (s, 1H); 4.989 (q, 1H, J=6.60 Hz); 7.38-7.48 (m, 5H) ppm. ^{19}F NMR ($CDCl_3$/pyridine)($CFCl_3$) δ: -78.680 (d, J_{F-H}=6.1 Hz) ppm. MS *m/z* 176 (M^+), 159, 127, 107, 89, 79, 51. Anal. Calcd for $C_8H_7F_3O$: C, 54.55; H, 4.01; F, 32.36. Found: C, 54.58 H, 3.99; F, 32.40. 97% yield.

9. ^{1}H NMR (Acetone-D6)(TMS) δ: 5.073 (q, 1H, J=7.34 Hz); 5.30-6.30 (s, b, 1H); 6.658 (m, 2H); 7.359 (m, 2H); 7.80-8.90 (s, b, 1H) ppm. ^{19}F NMR (C_2D_6O)($CFCl_3$) δ: -77.745 (d, J_{F-H}=6.1 Hz) ppm. ^{19}F NMR ($CDCl_3$/pyridine)($CFCl_3$) δ: -77.901 (d, J_{F-H}=6.1 Hz) ppm. MS *m/z* (silylated) 336 (M^+), 267, 249, 225, 197, 195, 151. Anal. Calcd for $C_8H_7F_3O_2$: C, 50.01; H, 3.67; F, 29.66. Found: C, 50.12; H, 3.71; F, 29.72. 98% yield.

10. ^{1}H NMR (Acetone-D6)(TMS) δ: 2.997 (s, b, 1H); 4.997 (m, 1H); 5.560 (m, 1H); 6.834(m, 2H); 7.976 (s, b, 1H); 8.035 (S, b, 1H) ppm. ^{19}F NMR (C_2D_6O)($CFCl_3$) δ: -77.587 (d, J_{F-H}=7.5 Hz) ppm. ^{19}F NMR ($CDCl_3$/pyridine)($CFCl_3$) δ: -77.691 (d, J_{F-H}=8.0 Hz) ppm. MS *m/z* (silylated) 424 (M^+), 409, 383, 356, 352, 283, 247. Anal. Calcd for $C_8H_7F_3O_3$: C, 46.17; H, 3.39; F, 27.38. Found: C, 46.25; H, 3.41; F, 27.37. 97% yield.

11. ^{1}H NMR ($CDCl_3$)(TMS) δ: 2.59 (s, 1H); 3.89 (s, 3H); 4.925 (q, 1H, J=6.78 Hz); 5.72 (s, 1H); 6.947 (d, 3H, J=13.93 Hz) ppm. ^{19}F NMR ($CDCl_3$/pyridine)($CFCl_3$) δ: -77.756 (d, J_{F-H}=8.0 Hz) ppm. MS *m/z* 222 (M^+), 205, 183, 153, 125, 93, 65, 51. Anal. Calcd for $C_9H_9F_3O_3$: C, 48.66; H, 4.08; F, 25.65. Found: C, 48.70; H, 4.11; F, 25.69. 95% yield.

12. ^{1}H NMR ($CDCl_3$)(TMS) δ: 2.18 (s, 1H); 3.85 (s, 6H); 4.924 (q, 1H, J=6.58 Hz); 6.68 (s, 2H) ppm. ^{19}F NMR ($CDCl_3$/pyridine)($CFCl_3$) δ: -77.633 (d, J_{F-H}=8 Hz) ppm. MS *m/z* 252 (M^+), 205, 183, 167, 155, 140, 123, 95. Anal. Calcd for $C_{10}H_{11}F_3O_4$: C, 47.63; H, 4.40; F, 22.60. Found: C, 47.62; H, 4.42; F, 22.58. 98% yield.

13. ^{1}H NMR ($CDCl_3$)(TMS) δ: 2.50 (s, 1H); 3.87 (s, 6H); 4.943 (q, 1H, J=6.64 Hz); 6.841 (t, 1H, J=4.88 Hz); 6.976 (d, 2H, J=3.42 Hz) ppm. ^{13}C NMR ($CDCl_3$)(TMS) δ: 55.73; 72.65 (q, J_{C-CF}=32.1 Hz); 110.19; 110.91; 120.29; 124.30 (q, J_{C-CF}=281.7 Hz); 126.44, 149.13; 149.99. ^{13}C NMR (DMSO) δ: 24.05; 70.37 (q, J_{C-F}=30.2 Hz); 114.89; 115.06; 118.85; 124.20 (q, J_{C-CF}=282.3 Hz); 126.59; 144.95; 145.79. ^{19}F NMR

($CDCl_3$/pyridine)($CFCl_3$) δ: -77.756 (d, J_{F-H}=7.5 Hz) ppm. MS *m/z* 236 (M^+), 219, 197, 167, 139, 124, 108, 96. Anal. Calcd for $C_{10}H_{11}F_3O_3$: C, 50.85; H, 4.69; F, 24.13. Found: C, 50.92; H, 4.66; F, 24.11. 99% yield.

14. ^1H NMR ($CDCl_3$)(TMS) δ: 2.97 (s, 1H); 4.58-4.66 (m, 1H); 6.20 (q, 1H, J=9.46 Hz); 6.842 (d, 1H, J=15.93 Hz); 7.31-7.44 (m, 5H) ppm. ^{19}F NMR ($CDCl_3$/pyridine)($CFCl_3$) δ: -78.229 (d, J_{F-H} =7.5 Hz) ppm. MS *m/z* 202 (M^+), 184, 165, 133, 115, 91, 77, 55. Anal. Calcd for $C_{10}H_9F_3O$: C, 59.41; H, 4.49; F, 28.19. Found: C, 59.45; H, 4.52; F, 28.17. 99% yield.

15. ^1H NMR ($CDCl_3$)(TMS) δ: 2.25 (s, 1H); 3.84 (s, 3H); 4.531 (t, 1H, J=13.19 Hz); 5.65 (s, 1H); 5.961 (q, 1H, J=9.12 Hz); 6.689 (d, 1H, J=15.73 Hz); 6.82-6.88 (m, 3H) ppm. ^{19}F NMR ($CDCl_3$/pyridine)($CFCl_3$) δ: -78.241 (d, J_{F-H} =6.1 Hz) ppm. MS *m/z* 248 (M^+), 219, 199, 179, 161, 147, 119, 91. Anal. Calcd for $C_{11}H_{11}F_3O_3$: C, 53.23; H, 4.47; F, 22.96. Found: C, 53.28; H, 4.44; F, 22.97. 99% yield.

16. ^1H NMR ($CDCl_3$) δ: 2.42 (br, 4H); 6.19 (s, 4H,); 6.27 (s, 4H,) ppm. ^1H NMR (DMSO) δ: 6.17 (s, 4H); 6.86 (s, 2H,) ppm. ^{13}C NMR (DMSO) δ: 67.18 (q, J_{C-CF}=29.4 Hz); 124.77 (q, J_{C-F}=286.4 Hz); 129.16. ^{13}C NMR (Acetone-D6) δ: 68.70 (q, J_{C-CF}=30.3 Hz); 125.64 (q, J_{C-F}=285.0 Hz); 130.26. ^{19}F NMR ($CDCl_3$/pyridine)($CFCl_3$) δ: -79.80 (s, major); -79.72 (s, minor) ppm. MS *m/z* 179 (M^+ - CF_3), 159, 143, 110, 83, 69, 53. Anal. Calcd for $C_8H_6F_6O_2$: C, 38.73; H, 2.44; F, 45.94. Found: C, 38.75; H, 2.49; F, 45.96. 96% yield.

17. ^1H NMR ($CDCl_3$) δ: 2.02-2.03 (d, 3H, J=1.16 Hz); 2.30 (br, 2H); 5.98-5.99 (d, 1H, J=1.72 Hz); 6.24-6.25 (t, 2H, J=2.16 Hz) ppm. ^{19}F NMR ($CDCl_3$/pyridine)($CFCl_3$) δ: -80.25 (s); -76.04 (s) ppm. MS *m/z* 193 (M^+ - CF_3), 173, 145, 124, 69, 51. Anal. Calcd for $C_9H_8F_6O_2$: C, 41.24; H, 3.08; F, 43.48. Found: C, 41.27; H, 3.15; F, 43.50. 95% yield.

18. ^1H NMR ($CDCl_3$) δ: 1.37-1.41 (d, 9H, J=8.60 Hz); 3.19-3.30 (d, 2H, J=21.23 Hz); 7.52-7.60 (m, 3H); 7.89-8.03 (m, 4H) ppm. ^{19}F NMR ($CDCl_3$/pyridine)($CFCl_3$) δ: -77.85 (s); -77.69 (s) ppm. MS *m/z* 335 (M^+ - CF_3), 320, 266, 251, 209, 181, 152, 112. Anal. Calcd for $C_{20}H_{18}F_6O_2$: C, 59.41; H, 4.49; F, 28.19. Found: C, 59.38; H, 4.46; F, 28.22. 94% yield.

19. ^1H NMR ($CDCl_3$) δ: 1.05 (s, 9H); 1.25 (s, 9H); 2.45 (s, 1H); 3.05 (s, 1H); 5.19 (s, 1H); 6.06 (s, 1H) ppm.^{19}F NMR ($CDCl_3$/pyridine)($CFCl_3$) δ: -68.78 (s); -74.86 (s) ppm. MS

m/z (silylated) 504 (M^+ - CF_3), 489, 399, 379, 327, 285, 259, 239. Anal. Calcd for $C_{16}H_{22}F_6O_2$: C, 53.33; H, 6.15; F, 31.63. Found: C, 53.40; H, 6.10; F, 31.59. 89% yield.

20. ^1H NMR ($CDCl_3$) δ: 4.75 (s, 2H); 7.25-7.34 (m, 2H); 7.41-7.55 (m, 6H); 7.67-7.72 (t, 2H, J=7.32 Hz) ppm. ^{19}F NMR ($CDCl_3$/pyridine)($CFCl_3$) δ: -75.66 (s) ppm. MS *m/z* 175 (M^+ -$C_8H_6F_3O$), 152, 105, 77, 51. Anal. Calcd for $C_{16}H_{12}F_6O_2$: C, 54.87; H, 3.45; F, 32.54. Found: C, 54.91; H, 3.50; F, 32.58. 98% yield.

21. ^1H NMR ($CDCl_3$)(TMS) δ: 3.63 (s, 1H); 3.78 (s, 3H); 3.863 (d, 6H, J=5.40 Hz), 4.07-4.12 (m, 2H); 4.449(t, 1H, J=1.80 Hz); 5.57 (s, 1H); 6.692 (q, 1H, J=3.60 Hz); 6.77-6.83 (m, 2H); 6.865 (d, 1H, J=5.10 Hz); 6.95-6.99 (m, 1H); 7.193 (d, 1H, J=4.80 Hz); 7.294 (d, 1H, J=1.2 Hz) ppm. ^{13}C NMR ($CDCl_3$/)(TMS) δ: 55.85; 56.04; 56.17; 61.36; 79.59 (q, $J_{C\text{-}CF}$=27.4 Hz); 82.64; 109.87; 110.48; 112.07; 118.25; 120.72; 121.66; 124.62; 124.97 (q, $J_{C\text{-}F}$=286.59 Hz); 128.93; 146.18; 148.56; 148.89; 151.53 ppm. ^{19}F NMR ($CDCl_3$/pyridine)($CFCl_3$) δ: -76.03 (s) ppm. MS *m/z* (silylated) 402 (M^+), 302, 278, 248, 235, 221, 181, 165. Anal. Calcd for $C_{19}H_{21}F_3O_6$: C, 56.72; H, 5.26; F, 14.16. Found: C, 56.74; H, 5.29; F, 14.22. 95% yield.

22. ^1H NMR ($CDCl_3$)(TMS) δ: 3.84 (s, 3H); 3.87 (s, 3H); 3.90 (s, 3H), 3.93 (d, 1H, J=3 Hz); 4.24 (d, 1H, J=12 Hz); 4.640 (d, 1H, J=12 Hz); 5.865 (d, 1H, J=3 Hz); 6.84-7.12 (m, 6H) ppm. ^{13}C NMR ($CDCl_3$)(TMS) δ: 56.11; 56.19; 56.64; 71.68; 75.62 (q, $J_{C\text{-}F}$=28.65 Hz); 108.78; 110.06; 111.44; 113.40; 120.41; 121.80; 122.95; 125.60 (q, $J_{C\text{-}F}$=286.59 Hz); 127.88; 147.37; 148.68; 149.16; 149.95 ppm. ^{19}F NMR ($CDCl_3$/pyridine)($CFCl_3$) δ: -76.57 (s) ppm. MS *m/z* 372 (M^+), 303, 248, 235, 217, 189, 180. Anal. Calcd for $C_{18}H_{19}F_3O_5$: C, 58.06; H, 5.14; F, 15.31. Found: C, 58.21; H, 5.20; F, 15.29. 96% yield.

23. ^1H NMR ($CDCl_3$)(TMS) δ: 2.25 (s, 3H); 3.75 (s, 1H); 3.79 (s, 3H), 3.88 (s, 3H); 3.935 (d, 1H, J=9 Hz); 4.12 (d, 1H, J=5.99 Hz); 4.33 (s, 1H); 5.60 (s, 1H,); 5.70 (s, 1H); 6.55-6.64 (m, 3H); 6.94 (d, 1H, J=5.40 Hz); 7.10 (d, 1H, J=4.80 Hz); 7.311 (d, 1H, J=1 Hz) ppm. ^{13}C NMR ($CDCl_3$)(TMS) δ: 21.19; 55.88; 55.93; 61.31; 79.85 (q, $J_{C\text{-}CF}$=28.9 Hz); 82.64; 109.59; 112.95; 113.93; 118.43; 121.01; 122.19; 125.07 (q, $J_{C\text{-}F}$=286.59 Hz); 128.71; 134.83; 143.81; 145.62; 146.35; 151.36 ppm. ^{19}F NMR ($CDCl_3$/pyridine)($CFCl_3$) δ: -75.93 (s) ppm. MS *m/z* (silylated) 618 (M^+), 480, 451, 411. 365, 343, 323, 271. Anal. Calcd for $C_{19}H_{21}F_3O_6$: C, 56.72; H, 5.26; F, 14.16. Found: C, 56.78; H, 5.19; F, 14.18. 93% yield.

6.2.1.3.2. Characterization of Trifluoromethylated Lignins

1. Dioxane lignin:

^{19}F NMR ($CDCl_3$/pyridine)($CFCl_3$) δ: -67.71 to -67.79 (m); -72.70 to -72.99 (b); -74.23 (s); -74.54 (s); -75.20 (b); -75.83 (s); -76.87 to -77.11 (b); -77.78 (d, J_{HF}= 6.6 Hz); -78.21 to -78.26 (b); -78.78 (d, J_{HF}= 7.0 Hz); -82.66 (s); -84.25 (d, J_{HF}= 5.2 Hz) ppm.

2. Kraft lignin:

^{19}F NMR ($CDCl_3$/pyridine)($CFCl_3$) δ: -73.78 (s); -74.29 (s); -74.48 (s); -74.92 (s); -76.06 (s); -76.40 (s); -77.61 (b); -77.78 (d, J_{F-H}=6.6 Hz); -79.14 (d, J_{F-H}=6.6 Hz); -79.24 (d, J_{F-H}=7.1 Hz); -83.42 (s); -84.22 (d, J_{F-H}= 4.2 Hz) ppm.

3. Sucrolin acid hydrolysis:

^{19}F NMR ($CDCl_3$/pyridine)($CFCl_3$) δ: -74.28 (s); -75.77 (s); -75.81 (s); -76.53 (b); -76.64 (s); -77.65 (d, J_{F-H}=6.6 Hz); -77.76 (d, J_{F-H}=7.5 Hz); -77.89 (d, J_{F-H}= 7.0 Hz); -79.13 (d, J_{F-H}=6.6 Hz); -84.32 (s); -85.35 (b) ppm.

4. Alcell Organosolv:

^{19}F NMR ($CDCl_3$/pyridine)($CFCl_3$) δ: -66.19 (s); -66.23 (s); -72.84 (s); -73.20 (b); -73.65 (s); -74.27 (s); -74.81 (t, J_{F-H}=13.2 Hz); -75.81 (s); -76.37 (b); -77.29 (d, J_{F-H}=7.5 Hz); -77.35 (b); -77.46 (b); -77.54 (b); -77.65 (d, J_{F-H}=7.1 Hz); -77.04 (b); -77.75 (s); -77.76 (s); -78.13 to -78.23 (b); -78.63 (s); -84.32 (s) ppm.

5. Steam Explosion lignin:

^{19}F NMR ($CDCl_3$/pyridine)($CFCl_3$) δ: -72.84 (s); -73.65 (s); -74.27 (s); -75.81 (s); -76.37 (b); -77.16 (d, J_{F-H}=4.2 Hz); -77.29 (d, J_{F-H}=7.5 Hz); -77.32 (b); -77.54 (b); -77.64 (d, J_{F-H}=8.0 Hz); -77.75 (d, J_{F-H}=7.1 Hz); -78.18 (b); -78.28 (d, J_{F-H}=6.6 Hz); -78.63 (s); -78.76 (b); -79.13 (b); -79.22 (d, J_{F-H}=3.8 Hz); -84.32 (s) ppm.

6. Straw Lignin:

^{19}F NMR ($CDCl_3$/pyridine)($CFCl_3$) δ: -67.67 (b); -74.26 (s); -75.15 (b); -75.80 (s); -76.52 (b); -76.64 (s); -77.04 (b); -77.25 (s); -77.69 (b); -78.19 (s); -79.05 (s); -79.15 (s); -83.27 (b); -83.95 (b); -84.39 (s) ppm.

7. Softwood Milled wood lignin:

^{19}F NMR ($CDCl_3$/pyridine) ($CFCl_3$) δ: -74.23 (s); -75.55 (b); -76.41 (b); -76.64 (b); -78.18 (b); -79.13 (d, J_{F-H}=6.6 Hz); -79.21 (d, J_{F-H}=6.6 Hz); -79.80 (b); -84.20 (b) ppm.

6.3. RESULTS and DISCUSSION

The detailed chemical reactions used to quantitatively trifluoromethylate the carbonyl groups (including quinones) that are present in lignin are shown in Figure 6.1. The precise trifluoromethylation conditions used for lignins were developed from an understanding of the reaction details for various model compounds[55].

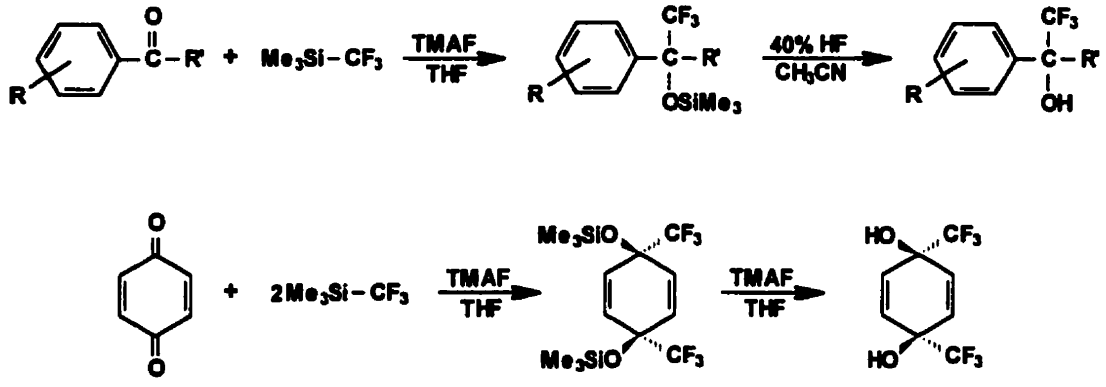

Figure 6.1. Trifluoromethylation of carbonyl-containing (including quinones) lignin-like model compounds.

The acquisitions of the ^{19}F NMR spectra for all trifluoromethylated lignins were carried out in a mixture of $CDCl_3$ and pyridine 1:1.6 (v/v), due to the relative low solubility of lignins in common organic solvents. The particular choice of $CDCl_3$ /pyridine (1:1.6 v/v) was made based on our previous work which requires to acquire ^{31}P NMR spectra of phosphitylated lignins[45-48]. For this reason all ^{19}F chemical shift values for trifluoromethylated carbonyl-containing lignin model compounds were recorded in $CDCl_3$/Py[1], (Tables 6.1 - 6.4).

A closer examination of these data shows that the ^{19}F NMR signals of trifluoromethylated ketones for lignin end-groups range between -80.28 to -80.42 ppm (upfield from $CFCl_3$), while those of dimeric units are confined between -73.39 to -76.57 ppm. Trifluoromethylated derivatives of cinnamic-like aldehydes appeared between

[1] DMF and DMSO were not suitable.

Table 6.1. Fluoride ion induced trifluoromethylation of carbonyl compounds of ketones with trifluoromethyltrimethylsilane.

Entry	Precursor	Product	Overall % Yield	^{19}F NMR(ppm) $CDCl_3$	$CDCl_3$/Pyridine	GC-MS m/e
1)	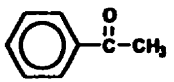	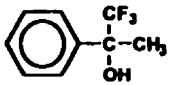	96	-81.35	-80.30	MS m/z 190 (M^+), 151, 127, 121, 105, 91.
2)	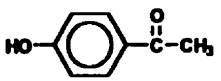	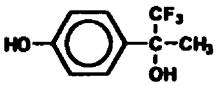	98	-81.76	-80.57	MS m/z 206 (M^+), 188, 167, 149, 137, 119.
3)	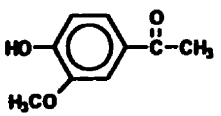	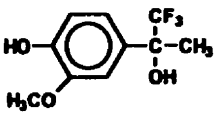	96	-81.60	-80.38	MS m/z 236 (M^+), 197, 167, 151, 124, 110.
4)	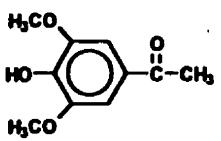	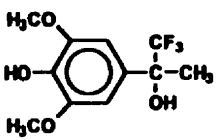	95	-81.47	-80.28	MS m/z 266 (M^+), 227, 197, 181, 155, 123.
5)	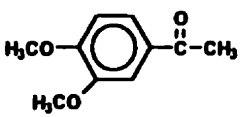	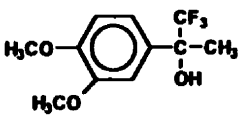	95	-81.56	-80.42	MS m/z 250 (M^+), 211, 181, 139, 124, 107.
6)	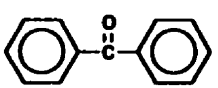	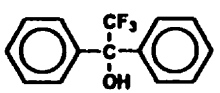	94	-74.79	-73.39	MS m/z 252 (M^+), 253, 213, 183, 165, 127.
7)	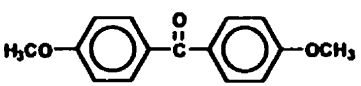	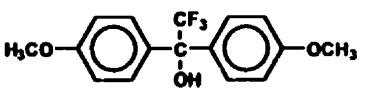	96	-75.11	-73.76	MS m/z 312 (M^+), 273, 243, 212, 135, 108.

Table 6.2. Fluoride ion induced trifluoromethylation of carbonyl compounds of aldehydes with trifluoromethyltrimethylsilane.

Entry	Precursor	Product	Overall % Yield	^{19}F NMR(ppm) $CDCl_3$	$CDCl_3$/Pyridine	GC-MS m/e
8)	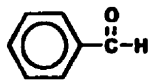	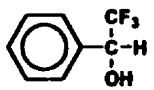	97	-78.848 (d, J_{F-H} = 6.1 Hz)	-77.680 (d, J_{F-H} = 6.1 Hz)	MS m/z 176 (M^+), 159, 127, 107, 89, 79.
9)	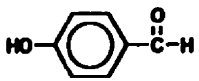	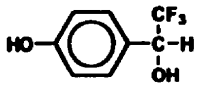	98	-77.745 (Acetone-D_6) (d, J_{F-H} = 6.1 Hz)	-77.901 (d, J_{F-H} = 6.1 Hz)	MS m/z (silylated) 336 (M^+), 267, 249, 225, 197, 151.
10)	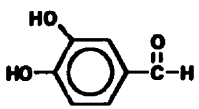	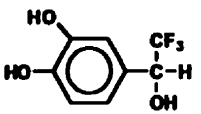	99	-77.587 (Acetone-D_6) (d, J_{F-H} = 7.5 Hz)	-77.691 (d, J_{F-H} = 8.0 Hz)	MS m/z (silylated) 424 (M^+), 409, 383, 356, 283, 247.
11)	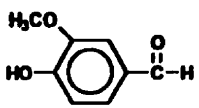	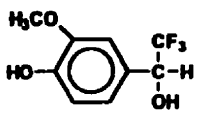	95	-78.981 (d, J_{F-H} = 6.1 Hz)	-77.756 (d, J_{F-H} = 8.0 Hz)	MS m/z 222 (M^+), 205, 183, 153, 125, 93.
12)	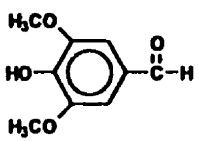	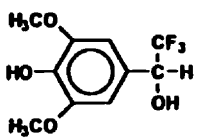	98	-78.890 (d, J_{F-H} = 6.1 Hz)	-77.633 (d, J_{F-H} = 8.0 Hz)	MS m/z 252 (M^+), 205, 183, 167, 155, 140.
13)	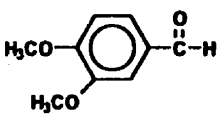	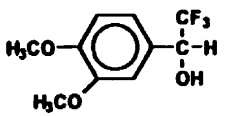	99	-78.916 (d, J_{F-H} = 6.1 Hz)	-77.756 (d, J_{F-H} = 7.5 Hz)	MS m/z 236 (M^+), 219, 197, 167, 139, 124.
14)	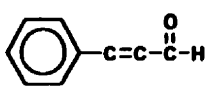	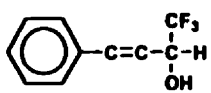	99	-79.458 (d, J_{F-H} = 6.1 Hz)	-78.229 (d, J_{F-H} = 7.5 Hz)	MS m/z 202 (M^+), 184, 165, 133, 115, 91.
15)	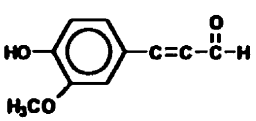	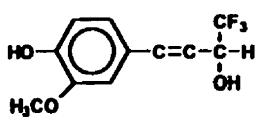	99	-79.607 (d, J_{F-H} = 6.1 Hz)	-78.241 (d, J_{F-H} = 6.1 Hz)	MS m/z 248 (M^+), 219, 199, 179, 161, 147.

Table 6.3. Fluoride ion induced trifluoromethylation of quinones with trifluoromethyltrimethylsilane.

Entry	Precursor	Product	Overall % Yield	^{19}F NMR(ppm) $CDCl_3$	$CDCl_3$/Pyridine	GC-MS m/e
16)	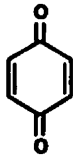	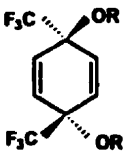	96	16 {-80.75 -80.81	16 {-79.72 (minor) -79.80 (major)	MS m/z 179 (M^+- CF_3), 159, 143, 110, 83, 69.
17)	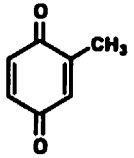	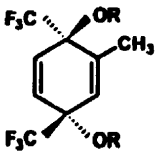	95	17 {-77.25 -81.21	17 {-76.04 -80.25	MS m/z 193 (M^+- CF_3), 173, 145, 124, 69, 51.
18)	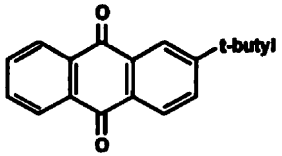	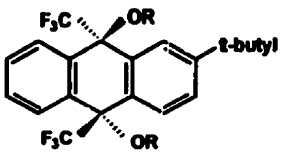	94	18 {-78.29 -78.61	18 {-77.69 -78.85	MS m/z 335 (M^+- CF_3), 320, 268, 251. 209, 181.
19)	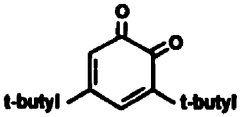	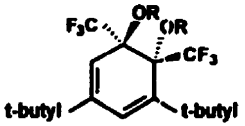	89	19 {-69.59 -75.87	19 {-68.78 -74.86	MS m/z 504 (silylated), (M^+ - CF_3), 489, 399, 379, 327, 285.
20)	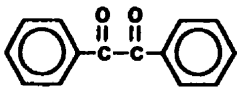	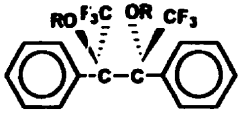	98	20 {-73.55	20 {-75.66	MS m/z 175 (M^+- $C_8H_6F_3O$), 152, 105, 77, 51.

Table 6.4. Fluoride ion induced trifluoromethylation of carbonyl groups with trifluoromethyltrimethylsilane.

Entry	Precursor	Product	Overall % Yield	^{19}F NMR (ppm) $CDCl_3$	$CDCL_3$/Pyridine	GC-MS m/e
21)	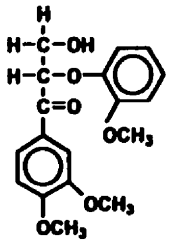	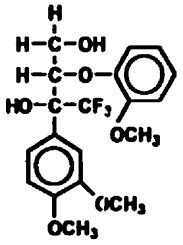	95	-75.53	-76.03	Ms m/z (silylated) 402, (M^+), 302, 278, 248, 235, 221.
22)	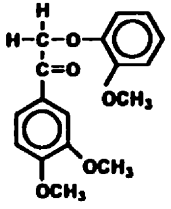	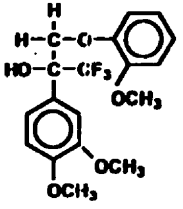	96	-77.63	-76.57	Ms m/z 372, (M^+), 303, 248, 235, 217, 189.
23)	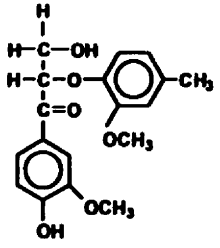	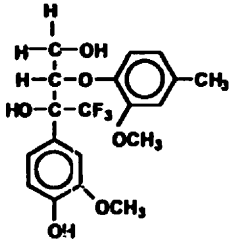	93	-75.48	-75.93	Ms m/z (silylated) 618, (M^+), 480, 451, 411, 365, 343.

-78.23 to -78.24 ppm, while benzaldehyde analogues occupied the range from -77.63 to -77.90 ppm. The latter signals appeared as doublets due to the coupling of fluorine to the adjacent proton present on the trifluoromethylated carbon, with coupling constants ranging between 6.1 to 8.0 Hz[55].

The ^{19}F NMR chemical shifts of trifluoromethylated *ortho* and *para*-quinones were spread over a wide range and their position was found to be sensitive to steric effects. The ^{19}F NMR spectra of trifluoromethylated *ortho*-quinone model compound showed two signals at -68.8 and -74.9 ppm while the signals of trifluoromethylated *para*-quinone model compounds ranged from -76.0 to -80.2 ppm (upfield from $CFCl_3$).

Figure 6.2-6.4 show the ^{19}F NMR spectra for a variety of trifluoromethylated lignin samples; namely: black spruce milled wood lignin, residual kraft lignin, Sucrolin, Alcell organosolv, steam explosion lignin from yellow poplar and milled straw lignin. Apparently, these spectra contain a number of ^{19}F NMR signals that spread over 20 ppm with a number of common signals for all lignins.

To ensure that the trifluoromethylation reaction was selectively carried out on the carbonyl groups in lignin, ^{19}F NMR spectra of lignin samples before and after reduction with sodium borohydride, were acquired. As anticipated the ^{19}F NMR spectra of the reduced and trifluoromethylated lignins showed no signals (Figure 6.5).

6.3.1. Signal Assignment

Initial attempts aimed at structural elucidation of several trifluoromethylated carbonyl-containing moieties in lignins were first carried out by comparing their ^{19}F NMR chemical shifts to the various trifluoromethylated lignin-model compounds. The ^{19}F NMR spectral analyses of different fluorinated lignins displayed a numerous well resolved sharp signals ranging from -64 to -87 ppm, corresponding exactly to the region of various trifluoromethylated lignin model compounds, allowing for some tentative signal assignments. These assignments were tentative because the ^{19}F NMR chemical shifts of trifluoromethylated quinones were found to occupy a wide range, overlapping with those of ketones[55]. As such, complete signal identification could not be carried out based solely on model compound chemical shift information.

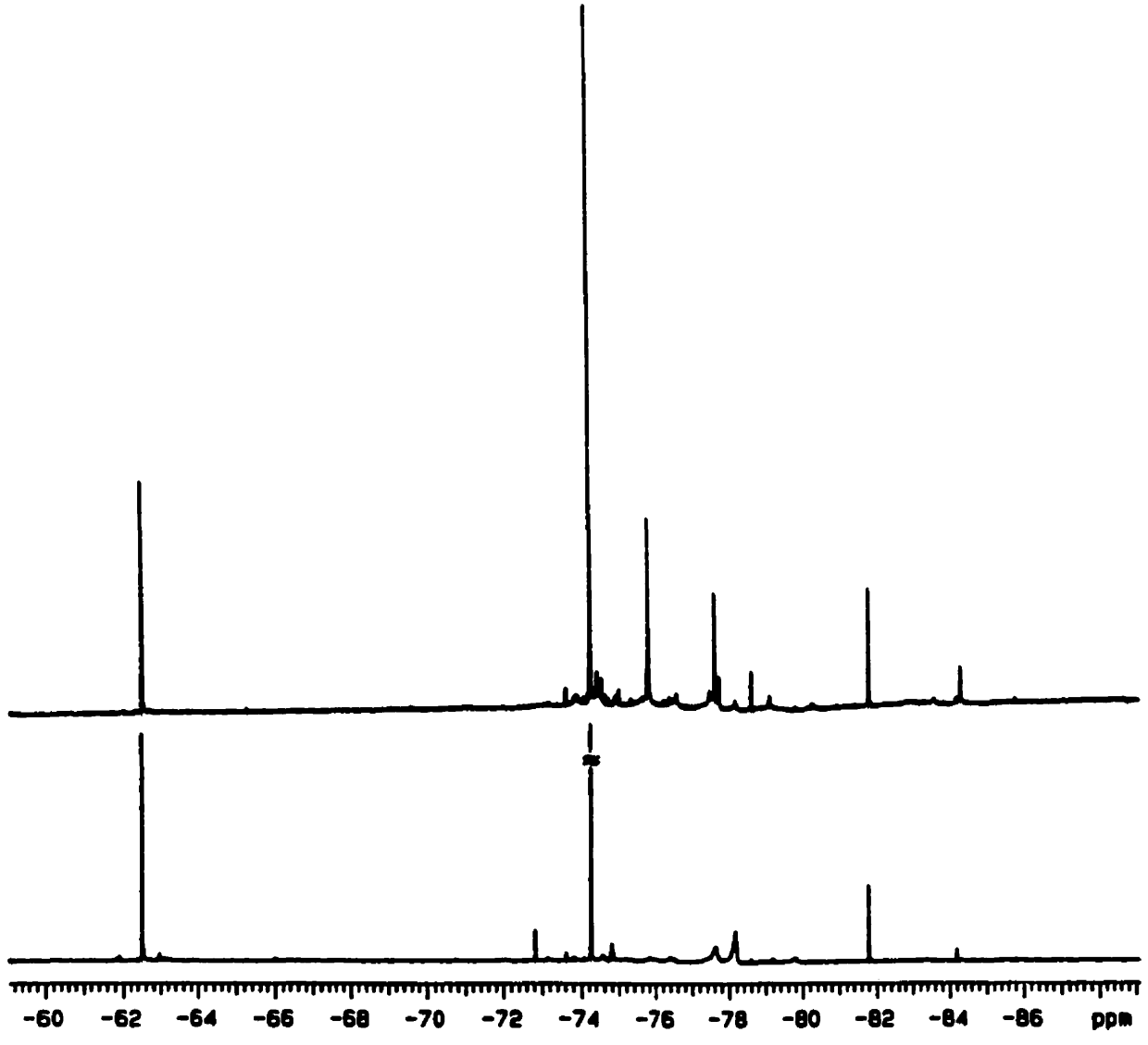

Figure 6.2. Quantitative ^{19}F NMR spectra of steam explosion yellow poplar (top) and black spruce milled wood (bottom) lignins.

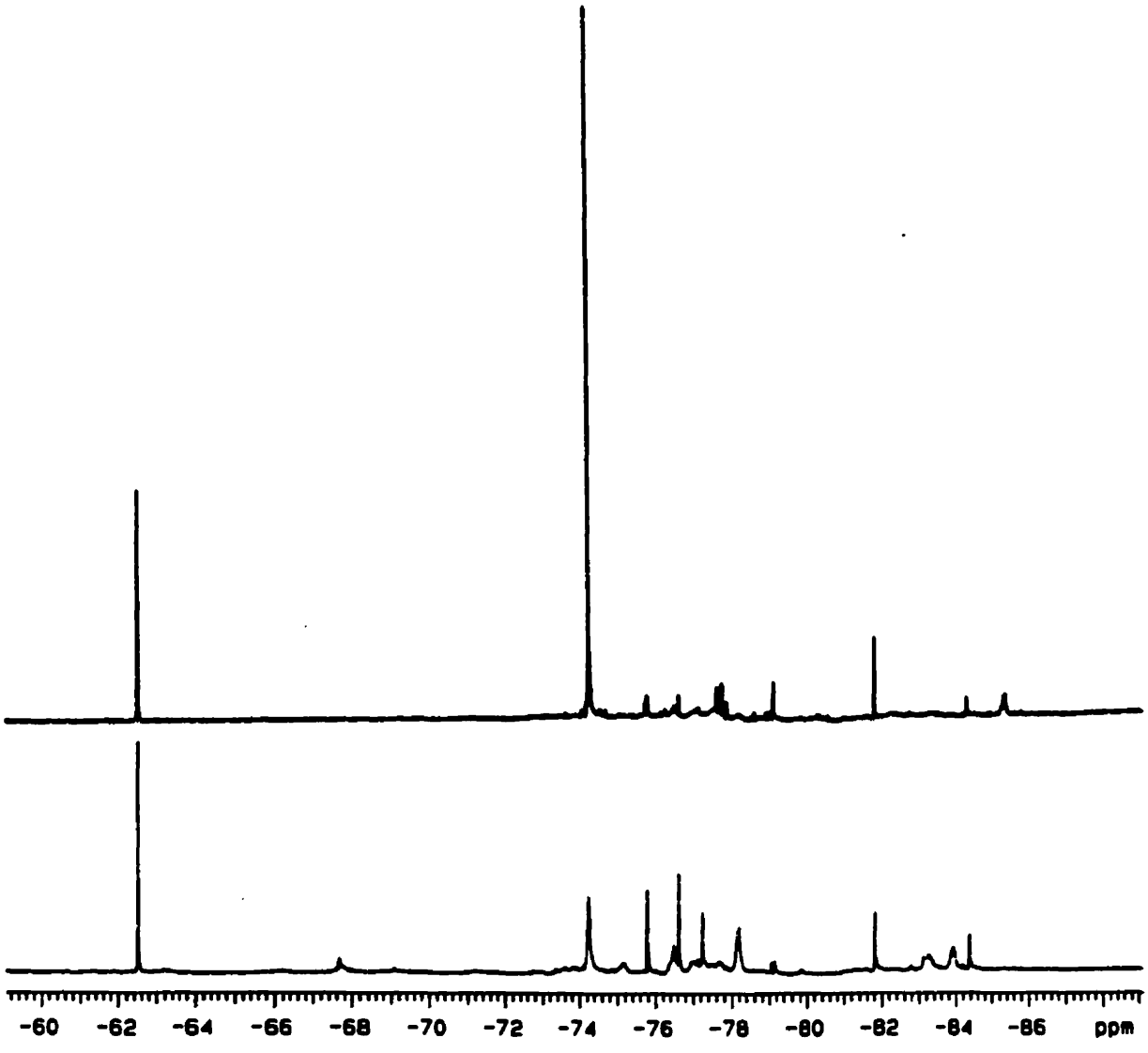

Figure 6.3. Quantitative ^{19}F NMR spectra of Sucrolin (top) and milled straw (bottom) lignins.

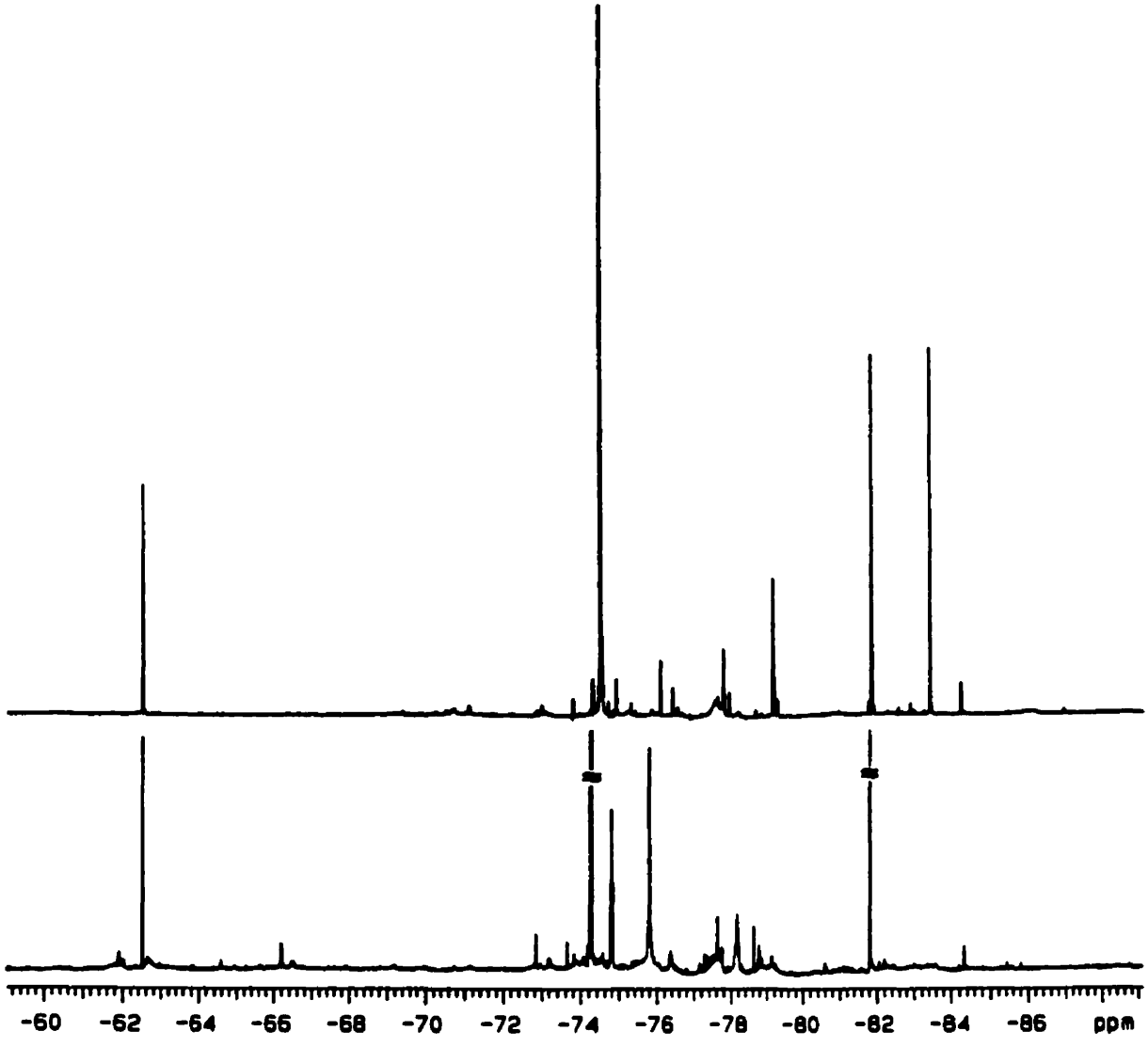

Figure 6.4. Quantitative ^{19}F NMR spectra of residual kraft (top) and Alcell organosolv (bottom) lignins.

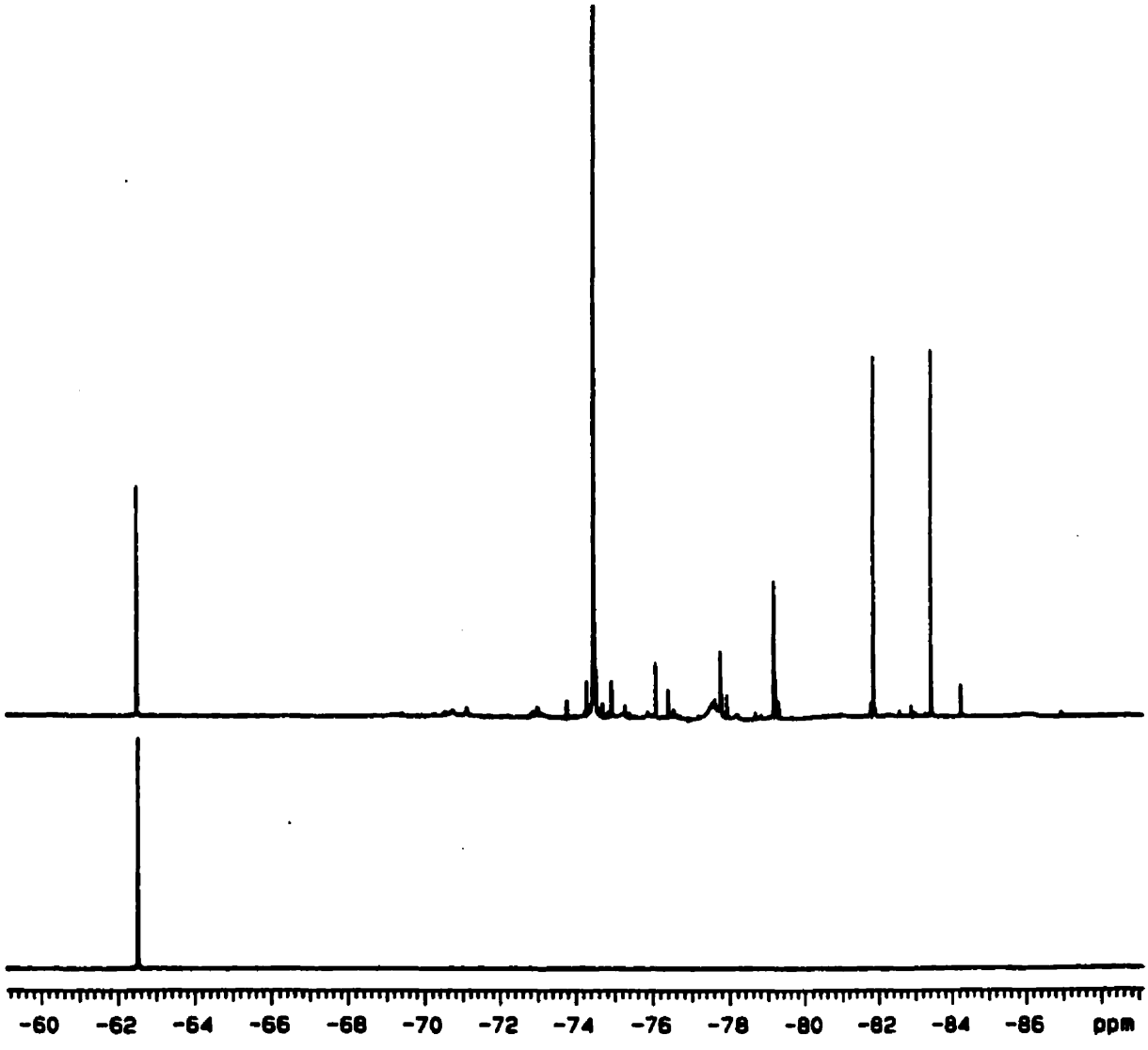

Figure 6.5. ^{19}F NMR spectra of trifluoromethylated kraft lignin before (top) and after (bottom) reduction of carbonyls by sodium borohydride.

The presence of different aldehydes in trifluoromethylated lignins were detected on the basis of their ^{19}F NMR chemical shifts and coupling constants (J_{F-H}). The ^{19}F NMR spectral analyses of trifluoromethylalted aldehydes showed that their signals were spread over two regions i.e. from -77.6 to -77.9 ppm and from -78.8 to -79.1 ppm. These regions were assigned to benzoic and cinnamic-aldehyde type structures respectively. However, the absence of the characteristic aldehydic doublets signals from the ^{19}F NMR spectra of some lignins could be due to signal overlap.

Further clarification of signal assignments was attempted by acquiring two dimensional ^{19}F-^{13}C heteronuclear NMR experiments in anticipation of ^{13}C NMR signal splitting by fluorine nuclei. This is because the ^{13}C NMR spectra for a number of trifluoromethylated model compounds showed distinct signals with appreciably different *J*-coupling constants. More specifically, the ^{13}C NMR chemical shifts for CF_3 groups (quartet) appeared between 123 to 126 ppm, with a ^1J C-F coupling constant of about 285 Hz. Furthermore, a long range ^2J C-F coupling constant was found to be about 30 Hz, confined (quartet) between 68 to 80 ppm, allowing for the differentiation of the ketonic from the quinonic signals.

Table 6.5. Carbon-13 NMR chemical shifts and coupling constants of some trifluoromethylated model compounds.

Compounds	C-13 NMR δ (ppm)		*J* C-F (Hz)	
	CF_3	C-CF_3	^1J	^2J
Dimer β-O-4 **(21)**	125.1	79.6	285	26
Dimer β-O-4 **(22)**	125.1	79.8	285	27
Dimer β-O-4 **(23)**	125.5	75.6	285	47
p-hydroxyacetophenone **(2)**	130.8	74.5	290	29
3,4'-dimethoxybenzaldehyde **(13)**	124.1	72.6	282	32
p-benzoquinone **(16)**	123.0	68.7	285	30

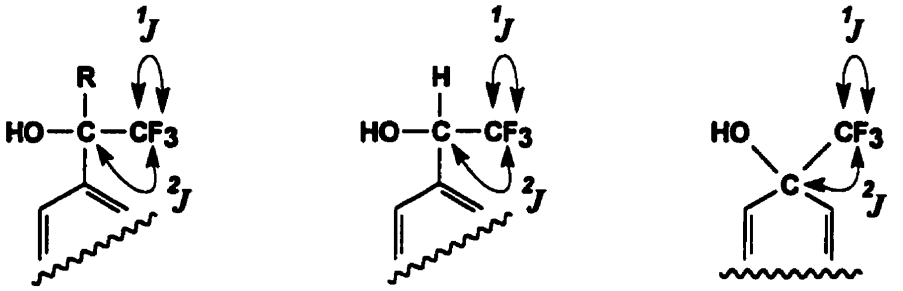

Figure 6.6. ^{19}F-^{13}C coupling constants for different classes of carbonyl groups.

In an effort to select a suitable set of parameters that would cover all possible ^{19}F-^{13}C long range coupling constants that may be encountered in lignin, several HMQC (Heteronuclear Multiple Quantum Correlation) experiments were conducted on different carbonyl-containing lignin model compounds. These studies revealed that, during an HMQC experiment, minor variations in the selected *J*-coupling constants could have serious implications on cross peak intensity. For example, Figure 6.7 (A-D) shows HMQC spectra of trifluoromethylated 3,4'-dimethoxybenzaldehyde (**13**) with *J*-values 28, 30, 32 and 282 Hz. The cross peak at -72.25 & 73.70 ppm (Figure 6.7 signal **I**) is our target signal. However, by varying the *J*-value, another cross peak at -72.37 & 130.9 ppm (Figure 6.7 B, C, D signal **II**) was apparent as a result of an isotope shift effect due to the ^{13}C-^{19}F interaction. This is not surprising since isotopic substitution causes changes in shielding effects: for instance, ^{19}F NMR chemical shift of CF_3I is shielded by 0.149 ppm more for the $^{13}CF_3I$ isotopomer than in $^{12}CF_3I$[58]. This signal, however, was easily distinguished from the primary correlation since it was confined in the $-CF_3$ ^{13}C chemical shift region, and in addition it was slightly shifted (about 0.1 ppm) from the parent ^{19}F peak. Nevertheless, isotope shift effects in HMQC spectra of trifluoromethylated lignins could increase the complexity of signal assignment. Being aware of such potential problems, a number of trifluoromethylated lignins were subjected to HMQC experiments. The accumulated spectral data, however, despite the long acquisition times (24 hours), were inconclusive due to the low carbonyl contents of lignins that gave low signal to noise ratios.

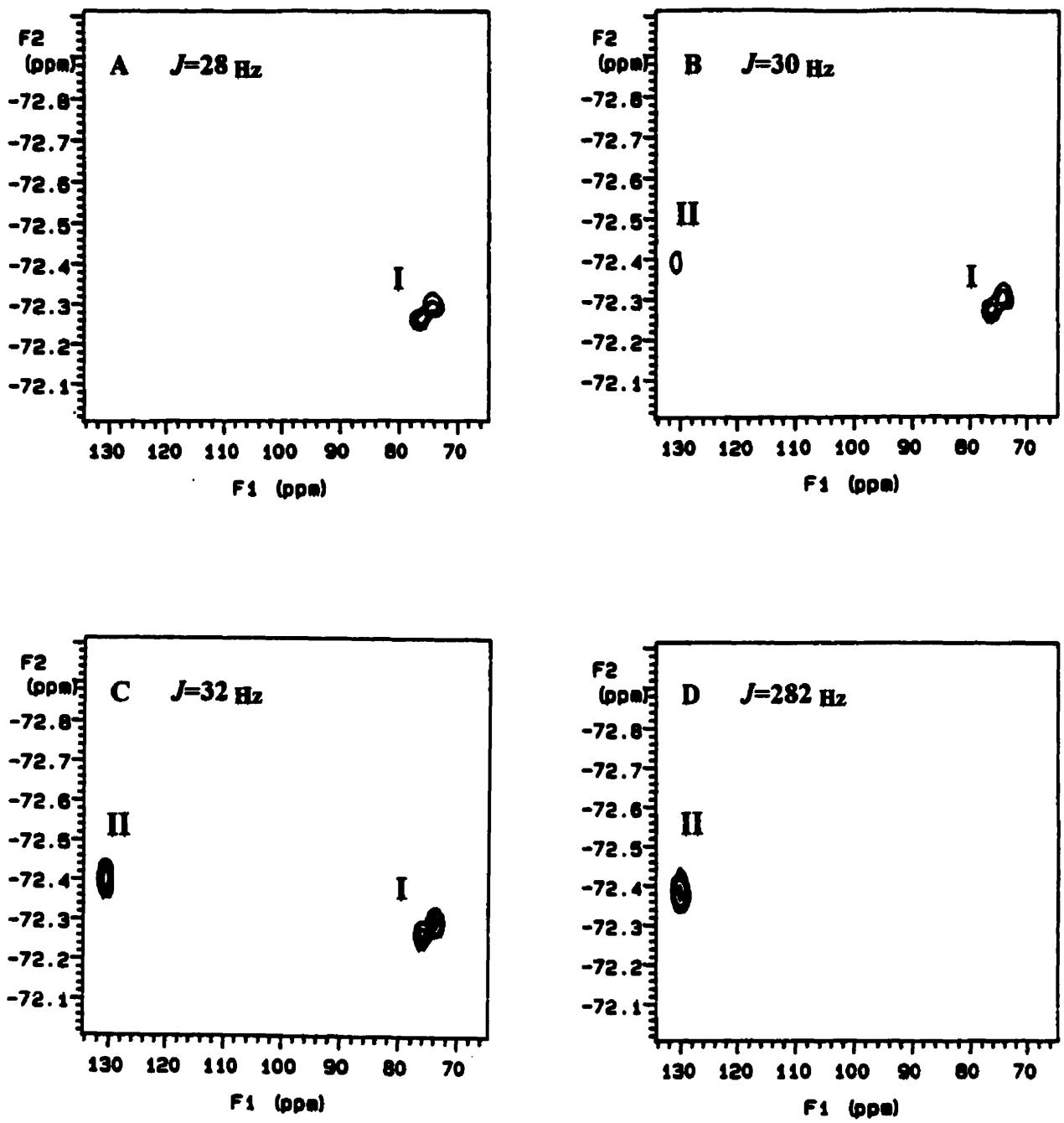

Figure 6.7. ^{19}F-^{13}C HMQC spectra of trifluoromethylated 3,4′-dimethoxybenzaldehyde acquired by selecting different J values.

Since 2D NMR was of limited utility toward aiding the ^{19}F NMR signal assignments for trifluoromethylated lignins, our attention was focused to the application of selective chemical derivatization techniques. In particular two different reactions were considered, namely; the Dakin oxidation[59, 60] and sodium hydrosulphite reduction[61-63].

The Dakin reaction has been shown to cause the selective oxidation of various carbonyl groups present in lignins[60]. More specifically, α-carbonyl groups are known to be oxidized to *para*-quinones when a free hydroxyl group is present *para* to the side-chain. In contrast, when the phenolic group is etherified the system is totally unreactive. Furthermore, α,β-unsaturated aldehydes react with alkaline hydrogen peroxide with the formation of the corresponding benzaldehydes and benzoic acids, while non-phenolic benzaldehydes are converted directly to the corresponding benzoic acids.

Therefore, a lignin sample subjected to the Dakin reaction should be enriched in *para*-quinones and depleted of aldehydes and α-carbonyls that bear free phenolic hydroxyl groups. The total concentration of etherified α-carbonyl structures, however, should remain the same before and after the Dakin reaction.

Sodium hydrosulphite is a mild reducing agent that has been reported[61-63] to selectively reduce quinones in the presence of aldehydes or ketones. In an effort to select the proper set of reaction conditions suitable for conducting such selective reductions on lignins a series of exploratory experiments were carried out. Furthermore, these experiments were also aimed at confirming that cinnamic and benzoic aldehydes as well as model α-ketones would not be reduced by sodium hydrosulphite. More specifically, di-*tert*-butyl-*o*-quinone, *p*-quinone, acetovanillone and syringaldehyde were reduced by sodium hydrosulphite. Both *o*- and *p*-quinones were found to be reduced quantitatively to their corresponding alcohol in 15 minutes, while acetovanillone and syringaldehyde were not affected even after a 4 hour reaction. Nevertheless, the reduction of lignin with sodium hydrosulphite was complete within one hour.

Figure 6.8 shows the ^{19}F NMR spectra of trifluoromethylated samples of residual dioxane lignin (A), after Dakin oxidation (B) and after sodium hydrosulphite reduction (C). On the basis of the above accounts, coupled with the accumulated chemical shift data bank of Tables 6.1-6.4, a number of major carbonyl signals are tentatively assigned.

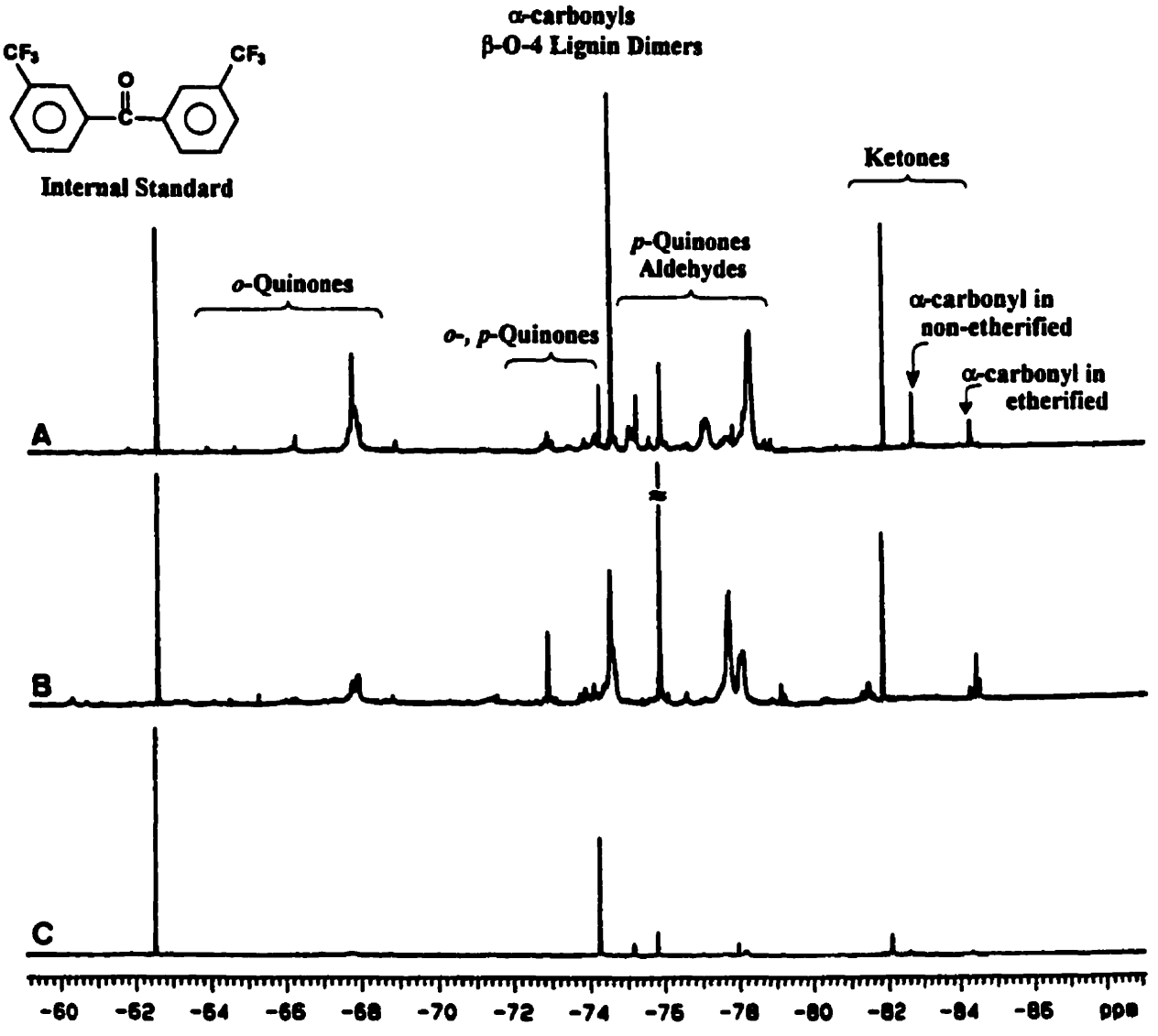

Figure 6.8. ^{19}F NMR spectra of trifluoromethylated dioxane lignin (A), after Dakin reaction (B) and reduction (C) with sodium hydrosulphite.

The comparison of ^{19}F NMR spectral analyses of trifluoromethylated dioxane lignin showed a number of prominent signals that were significantly affected by the Dakin and sodium hydrosulfite reactions. For example, the intensity of signals located at -67.7, -73.0 and -78.2 ppm in the original spectrum of the dioxane lignin [Figure 6.8 (A)] were reduced almost completely [Figure 6.8 (C)] after their reaction with sodium hydrosulfite. Therefore, these signals were assigned to *o*- and *p*-quinones on the basis in chemistry known to occur between sodium hydrosulfite and quinones.

Another important signal, centred at -74.5 ppm, which appeared consistently in all the different trifluoromethylated lignin samples (Figure 6.2-6.4) was also identified. This signal which was assumed to represent α-carbonyl containing β-O-4 structures or quinones (Tables 6.4) was found to be drastically reduced after Dakin oxidation, while it remained unaffected upon treatment with sodium hydrosulfite (Figure 6.8). As such, this signal was assigned to be due exclusively to α-carbonyl groups of β-O-4 units bearing a free phenolic hydroxyl group *para* to the side-chain.

The fine structural elucidation for a number of signals located at -75 to -79 ppm (Figure 6.8) was restricted since various trifluoromethylated carbonyl signals in lignin partially overlap in this region. For instance, the ^{19}F NMR signals of aldehydes, quinones and also α-carbonyls could be all found in this region.

The last set of ^{19}F NMR signals in trifluoromethylated lignin spectra located between -82 to -85 ppm (Figure 6.8) were assigned to different unhindered ketones. The comparison with model compound data (Table 6.1) allowed the assignments of two different classes of ketones in this region. The signal that was not affected by the Dakin oxidation appeared at -84.2 ppm was assigned as being due to the α-carbonyl of etherified lignin end-groups. However, the signal at -82.7 ppm was found to be seriously reduced by Dakin oxidation. This signal was assigned to the ketonic structures bearing a free phenolic hydroxyl group in the *para* position of the aromatic ring such as 5-5′ biphenyl or 4-O-5′ units. Traces of acetone used to wash and dry the glassware was found to give rise to the signal at -82.15 ppm. Therefore, the sensitivity of this technique dictates that when acetone is used for cleaning purposes should be thoroughly removed.

6.3.2. Quantitative evaluation of the carbonyl groups in lignins

The quantification of the total amount of carbonyl groups in lignin was carried out by using 3,3'-bis(trifluoromethyl)benzophenone as an internal standard. This compound had all the characteristics of a reliable internal standard required for accurate measurements: it is a pure crystalline solid possessing two equivalent CF_3 groups giving a sharp signal at -62.511 ppm. Its position is in the proximity of the lignin signals, so as to allow the use of a narrow sweep width during spectral acquisition, and at the same time does not overlap with any of the lignin signals allowing for precise integrations. The use of this internal standard permitted the quantitative determination of all carbonyl groups present in all examined lignins. This was made possible because adequate delay time between pulses was used (10 sec). This selection was based on detailed measurements of the ^{19}F spin-lattice relaxation times for trifluoromethylated lignins and the internal standard. As anticipated, the longest T_1, was found to be that of the internal standard.

Table 6.6. Quantitative analyses of carbonyl groups in several lignins by using F-19 NMR spectroscopy.

Lignin sample	CO/C9		W.t. %		M.W. (g/mol)
	$\bar{x}$	s	$\bar{x}$	s	
Sucrolin Acid Hydrolysis (Bagasse)	0.12 ± 0.01	0.0097	1.89 ± 0.2	0.15	177.4
Alcell Organosolv (Mixed Hardwoods)	0.11 ± 0.01	0.0086	1.56 ± 0.2	0.13	178.5
Steam Explosion (Yellow Poplar)	0.13 ± 0.01	0.010	1.57 ± 0.2	0.18	194.8
Dioxane Acidolysis	0.15 ± 0.01	0.0095	2.27 ± 0.2	0.15	189.4
Kraft Residual*	—	—	2.90 ± 0.2	—	—
Straw	0.018 ± 0.005	0.0011	0.25 ± 0.05	0.012	291.1

$\bar{x}$ = Mean value

s = Standard deviation

* The amount of CO/C9 is not reported since the C9 unit can not be defined

Furthermore, in an effort to examine the reproducibility and quantitative reliability of our measurements, several native and technical lignins were selected and their carbonyl contents were determined after trifluoromethylation. The total carbonyl content for each lignin sample was determined four times and the calculated mean values and standard deviations are shown in Table 6.6. Notably, the total amount of carbonyls determined by ^{19}F NMR were found to be different from sample to sample with high precision. A further investigation aimed at substantiating the present technique as an analytical tool for the quantification of the various carbonyl groups in different soluble lignins was conducted. In particular the quantitative derivatization of carbonyls by trifluoromethylation was examined by selecting lignin samples whose carbonyl content were examined by two different techniques i.e. oximation and UV spectroscopy during the *1991 International Round Robin* effort[56, 57]. It was thus possible to compare the results furnished by quantitative ^{19}F-NMR with those produced by independent methods in other laboratories for the same samples as presented in Table 6.7.

Table 6.7. Determination of total amount of carbonyl groups in lignins by different techniques.

Lignin sample	Detection method			M.W. (g/mol)	Formula
	F-19 NMR	Oximation	UV-VIS*		
Sucrolin Acid Hydrolysis (Bagasse)	0.12 ± 0.01	0.12 ± 0.12	0.03 ± N.R.	177.4	$C_9H_{8.3}O_{2.2}(OCH_3)_{0.83}$
Alcell Organosolv (Mixed Hardwoods)	0.11 ± 0.01	0.10 ± 0.0	0.11 ± N.R.	178.5	$C_9H_{7.7}O_{1.9}(OCH_3)_{1.04}$
Steam Explosion (Yellow Poplar)	0.13 ± 0.01	0.11 ± 0.04	0.09 ± N.R.	194.8	$C_9H_{7.8}O_{2.5}(OCH_3)_{1.25}$

* Reduction with sodium borohydride followed by UV-VIS (standard deviation was not reported - N.R.).

The proximity of the two sets of data in Table 6.7 qualifies the ^{19}F NMR technique as a novel and promising analytical tool for detecting and determining the most prominent carbonyl-containing groups present in different soluble lignins.

6.4. CONCLUSIONS

The quantitative trifluoromethylation of carbonyl groups in some technical and native lignins was examined. These studies demonstrated that such a technique can be applied for the detection and quantitative determination of the various carbonyl groups present in lignins. By applying a set of selective reactions onto a sample of lignin i.e. borohydride and hydrosulphite reductions and Dakin oxidation it became possible to assign a number of prominent ^{19}F NMR signals in trifluoromethylated lignins. The actual quantification of the total amount of carbonyls can be carried out using 3,3'-bis(trifluoromethyl)benzophenone as an internal standard. The total amount of carbonyls determined by the proposed technique in a variety of samples was found to be different from one another and yet close to reported values using independant techniques. The proximity of these data for three lignin samples qualifies the ^{19}F NMR technique as a new analytical tool for detecting and determining carbonyl groups in lignins.

6.5. REFERENCES

1. Harkin, J. M., Lignin-A natural polymeric product of phenol oxidation., In: The chemistry of phenolic resins; the formation, structure and reactions, of phenolic resins and related products., John Wiley & Sons, New York, Chapter 6., pp. 243-312, 1956.

2. Jansherkar, H., Fiechter, A., Lignin: biosynthesis, application, and biodegradation., Advances in Biochemical Engineering/Biotechnology., 27, 119-178, 1983.

3. Glasser, W. G., Kelley, S. S., Light stability of polymers., J. Pulp and paper Can., 8, 795-851, 1987.

4. Argyropoulos, D. S., Menachem, S. B., Lignin., Advances in Biochemical Engineering/Biotechnology., 57, 127-158, 1997.

5. Adler, E., Ellmer, L., Coniferylaldehydgruppen im Holz und in isolierten Lignin praparaten., Acta Chem. Scand., 2, 839-840, 1948.

6. Adler, E., Marton, J., Zur Kenntnis der Carbonylgruppen im Lignin. I., Acta Chem. Scand., 13, 75-96, 1959.

7. Marton, J., Adler, E., Carbonyl groups in lignin III. Mild catalytic hydrogenation of Björkman lignin., Acta Chem. Scand., 15, 370-383, 1961.

8. Gierer, J., and Söderberg, S., Über die Carbonylgruppen des Lignins., Acta Chem. Scand., 13, 127-137, 1959.

9. Geiger, H., Fuggerer, H., Über den Chemismus der Wiesener-Reaktion auf Lignin. Z. Naturforsch., 34, 1471-1472, 1979.

10. Lin, S. Y., Dence, C. W., Methods in Lignin Chemistry., Springer Series in Wood Science., Springer-Verlag Berlin Heidelberg., Chapter 7.4., pp. 446-457, 1992.

11. Sarkanen, K. V., Ludwig., C. H., In Lignins: occurrence, formation, structure and reactions., Wiley-Interscience, John Wiley & Sons, Inc., New York, London, Sydney, Toronto, 1971.

12. Hon, D. N. S., and Glasser, W., On possible chromophore structures in wood and pulps-a survey of the present state of knowledge., Polym. Plast. Technol. Eng., 12, 157-159, 1979.

13. Lebo, S. E., Lonsky, W. F., McDonough, T. J., Medvecz, P. J., Dimmel, D. R., The occurrence of light-induced formation of *ortho*-quinonoid lignin structures in white spruce refiner mechanical pulp., J. Pulp and Pap. Sci., 16, 5, 139-143, 1990.

14. Brunow, G., Eriksson, B., α-carbonyl groups as sensitizers in the photo-dehydrogenation of phenolic structures in lignin., Acta Chem. Scand., 25, 2779-2781, 1971.

15. Argyropoulos, D. S., Heitner, C. and Morin, F. G., ^{31}P NMR spectroscopy in wood chemistry. Part III. Solid state ^{31}P NMR of trimethyl phosphite derivatives of chromophores in mechanical pulp., Holzforschung, 46, 211-218, 1994.

16. Argyropoulos, D. S., Heitner, C., ^{31}P NMR spectroscopy in wood chemistry. Part VI. Solid state ^{31}P NMR of trimethyl phosphite derivatives of chromophores and carboxcylic acids present in mechanical pulps: A method for the determination of *ortho*-quinones., Holzforschung Suppl., 48, 112-116, 1994.

17. Lin, S. Y. and Kringstad, K. P., Some reactions in the photoinduced discoloration of lignin., Norsk. Skiksind., 25, 252-256, 1971.

18. Forsskåhl, I., Tylli, H., Olkkonen, C. and Janson, J., Photochemistry of quinones and hydroquinones on solid matrices., Int. Symp. of Wood and Pulping Chemistry, Melbourne Australia, 2, 325-332, 1991.

19. Castellan, A., Nourmamode, A., Jeager, C. and Forsskåhl, I., Photochemistry of lignocellulosic materials., Eds. Heitner, C. and Scaiano, J. C., ACS Symp. Ser., 531, pp. 60-76, 1993.

20. Gellersted, G. and Pattersson, E. L., Light-induced oxidation of lignin. Part2. The oxidative degradation of aromatic rings, Svensk. Papperstidn., 77, 15-21, 1977.

21. Green, J. W., Determination of carbonyl group. In: Whistler, R. I., (ed) Methods in carbohydrates Chem., Vol. III. Academic Press, New York, 49-54, 1963.

22. Lindberg, B., Misiorny, A., Quantitative analysis of reducible carbohydrates by means of sodium borohydride., Svensk. Papperstidn., 55, 13-14, 1952.

23. Lindberg, B., Theander, O., Quantitative determination of carbonyl groups in oxycellulose by means of sodium borohydride., Svensk. Papperstidn., 57, 83-85, 1954.

24. Heuser, E., Analytik von Chinonen., In: Müller E., Bayer, O., Meerwein H.,

Ziegler, K., (eds) Methoden der organischen Chemie (Houben-Weyl) 4. Aufl., Bd II Analytische Methoden. George Thieme, Stuttgart, Federal Republic of Germany, 434-472, 1953.

25. Miyake, M., Kraft cooking with addition of reducing agents. III. Effect of yield increase by hydrazine or hydroxylamine and its mechanism., J. Jap. Tappi, 24, (2), 74-80, 1970.

26. Zakis, G. F., "Functional analysis of lignins and their derivatives", Tappi press, Riga, Latvia, Tappi, pp. 61-76, 1994.

27. Kolboe, S., and Ellefsen, O., Infrared investigations of lignin; A discussion of some recent results., Tappi, 45(2), 163-166, 1962.

28. Faix, O., Classification of lignins from different botanical origins by FTIR spectroscopy, Holzforschung Suppl., 45, 21-27, 1991.

29. Hergert, H., Inrared spectra. In: Lignins-Occurrence, Formation, Structure and Reaction, Eds. K. Sarkanen and C. Ludwig, Wiley Interscience, New York, pp. 267-297, 1971.

30. Marton, J., Adler, E., and Persson, K. I., Carbonyl groups in lignin IV*. Infrared absorption studies and examination of the volumetric borohydride method**., Acta Chem. Scand., 15(2), 384-392, 1961.

31. Hortling, B., Tamminen, T., and Kenttä, E., Determination of carboxyl and non-conjugated carbonyl groups in dissolved and residual lignins by IR spectroscopy., Holzforschung, 51, 405-410, 1997.

32. Argyropoulos, D. S., ^{31}P NMR in Wood Chemistry, A review of recent progress., Research on chemical intermediates., 21, No. 3-5, pp. 373-395, 1995.

33. Lundquist, K., NMR studies of lignins. 2. Interpretation of the ^{1}H NMR spectrum of acetylated brich lignin., Acta. Chem. Scand., B33, 27-30, 1979.

34. Lundquist, K., NMR studies of lignins. 3. ^{1}H NMR spectroscopic data for lignin model compounds., Acta. Chem. Scand., B33, 418-420, 1979.

35. Lundquist, K., NMR studies of lignins. 4. Investigation of spruce lignin by ^{1}H NMR spectroscopy., Acta. Chem. Scand., B34, 21-26, 1980.

36. Lapierre, C., Monties, B., Guittet, E., Lallemand, J. Y., Quantitative measurements in hardwood lignin ^{13}C NMR spectra., Holzforschung, 39, 367-368, 1984.

37. Robert, D., Brunow, G., Quantitative estimation of hydroxyl groups in milled wood lignin from spruce and in a dehydrogenation polymer from coniferyl alcohol using ^{13}C NMR spectroscopy., Holzforschung, 38, 85-90, 1984.

38. Obst, J. R., Landucci, L. L., Quantitative ^{13}C NMR of lignins. Methoxyl: aryl ratio., Holzforschung Suppl., 40, 87-92, 1986.

39. Pan., X., and Lachenal, D., Structure and reactivity of spruce mechanical pulp lignins IV: ^{13}C-NMR spectral studies of isolated lignins., J. Wood Chem. Technol., 14(4), 483-506, 1994.

40. Brezny, R., and Schraml, J., Silicon-29 NMR spectral studies of kraft lignin and related model compounds., Holzforschung, 41, 293-298, 1987.

41. Nieminen, O. J., Pulkkinen, E., and Rahkamaa, E., Determination of hydroxyl groups in kraft pine lignin by Silicon-29 NMR spectroscopy., Holzforschung, 43, 303-307, 1989.

42. Archipov, Y., Argyropoulos, D. S., Bolker, H. I. and Heitner, C., ^{31}P NMR spectroscopy in wood chemistry. Part I, Model compounds., J. Wood Chem. Technol., 11(2), 137-157, 1991.

43. Archipov, Y., Argyropoulos, D. S., Bolker, H. I. and Heitner, C., ^{31}P NMR spectroscopy in wood chemistry. Part II, Phosphite derivatives of carbohydrates., Carbohydrate Research, 220, 49-61, 1991.

44. Argyropoulos, D. S., Archipov, Y., Bolker, H. I. and Heitner, C., ^{31}P NMR spectroscopy in wood chemistry. Part IV, Lignin models: Spin-lattice relaxation times and solvent effects in ^{31}P NMR, Holzforschung, 47, 50-56, 1992.

45. Argyropoulos, D. S., Bolker, H. I., Heitner, C. and Archipov, Y., ^{31}P NMR spectroscopy in wood chemistry. Part V, Qualitative analysis of lignin functional groups., J. Wood Chem. Technol., 13(2), 187-212, 1993.

46. Argyropoulos, D. S., Quantitative phosphorus-31 NMR analysis of lignins, A new tool for the lignin chemist., J. Wood Chem. Technol., 14(1), 45-63, 1994.

47. Argyropoulos, D. S., Quantitative phosphorus-31 NMR analysis of six soluble lignins., J. Wood Chem. Technol., 14(1), 65-82, 1994.

48. Fillppov, V., Archipov, Y., Argyropoulos, D. S., 4,4,5,5-tetramethyl-1,3,2-dioxaphospholanyl chloride-derivatization reagent for lignin functional group analysis materials., 7th Int. Conf. Young Scientists, Riga, Latvia, 1991.

49. Manatt, S. L., Characterization of functional groups by nuclear magnetic resonance. I. Classification of alcohols from the fluorine-19 spectra of trifluoroacetates., J. Am. Chem. Soc., 88(6), 1323-1324, 1966.

50. Barrelle, M., Improvements in the structural investigation of lignins by ^{19}F NMR spectroscopy., J. Wood Chem. Technol., 15(2), 179-188, 1995.

51. Argyropoulos, D. S., Heitner, C. and Schmidt, J. A., Observation of quinonoid groups during the light-induced yellowing of softwood mechanical pulp., Res. Chem. Intermed., 9, No. 3-5, pp. 263-274, 1995.

52. Barrelle, M., A new method for the quantitative ^{19}F NMR spectroscopic analysis of hydroxyl groups in lignins., Holzforschung, 47, 261-267, 1993.

53. Lachenal, D., Fernandes, J. C., and Froment, P., Behaviour of residual lignin in kraft pulp during bleaching., J. Pulp and Pap. Sci., 21, 173-177, 1995.

54. Ahvazi, B. C., and Argyropoulos, D. S., Quantitative trifluoromethylation of carbonyl-containing lignin model compounds., J. Fluorine Chem., 78, 195-198, 1996.

55. Ahvazi, B. C., and Argyropoulos, D. S., ^{19}F Nuclear magnetic resonance spectroscopy for the elucidation of carbonyl groups in lignins: Part 1. Model compounds., J. Agric. Food Chem., 44, 8, 2167-2175, 1996.

56. Andersons, B., and Faix O., Carbonyl group determination of lignins., 8th International Symposium on Wood and Pulping Chemistry., Helsinki, Finland., Vol. I, 559-566, June 6-9, 1995.

57. Milne, T. A., Chum, H. L., Agblevor, F., and Johnson, D. K., Standardized analytical methods., Biomass and Bioenergy, 2, 341-366, 1992.

58. Harris, R. K., Nuclear magnetic resonance spectroscopy; A Physiochemical view., The Universities Press (Belfast) Ltd., Pitman eds., Chap. 8, p. 189, 1983.

59. Bailey, C. W., and Dence, C. W., Reactions of alkaline hydrogen peroxide with softwood lignin model compounds, spruce milled-groundwood lignin and spruce groundwood., Tappi, 52(3), 491-500, 1969.

60. Reeves, R. H., and Pearl, I. A., Reaction products formed upon the alkaline peroxide oxidation of lignin-related model compounds., Tappi, 48(2), 121-125, 1965.

61. Rabjohn, N., Organic Syntheses: Collective Volume IV., A revised edition of

annual volumes 30-39, John Wiley & Sons, Inc., New York, London, pp. 13-18, 1963.

62. Fieser, F., and Fieser, M., Reagents for organic synthesis., John Wiley & Sons, Inc., New York, London, Sydney, pp. 1080-1082, 1967.

63. Grundmann, C., Chinone: p-Chinone der Benzol-und Naphthalin-Reihe., In: Methoden der Organischen Chemie., Ed. by Müller, E., Houben-Weyl., Georg Thieme Verlag Stuttgart., Vol. VII/3a., pp. 648-650, 1977.

Original Contributions to Knowledge and Ideas for Continued Research

Wood is a unique organic material. It is unique in virtually every one of its properties and characteristics: its strength-to-weight ratio, its machinability, its warmth and beauty, its chemical make-up, its insulating properties, its anisotropy, and its great variability. There is no other material embodying all of these properties in a single complex.

While there exists a great accumulation of information about wood properties--physical, mechanical, chemical--and a substantial body of knowledge is available on its cellular structure, still there are many gaps to be filled. Advancement depends in part on understanding the molecular origins of macroscopic behaviour; It is here nuclear magnetic resonance spectroscopy techniques make notable contributions to comprehend the various physico-chemical properties of wood structure.

The work carried out during this effort contributes in the development and application of solid-state and solution NMR spectroscopic techniques, revealing fine structural details of lignin when exposed to a range of pH's and pulping processes.

1. The solid-state proton spin-lattice relaxation measurements for carbohydrates and lignin over a wide range of pH's were examined. These studies indicated that ionization of various functional groups can influence the mobility of these biopolymers and consequently their physico-chemical properties. The analyses of the T_{1H} data showed that as the pH increased from acidic to near neutrality ($2 \rightarrow 6$), the T_{1H} values of carbohydrates and lignin increased, reaching a maximum at pH 6. However, as the pH changed from near neutrality toward alkalinity ($6 \rightarrow 13$), the T_{1H} values decreased, promoting the softening of these biopolymers under alkaline conditions. Further studies aimed at a better understanding of the ultrastructure of wood and the architectural association of lignin with carbohydrates can be carried out by evaluating the proton spin-lattice relaxation times (T_{1H}) of several isolated samples of black spruce softwood as a function of degree of delignification.

2. The pseudo-first order rate kinetics for the stereoselective degradation of arylglycerol-β-aryl ether linkages present in softwood milled wood lignin were investigated by using quantitative ^{31}P NMR spectroscopy. The *erythro* and *threo* forms of β-aryl ethers units were measured quantitatively by ^{31}P spectroscopy as a function of time and temperature. The activation energy of the *erythro* isomer was found to be always lower than its counterpart for both the initial and the bulk phases of delignification. The stereoselectivity of both arylglycerol-β-aryl ether isomers and the stability of the *threo* over their *erythro* counterparts can be further investigated by enzymatic degradation of these structural units in lignin. This will be followed by quantitative ^{31}P NMR spectral analyses aimed at revealing more information on this issue.

3. By using quantitative ^{31}P NMR spectroscopy it is possible to identify, quantify and follow the formation of phenolic hydroxyl groups that belong to diphenylmethane units under kraft and soda pulping conditions. Data derived during the course of this work implied that diphenylmethanes are formed in higher quantities during conventional pulping as opposed to its EMCC$^{\bullet}$ counterpart, at the same kappa number. Further studies may involve the kinetic investigation for the formation of overall condensed structures and particularly diphenylmethane units in milled wood lignin under homogeneous kraft pulping conditions. This will provide vital information on the magnitude of their activation energies, indicating on how and to what extent the formation of condensed structures hamper the rate of delignification processes.

4. The quantitative trifluoromethylation of carbonyl groups for a series of carbonyl-containing lignin-like model compounds has been accomplished by using trifluorotrimethylsilane (Ruppert's reagent) in the presence of TMAF. This reagent was found to be an efficient nucleophilic trifluoromethylating

agent for derivatizing a variety of carbonyl-containing compounds that may have been present in lignin. This was followed by studying the ^{19}F NMR chemical shifts of fluorine containing derivatives.

5. The quantitative trifluoromethylation of carbonyl groups in some technical and native lignins was also examined. These studies demonstrated that such a technique can be applied for the detection and quantitative determination of the various carbonyl groups present in lignins. The actual quantification of the total amount of carbonyls was carried out using 3,3'-bis(trifluoromethyl)benzophenone as an internal standard qualifying this technique as a new analytical tool for detecting and determining carbonyl groups in lignins. Further investigation may be carried out by trifluoromethylating more carbonyl-containing lignin-like model compounds (i.e. *o*-quinones, dimeric model compounds) followed by recording their ^{19}F NMR chemical shifts. Experimentation with various organic solvents other than THF aimed at dissolving a greater variety of lignin samples can also be carried out.